



Norwegian University of  
Science and Technology

# Asymmetric Synthesis of 2- Phenylpyrrolidines for SAR Study of Thienopyrimidine-based EGFR Kinase Inhibitors

**Andreas Behne Ramsnes**

Chemical Engineering and Biotechnology

Submission date: June 2018

Supervisor: Bård Helge Hoff, IKJ

Co-supervisor: Thomas Aarhus, IKJ


Norwegian University of Science and Technology  
Department of Chemistry



---

I hereby declare that the work done in this thesis is independent and in accordance with the exam regulations of the Norwegian University of Science and Technology.

June 18, 2018

  
\_\_\_\_\_  
Andreas Behné Ramsnes

---



# Acknowledgements

This master's thesis has been completed at the Department of Chemistry at the Norwegian University of Science and Technology during the spring of 2018. The project has been supervised by Professor Bård Helge Hoff, and PhD-candidate Thomas Ihle Aarhus. Thank you for giving me a truly fascinating project to work with, and for your encouragement and guidance along the way. I have learned incredibly much from working with you both, and you have inspired me to work hard and challenge myself along the way.

I wish to thank Torun Margareta Melø for being incredibly helpful with any problems related to NMR analyses. A big thank you to Roger Aarvik for ordering chemicals and helping out with any practical issues around the lab, and of course to Susana Villa Gonzalez for performing all my MS analyses.

Thank you to my family for their continuous support and encouragement throughout my study, and for helping me with the laborious task of proofreading this thesis. Last but not least I would like to thank my fellow master students, both inside and outside of the laboratory. Thank you for all your professional advice, for the time spent during (over)extended lunch breaks, and generally for making my time here truly enjoyable. A special mention goes to David Moe Almenningen, for your invaluable inputs and company.



# Abstract

The aim of this master's thesis was to carry out a preliminary structure-activity relationship (SAR) study of thieno[2,3-*d*]pyrimidines with racemic and enantioenriched 2-phenylpyrrolidine as a substituent on C-4. One objective was to investigate if secondary amines are essential substituents at C-4 by preparing thieno[2,3-*d*]pyrimidines with a tertiary heterocyclic amine. This study has also included compounds with pyrrolidine as a C-4 substituent, to study the contribution of the phenyl moiety on the amine on the EGFR-TK activity. All amines and thieno[2,3-*d*]pyrimidines have been synthesized as part of the project, and a second objective of this master's thesis was to investigate viable synthetic routes to obtain enantioenriched 2-phenylpyrrolidine with high chemical and enantiopurity.

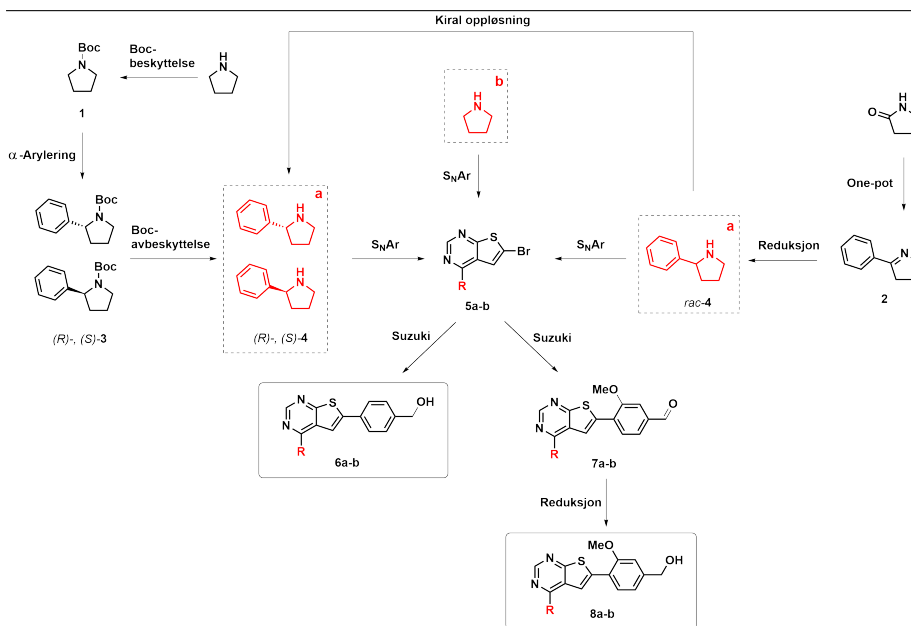
Enantioenriched 2-phenylpyrrolidines were prepared in three synthetic steps, starting with Boc protection of pyrrolidine. Palladium-catalyzed  $\alpha$ -arylation gave enantioenriched, Boc-protected intermediates, followed by Boc deprotection to achieve enantioenriched amines with 81-96 % ee. Enantioenriched amine was also obtained from racemic 2-phenylpyrrolidine via chiral resolution, employing a chiral acid. Racemic 2-phenylpyrrolidine was prepared in two synthetic steps, starting with a two-step, one-pot synthesis from pyrrolidin-2-one, followed by reduction of a conjugated double bond. Access to the target thieno[2,3-*d*]pyrimidines required further two to three synthetic steps, including nucleophilic aromatic substitution, Suzuki cross-coupling, and reduction of aldehyde to primary alcohol. The synthetic routes are illustrated in Scheme 0.0.1.



# Sammendrag

Hensikten med denne masteroppgaven har vært å utføre en innledende struktur-aktivitet relasjonsstudie av tieno[2,3-*d*]pyrimidiner med rasemisk og enantioanrikt 2-fenylpyrrolidine som substituent på C-4. Målet var å undersøke om det er nødvendig med et sekundært amin på C-4 for å oppnå EGFR-TK aktivitet, eller om det er mulig å oppnå god aktivitet med tertiære heterosykliske aminer. Denne studien har også inkludert strukturer med pyrrolidin som C-4 substituent, for å studere bidraget av fenylgruppen på aminet til EGFR-TK aktiviteten. Alle aminer og tieno[2,3-*d*]pyrimidiner har blitt syntetisert som en del av prosjektet, og et annet mål med denne masteroppgaven har vært å undersøke mulige synteseveier for å oppnå enantioanrikt 2-fenylpyrrolidin med høy kjemisk og enantiomer renhet.

Enantioanrikt 2-fenylpyrrolidin ble syntetisert i tre steg, med utgangspunkt i en Boc beskyttelse av pyrrolidin. Palladium-katalysert  $\alpha$ -arylering gav Boc-beskyttede mellomprodukter, som ved avbeskyttelse gav enantioanrikt amin. En alternativ syntesevei til enantioanrikt amin via kiral oppløsning av rasemisk amin ble også utforsket, ved bruk av en kiral syre. Rasemisk 2-fenylpyrrolidin ble syntetisert i to steg, med utgangspunkt i en to-steg, one-pot syntese fra pyrrolidin-2-on, etterfulgt av reduksjon av et konjugert dobbelbånd. Målstrukturene ble videre syntetisert gjennom to til tre syntetiske steg, herunder nukleofil aromatisk substitusjon, Suzuki kobling, og reduksjon av aldehyd til primær alkohol. Synteseveiene i denne masteroppgaven er illustrert i Skjema 0.0.2



**Scheme 0.0.2:** Synteseveier til målstrukturene **6a-b**, og **8a-b**.

Denne oppgaven har resultert i 14 nye strukturer, hvorav to ble funnet å inneha god EGFR-TK-aktivitet og med potensial til å åpne nye forskningsområder. Fenygruppen på C-4 aminet har vist seg å ha en signifikant påvirkning på EGFR-TK-aktiviteten, ettersom fjerning av denne gruppen hadde en betydelig negativ innvirkning. Også kiraliteten på fenygruppen har vist seg å ha en påvirkning på EGFR-TK-aktiviteten, med en markant økning i aktivitet for (*R*)-enantiomeren relativt til rasematet, og dårlig aktivitet for (*S*)-enantiomeren. Resultatene fra denne masteroppgaven har vist at det er mulig å oppnå god EGFR-TK aktivitet med et tertiært heterosyklisk amin på C-4.

# Symbols and Abbreviations

$\delta$	Chemical shift [ppm]
$^{13}\text{C}$ NMR	Carbon Nuclear Magnetic Resonance
$^1\text{H}$ NMR	Proton Nuclear Magnetic Resonance
APCI	Atmospheric Pressure Chemical Ionization
Ar	Aryl
ATP	Adenosine Triphosphate
bp	Boiling Point [ $^{\circ}\text{C}$ ]
br	Broad signal
Conv	Conversion
COSY	Correlation Spectroscopy
CSF1R	Colony Stimulating Factor 1 Receptor
CSP	Chiral Stationary Phase
d	Doublet
Decomp	Decomposition
ee	Enantiomeric Excess
EGFR	Epidermal Growth Factor Receptor
eq	Equivalent(-s)
ESI	Electrospray Ionization
FGFR	Fibroblast Growth Factor Receptor
FRET	Fluorescence Resonance Energy Transfer
h	Hours

HMBC	Heteronuclear Multiple Bond Correlation
HPLC	High Performance Liquid Chromatography
HRMS	High Resolution Mass Spectrometry
HSQC	Heteronuclear Single Bond Correlation
IC <sub>50</sub>	Half maximal inhibitory concentration
IR	Infrared
IRED	Imine Reductase
J	Coupling constant [Hz]
m	Multiplet
m/z	Mass per charge
min	Minutes
mp	Melting Point [°C]
MS	Mass Spectroscopy
NSCLC	Non-Small Cell Lung Cancer
q	Quartet
R <sub>f</sub>	Retention Factor
rt	Room Temperature
s	Singlet
t	Triplet
t <sub>R</sub>	Retention Time [min]
TK	Tyrosine Kinase
TKI	Tyrosine Kinase Inhibitor
TKR	Tyrosine Kinase Receptor
TLC	Thin Layer Chromatography
UV	Ultraviolet
VEGFR	Vascular Endothelial Growth Factor Receptor



# Contents

<b>Abstract</b>	<b>iii</b>
<b>List of Symbols and Abbreviations</b>	<b>iv</b>
<b>List of Tables</b>	<b>ix</b>
<b>List of Figures</b>	<b>xi</b>
<b>Numbered Compounds</b>	<b>xiii</b>
<b>1 Background</b>	<b>1</b>
<b>2 Introduction and Theory</b>	<b>5</b>
2.1 EGFR . . . . .	5
2.2 EGFR-TKI . . . . .	6
2.3 Bioactive thienopyrimidines . . . . .	8
2.4 Bioactive pyrrolidines . . . . .	9
2.5 Biological assay . . . . .	10
2.6 Synthesis and choice of strategy . . . . .	11
2.6.1 Asymmetric synthesis of 2-substituted pyrrolidines . . . . .	11
2.6.2 One-pot synthesis of 2-substituted pyrroline . . . . .	18
2.6.3 Synthetic route for thieno[2,3- <i>d</i> ]pyrimidines . . . . .	19
2.6.4 Nucleophilic aromatic substitution . . . . .	21
2.6.5 Suzuki cross-coupling . . . . .	22
2.6.6 Reductions with NaBH <sub>4</sub> . . . . .	23
<b>3 Results and Discussion</b>	<b>27</b>
3.1 Boc protection . . . . .	28
3.2 One-pot silylation and Grignard . . . . .	28
3.3 Reduction of 2-phenylpyrroline . . . . .	32
3.4 Palladium-catalyzed $\alpha$ -arylation . . . . .	32
3.5 Boc deprotection . . . . .	34
3.6 Chiral resolution of <i>rac</i> -2-phenylpyrrolidine . . . . .	35
3.7 Amination of thienopyrimidines . . . . .	36
3.8 Suzuki cross-coupling . . . . .	37

3.9	Reduction of aldehydes by sodium borohydride . . . . .	39
3.10	<i>In vitro</i> testing of target compounds . . . . .	40
3.11	Compound characterization . . . . .	45
3.11.1	Compound <i>rac</i> - <b>5a</b> . . . . .	49
3.11.2	Compound <b>5b</b> . . . . .	50
3.11.3	Compound <i>rac</i> - <b>6a</b> . . . . .	51
3.11.4	Compound <b>6b</b> . . . . .	52
3.11.5	Compound <i>rac</i> - <b>7a</b> . . . . .	53
3.11.6	Compound <b>7b</b> . . . . .	55
3.11.7	Compound <i>rac</i> - <b>8a</b> . . . . .	56
3.11.8	Compound <b>8b</b> . . . . .	58
<b>4</b>	<b>Concluding Remarks and Further Work</b> . . . . .	<b>59</b>
4.1	Summary . . . . .	59
4.2	Further work . . . . .	60
<b>5</b>	<b>Experimental</b> . . . . .	<b>63</b>
5.1	General . . . . .	63
5.1.1	Separation techniques . . . . .	63
5.1.2	Spectroscopic analysis . . . . .	63
5.1.3	Melting point . . . . .	64
5.1.4	Optical rotation . . . . .	64
5.2	General procedure for $\alpha$ -arylations . . . . .	64
5.3	General procedure for Boc-deprotection . . . . .	65
5.4	General procedure for nucleophilic aromatic substitution . . . . .	65
5.5	General procedure for Suzuki cross-coupling . . . . .	65
5.6	General procedure for reduction using NaBH <sub>4</sub> . . . . .	65
5.6.1	Synthesis of <b>1</b> . . . . .	66
5.6.2	Synthesis of ( <i>R</i> )- <b>3</b> . . . . .	66
5.6.3	Synthesis of ( <i>R</i> )- <b>4</b> . . . . .	66
5.6.4	Synthesis of ( <i>S</i> )- <b>3</b> . . . . .	67
5.6.5	Synthesis of ( <i>S</i> )- <b>4</b> . . . . .	67
5.6.6	Synthesis of <b>2</b> . . . . .	68
5.6.7	Synthesis of <i>rac</i> - <b>4</b> . . . . .	68
5.6.8	Synthesis of <i>rac</i> - <b>5a</b> . . . . .	69
5.6.9	Synthesis of ( <i>R</i> )- <b>5a</b> . . . . .	69
5.6.10	Synthesis of ( <i>S</i> )- <b>5a</b> . . . . .	69
5.6.11	Synthesis of <b>5b</b> . . . . .	70
5.6.12	Synthesis of <i>rac</i> - <b>6a</b> . . . . .	70
5.6.13	Synthesis of ( <i>R</i> )- <b>6a</b> . . . . .	71
5.6.14	Synthesis of ( <i>S</i> )- <b>6a</b> . . . . .	71
5.6.15	Synthesis of <b>6b</b> . . . . .	72
5.6.16	Synthesis of <i>rac</i> - <b>7a</b> . . . . .	72
5.6.17	Synthesis of <i>rac</i> - <b>8a</b> . . . . .	73
5.6.18	Synthesis of ( <i>R</i> )- <b>7a</b> . . . . .	73
5.6.19	Synthesis of ( <i>R</i> )- <b>8a</b> . . . . .	74

---

5.6.20 Synthesis of <b>7b</b> . . . . .	74
5.6.21 Synthesis of <b>8b</b> . . . . .	75
<b>Appendix</b>	<b>i</b>
<b>A Spectroscopic Data - Compound I</b>	<b>iii</b>
<b>B Spectroscopic Data - Compound 2</b>	<b>v</b>
<b>C Spectroscopic Data - Compound (R)-3</b>	<b>vii</b>
<b>D Spectroscopic Data - Compound (S)-3</b>	<b>ix</b>
<b>E Spectroscopic Data - rac-4</b>	<b>xi</b>
<b>F Spectroscopic Data - Compound (R)-4</b>	<b>xiii</b>
<b>G Spectroscopic Data - Compound (S)-4</b>	<b>xv</b>
<b>H Spectroscopic Data - Compound rac-5a</b>	<b>xvii</b>
<b>I Spectroscopic Data - Compound (R)-5a</b>	<b>xxv</b>
<b>J Spectroscopic Data - Compound (S)-5a</b>	<b>xxxiii</b>
<b>K Spectroscopic Data - Compound 5b</b>	<b>xli</b>
<b>L Spectroscopic Data - Compound rac-6a</b>	<b>xlix</b>
<b>M Spectroscopic Data - Dimer by-product</b>	<b>lvii</b>
<b>N Spectroscopic Data - Compound (R)-6a</b>	<b>lix</b>
<b>O Spectroscopic Data - Compound (S)-6a</b>	<b>lxvii</b>
<b>P Spectroscopic Data - Compound 6b</b>	<b>lxxv</b>
<b>Q Spectroscopic Data - Compound rac-7a</b>	<b>lxxxiii</b>
<b>R Spectroscopic Data - Compound (R)-7a</b>	<b>xc i</b>
<b>S Spectroscopic Data - Compound 7b</b>	<b>xcix</b>
<b>T Spectroscopic Data - Compound rac-8a</b>	<b>cvii</b>
<b>U Spectroscopic Data - Compound (R)-8a</b>	<b>cxv</b>
<b>V Spectroscopic Data - Compound 8b</b>	<b>cxxiii</b>



# List of Tables

3.1	Scale, solvent volume, reflux time, stirring apparatus, conversion, and yield of the one-pot synthesis of compound <b>2</b> . . . . .	29
3.2	Scale, reaction time, conversion, and yield for the reduction of compound <b>2</b> to <i>rac</i> - <b>4</b> . . . . .	32
3.3	Optimization of base line separation for the enantiomers of ( <i>R</i> )- and ( <i>S</i> )- <b>3</b> . . . . .	33
3.4	Yields, conversion and reaction times for the synthesis of compounds <b>5a-b</b> . . . . .	37
3.5	Yields, scale, conversion, and reaction times for the synthesis of compounds <b>6a-b</b> and <b>7a-b</b> . . . . .	38
3.6	Yields, scale, conversion, reaction times, and yields for the synthesis of compounds <b>8a-b</b> . . . . .	39
3.7	EGFR inhibitory potency of target compounds . . . . .	41
3.8	EGFR inhibitory potency of reference compounds . . . . .	43
3.9	CSF1R inhibitory potency of reference compounds and target compounds . . . . .	44
3.10	Assigned <sup>1</sup> H and <sup>13</sup> C NMR shifts for compound <i>rac</i> - <b>5a</b> . . . . .	50
3.11	Assigned <sup>1</sup> H and <sup>13</sup> C NMR shifts for compound <b>5b</b> . . . . .	51
3.12	Assigned <sup>1</sup> H and <sup>13</sup> C NMR shifts for compound <i>rac</i> - <b>6a</b> . . . . .	52
3.13	Assigned <sup>1</sup> H and <sup>13</sup> C NMR shifts for compound <b>6b</b> . . . . .	53
3.14	Assigned <sup>1</sup> H and <sup>13</sup> C NMR shifts for compound <i>rac</i> - <b>7a</b> . . . . .	55
3.15	Assigned <sup>1</sup> H and <sup>13</sup> C NMR shifts for compound <b>7b</b> . . . . .	56
3.16	Assigned <sup>1</sup> H and <sup>13</sup> C NMR shifts for compound <i>rac</i> - <b>8a</b> . . . . .	57
3.17	Assigned <sup>1</sup> H and <sup>13</sup> C NMR shifts for compound <b>8b</b> . . . . .	58



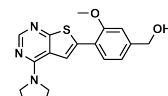
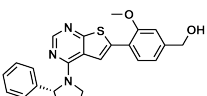
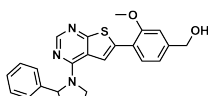
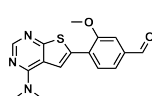
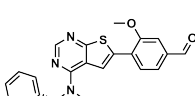
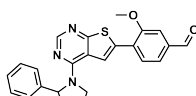
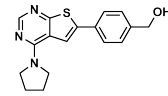
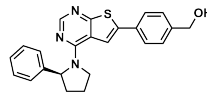
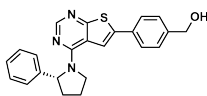
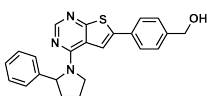
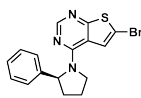
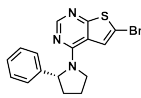
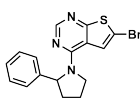
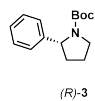
# List of Figures

1.1	Hallmarks of cancer . . . . .	2
1.2	Structure-activity relationship model for thieno[2,3- <i>d</i> ]pyrimidines . . . . .	3
2.1	Activation of receptor tyrosine kinase signalling (TKR) . . . . .	6
2.2	Blocking of receptor tyrosine kinase (TKR) signalling by use of tyrosine kinase inhibitor (TKI) . . . . .	7
2.3	Structures of some different generation EGFR-TKIs . . . . .	8
2.4	Structures of potent thienopyrimidine-based EGFR inhibitors . . . . .	9
2.5	Structures of some natural products, pharmaceuticals, and bioactive compounds with substituted pyrrolidine as a structural unit. . . . .	10
2.6	Biochemical assay of kinase inhibitors . . . . .	11
3.1	Structures of new thieno[2,3- <i>d</i> ]pyrimidines . . . . .	27
3.2	By-products in the <sup>1</sup> H NMR of crude compound <b>2</b> . . . . .	30
3.3	Illustration of the two rotamers of ( <i>R</i> )- <b>3</b> . . . . .	33
3.4	Temperature gradient <sup>1</sup> H NMR of ( <i>R</i> )- <b>3</b> . . . . .	34
3.5	<sup>19</sup> F NMR of ( <i>S</i> )- <b>4</b> . . . . .	35
3.6	IC <sub>50</sub> -curves for compounds ( <i>R</i> )- and ( <i>S</i> )- <b>6a</b> , and ( <i>R</i> )- <b>8a</b> . . . . .	42
3.7	General numbering of positions in compounds <b>5-8</b> . . . . .	46
3.8	HMBC coupling in compound <b>6b</b> . . . . .	47
3.9	HMBC coupling in <i>rac</i> - <b>4</b> . . . . .	48
3.10	HMBC couplings in compounds <b>6-8</b> . . . . .	48
3.11	COSY couplings in compounds <b>6a-b</b> , and <b>8a-b</b> . . . . .	49
3.12	Numbering of positions in compound <i>rac</i> - <b>5a</b> . . . . .	49
3.13	Numbering of positions in compound <b>5b</b> . . . . .	51
3.14	Numbering of positions in compound <i>rac</i> - <b>6a</b> . . . . .	52
3.15	Numbering of positions in compound <b>6b</b> . . . . .	53
3.16	Numbering of positions in compound <i>rac</i> - <b>7a</b> . . . . .	54
3.17	Numbering of positions in compound <b>7b</b> . . . . .	56
3.18	Numbering of positions in compound <i>rac</i> - <b>8a</b> . . . . .	57
3.19	Numbering of positions in compound <b>8b</b> . . . . .	58





# Numbered Compounds





# 1 | Background

Cancer is one of the leading causes of death globally, as an affliction with high prevalence and mortality rates.<sup>[1]</sup> Three decades of research into the mechanisms of cancer pathogens have led to the development of molecular targeted cancer therapy: the use of drugs or other substances to target specific biomacromolecules involved in the growth and spread of cancer.<sup>[2,3]</sup> Despite major advances in cancer therapy and drug development, targeted cancer therapy is inevitably challenged by drug resistance. As drug resistance is almost invariably succeeded by disease progression, the development of new anti-cancer agents remains an important objective in targeted cancer therapy.<sup>[4]</sup>

The growing arsenal of targeted anti-cancer agents can be categorized according to their respective effect on one or more hallmarks of cancer, as illustrated in Figure 1.1.<sup>[5]</sup> Sustained proliferative signalling is one such trait, allowing malignant cells to maintain constant growth by avoiding growth suppression.<sup>[6]</sup> Inhibition of sustained proliferative signalling may be done by use of tyrosine kinase inhibitors (TKIs), as for instance by targeting the epidermal growth factor receptor (EGFR). This treatment is primarily associated with lung-, breast-, and pancreatic cancer, with commercially available drugs like Erlotinib and Gefitinib.<sup>[7,8]</sup>

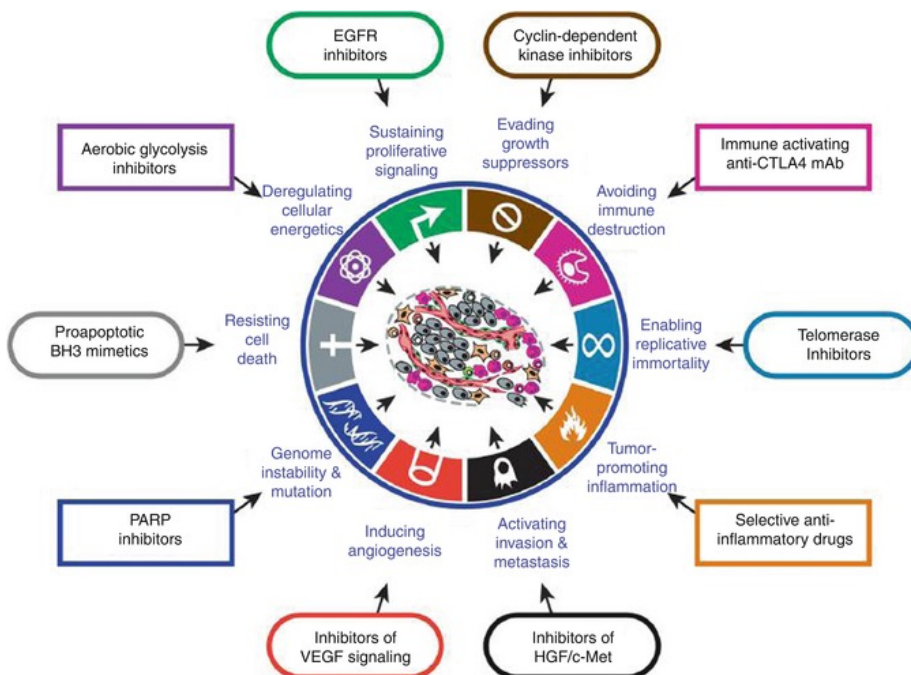


**Figure 1.1:** The hallmarks of cancer form the basis of contemporary drug development and targeted anti-cancer treatment.<sup>[5]</sup>

The Hoff/Sundby research group has focused on developing thieno-, pyrrolo-, and furo-pyrimidines as new EGFR-TKIs for use as anti-cancer agents. This work has resulted in a number of structure-activity studies, identifying several compounds with activity in the nanomolar range.<sup>[9–11]</sup> A biological assay of the purine TIA02-176 (Aarhus, Sundby, Hoff, work in progress), illustrated in Figure 1.2, found this compound to possess excellent EGFR-TK activity. Previous structure-reactivity studies on thieno[2,3-*d*]pyrimidines by Bugge, et al.,<sup>[11]</sup> have found that a secondary amine at C-4 is essential for the EGFR-TK activity, as illustrated in Figure 1.2. Preliminary results in the research group indicate that this is not necessarily the case.

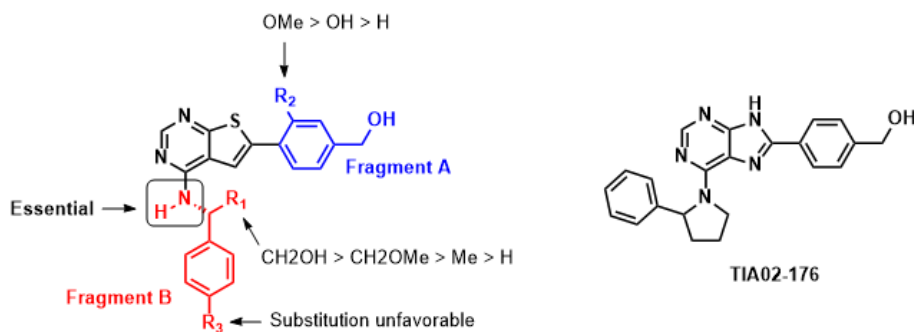


**Figure 1.2:** Structure-activity relationship model for thieno[2,3-*d*]pyrimidines.

The aim of this master's thesis was to perform a preliminary structure-activity relationship (SAR) study of thieno[2,3-*d*]pyrimidines with racemic and enantioenriched 2-phenyl-pyrrolidine as a substituent on C-4. An objective was investigate if secondary amines are essential substituents at C-4 by preparing thieno[2,3-*d*]pyrimidines with a tertiary heterocyclic amine. Compounds with pyrrolidine as a C-4 substituent were also investigated, to study the contribution of the phenyl moiety on the amine on the EGFR-TK activity. All amines and thieno[2,3-*d*]pyrimidines were synthesized as part of this project, and a secondary objective of this master's thesis was to investigate viable synthetic routes to obtain enantioenriched 2-phenylpyrrolidine with high chemical and enantiopurity.



## 2 | Introduction and Theory

### 2.1 EGFR

The epidermal growth factor receptor (EGFR, also known as ErbB-1/HER1) is a transmembranal protein belonging to the ErbB class of receptor tyrosine kinases (TKR).<sup>[12]</sup> The EGFR consists of an intracellular tyrosine kinase domain, a transmembrane lipophilic domain, and an extracellular ligand-binding domain which will bind to receptor-specific ligands.<sup>[13]</sup> The EGFR, along with other tyrosine kinase receptors, including vascular endothelial growth factor receptors (VGEFR) and fibroblast growth factor receptors (FGFR), play a key role in regulating cellular processes such as cellular growth, differentiation and metabolism.<sup>[14]</sup>

Activation of the EGFR, illustrated in Figure 2.1, occur by binding of receptor-specific polypeptide ligands (growth factors) to the extracellular domain of the receptors. This induces receptor dimerization, forming homo- or heterodimeric receptor complexes, which leads to activation of the tyrosine kinase domain by phosphorylation of specific tyrosine residues.<sup>[12,14,15]</sup> These residues serve as docking sites for proteins containing specific domains, including the phosphotyrosine binding domain.<sup>[12]</sup> The introduction of these proteins leads to activation of the intracellular signalling pathways.

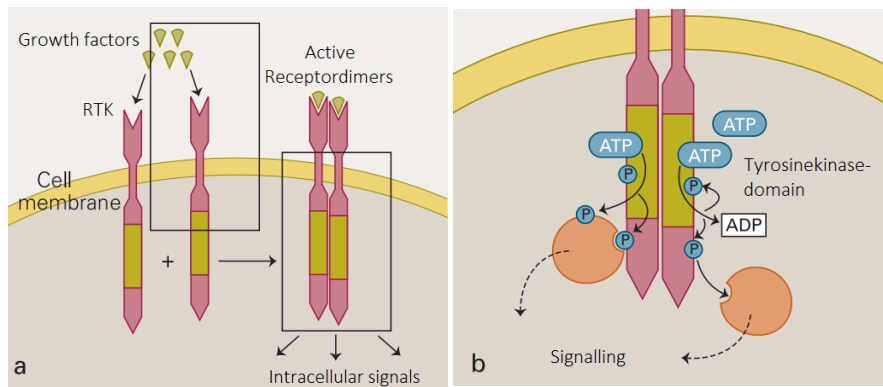


**Figure 2.1:** Activation of intracellular signalling of receptor tyrosine kinase (TKR). Binding of growth factors (a) induces receptor dimerization, which leads to activation of the tyrosine kinase domain by autophosphorylation (b).<sup>[16]</sup>

## 2.2 EGFR-TKI

Overexpression of the EGFR is associated with a variety of malignancies, including lung, breast and pancreatic cancer.<sup>[17]</sup> Aberrant activity of these receptors has been shown to play a key role in the development of tumor cells, making these receptors attractive targets in targeted cancer therapy.<sup>[18]</sup>

Several approaches have been developed for targeting, and inhibiting the EGFR signalling pathways, including the use of monoclonal anti-EGFR antibodies and recombinant proteins.<sup>[18]</sup> The use of tyrosine kinase inhibitors (TKI) as small, adenine triphosphate (ATP) analogues, has proven effective against human EGFR, and is now a standard clinical treatment for patients with advanced EGFR mutant non-small-cell lung cancer.<sup>[19]</sup> These molecules work by binding to the ATP binding sites on the tyrosine kinase domain, thus preventing autophosphorylation and activation of further downstream signalling pathways (as illustrated in Figure 2.2).<sup>[18]</sup>



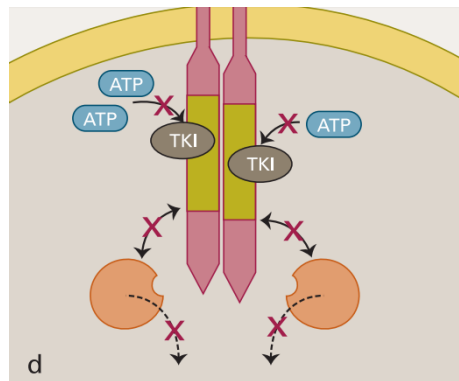


**Figure 2.2:** Blocking of the intracellular signalling of receptor tyrosine kinase (TKR) by use of a tyrosine kinase inhibitor (TKI).<sup>[16]</sup>

Several EGFR-TKIs are approved for therapeutic use worldwide, including Erlotinib, Gefitinib, and Afatinib for the treatment of non-small cell lung cancer (NSCLC) harbouring EGFR mutations (Figure 2.3).<sup>[20]</sup> Erlotinib and Gefitinib are first-generation EGFR-TKIs and act to block autophosphorylation and activation of downstream signalling. Unfortunately, most patients with EGFR-mutant NSCLC treated with EGFR-TKIs develop resistance within 9-14 months, and second-generation EGFR-TKIs, such as Afatinib, has therefore been developed to overcome the acquired resistance of the first-generation EGFR-TKIs.<sup>[21]</sup> Afatinib is an irreversible EGFR-TKI, unlike the reversible Erlotinib and Gefitinib, and acts to block the enzymatic activity of active ErbB receptor family members by forming irreversible covalent bonds. These bonds can inhibit the kinase activity until new receptors are formed, which may give longer action time of Afatinib compared to reversible EGFR-TKIs.<sup>[20]</sup> New generations of EGFR-TKIs continue to appear with the development of third-generation EGFR-TKIs (Osimertinib, Olmutinib)<sup>[22]</sup> to combat mutations altering the EGFR affinity for ATP (e.g. T790M mutation), and fourth-generation inhibitors (EAI045)<sup>[23]</sup> to battle mutations preventing irreversible EGFR-TKIs from forming covalent bonds (e.g. C797S mutation).<sup>[20]</sup>

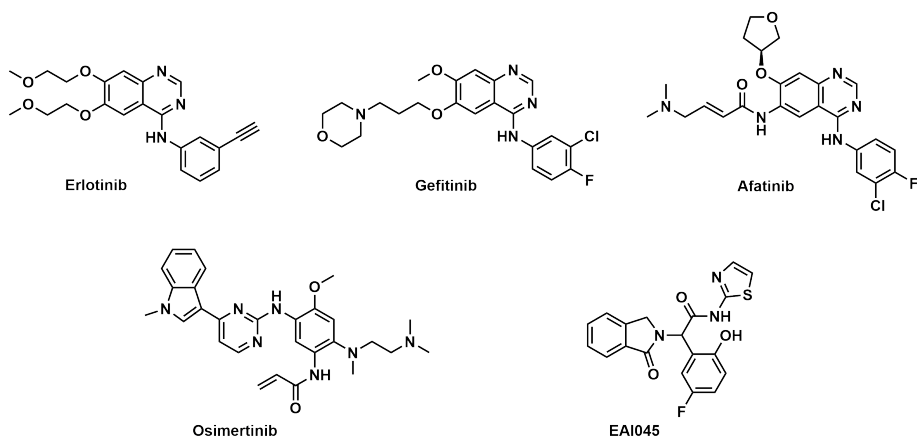


**Figure 2.3:** Structures of some different generation EGFR-TKIs: Erlotinib (first generation), Gefitinib (first generation), Afatinib (second generation), Osimertinib (third generation), EAI045<sup>[24]</sup> (fourth generation).

## 2.3 Bioactive thienopyrimidines

Thienopyrimidines are heterocycles with a large diversity in bioactivity, and derivatives of these compounds have been found to possess antimicrobial-,<sup>[25]</sup> antitubercular-,<sup>[26]</sup> antiviral-,<sup>[27]</sup> anti-inflammatory-,<sup>[28]</sup> and anti-tumour<sup>[29]</sup> activity.

The use of thienopyrimidines as EGFR kinase inhibitors can be traced back to the 1990s, as scaffold hopping of quinazolines and pyrrolopyrimidines found thienopyrimidines to be potent EGFR-TKIs.<sup>[30,31]</sup> The recent years have seen a growing interest in thienopyrimidines, as a number of potent thienopyrimidine-based EGFR inhibitors have been published (Figure 2.4).<sup>[11,32,33]</sup> However, to the best of the author's knowledge, as of June 2018, the only thienopyrimidine-based EGFR-TKI to be approved for therapeutic use is Olmutinib (approved in South Korea in 2016<sup>[34]</sup>).<sup>[24,35]</sup>

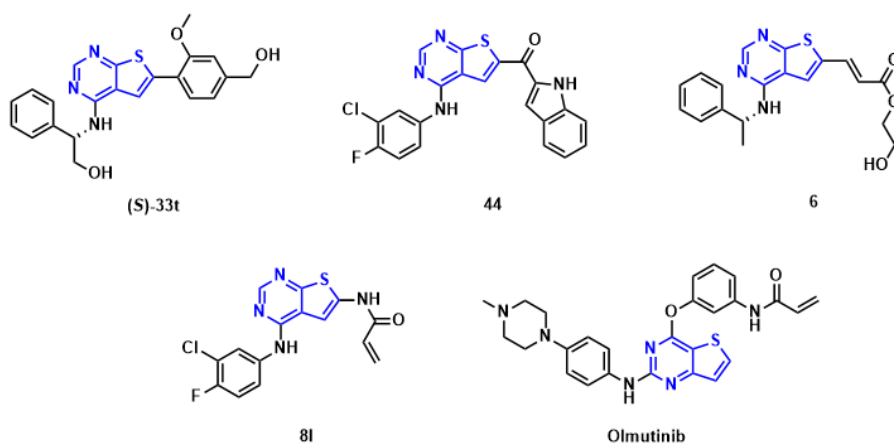


**Figure 2.4:** Structures of potent thienopyrimidine-based EGFR inhibitors, (S)-33t,<sup>[11]</sup> 44,<sup>[32]</sup> 6,<sup>[33]</sup> 8l,<sup>[36]</sup> Olmutinib.<sup>[37]</sup>

## 2.4 Bioactive pyrrolidines

*N*-Heterocycles are important structural units in many biologically active compounds, and are attractive scaffolds in pharmaceutical development.<sup>[38]</sup> Substituted pyrrolidines are found in a large array of natural products, pharmaceuticals, and bioactive compounds (Figure 2.5). Some examples are Nicotine; alkaloid found in the nightshade family of plants (Solanaceae),<sup>[39]</sup> Kainic acid; naturally occurring neurotoxin isolated from seaweed (*Digenea simplex*),<sup>[40]</sup> Vildagliptin; an oral anti-diabetic drug,<sup>[41]</sup> Anisomycin; antibiotic inhibiting protein synthesis,<sup>[42]</sup> and Kaitocephalin; a glutamate receptor antagonist.<sup>[43]</sup>

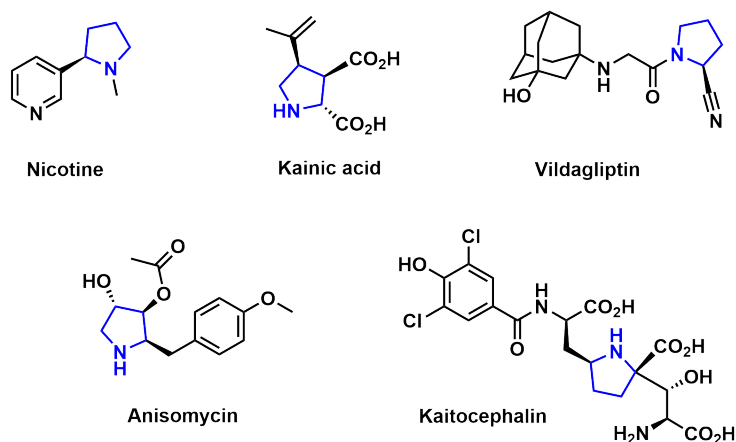


**Figure 2.5:** Structures of some natural products, pharmaceuticals, and bioactive compounds with substituted pyrrolidine as a structural unit.

## 2.5 Biological assay

Biological tests of the target compounds in this project have been done by Invitrogen, using the Z'-LYTE<sup>®</sup> biochemical assay. This assay employs a fluorescence-based, coupled-enzyme format in which the peptide substrate is labeled with two fluorophores, one at each end.<sup>[44]</sup> As illustrated in Figure 2.6, this allows for intramolecular fluorescence resonance energy transfer (FRET) from the donor to the acceptor fluorophore, thus referred to as a FRET pair.<sup>[45]</sup> In this process, the excited donor fluorophore (e.g. Coumarin) transfers its excitation energy non-radiatively to the acceptor fluorophore (e.g. Fluorescein), thus causing the acceptor fluorophore to emit its characteristic fluorescence.<sup>[45]</sup>

During testing, the kinase transfers the gamma-phosphate of ATP to a single tyrosine residue in a synthetic FRET-peptide.<sup>[44]</sup> In the case of a good kinase inhibitor the phosphate transfer is counteracted, yielding more non-phosphorylated peptide, as illustrated in Figure 2.6. In the following step, a site-specific protease recognizes and cleaves only the non-phosphorylated peptides, as phosphorylation suppresses cleavage by the Development Reagent.<sup>[44]</sup> The cleavage disrupts the FRET of the non-phosphorylated peptides, while FRET of the phosphorylated peptides is maintained.<sup>[44]</sup> This yields highly fluorescent cleaved peptide fragments and uncleaved FRET-peptides, both contributing to the fluorescence signals, as illustrated in Figure 2.6. Detection of the fluorescence signals gives the emission ratio as the ratio of donor emission to acceptor emission.<sup>[44]</sup> High emission ratio indicates larger amounts of non-phosphorylated FRET-peptide, hence better kinase inhibition.

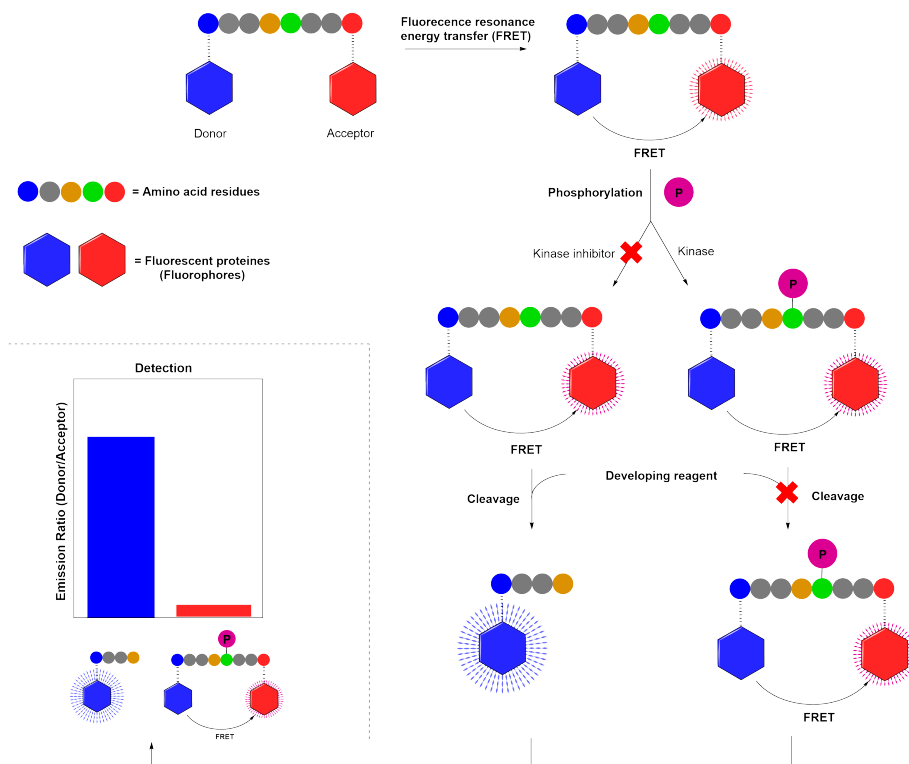


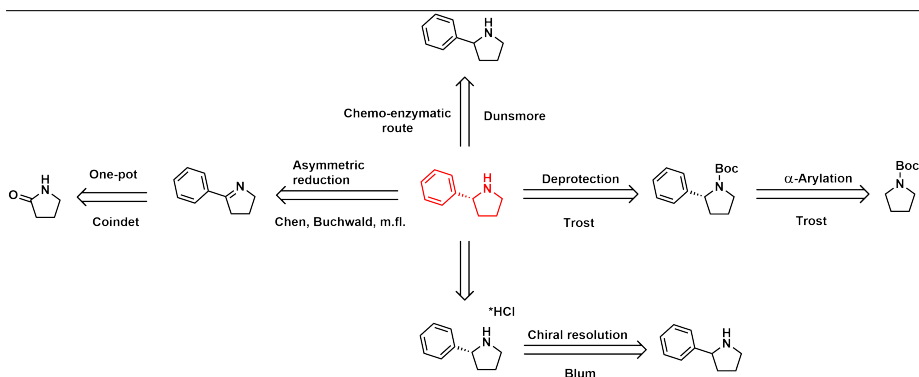
Figure 2.6: Biochemical assay of kinase inhibitors by use of the Z'-LYTE<sup>®</sup> biochemical assay.

## 2.6 Synthesis and choice of strategy

### 2.6.1 Asymmetric synthesis of 2-substituted pyrrolidines

The term *asymmetric synthesis* is used of “a chemical reaction (or reaction sequence) in which one or more new elements of chirality are formed in a substrate molecule and which produces the stereoisomeric (enantiomeric or diastereoisomeric) products in unequal amounts.” (IUPAC def.<sup>[46]</sup>). As pyrrolidines are important precursors to biologically active compounds, asymmetric synthesis of these compounds is well documented, with possible synthetic routes including cycloaddition,<sup>[47,48]</sup> intramolecular addition of nucleophiles into imines,<sup>[49,50]</sup> and the reaction of organic azides with alkylidifluoroborane intermediates.<sup>[51]</sup>

The 2-substituted pyrrolidines (*R*)- and (*S*)-**4** have previously been prepared by asymmetric synthesis, employing a variety of synthetic routes.<sup>[52–55]</sup> Scheme 2.6.1 illustrates a selection of possible synthetic routes to (*R*)-**4**, of which the  $\alpha$ -arylation and chiral resolution routes are employed in this master’s thesis.



**Scheme 2.6.1:** Retrosynthetic analysis of (*R*)-2-phenylpyrrolidine ((*R*)-**4**). References: Trost *et al.*,<sup>[52]</sup> Dunsmore *et al.*,<sup>[53]</sup> Blum *et al.*,<sup>[54]</sup> Chen *et al.*,<sup>[55]</sup> Buchwald *et al.*,<sup>[56]</sup> Coindet *et al.*<sup>[57]</sup>

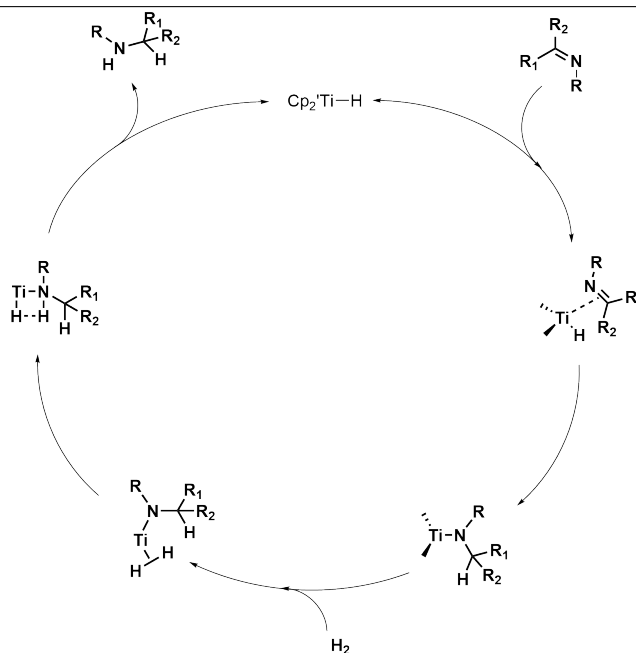
### Asymmetric hydrogenation

Asymmetric hydrogenation, or asymmetric reduction, is widely regarded as a highly efficient method for obtaining optically active amines.<sup>[55,58,59]</sup> The development of the technique originated in 1968,<sup>[60,61]</sup> and was pioneered by William S. Knowles<sup>[62]</sup> and Ryoji Noyori,<sup>[63]</sup> for which they were both rewarded with the Nobel Prize in Chemistry 2001.

Enantioselective asymmetric hydrogenation allows for selective generation of chiral centres by use of specially designed catalysts, thus providing the possibility of synthesizing optically active 2-substituted pyrrolidines from cyclic imines. The hydrogenation of compound **2** to form (*R*)- or (*S*)-**3** or **4** has already been investigated, and some known catalysts for these reactions includes Ru-,<sup>[55]</sup> Ti-,<sup>[56,64–66]</sup> and Ir-based catalysts.<sup>[67–69]</sup> Amine compounds are known to have a deleterious effect on the performance of both heterogeneous<sup>[70]</sup> and homogeneous<sup>[71]</sup> hydrogenation systems, and in-situ protection of the resulting 2-substituted pyrrolidine compound has therefore been found to be favourable to reduce the potential for product inhibition.<sup>[55,72,73]</sup> The synthesis of (*R*)-**3** from **2** was planned as a synthetic route in this master project.

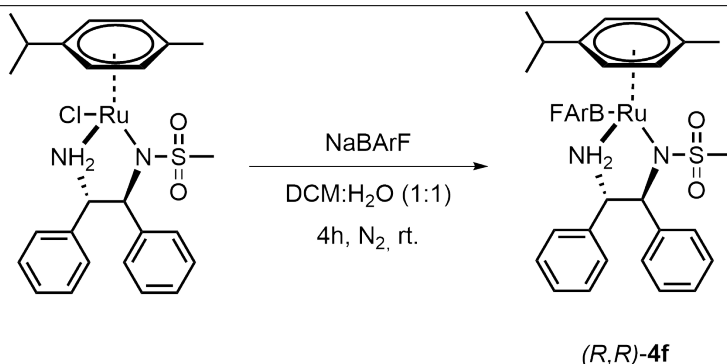
Several mechanistic studies on asymmetric hydrogenation of cyclic amines have been conducted in an attempt to understand how the substrate coordinates to the metal center of the catalysts, and how hydrogen is transferred to the C=N.<sup>[56,65,74]</sup> A proposed catalytic cycle by Willoughby & Buchwald, using a chiral titanocene catalyst,<sup>[75]</sup> suggests a mechanism in which the imine reacts with a titanium hydride in a fast 1,2-insertion step, forming a titanium amide intermediate. This is followed by a slow reaction of the amide complex with hydrogen to produce the amine, which also regenerates the titanium hydride.<sup>[56]</sup> Later studies have found the formation of a dihydrido complex containing the imine, coordinated via the nitrogen atom, to play a key role in this catalytic cycle.<sup>[74]</sup> The proposed catalytic cycle for asymmetric

hydrogenation of cyclic amines is illustrated in Scheme 2.6.2. The mechanisms for reactions involving rhodium-, irridium-, and ruthenium-complexes are still under investigation.<sup>[55,76]</sup>



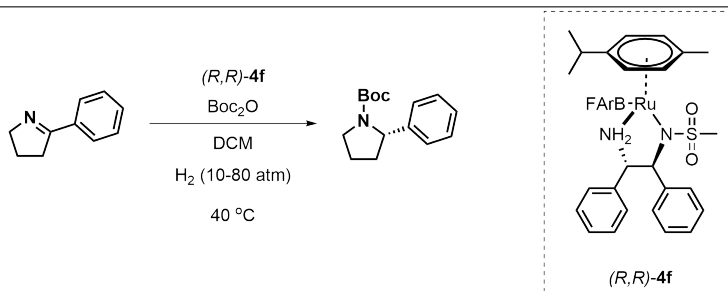
**Scheme 2.6.2:** Proposed catalytic cycle for the hydrogenation of cyclic amines, using a chiral titanocene catalyst.<sup>[56,65,74]</sup>

Despite the simplicity, good atom economy, and environmental friendliness of these reactions, enantioselective asymmetric hydrogenation reactions possess some practical limitations.<sup>[77]</sup> The specialized metal catalysts are often hard to obtain due to scarcity of the metals, patent-protected syntheses, and the high cost associated with them. The chosen ruthenium-based catalyst for the synthesis of (*R*)-**3**,  $[\text{RuBARF}(p\text{-cymene})(R,R)\text{-MsDPEN}]$ ,<sup>[55]</sup> could be prepared from the precursor  $[\text{RuCl}(p\text{-cymene})(R,R)\text{-MSDPEN}]$ , by undergoing a simple ligand-exchange, as illustrated in Scheme 2.6.3.<sup>[78]</sup>



**Scheme 2.6.3:** Preparation of  $[\text{RuBArF}(p\text{-cymene})(R,R)\text{-MsDPEN}]$  ( $(R,R)$ -**4f**)<sup>[55]</sup> from  $[\text{RuCl}(p\text{-cymene})(R,R)\text{-MSDPEN}]$ .<sup>[78]</sup>

The following synthesis of  $(R)$ -**3**, employing catalyst  $(R,R)$ -**4f**, utilizes pressurized  $\text{H}_2$  at 10-80 atm. and 40 °C, as presented in Scheme 2.6.4.<sup>[55]</sup> Due to technical restrictions,  $\text{H}_2$  at this pressure proved difficult to obtain. It may be possible to run the synthesis at lower hydrogen pressure, as the enantioselectivity is reportedly insensitive to changes in pressure.<sup>[55,56]</sup> However, along with difficulties obtaining the precursor for catalyst  $R,R$ -**4f** and time constraints, this reaction was ultimately not attempted.



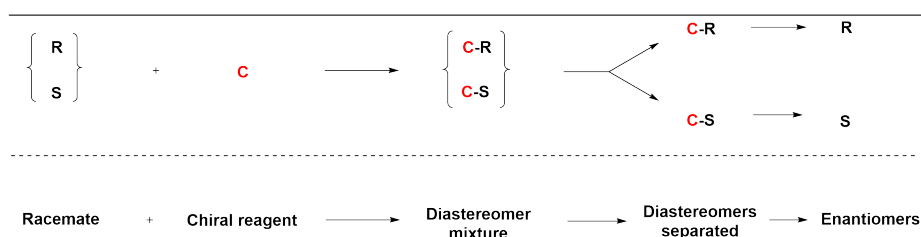
**Scheme 2.6.4:** Enantioselective asymmetric hydrogenation of **2** to  $(R)$ -**3**, using  $(R,R)$ -**4f** as the catalyst.<sup>[55]</sup>

### Chiral resolution

Chiral resolution is a process in which a racemic compound is separated into its enantiomers, and is still an important tool for obtaining enantiopure products.<sup>[79,80]</sup> A downside of chiral resolution of racemates, compared to other asymmetric syntheses, is that a maximum yield of 50 % of the desired product can be obtained, with another 50 % being the undesired enantiomer.

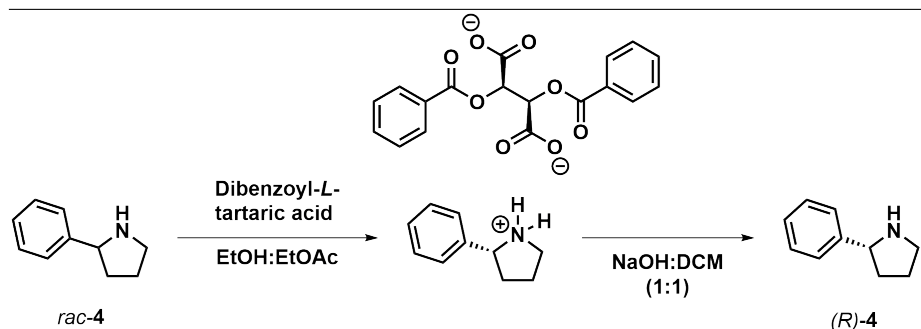


Separation of enantiomers in a racemate may be achieved by reaction with enantio-pure chiral reagents, such as chiral acids or bases, to form a mixture of diastereomer intermediates.<sup>[54]</sup> Whereas the enantiomers are identical, the diastereomers may possess different chemical and physical properties and can be separated, as illustrated in Scheme 2.6.5. It is possible to also exploit the difference in reaction rates of enantiomers with chiral reagents in so-called kinetic resolution: one of the enantiomers reacts more rapidly, thus leaving an excess of the other enantiomers behind.<sup>[81]</sup> A widely utilized version of kinetic resolution is enzymatic kinetic resolution, employing biocatalysts, especially hydrolytic enzymes, to achieve high enantioselectivity and good yields.<sup>[82]</sup> A third method is the use of preparatory chromatography, such as chiral stationary phase HPLC (CSP-HPLC). For CSP-HPLC, the stationary phase is a chiral reagent that adsorbs one enantiomer more strongly than the other, allowing for direct separation of the enantiomers from the racemate.<sup>[83–85]</sup>



**Scheme 2.6.5:** Chiral resolution of a racemate by formation and separation of diastereomers.

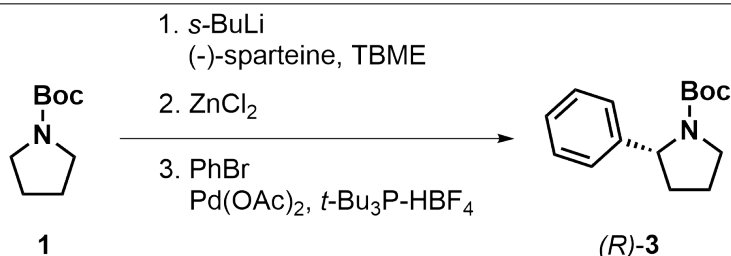
Chiral resolution of *rac*-**4** to (*R*)-**4** has been reported by using dibenzoyl-*L*-tartaric acid as a chiral acid.<sup>[54]</sup> The (*R*)-enantiomer precipitates in the solution as a salt, allowing for recrystallization and removal of the salt for the formation of enantiopure (*R*)-**4**. To achieve high ee, the enantioenriched salt is submitted to sequential recrystallizations, with each cycle increasing the ee of the final product. Scheme 2.6.6 illustrates the chiral resolution of *rac*-**4** to (*R*)-**4**. Synthesis of the (*S*)-enantiomer is possible by substituting the chiral acid for dibenzoyl-*D*-tartaric acid.



**Scheme 2.6.6:** Chiral resolution of *rac*-**4** to (*R*)-**4** by crystallization with dibenzoyl-*L*-tartaric acid.<sup>[54]</sup>

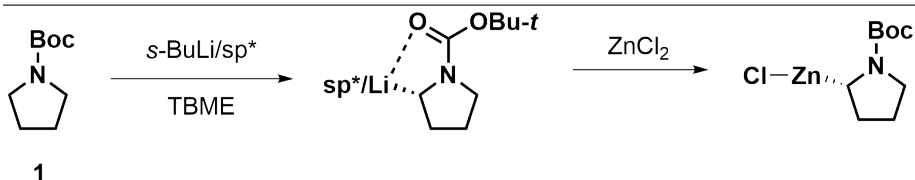
**$\alpha$ -Arylation**

An effective synthesis of 2-substituted pyrrolidines is the enantioselective, palladium-catalyzed  $\alpha$ -arylation of *N*-Boc-pyrrolidine, illustrated in Scheme 2.6.7.<sup>[52,86]</sup> The reaction proceeds via an in-situ generated 2-pyrrolidinozinc reagent, allowing for a direct palladium-catalyzed arylation from **1** to (*R*)- or (*S*)-**3**. What makes this procedure favourable is that it provides a more direct route to enantioenriched 2-arylpyrrolidines, compared to longer synthetic routes,<sup>[87]</sup> while maintaining good yields and excellent enantiomeric excess.<sup>[86]</sup>



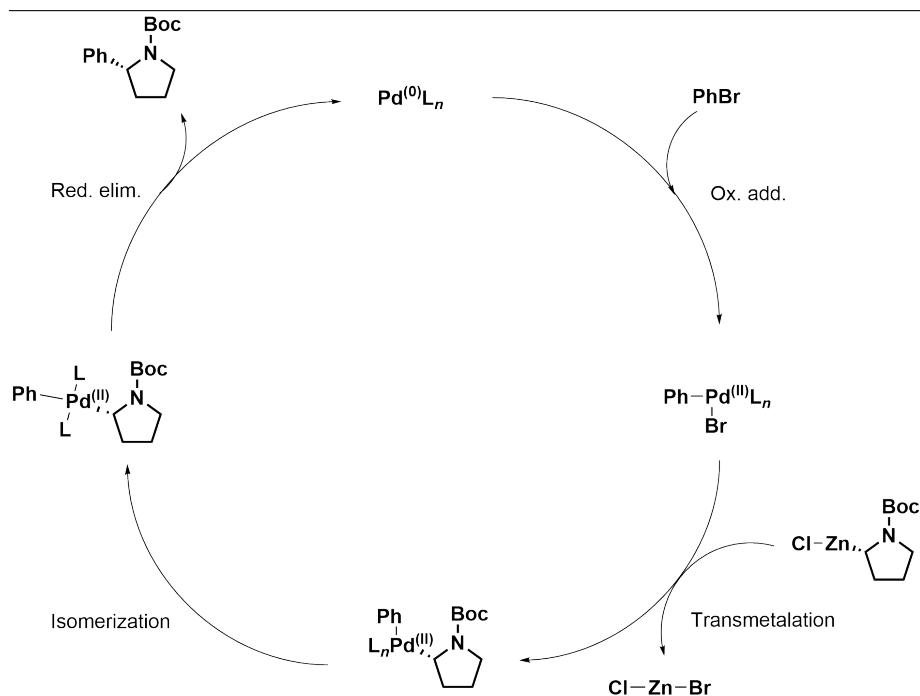
**Scheme 2.6.7:** Enantioselective, palladium-catalyzed  $\alpha$ -arylation of *N*-boc-pyrrolidine to (*R*)-**3**.<sup>[52,86]</sup>

This methodology is based on Beak's sparteine-mediated, enantioselective deprotonation and lithiation of *N*-boc-pyrrolidine to form 2-pyrrolidinolithium compounds in high enantioselectivity.<sup>[88]</sup> The lithiation is followed by transmetalation with ZnCl<sub>2</sub> to generate a stereochemically rigid 2-pyrrolidinozinc reagent, which is coupled with aryl bromide in a Pd-catalyzed Negishi coupling.<sup>[86,89]</sup> Scheme 2.6.8 illustrates the enantioselective, sparteine mediated deprotonation and lithiation of *N*-Boc-pyrrolidine, followed by generation of the 2-pyrrolidinozinc reagent.



**Scheme 2.6.8:** Enantioselective, (-)-sparteine mediated deprotonation and lithiation of **1**. Transmetalation with ZnCl<sub>2</sub> generates the stereochemically rigid 2-pyrrolidinozinc.<sup>[86,89-91]</sup>

The lithiation is the enantiodiscriminating step of this synthesis, and thus the final enantiomeric excess is independent of the aryl bromide utilized in the Negishi-coupling.<sup>[52,89,91]</sup> Scheme 2.6.9 presents the catalytic cycle for the Negishi-coupling of this synthesis. The potential for  $\beta$ -H elimination in this catalytic Negishi cycle has been evaluated, and found products resulting from this pathway to be less than 8%.<sup>[86]</sup>

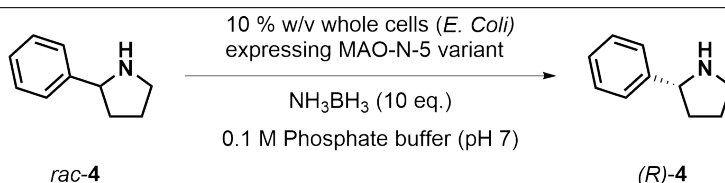


**Scheme 2.6.9:** Catalytic cycle for the transmetalation and Negishi-coupling in the one-pot  $\alpha$ -arylation from **1** to (*R*)-**3**.<sup>[92]</sup>

### Chemo-enzymatic route

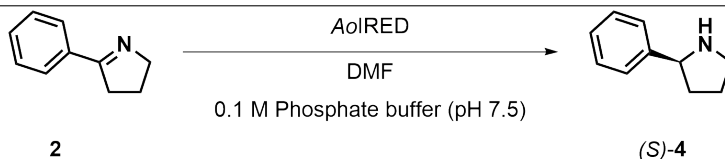
The utilization of both chemical and biological approaches combined, have proven to be powerful tools for organic synthesis and has long been a topic of interest in asymmetric synthesis.<sup>[93,94]</sup> Such reactions combine the flexibility of chemical synthesis with the selectivity and efficiency of enzymatic methods, which also makes for “greener” synthesis by reducing downstream processing steps and allowing for potential in-situ regeneration of expensive co-factors.<sup>[93,95]</sup>

Several approaches have been suggested for chemo-enzymatic synthesis of cyclic amines, including asymmetric synthesis with transaminase,<sup>[96]</sup> deracemization with monoamine oxidase,<sup>[97]</sup> kinetic resolution with hydrolase,<sup>[98]</sup> and imine reductase.<sup>[99]</sup> Chemo-enzymatic deracemization of *rac*-**4** to (*R*)-**4** has been reported, using the specific monoamine oxidase Ile246Met/Asn336Ser/Met348Lys/Thr384Asn/Asp385Ser (MAO-N-5) from *Aspergillus niger*. The process proceeds via a two-step, one-pot synthesis, in which the enzyme oxidizes only the (*S*)-enantiomer to the corresponding imine. The imine is reduced in-situ back to the racemic amine, with repeated cycles accumulating (*R*)-**4** in high yield and enantiomeric excess.<sup>[53]</sup> Scheme 2.6.10 presents this reaction.



**Scheme 2.6.10:** Chemo-enzymatic deracemization of *rac-4* to *(R)-4*, by use of the enzyme Ile246Met/ Asn336Ser/Met348Lys/Thr384Asn/Asp385Ser (MAO-N-5) from *Aspergillus niger*.<sup>[53]</sup>

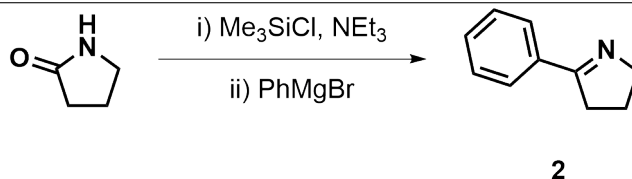
The direct reduction of prochiral imines is possible by NAD(P)H-dependent oxidoreductases, termed imine reductase (IRED). Reduction of **2** to *(S)-4* has been reported using *AoIRED* from *Amycolatopsis orientalis* (Uniprot R4SNK4), with ee's up to 95%.<sup>[100]</sup> The mechanism of IRED is not well understood, and it appears that the use of different oxidoreductases changes the mechanistic pathways as these employ different amino acid residues within the active site for substrate recognition.<sup>[100]</sup> Scheme 2.6.11 illustrates the imine reductase of **2** to *(S)-4* by *AoIRED*.



**Scheme 2.6.11:** Imine reductase (IRED) of **2** to *(S)-4*, using *AoIRED* from *Amycolatopsis orientalis* (Uniprot R4SNK4).<sup>[100]</sup>

## 2.6.2 One-pot synthesis of 2-substituted pyrroline

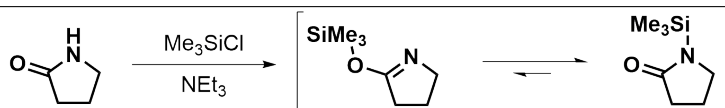
Compound **2** can be synthesized from pyrrolidin-2-one in a two-step, one-pot reaction, starting with the protection of the amine by silylation, followed by a Grignard reaction.<sup>[57]</sup> Scheme 2.6.12 illustrates this reaction.



**Scheme 2.6.12:** Two-step, one-pot synthesis of **2** from pyrrolidin-2-one.<sup>[57]</sup>

Trimethylsilyl chloride may be used as the silylating agent, which acts as both a protecting group in the first reaction step, and a leaving group in the second step.<sup>[57]</sup> The

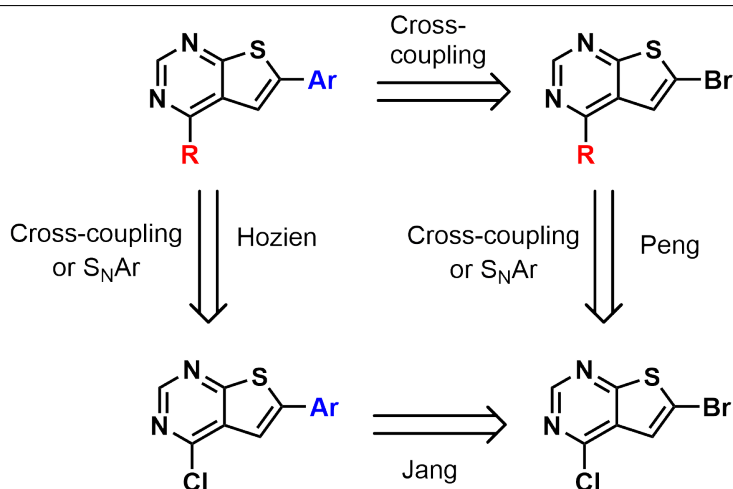
silyl group is predominantly located on the amine with some protection of the ketone group, as illustrated in Scheme 2.6.13.<sup>[57]</sup> Formation of **2** occur by a spontaneous de-protection, allowing for the formation of the double bond in the pyrroline moiety.



**Scheme 2.6.13:** Blocking of pyrrolidin-2-one with a trimethylsilyl group gives two products. The silyl group is predominantly located on the amine.<sup>[57]</sup>

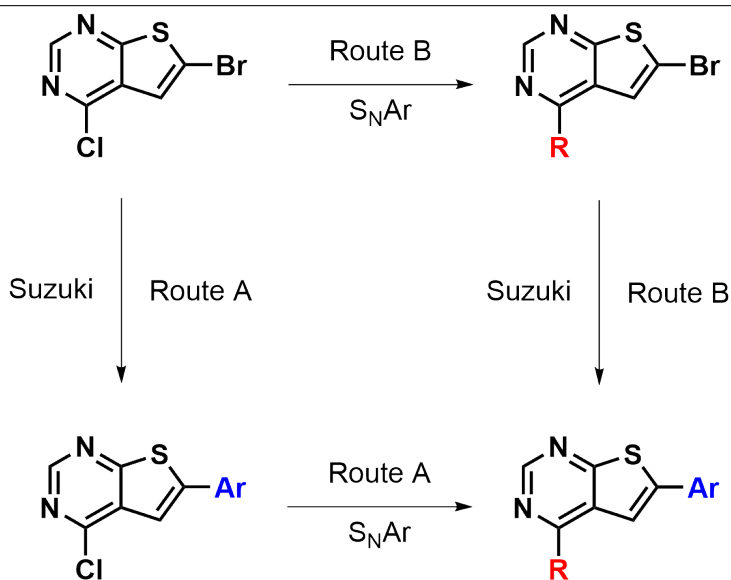
### 2.6.3 Synthetic route for thieno[2,3-*d*]pyrimidines

Synthetic routes for preparing thieno[2,3-*d*]pyrimidines have been thoroughly investigated by Bugge.<sup>[101]</sup> A retrosynthetic analysis with 6-bromo-4-chlorothieno[2,3-*d*]pyrimidine as the initial core, illustrated in Scheme 2.6.14, found nucleophilic aromatic substitution and Suzuki cross-coupling reactions to be viable options for the synthetic route of target structures **6-8**.



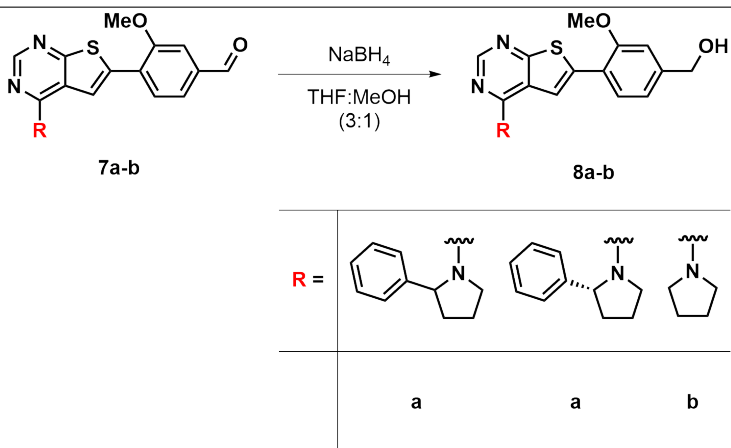
**Scheme 2.6.14:** Retrosynthetic analysis with 6-bromo-4-chlorothieno[2,3-*d*]pyrimidine as the initial core. References: Hozien *et al.*,<sup>[102]</sup> Peng *et al.*<sup>[103]</sup>

Scheme 2.6.15 presents two synthetic routes, A and B, to the target structures. On similar structures, it has been found that nucleophilic aromatic substitution, followed by Suzuki cross-coupling (route B) was the most efficient synthetic route, due to low selectivity or incomplete conversion of route A. Route B was found to circumvent the selectivity issues, and also gave the highest overall yields.<sup>[101]</sup>



**Scheme 2.6.15:** Two possible routes, A and B, from 6-bromo-4-chlorothieno[2,3-*d*]pyrimidine to the target structures.

The reduction of aldehydes **7a-b** to the corresponding primary alcohols **8a-b**, illustrated in Scheme 2.6.16, was done using sodium borohydride ( $\text{NaBH}_4$ ) in THF:MeOH (3:1), as previously reported on similar structures.<sup>[9]</sup>



**Scheme 2.6.16:** Reduction of aldehydes **7a-b** to primary alcohols **8a-b**, using sodium borohydride ( $\text{NaBH}_4$ ) as the reducing agent.<sup>[9]</sup>

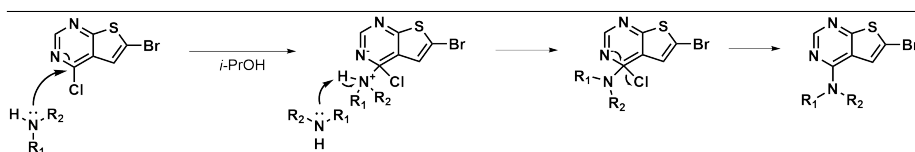
### 2.6.4 Nucleophilic aromatic substitution

Thieno[2,3-*d*]pyrimidines consist of a fused pyrimidine- and thiophene moiety. While six-membered heterocycles such as pyrimidine are generally electron deficient, thiophene is an electron rich heterocycle, allowing for regioselective nucleophilic aromatic substitution on thieno[2,3-*d*]pyrimidines under the right conditions.<sup>[104]</sup>

Nucleophilic aromatic substitution may proceed through several mechanisms, including:

- Addition-elimination
- Elimination-addition
- Metal-catalyzed processes

Thieno[2,3-*d*]pyrimidines favour the addition-elimination mechanism, as the nitrogen atoms in the pyrimidine moiety acts to stabilize the reaction intermediate (Meisenheimer complex), thus activating the ring towards nucleophilic attack. The addition of the nucleophile forms a resonance-stabilized anion, followed by an elimination of the halogen leaving group, as illustrated in Scheme 2.6.17.



**Scheme 2.6.17:** Nucleophilic aromatic substitution via an addition-elimination mechanism.

The reaction rate of the nucleophilic aromatic substitution reaction is a product of several factors, including the chosen solvent, the leaving group, and the nucleophile. Considerably higher reaction rates has been found for  $S_NAr$  in dipolar aprotic solvents as opposed to polar solvents, due to increased stability of the Meisenheimer complex and increased basicity of the amine in aprotic solvents.<sup>[105,106]</sup> The addition of a hydrogen-bond acceptor co-solvent, such as a more basic non-nucleophilic amine, also has a favourable effect on the reaction rate. In addition to its inherent catalytic effect, the use of a co-solvent amine with higher  $pK_a$  than the nucleophilic amine gives an amine-amine aggregate which acts as a better nucleophile, compared to the amine without the co-solvent.<sup>[107]</sup>

The nature of the leaving group is a key factor for the reaction rate of nucleophilic aromatic substitution. Common leaving group are halides, although alkoxy, cyano, nitro and sulfonyl groups may also be displaced in highly activated systems. Because the addition of the nucleophile is the rate determining step of this reaction, the leaving group order of the halides is divergent from general  $S_N2$  reactions, with  $F > Cl > Br > I$ . The rate determining step is also greatly facilitated by electron deficient aromatic reactants, hence perfect for regioselective substitution of thieno[2,3-*d*]pyrimidines.

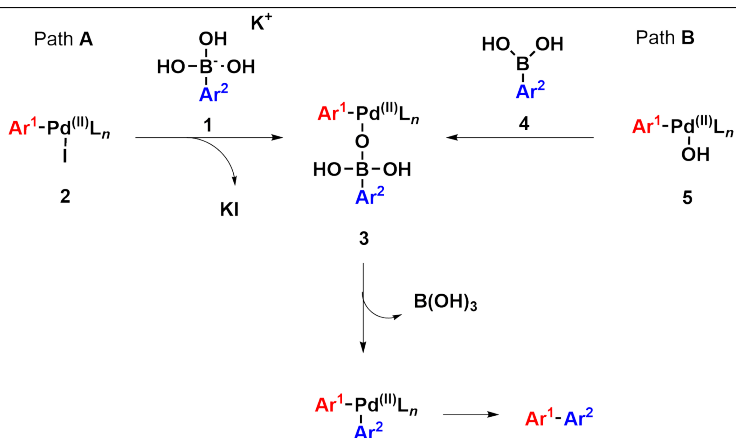
## 2.6.5 Suzuki cross-coupling

The choice of method for the carbon-carbon coupling of thieno[2,3-*d*]pyrimidines **5a-b** with their respective aryl groups, was the Suzuki cross-coupling reaction. This palladium-catalyzed cross-coupling reaction has been a pioneer in cross-coupling since it was first published in 1981, as the large diversity of available boronic acids allows for a high degree of customization.<sup>[108]</sup> In combination with low cost and toxicity of substrates and catalysts, and mild reaction conditions, the Suzuki cross-coupling reaction has become the “golden standard” for preparation of biaryls and is ubiquitous in modern medicinal chemistry.<sup>[109]</sup>

The mechanism of Suzuki cross-coupling involves four steps:<sup>[110]</sup>

- Oxidative addition of aryl-halide to Pd(0) to form a Pd(II)-complex
- Exchange of the anion attached to Pd(II) for the anion of the base (Metathesis)
- Transfer of the organic group from the organo-metal to the Pd(II)-complex (Transmetallation)
- Reductive elimination of the substituted Pd(II)-complex to give carbon bond formation, and to re-form the Pd(0) catalyst.

The mechanism of the transmetallation step has long been a subject of debate, concerning the activation of the organoboron compound by the base.<sup>[111]</sup> Two prominent pathways have been considered (path A and B in Scheme 2.6.18), which differ in the way transmetallation is initiated by the hydroxide ion.<sup>[112]</sup>



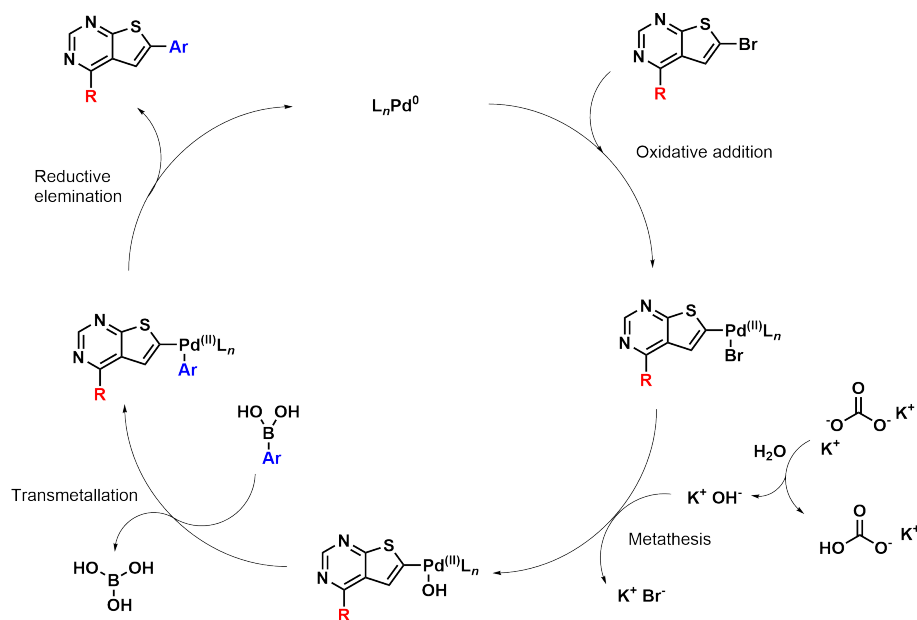
**Scheme 2.6.18:** Transmetallation pathways in Suzuki cross-coupling.<sup>[112,113]</sup>

Path A proceeds from a palladium halide complex (**2**), via a negatively charged aryl-trihydroxyboronate, while path B proceeds from a palladium hydroxide complex via a neutral arylboronic acid.<sup>[112]</sup> Both pathways converge at the same intermediate containing a Pd-O-B unit (**3**), whose structure was confirmed fairly recently.<sup>[113]</sup> Extensive



kinetic studies have established path B as the favoured route, and the generally accepted catalytic cycle for the Suzuki cross-coupling is presented in Scheme 2.6.19.<sup>[112,114–116]</sup>

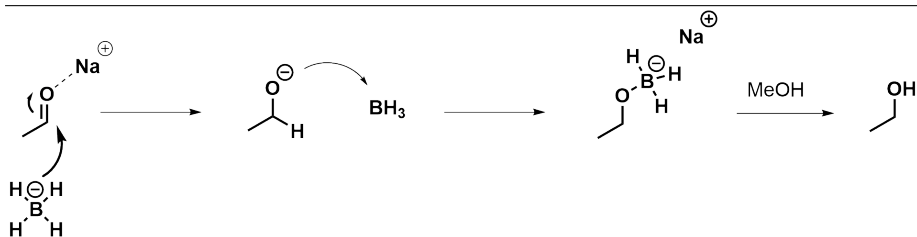
**Scheme 2.6.19:** General catalytic cycle for the Suzuki cross-coupling reaction of arylhalides.<sup>[117]</sup>



## 2.6.6 Reductions with NaBH<sub>4</sub>

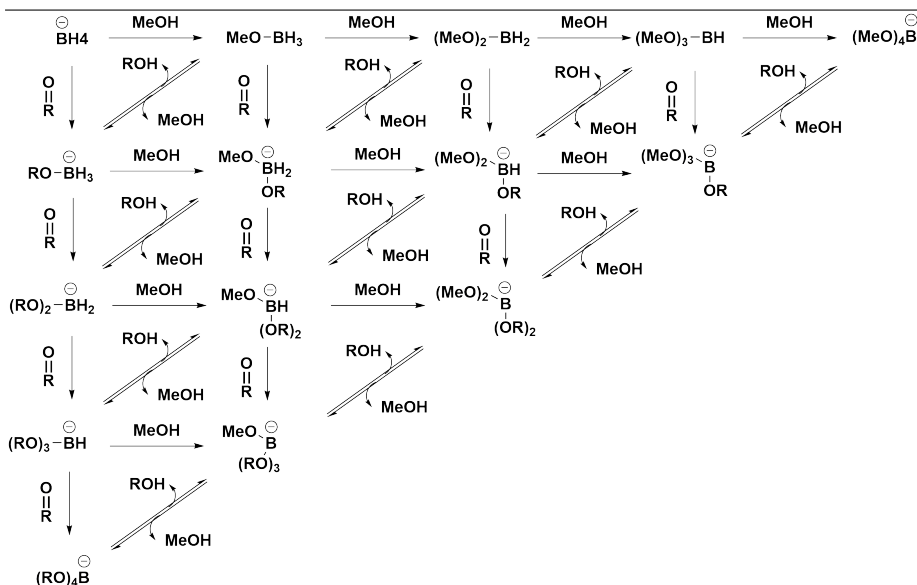
### Reduction of aldehydes

The reduction of aldehydes to primary alcohols is done by treatment with either NaBH<sub>4</sub> or LiAlH<sub>4</sub>. While both give the same overall result, the reaction conditions for using either one are rather different. Due to the high reactivity of LiAlH<sub>4</sub>, this one reacts rapidly and violently with protic solvents, such as water or alcohols, and reactions employing this reducing agent must be protected from moisture. NaBH<sub>4</sub> is a milder reagent and allows for reductions to be carried out in water or methanol solution, which makes for an easier workup.<sup>[118,119]</sup> A general mechanism for the reduction of an aldehyde to a primary alcohol using NaBH<sub>4</sub> is presented in Scheme 2.6.20, illustrating the nucleophilic attack from the hydride ion on the carbonyl carbon, followed by protonation of the resulting alkoxide.



**Scheme 2.6.20:** Reduction of aldehyde with NaBH<sub>4</sub>.

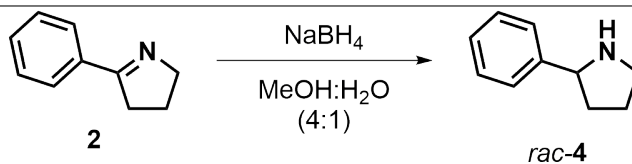
The mechanism of NaBH<sub>4</sub> reduction becomes more complex when taken into account that all four of the hydrides may eventually be transferred, meaning that several distinct reducing agents may be functioning throughout the course of the reaction.<sup>[120]</sup> Scheme 2.6.21 helps illustrate this complexity, as all species containing a B-H group may react either with the carbonyl or the solvent alcohol. As pointed out in this scheme, NaBH<sub>4</sub> may be used to reduce up to four equivalents of aldehyde, depending on the substrates and reaction conditions. This may be used along with methanol workup to form trimethyl borate from the boron complex, allowing for removal of the boron by drying to constant weight due to the low boiling point of trimethyl borate (bp. 69°C).<sup>[121–123]</sup>



**Scheme 2.6.21:** Possible pathways in NaBH<sub>4</sub> carbonyl reduction. R=O in this case represents an aldehyde.

### Reduction of imines

$\text{NaBH}_4$  has applications in a wide range of functional groups, and the use of this reducing agent for the reduction of imines conjugated with aromatic rings is well established.<sup>[119,124,125]</sup> As an inexpensive and mild reagent it was chosen for the reduction of compound **2** to *rac*-**4**, as illustrated in Scheme 2.6.22.<sup>[53]</sup> In this reaction, delocalization of the  $\pi$ -electrons occurs through conjugation of the carbon-nitrogen double bond with the phenyl group. This creates an electrophilic center, capable of being attacked by the nucleophilic borohydride anion.



**Scheme 2.6.22:** Reduction of imine **2** with sodium borohydride ( $\text{NaBH}_4$ ) to *rac*-**4**.

---



### 3 | Results and Discussion

The main focus of this master's thesis has been to carry out a preliminary SAR study of thieno[2,3-*d*]pyrimidines with a tertiary heterocyclic amine as a substituent on C-4. A second objective has been to prepare these thieno[2,3-*d*]pyrimidine-based kinase inhibitors, using enantioenriched and racemic 2-phenylpyrrolidine, and pyrrolidine as the substituent. The aim was to prepare new compounds with high chemical and enantiopurity, to study both the effect of chirality of the phenyl group of the C-4 amine, and the contribution it may provide to the EGFR-TK activity of these structures. This work has resulted in 14 new compounds, of which two show promising activity and may open new areas of research.

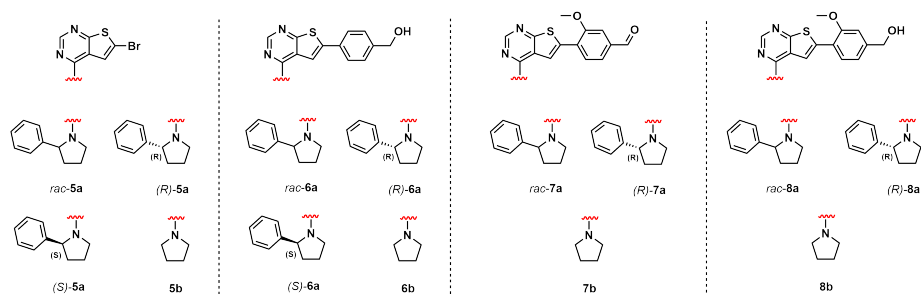
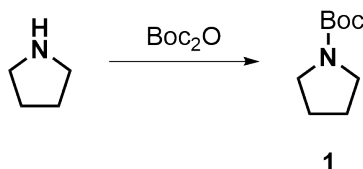


**Figure 3.1:** Structures of new thieno[2,3-*d*]pyrimidines **5-8**

This section will address the synthesis of precursor molecules, intermediates, and the synthesis and structure elucidation of structures **5-8**, followed by a review of the results from the bioassay of target structures **6a-b** and **8a-b**. The focus of the syntheses has been to achieve the target molecules with high purity, so the listed reaction parameters may not be optimized with respect to yield.

### 3.1 Boc protection

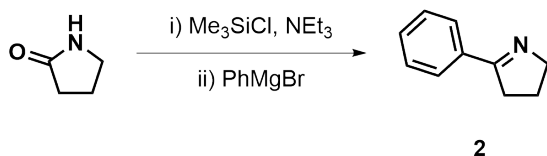


**Scheme 3.1.1:** Boc protection of pyrrolidine to compound **1**.

---

Compound **1** was synthesized as a precursor to (*R*)- and (*S*)-**3**. The compound was synthesized via Boc protection of pyrrolidine, using  $\text{Boc}_2\text{O}$ .<sup>[126]</sup> The reaction time was 2 minutes, yielding 92-94 % of **1** as a yellowish liquid without the need for purification.

### 3.2 One-pot silylation and Grignard



**Scheme 3.2.1:** Two-step, one-pot reaction of pyrrolidin-2-one to **2**.

---

Compound **2** was synthesized as a precursor to *rac*-**4**. The compound was synthesized in a two-step, one-pot reaction starting with a silylation, followed by addition of a Grignard reagent.<sup>[57]</sup> The obtained yields for this reaction were 12 - 36 %, with literature values ranging from 30 - 90 %.<sup>[53,57]</sup> The synthesis was performed several times under different conditions to tune conversion and yield.

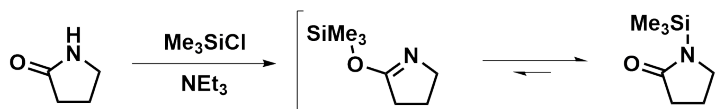
The main issue of this reaction was to achieve full conversion of pyrrolidin-2-one during the initial silylation. The challenge encountered in this step was that the addition of  $\text{Me}_3\text{SiCl}$  to the reaction mixture caused a massive increase in viscosity of the solution. This made reflux and stirring of the reaction difficult, which in turn impacted the conversion of starting material. Small tweaks were done to improve this step, such as adding more solvent, changing reflux time, and substituting magnetic stirring for mechanical stirring. Table 3.1 presents an overview of these changes, and the overall effect on conversion and yield of the one-pot reaction.

**Table 3.1:** Scale, solvent volume, reflux time, stirring apparatus, conversion, and yield of the one-pot synthesis of compound **2**.

Scale [g]	Volume [mL] <sup>a</sup>	Eq. <sup>b</sup>	Time [h] <sup>c</sup>	Stirring	Conv. [%] <sup>d</sup>	Yield [%] <sup>e</sup>
1.03	15	1	24	Mag.	69	12
0.50	7.5	1	0.5	Mag.	95	14
0.71	10	2	4.5	Mag.	80	22
1.81	15	1.3	0.5	Mag.	89	35
5.07	75	1.1	2	Mech.	53	33
0.88	15	2.1	1	Mech.	92	35
0.52	10	2	0.5	Mech.	92	36

<sup>a</sup> Diethyl ether.<sup>b</sup> Grignard reagent.<sup>c</sup> Reflux time during silylation.<sup>d</sup> Estimated from <sup>1</sup>H NMR.<sup>e</sup> Isolated yield.

It is difficult to draw conclusions based on the results of Table 3.1, as there are considerable divergences in conversion and yield with the various parameters. The results obtained during these experiments were difficult to reproduce, something that has been previously noted with the use of a Grignard reagent in this transformation.<sup>[57]</sup> Some explanation for the erratic results may be the equilibrium that conforms during the silylation, where Me<sub>3</sub>Si is attached to either the nitrogen or the oxygen of the lactam (Scheme 3.2.2). Provided only the N-protected isomer may react with the Grignard reagent to form **2**, this means that the yield is dependent on, inter alia, the amount of silyl-protected oxygen.

**Scheme 3.2.2:** The equilibrium between the O- or N-protected lactam of pyrrolidin-2-one after silylation. The equilibrium is shifted towards the protected nitrogen.

The formation of by-products could also be an explanation for the irregularities in the results. Some by-products are observed in the crude <sup>1</sup>H NMR of compound **2**, especially in the aromatic region, as presented in Figure 3.2.

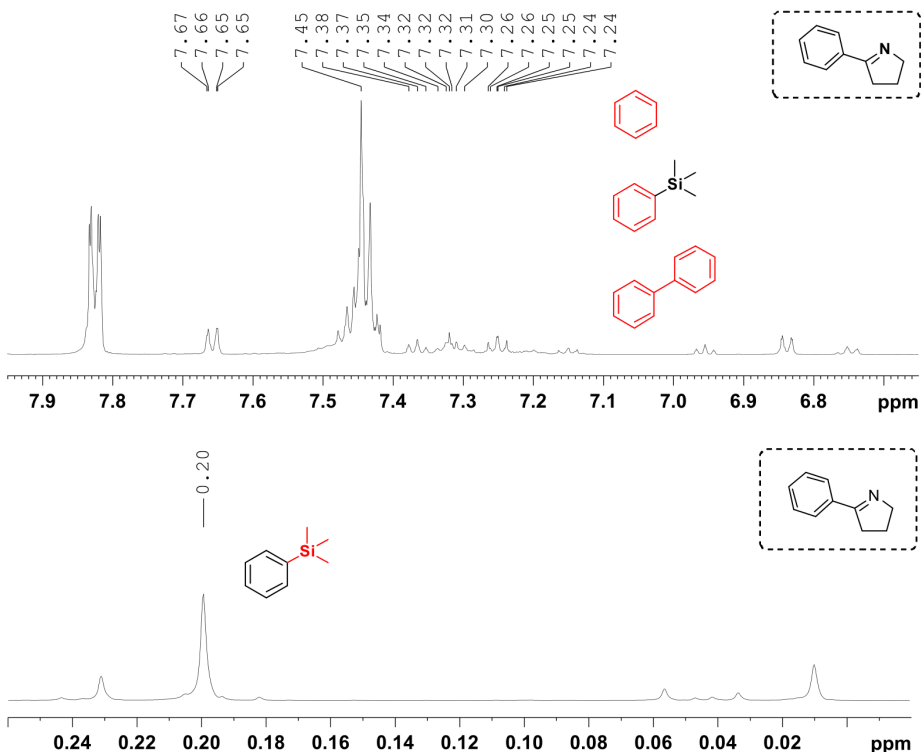
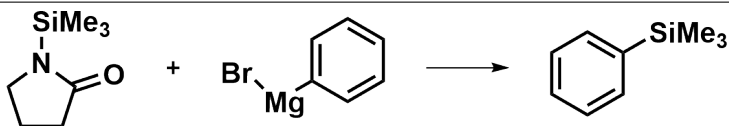


**Figure 3.2:** Presumed signals from trimethyl(phenyl)silane, benzene, and 1,1'-biphenyl in the  $^1\text{H}$  NMR of crude material of compound **2**.

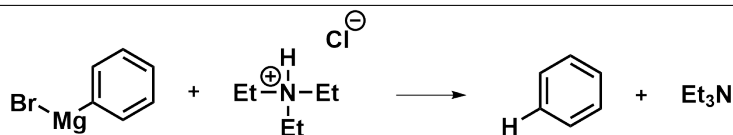
Some of these by-products arise from the reaction between the Grignard reagent and the silyllactam at silicon, as previously reported by Hua.<sup>[127]</sup> Scheme 3.2.3 illustrates this side reaction to form trimethyl(phenyl)silane.  $^1\text{H}$  NMR spectrum of trimethyl(phenyl)silane in DMSO has not been found in the literature for reference; however,  $^1\text{H}$  NMR modelling using integrated software on the computer-application “ChemBioDraw Ultra 14.0” suggest that this compound is present in the NMR of crude material of compound **2** as signals at 7.35-7.27 ppm.<sup>[128]</sup> Figure 3.2 shows the presumed signals of trimethyl(phenyl)silane in the  $^1\text{H}$  NMR spectrum of crude **2**.



**Scheme 3.2.3:** Formation of the by-product trimethyl(phenyl)silane from the reaction between the Grignard reagent and the silyllactam at silicon.<sup>[127]</sup>



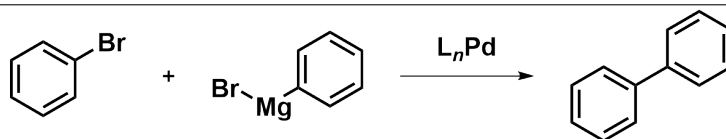
Addition of the Grignard reagent was done without purification of the silylated intermediate, which could lead to formation of by-products such as benzene due to insufficient removal of ammonium salt from the silylation, as illustrated in Scheme 3.2.4.<sup>[129]</sup> Benzene may be present in the crude product of compound **2**, as a signal at 7.37 ppm in Figure 3.2.<sup>[130]</sup>



**Scheme 3.2.4:** Formation of the by-product benzene by reaction of the Grignard reagent with ammonium salt.

---

Another possibility for by-product is the formation of a 1,1'-biphenyl by homocoupling of the Grignard reagent. This reaction could proceed via a radical type coupling or a Kumada cross-coupling, likely catalyzed by palladium-residues or other heavy-metal residues in the glassware or reagents, as illustrated in Scheme 3.2.5. Biphenyl may also be an impurity present in the Grignard reagent itself.  $^1\text{H}$  NMR spectrum of 1,1'-biphenyl in DMSO has not been found in the literature for reference; however,  $^1\text{H}$  NMR modelling using integrated software on the computer-application “ChemBio-Draw Ultra 14.0” suggest that this compound may be present in the crude material of **2** as signals at 7.66 ppm, 7.44 ppm, and 7.35 ppm.<sup>[131–133]</sup> Figure 3.2 shows the presumed signals of 1,1'-biphenyl in the  $^1\text{H}$  NMR spectrum of crude **2**.

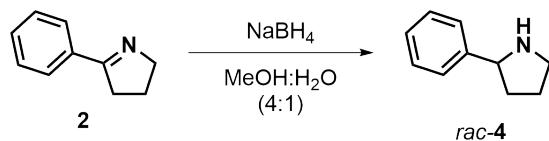


**Scheme 3.2.5:** Homocoupling of the Grignard reagent via a palladium-catalyzed Kumada cross-coupling.

---

Purification of the intermediate by distillation is a viable option to help avoid these side reactions; however, the gains of doing so have been reported as minuscule.<sup>[57]</sup>

### 3.3 Reduction of 2-phenylpyrroline



**Scheme 3.3.1:** Reduction of imine **2** to *rac-2*.

The reduction of imine **2** to *rac-4* was done using NaBH<sub>4</sub> as a reducing agent, and MeOH:H<sub>2</sub>O (4:1) as solvent. The reaction was left for >12 hours, as previously reported by Dunsmore *et al.*<sup>[53]</sup> Yields were in the range from 72-89 %, with a literature value of 97 % for this reaction.<sup>[53]</sup> Table 3.2 lists scale, reaction times, conversions, and yields for this reaction.

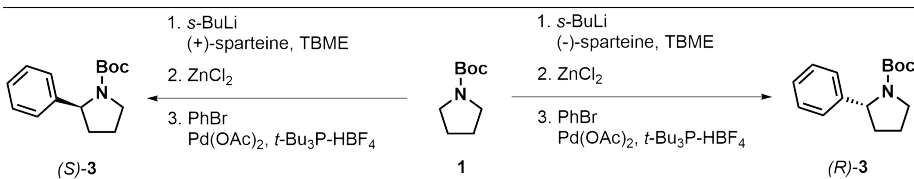
**Table 3.2:** Scale, reaction time, conversion, and yield for the reduction of compound **2** to *rac-4*.

Scale [g]	Time [h]	Conversion [%] <sup>a</sup>	Yield [%] <sup>b</sup>
3.16	17	>97	72
0.3	22	>97	77
1.36	22	>97	89

<sup>a</sup> Conversion determined by <sup>1</sup>H NMR.

<sup>b</sup> Isolated yield.

### 3.4 Palladium-catalyzed $\alpha$ -arylation



**Scheme 3.4.1:** Palladium-catalyzed  $\alpha$ -arylation of compound **1** to (*R*)- and (*S*)-**3**.

The (*R*)- and (*S*)-enantiomers of **3** were synthesized from **1** in a palladium-catalyzed  $\alpha$ -arylation, employing (-)-sparteine for the preparation of (*R*)-**3** and (+)-sparteine for (*S*)-**3**.<sup>[52,86]</sup> Both reactions were left for >12 hours, and achieved full conversion of starting material. Yields were 62 % for (*R*)-**3** and 70 % (*S*)-**3**. No other compounds were observed.

Enantiomeric analyses were done by analytical chiral stationary phase HPLC (CSP-HPLC), using a Chiralpak AD column. The analyses were done for these compounds, as opposed to the deprotected (*R*)- and (*S*)-**4**, due to more available experimental data and availability of HPLC-columns.<sup>[52][86]</sup> By tuning the available parameters, a near base line resolution was achieved with  $R = 2.3$ . Enantiomeric excess was found to be 86 % for (*R*)-**3**, and 96 % for (*S*)-**3** under these conditions. Parameters and corresponding retention times are listed in Table 3.3. Differences in ee are suspected due to divergences in the enantiopurity of (-)- and (+)-sparteine, as the experimental preparation of (*R*)- and (*S*)-**3** are close to identical.

Flow [mL]	iPrOH/Hexane	$t_{R,1}$ [min.]	$t_{R,2}$ [min.]	$\alpha$	R	N
0.8	1/99	8.5	9.0	1.05	1.79	10071
0.5	1/99	10.9	11.6	1.07	2.24	25688
0.3	1/99	24.9	26.7	1.07	2.3	23958
0.2	1/99	34.8		1	0	-
0.5	2/98	10.0		1	0	-
0.3	2/98	10.9	11.2	1.03	1.76	102949
0.2	2/98	24.0		1	0	-

**Table 3.3:** Optimization of base line separation for the enantiomers of (*R*)- and (*S*)-**3**.

<sup>1</sup>H NMR spectra of (*R*)- and (*S*)-**3** (Appendix C to D) show the presence of rotamers (~40:60) by splitting of the CH proton on the pyrrolidine moiety at 4.75 ppm, and the (CH<sub>3</sub>)<sub>3</sub> protons of the Boc-group at 1.25 ppm. Figure 3.3 illustrates the rotamers of (*R*)-**3**.

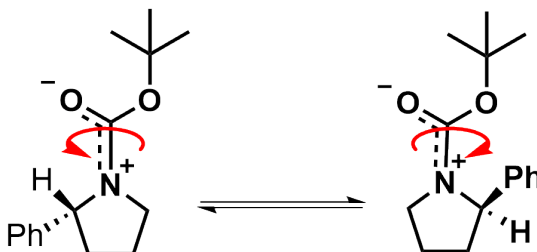


**Figure 3.3:** Illustration of the two rotamers of (*R*)-**3**.

To confirm that this splitting is indeed caused by rotamers, the compounds were analyzed by temperature gradient <sup>1</sup>H NMR. By increasing the temperature to 50 °C, the two CH peaks merge, while the (CH<sub>3</sub>)<sub>3</sub> peaks only fully merge at around 80 °C. Figure 3.4 shows the effect of increased temperature on the <sup>1</sup>H NMR spectrum of (*R*)-**3**. The effect is the same for (*S*)-**3**, and the <sup>1</sup>H NMR spectra of the two compounds are close to identical.

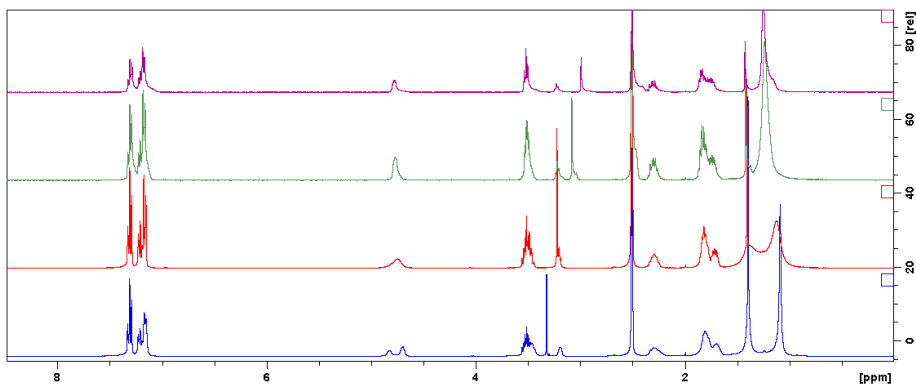
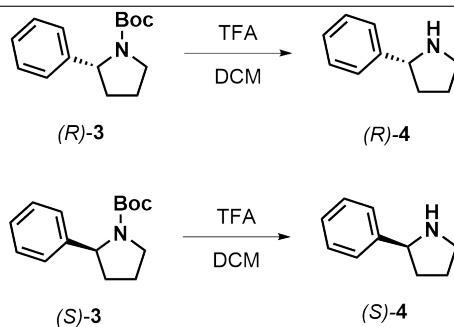


**Figure 3.4:** Temperature gradient  $^1\text{H}$  NMR (400 MHz,  $\text{DMSO-}d_6$ ) of  $(R)$ -**3**. From top to bottom: 100 °C, 80 °C, 50 °C, room temperature. Rotamers are visible at 4.75 ppm, and 1.25 ppm.

### 3.5 Boc deprotection



**Scheme 3.5.1:** Boc deprotection of compounds  $(R)$ - and  $(S)$ -**3** to  $(R)$ - and  $(S)$ -**4**.

$(R)$ - and  $(S)$ -**4** were synthesized by Boc deprotection of  $(R)$ - and  $(S)$ -**3**. The deprotection was done using trifluoroacetic acid as described by Trost *et al.*,<sup>[52]</sup> with a reaction time of 4 hours. The reactions gave  $(R)$ - and  $(S)$ -**4** as mixtures with 0.61 eq. of TFA salt. The yields were 56 % and 49 % for  $(R)$ - and  $(S)$ -**4**, respectively.

Identification of the TFA salt was done by  $^{19}\text{F}$  NMR, using hexafluorbenzene as an internal standard. The salt is visible as a signal at -73.5 ppm, with hexafluorbenzene at -162.6 ppm, as presented in Figure 3.5. The amount of TFA salt formed in the reactions was found by quantitative  $^{19}\text{F}$  NMR, by referencing known amounts of  $(S)$ -**4** TFA salt with the internal standard. Calculations were done using the formula

$$\frac{M_P}{M_I} = \frac{I_P}{I_I} * \frac{N_I}{N_P},$$

where  $M_P/M_I$  is the molar ratio between product and internal standard,  $I_P/I_I$  is the integral ratio between product and internal standard, and  $N_I/N_P$  is the ratio between the number of  $^{19}\text{F}$  atoms in the internal standard and the product.<sup>[134]</sup> As the experimental procedure for the preparation of (*R*)- and (*S*)-**4** are close to identical, it was estimated that both reactions yielded 0.61 equivalents of TFA salt. The yields were calculated based on the estimate of the formation of 39 % desired product.

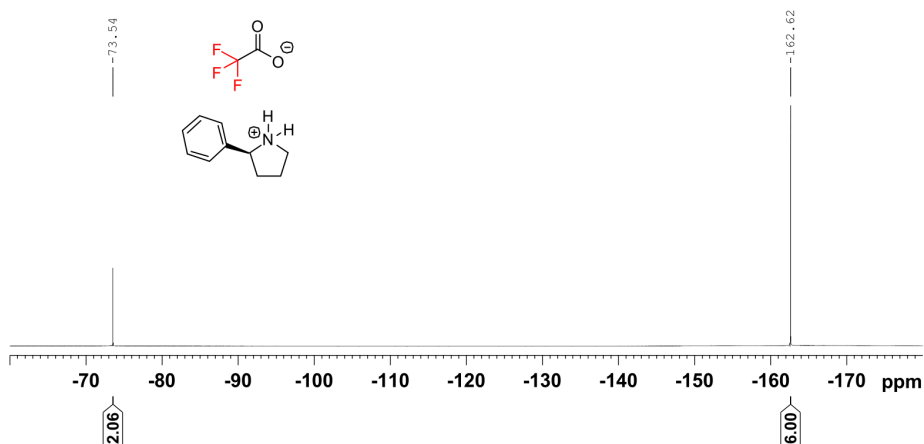
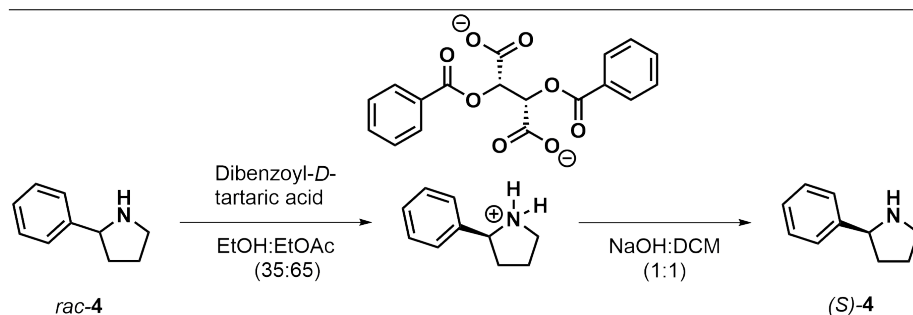


**Figure 3.5:**  $^{19}\text{F}$  NMR of (*S*)-**4**, with hexafluorobenzene as the internal standard.

### 3.6 Chiral resolution of *rac*-2-phenylpyrrolidine



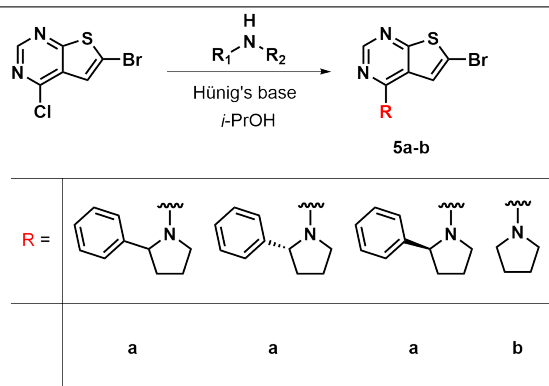
**Scheme 3.6.1:** Chiral resolution of compound *rac*-**4** to (*S*)-**4**.

Chiral resolution of racemic 2-phenylpyrrolidine was investigated as a synthetic route to enantioenriched 2-phenylpyrrolidines. Racemic **4** (*rac*-**4**) was mixed with dibenzoil-*D*-tartaric acid and dissolved in a solution of 35 % ethanol in ethyl acetate. The solution was heated to boiling for 10 minutes and then slowly cooled to room temperature, to allow crystallization of the salt. The procedure yielded 31 % salt as

white crystals, which were then vigorously stirred in a mixture of NaOH:DCM (1:1) to remove the salt. (*S*)-2-phenylpyrrolidine was obtained in 49 % yield as an orange oil.

A sample of (*S*)-2-phenylpyrrolidine was Boc protected and analysed by CSP-HPLC to check the ee. Using the established eluent system for compounds (*R*)- and (*S*)-**3**, the ee was found to be 24 %, indicating a slight excess of the (*S*)-enantiomer. Subsequent recrystallization of the intermediary (*S*)-2-phenylpyrrolidine salt has been reported as a way to improve the enantioselectivity in this procedure;<sup>[54]</sup> however, due to time constraints this was not investigated in this project. Despite the low enantiopurity, this procedure succeeds in providing an alternate path to enantioenriched 2-phenylpyrrolidines from the racemic amine.

### 3.7 Amination of thienopyrimidines



**Scheme 3.7.1:** Nucleophilic aromatic substitution of 6-bromo-4-chloro-2-thienopyrimidine to compounds **5a-b**.

Compounds **5a-b** were synthesized by nucleophilic aromatic substitution, using *i*-PrOH as solvent.<sup>[10]</sup> The reactions were stirred at 80 °C under an N<sub>2</sub> atmosphere, and all of the compounds were purified by silica gel column chromatography. Table 3.4 lists conversion, reaction times and yields for these reactions.

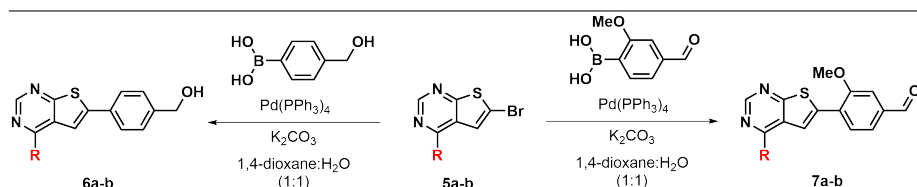
**Table 3.4:** Yields, conversion and reaction times for the synthesis of compounds **5a-b**

Reactant	Scale [mg]	Eq. <sup>a</sup>	Eq. <sup>b</sup>	Time [h]	Conv. [%] <sup>c</sup>	Yield [%] <sup>d</sup>	Product
<i>rac</i> - <b>4</b>	200	1.5	1.5	1.25	>97	80	<i>rac</i> - <b>5a</b>
( <i>R</i> )- <b>4</b>	302	14	1.4	24	82	74	( <i>R</i> )- <b>5a</b>
( <i>S</i> )- <b>4</b>	206	1.5	1.4	24	59	50	( <i>S</i> )- <b>5a</b>
Pyrrolidine	416	1.5	1.5	1.6	>97	91	<b>5b</b>

<sup>a</sup> Amine.<sup>b</sup> Hünig's base.<sup>c</sup> Conversion determined by <sup>1</sup>H NMR.<sup>d</sup> Isolated yield.

Suboptimal conversion of starting material was observed in the synthesis of (*R*)- and (*S*)-**5a**, likely due to the presence of TFA salt in (*R*)- and (*S*)-**4**. With 0.61 equivalents of TFA salt, most of the amines would be unavailable as a nucleophile. It was thought that by adding a surplus of Hünig's base, this would act to deprotonate salt in addition to acting as co-base for the nucleophilic aromatic substitution. This was tested in the synthesis of (*R*)-**5a**, giving considerably better conversion compared to the synthesis of (*S*)-**5a**. To improve the conversion and yield of these two reactions, more co-base is needed to fully deprotonate the TFA salt. Alternatively, (*R*)- and (*S*)-**4** can be deprotonated prior to the nucleophilic aromatic substitution.

### 3.8 Suzuki cross-coupling

**Scheme 3.8.1:** Suzuki cross-coupling of **5a-b** to **6a-b** and **7a-b**.

Compounds **6a-b** were synthesized by Suzuki cross-coupling with the appropriate arylboronic acids. The reactions were stirred at 80 °C under an N<sub>2</sub> atmosphere, and all compounds were purified by silica gel column chromatography. Table 3.5 lists conversion, reaction times and yields for these reactions.

**Table 3.5:** Yields, scale, conversion, and reaction times for the synthesis of compounds **6a-b** and **7a-b**

Reagent	Scale [mg]	Time [min.]	Conv. <sup>a</sup> [%]	Yield <sup>b</sup> [%]	Product
<i>rac</i> - <b>5a</b>	111	25	>97	60	<i>rac</i> - <b>6a</b>
<i>rac</i> - <b>5a</b>	100	55	>97	93	<i>rac</i> - <b>6a</b>
<i>rac</i> - <b>5a</b>	131	30	>97	56	<i>rac</i> - <b>7a</b>
<i>rac</i> - <b>5a</b>	372	90	>97	99	<i>rac</i> - <b>7a</b>
( <i>R</i> )- <b>5a</b>	146	45	>97	92	( <i>R</i> )- <b>6a</b>
( <i>R</i> )- <b>6a</b>	172	45	>97	92	( <i>R</i> )- <b>7a</b>
( <i>S</i> )- <b>5a</b>	131	45	>97	92	( <i>S</i> )- <b>6a</b>
<b>5b</b>	103	55	>97	58	<b>6b</b>
<b>5b</b>	418	45	>97	94	<b>7b</b>

<sup>a</sup> Conversion determined by <sup>1</sup>H NMR.

<sup>b</sup> Isolated yield.

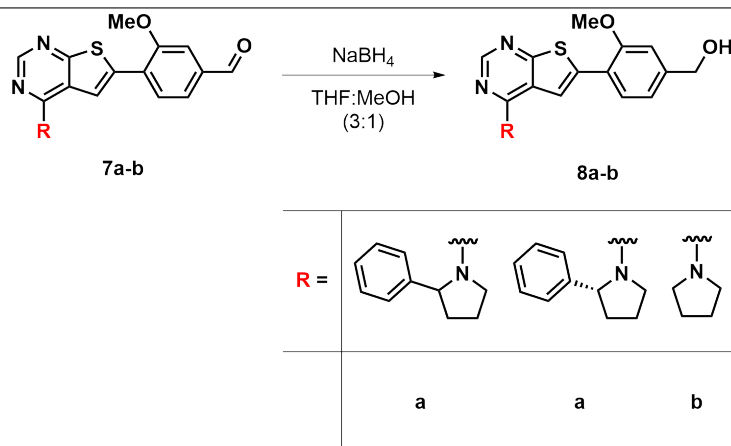
In the initial Suzuki cross-coupling reactions of *rac*-**5a** to *rac*-**6a** and *rac*-**7a**, ~24 % of by-products were formed, giving low yield of the desired products. The by-product from the synthesis of *rac*-**6a** was isolated and analysed, identifying this compound to be the product of dimerization of the arylboronic acid. The <sup>1</sup>H NMR spectrum of the dimer, 4,4'-bis(hydroxymethyl)biphenyl, is given in Appendix M, and NMR data are in accordance with previously reported values.<sup>[135]</sup> It is suspected that the dimerization was the result of insufficient degassing of the solvent, causing oxidation of the phosphine ligands of tetrakis(triphenylphosphine)palladium(0) and of Pd(0) to Pd(II), thus favouring formation of the dimer.<sup>[136,137]</sup> Evidence of this is that proper degassing resulted in minute amounts of by-product and increased the yield in later experiments.

CSP-HPLC analyses were done for compounds (*R*)- and (*S*)-**6a**, and (*R*)-**8a**, to cross-reference the ee of the final products to that of compounds (*R*)- and (*S*)-**3**. A chiral analysis of these compounds was developed, based on an analytic procedure on similar compounds by Bugge *et al.*,<sup>[11]</sup> using a Lux 5u Cellulose HPLC column. The ee of compounds (*R*)- and (*S*)-**6a** were both found to be 65 %, which marks a significant drop from the 86-96 % ee of (*R*)- and (*S*)-**3**, respectively. The ee of compound (*R*)-**8a** was found to be 84 %, which may be within standard deviation of the HPLC data. While no clear sources of racemization of compounds (*R*)- and (*S*)-**6a** have been found, a possibility may be palladium-catalyzed racemization. This has been reported for (*S*)-2-phenylpyrrolidine in a Buchwald-Hartwig N-Arylation,<sup>[138]</sup> and for amino acid derivatives in palladium-catalyzed cross-coupling reactions with the use of the Pd(PPh<sub>3</sub>)<sub>4</sub> catalyst.<sup>[139]</sup> In these cases, racemization is possible due to β-hydrogen elimination or the presence of an acidic α-proton. Neither of these are likely sources for racemization in the Suzuki cross-coupling reactions in this project, as the amine is attached to the thieno[2,3*d*]pyrimidine core prior to the cross-coupling reactions. Racemization would most likely occur with the presence



of palladium-residues, either from glassware or reagents, during the  $S_NAr$  reactions; however, further studies are required to clarify these findings.

### 3.9 Reduction of aldehydes by sodium borohydride



**Scheme 3.9.1:** Reduction of **7a-b** to **8a-b** with sodium borohydride ( $\text{NaBH}_4$ ).

Compounds **8a-b** were synthesized by reduction of aldehyde to primary alcohol, using  $\text{NaBH}_4$  as the reducing agent, and THF:MeOH as solvent. The reactions were stirred at room temperature under an  $\text{N}_2$  atmosphere, and all compounds were purified by silica gel column chromatography. Table 3.6 lists scale, conversion, reaction times, and yields for these reactions.

**Table 3.6:** Yields, scale, conversion, reaction times, and yields for the synthesis of compounds **8a-b**

Reagent	Scale [mg]	Time [min.]	Conv. [%] <sup>a</sup>	Yield [%] <sup>b</sup>	Product
<i>rac</i> - <b>7a</b>	350	60	>97	48	<i>rac</i> - <b>8a</b>
( <i>R</i> )- <b>7a</b>	145	50	>97	>99	( <i>R</i> )- <b>8a</b>
<b>7b</b>	199	90	>97	67	<b>8b</b>

<sup>a</sup> Conversion determined by  $^1\text{H}$  NMR.

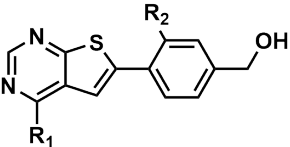
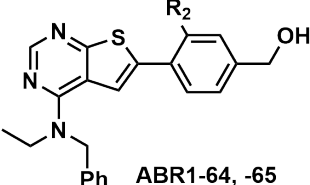
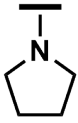
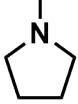
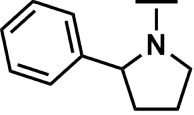
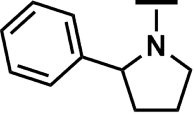
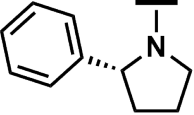
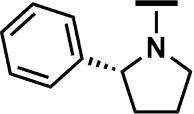
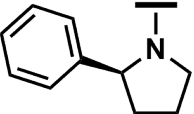
<sup>b</sup> Isolated yield.

The low yield in the synthesis of *rac*-**8a** and **8b**, compared to (*R*)-**8a**, was due to poor solubility of these compounds, making the purification processes difficult.

### 3.10 *In vitro* testing of target compounds

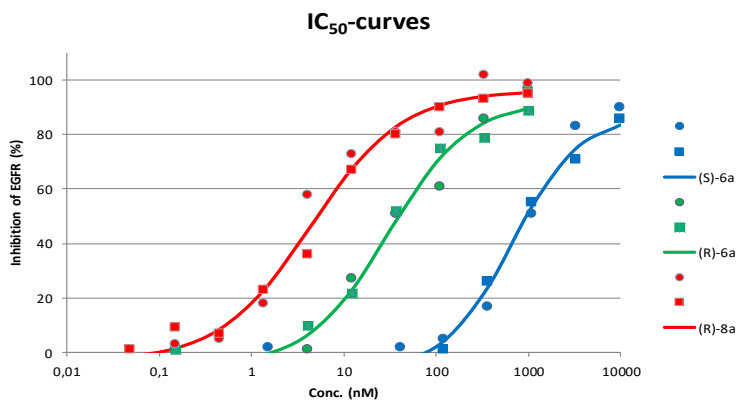
The biological activity of the target compounds was tested towards EGFR-TK and CSF1R-TK in an enzymatic assay. Single-point analyses were performed at 100 nM and 500 nM concentration of the inhibitors for EGFR and CSF1R, respectively, and the results of these tests are given in Tables 3.7 and 3.9. Two previously synthesized thieno[2,3-*d*]pyrimidines, compounds **ABR1-65** and **ABR1-64**,<sup>[140]</sup> are also included in this biological evaluation. Table 3.8 lists the EGFR inhibitory potency of some reference compounds.

**Table 3.7:** EGFR (ErbB1) inhibitory potency of target compounds **6a-b** and **8a-b**, in addition to previously synthesized compounds **ABR1-65** and **ABR1-64**.<sup>[140]</sup>

 <b>6a-b, 8a-b</b>		 <b>ABR1-64, -65</b>			
Comp.	R <sub>1</sub>	R <sub>2</sub>	ee [%]	Inhibition <sup>a</sup> [%]	IC <sub>50</sub> [nM]
<b>6b</b>		<b>H</b>	-	0	>1000
<b>8b</b>		<b>OMe</b>	-	-4	-
<i>rac</i> - <b>6a</b>		<b>H</b>	-	45	-
<i>rac</i> - <b>8a</b>		<b>OMe</b>	-	92	-
( <i>R</i> )- <b>6a</b>		<b>H</b>	65	73	30.6
( <i>R</i> )- <b>8a</b>		<b>OMe</b>	84	92	5.8
( <i>S</i> )- <b>6a</b>		<b>H</b>	65	5	811
<b>ABR1-65</b> <sup>[140]</sup>	-	<b>H</b>	-	8	860
<b>ABR1-64</b> <sup>[140]</sup>	-	<b>OMe</b>	-	49	115

<sup>a</sup> Mean value of two measurements at 100 nM concentration of the inhibitor.

Compounds *rac*- and (*R*)-**8a** show promising results from the single-point analyses, with high activity towards EGFR. Considering the divergences in activity between *rac*-, (*R*)- and (*S*)-**6a**, it appears that the chirality of the phenyl moiety has a significant effect on the EGFR-TK activity. As expected, the (*S*)-enantiomer has low activity, compared to the racemate, while the (*R*)-enantiomer appears to be more favourable. Figure 3.6 presents the IC<sub>50</sub>-curves for compounds (*R*)- and (*S*)-**6a**, and (*R*)-**8a**, further illustrating the effect of the stereochemistry of the phenyl group on the activity of compounds (*R*)- and (*S*)-**6a**.

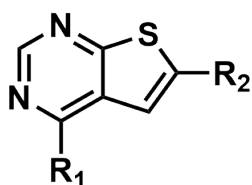


**Figure 3.6:** IC<sub>50</sub>-curves for compounds (*R*)- and (*S*)-**6a**, and (*R*)-**8a**.

The positive effect of a correctly spaced phenyl moiety towards EGFR-TK is visible in the low activity of compounds **6b** and **8b**, compared to compounds *rac*-**6a** and *rac*-**8a**. The removal of the 2-substituted phenyl group proves to be detrimental for the EGFR-TK activity, which demonstrates the significance of this substituent to the activity of these compounds.

The effect of the methoxy moiety is visible by comparing (*R*)-**6a** with compound (*R*)-**8a**, and **ABR1-65** with **ABR1-64**. As illustrated by the IC<sub>50</sub>-curves in Figure 3.6, the methoxy group appears to contribute favourably to the EGFR-TK activity, with a significant increase in activity from (*R*)-**6a** to (*R*)-**8a**. The contribution of the methoxy moiety has also been demonstrated in reference compounds (*R*)-**5e** and **5t**.<sup>[10,11]</sup> (Table 3.8).

One objective of the thesis was to investigate if secondary amines are essential substituents at C-4. Based on the inhibition data for compounds (*R*)-**5n** and **29n** (Table 3.8) and other previous work,<sup>[141]</sup> Bugge *et al.*<sup>[11]</sup> concluded that a secondary amine is essential for the EGFR-TK inhibitory activity; however, the findings of this master's thesis demonstrate that it is possible to achieve high activity towards EGFR with a tertiary heterocyclic amine. A hypothesis is that the EGFR-activity of thieno[2,3-*d*]pyrimidines is related to the conformation of the amino group, as opposed to the hydrogen donor ability. Further modelling and X-ray co-crystal structure determination are needed to fully answer these questions.

**Table 3.8:** EGFR inhibitory potency of reference compounds (*R*)-**1w**, **-5n**, **-29n**, **-5e**, and **5t**.<sup>[10,11]</sup>

Comp.	R <sub>1</sub>	R <sub>2</sub>	Inhibition <sup>a</sup> [%]	IC <sub>50</sub> <sup>b</sup> [nM]	SD <sup>c</sup>
( <i>R</i> )- <b>1w</b> <sup>[10]</sup>		Br	0	-	-
( <i>R</i> )- <b>5n</b> <sup>[11]</sup>			79	35	14
( <i>R</i> )- <b>29n</b> <sup>[11]</sup>			5	>1000	-
( <i>R</i> )- <b>5e</b> <sup>[11]</sup>			86	7	1
( <i>R</i> )- <b>5t</b> <sup>[11]</sup>			100	0.7 <sup>d</sup>	0.2

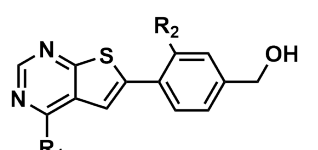
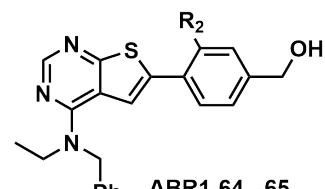
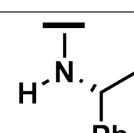
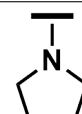
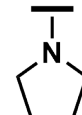
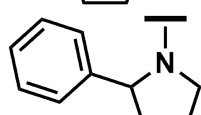
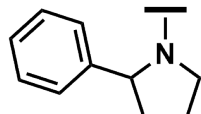
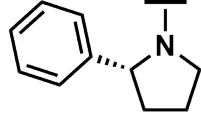
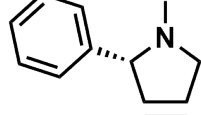
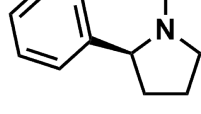
<sup>a</sup> Mean value of two measurements at 100 nM concentration of the inhibitor.

<sup>b</sup> Mean value of two titration curves (20 data points), unless otherwise stated.

<sup>c</sup> Standard deviation.

<sup>d</sup> Mean value of six titration curves (60 data points).

**Table 3.9:** CSF1R (FMS) inhibitory potency of reference compound (*R*)-**5t**,<sup>[11]</sup> target compounds **6a-b** and **8a-b**, and previously synthesized compounds **ABR1-65** and **ABR1-64**.<sup>[140]</sup>

 ( <i>R</i> )- <b>5t</b> , <b>6a-b</b> , <b>8a-b</b>		 <b>ABR1-64</b> , <b>-65</b>		
Comp.	R <sub>1</sub>	R <sub>2</sub>	ee [%]	Inhibition <sup>a</sup> [%]
( <i>R</i> )- <b>5t</b> <sup>[11]</sup>		OMe	ND	2
<b>6b</b>		H	-	55
<b>8b</b>		OMe	-	68
<i>rac</i> - <b>6a</b>		H	-	41
<i>rac</i> - <b>8a</b>		OMe	-	71
( <i>R</i> )- <b>6a</b>		H	65	65
( <i>R</i> )- <b>8a</b>		OMe	84	86
( <i>S</i> )- <b>6a</b>		H	65	20
<b>ABR1-65</b> <sup>[140]</sup>	-	H	3	
<b>ABR1-64</b> <sup>[140]</sup>	-	OMe	11	

<sup>a</sup> Mean value of two measurements at 500 nM concentration of the inhibitor.

Compound (*R*)-**8a** seems to possess good CSF1R activity, and is considerably more active than the racemic *rac*-**8a**. Looking at structures (*R*)-, (*S*)- and *rac*-**6a**, the conformation of the phenyl moiety on the C-4 substituent appears to have an impact on the CSF1R activity. However, compounds **6b** and **8b** without the phenyl group have activity almost on a par with, or higher than compounds *rac*-**6a** and -**8a**. It may be that the conformation of the pyrrolidine moiety is of importance, and that the addition of a 2-substituted phenyl group contributes either positively or negatively to the CFS1R activity, depending on the chirality of this substituent.

### 3.11 Compound characterization

Compounds **5-8**, excluding *rac*-**5a** and *rac*-**6a**, were previously unknown, and their structures are therefore elucidated in this section. Compounds *rac*-**5a** and *rac*-**6a** were synthesized as part of the specialization project of autumn 2017.<sup>[140]</sup> However, due to contamination of the final products, these structures have been resynthesized in this master project and are therefore included in this structure elucidation. <sup>1</sup>H NMR, <sup>13</sup>C NMR, IR and MS have been used for elucidation and confirmation of the target structures, and the spectra from these analyses can be found in the appendices.

#### General remarks

##### IR spectroscopy

IR spectroscopy of the elucidated compounds show generally similar results, and so the spectra are not discussed individually. Instead, some general remarks are discussed in this section.

Aromatic C-H and C=C stretches are visible in all spectra at  $3000\text{ cm}^{-1}$ , along with aromatic C-H bending at  $860\text{-}680\text{ cm}^{-1}$ . For compounds (*R*)- and *rac*-**7a**, a characteristic C=O stretch for aldehyde is visible at  $\sim 1690\text{ cm}^{-1}$ . For compounds **6a-b** and **8a-b** a broad O-H stretch at  $3307\text{-}3314\text{ cm}^{-1}$ , along with the strong C-O stretches at  $1050\text{-}1150\text{ cm}^{-1}$ , suggest the presence of an alcohol group.<sup>[142]</sup>

##### NMR

A general procedure for the structure elucidation of the target compounds from <sup>1</sup>H, <sup>13</sup>C, and 2D NMR, is elaborated in this section. Numbering of positions in the thieno[2,3-*d*]pyrimidine and pyrrolidine moiety are given in Figure 3.7

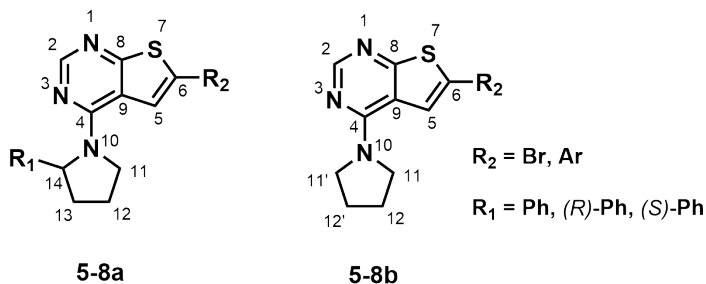


**Figure 3.7:** General numbering of positions in compounds **5-8**

The C-2 proton of the thieno[2,3-*d*]pyrimidine moiety is easily spotted in the  $^1\text{H}$  spectra as a singlet at 8.20-8.30 ppm, and is used as a landmark in the structure elucidations. From this proton, the C-4, C-8, and C-9 carbons may be assigned from long-range  $^1\text{H}$ - $^{13}\text{C}$  coupling (HMBC), as illustrated in Figure 3.8. Comparing this signal in the spectra of compounds **5-8a** and **5-8b** show a significant broadening in the signals of the former. This broadening is also applied to the proton on C-5, as it is easily spotted as a singlet at 7.74-8.17 ppm for compounds **5-8b** while appearing as a very broad signal in the aromatic region of compounds **5-8a**. These differences clearly show the effect of dynamic processes in the structures of compounds **5-8a** as a result of the 2-substituted phenyl group.

The broad signal of the C-5 proton in compounds **5-8a** makes it difficult to assign in these structures; however, the HMBC couplings to this proton are clearly visible in the spectra of compounds **5-8b**, which also allow for the identification of carbon C-6 by cross-referencing with the long-range coupling of the C-2 proton to C-8 and C-9 (see Figure 3.8). While these HMBC couplings are not always visible, especially in the spectra of compounds **5-8a**, the shifts of the thieno[2,3-*d*]pyrimidine moiety remain fairly consistent in all of the structures.



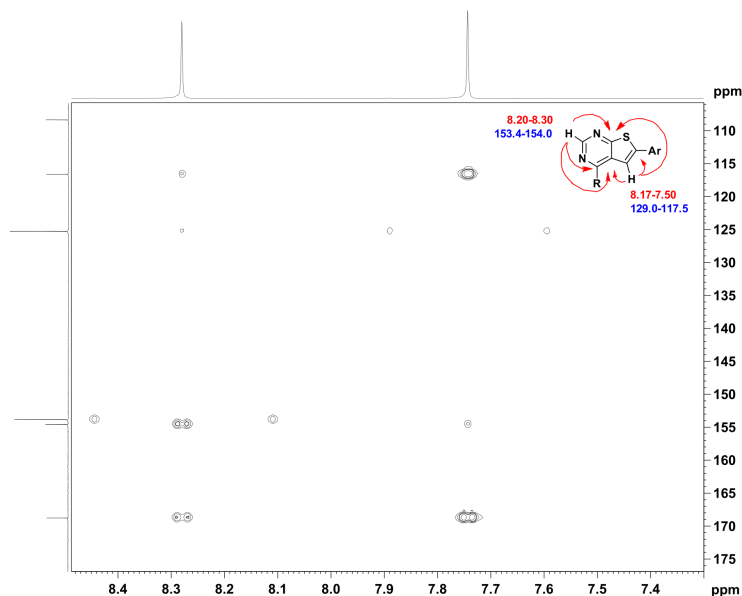


**Figure 3.8:** HMBC coupling of the proton on C-2 (8.29 ppm) to carbons C-4 (155.5 ppm), C-8 (167.3 ppm), and C-9 (117.4 ppm), and of the proton on C-5 (7.90 ppm) to C-6 (136.6 ppm), C-8 (167.3 ppm), and C-9 (117.4 ppm) in compound **6b**.

The protons on C-12 and C-13 for compounds **5-8a** are visible as broad signals in  $^1\text{H}$  NMR. The associated carbons of these signals are poorly visible in all the  $^{13}\text{C}$  spectra, and the C-H couplings are not visible in the HSQC spectra. These shifts are assigned from HMBC by coupling of the C-14 proton to C-12 and C-13, as illustrated in Figure 3.9. Although this coupling is only observed in the HMBC spectrum of *rac-4*, these shifts should be applicable to the other compounds as the introduction of the aryl-group at C-6 does not appear to have any significant impact on the chemical shifts of the C-4 substituent in Tables 3.10-3.17.

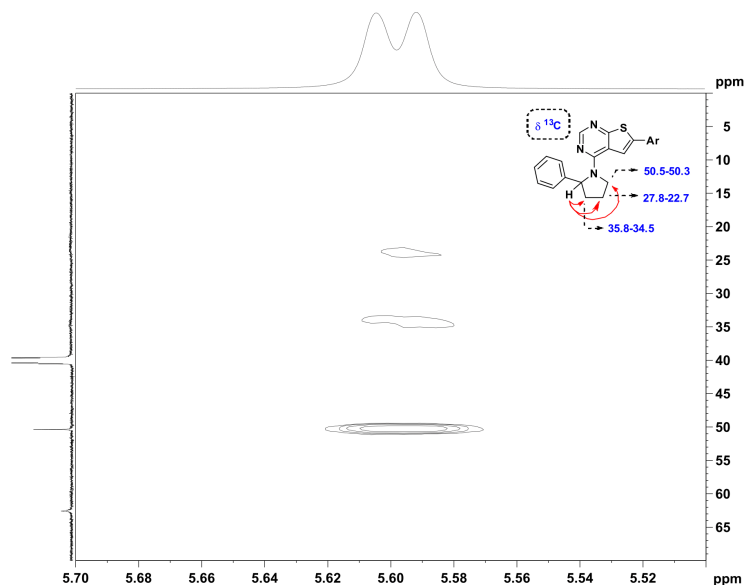


**Figure 3.9:** HMBC coupling of the C-14 proton to C-11-C-13 in compound *rac-4*

The aromatic shifts of compounds **6-8** may be difficult to elucidate, especially when attempting to distinguish these from the aromatic group on the C-4 substituent of compounds **6-8a**. Some key signals to help assign these shifts by HMBC are the CH<sub>2</sub>OH protons for compounds **6a-b** and **8a-b**, the aldehyde proton for compounds **7a-b**, and the methoxy protons for compounds **7a-b** and **8a-b**. Figure 3.10 illustrates the HMBC couplings of these protons to the C-6 aromatic carbons. The proton on C-5 also helps identify the shifts on the C-6 aryl group by HMBC coupling to the nearest carbon on the aromatic ring, as illustrated in Figure 3.10.

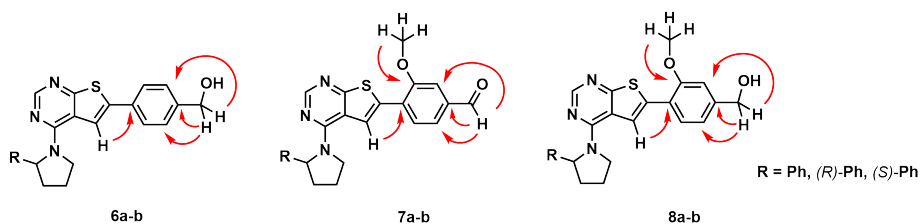


**Figure 3.10:** HMBC coupling of the CH<sub>2</sub>OH-, aldehyde-, and methoxy protons to the aromatic ring on C-6 in compounds **6-8**.

COSY spectra are primarily used to confirm the proton shifts in the pyrrolidine moiety on C-4, and to identify the neighbouring CH<sub>2</sub> protons to the alcohol group, as illustrated in Figure 3.11.

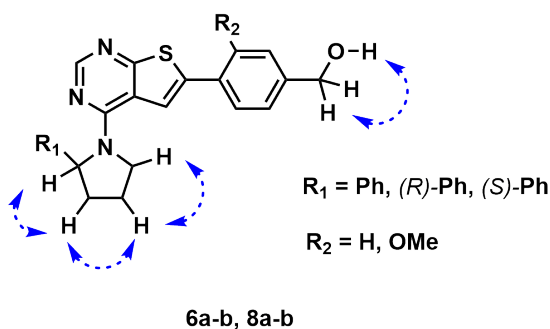


**Figure 3.11:** COSY coupling of the CH<sub>2</sub> and OH protons, and of the protons on C-11-C-13 in compounds **6a-b** and **8a-b**.

### 3.11.1 Compound *rac-5a*

Compounds *rac*-, (*R*)-, and (*S*)-**5a** have near identical <sup>1</sup>H and <sup>13</sup>C NMR shifts, and only the structure elucidation of *rac-5a* is therefore presented in this section. The structure of *rac-5a* with numbering positions is illustrated in Figure 3.12.

#### NMR

The results from <sup>1</sup>H and <sup>13</sup>C NMR of *rac-5a* are presented in Table 3.10. Long range <sup>1</sup>H-<sup>13</sup>C coupling was used to assign quaternary carbons. <sup>1</sup>H NMR, <sup>13</sup>C NMR, IR and MS spectra for compounds *rac*-, (*R*)-, and (*S*)-**5a** are given in Appendix H to J.

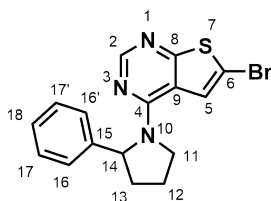


**Figure 3.12:** Numbering of positions in compound *rac-5a*

**Table 3.10:** Assigned  $^1\text{H}$  NMR (400 MHz) and  $^{13}\text{C}$  NMR (150 MHz) shifts for compound *rac*-**5a** in  $\text{DMSO-}d_6$ .

Position	$^{13}\text{C}$ [ppm]	$^1\text{H}$ [ppm] (mult., J [Hz], int.)	COSY	HMBC
2	153.7	8.24 (s, 1H)		
4	154.7			
5	128.9	7.78 (br s, 1H)		
6	108.7			
8	169.1			
9	116.6			
11	50.4	4.20 (br s, 1H) 3.92 (br s, 1H)	11, 12	
12	24.0 <sup>a</sup>	2.00 (br s, 1H) 1.89 (br s, 1H)		
13	34.4 <sup>b</sup>	2.40 (br s, 1H) 1.89 (br s, 1H)		
14	62.6	5.60 (d, J = 7.7, 1H)	13,16/16'	4,11-16
15	143.6			
16/16'	125.9	7.23-7.21 (m, 2H)	14,17,18	14-18
17/17'	128.9	7.31-7.30 (m, 2H)	16,17	15-18
18	127.1	7.23-7.21 (m, 1H)	17	16,17

<sup>a</sup> Poorly visible in  $^{13}\text{C}$  NMR. Shift confirmed by HMBC.

<sup>b</sup> Poorly visible in  $^{13}\text{C}$  NMR. Shift confirmed by HMBC.

### 3.11.2 Compound 5b

The structure of **5b** with numbering positions is illustrated in Figure 3.13.

#### NMR

The results from  $^1\text{H}$  and  $^{13}\text{C}$  NMR are presented in Table 3.11. Long range  $^1\text{H}$ - $^{13}\text{C}$  coupling was used to assign quaternary carbons.  $^1\text{H}$  NMR,  $^{13}\text{C}$  NMR, IR and MS spectra for compound **6b** are given in Appendix K.

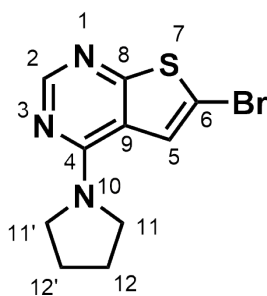


**Figure 3.13:** Numbering of positions in compound **5b**

**Table 3.11:** Assigned  $^1\text{H}$  NMR (600 MHz) and  $^{13}\text{C}$  NMR (150 MHz) shifts for compound **5b** in  $\text{DMSO-}d_6$ .

Position	$^{13}\text{C}$ [ppm]	$^1\text{H}$ [ppm] (mult., J [Hz], int.)	COSY	HMBC
2	153.8	8.28 (s, 1H)		4,8,9
4	154.6			
5	125.3	7.74 (s, 1H)		8,9
6	108.3			
8	168.8			
9	116.6			
11/11'	49.1	3.71 (br s, 4H)	12/12'	
12/12'	25.5	1.96 (br s, 4H)	11/11'	

### 3.11.3 Compound *rac*-**6a**

Compounds *rac*-, (*R*)-, and (*S*)-**6a** have near identical  $^1\text{H}$  and  $^{13}\text{C}$  NMR shifts, and only the structure elucidation of *rac*-**6a** is therefore presented in this section. The structure of *rac*-**6a** with numbering positions is illustrated in Figure 3.14.

#### NMR

The results from  $^1\text{H}$  and  $^{13}\text{C}$  NMR are presented in Table 3.14. Long range  $^1\text{H}$ - $^{13}\text{C}$  coupling was used to assign quaternary carbons.  $^1\text{H}$  NMR,  $^{13}\text{C}$  NMR, IR and MS spectra for compounds *rac*-, (*R*)-, and (*S*)-**6a** are given in Appendix L to O.

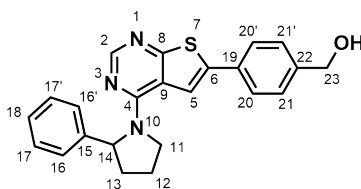


**Figure 3.14:** Numbering of positions in compound *rac*-**6a**

**Table 3.12:** Assigned  $^1\text{H}$  NMR (600 MHz) and  $^{13}\text{C}$  NMR (150 MHz) shifts for compound *rac*-**6a** in  $\text{DMSO-}d_6$ .

Position	$^{13}\text{C}$ [ppm]	$^1\text{H}$ [ppm] (mult., J [Hz], int.)	COSY	HMBC
2	153.5	8.27 (br s, 1H)		
4	155.6			
5	128.9	7.56-7.53 (m, 1H)		19
6	136.7			
8	167.6			
9	117.9			
11	50.5	4.29 (br s, 1H) 4.0 (br s, 1H)		
12	24.0 <sup>a</sup>	1.93 (br s, 1H) 2.04 (br s, 1H)	13	
13	34.4 <sup>b</sup>	2.43 (br s, 1H) 1.93 (br s, 1H)	12	
14	62.9	5.70 (br s, 1H)		
15	144.0			
16/16'	126.0	7.28 (br s, 2H)		
17/17'	129.0	7.31-7.30 (m, 2H)	15	
18	127.1	7.21-7.19 (m, 1H)		16/16'
19	132.5			
20/20'	132.0	7.64-7.61 (m, 2H)		
21/21'	127.6	7.39-7.38 (m, 2H)	23	19,23
22	143.5			
23	62.9	4.54 (d, J = 5.4 Hz, 2H)	21,OH	21,22
OH		5.27 (t, J = 5.7 Hz, 1H)	23	22,23

<sup>a</sup> Poorly visible in  $^{13}\text{C}$  NMR. Shift confirmed by HMBC.

<sup>b</sup> Poorly visible in  $^{13}\text{C}$  NMR. Shift confirmed by HMBC.

### 3.11.4 Compound **6b**

The structure of **6b** with numbering positions is illustrated in Figure 3.15.

## NMR

The results from  $^1\text{H}$  and  $^{13}\text{C}$  NMR are presented in Table 3.13. Long range  $^1\text{H}$ - $^{13}\text{C}$  coupling was used to assign quaternary carbons.  $^1\text{H}$  NMR,  $^{13}\text{C}$  NMR, IR and MS spectra for compound **6b** are given in Appendix P.

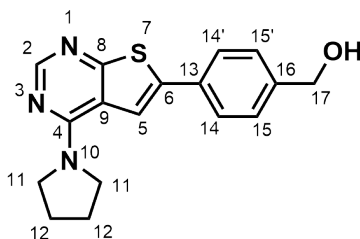


**Figure 3.15:** Numbering of positions in compound **6b**

**Table 3.13:** Assigned  $^1\text{H}$  NMR (600 MHz) and  $^{13}\text{C}$  NMR (150 MHz) shifts for compound **6b** in  $\text{DMSO-}d_6$ .

Position	$^{13}\text{C}$ [ppm]	$^1\text{H}$ [ppm] (mult., J [Hz], int.)	COSY	HMBC
2	153.6	8.29 (s, 1H)		4,8,9
4	155.5			
5	117.5	7.90 (s, 1H)		6,8,9,13,
6	136.6			
8	167.3			
9	117.4			
11/11'	49.2	3.82 (br s, 4H)	12/12'	
12/12'	25.5	1.99 (br s, 4H)	11/11'	
13	132.1			
14/14'	126.1	7.75-7.33 (m, 2H)	15/15'	6,14/14',16
15/15'	127.5	7.40-7.39 (m, 2H)	14/14',17	13,15,17
16	143.4			
17	63.0	4.54 (d, J = 5.7 Hz, 2H)	15/15',OH	15/15',16
OH		5.26 (t, J = 5.7 Hz, 1H)	17	16,17

### 3.11.5 Compound *rac*-7a

Compounds *rac*-, and (*R*)-**7a** have near identical  $^1\text{H}$  and  $^{13}\text{C}$  NMR shifts, and only the structure elucidation of *rac*-**7a** is therefore presented in this section. The structure of *rac*-**7a** with numbering positions is illustrated in Figure 3.16.

## NMR

The results from  $^1\text{H}$  and  $^{13}\text{C}$  NMR are presented in Table 3.16. Long range  $^1\text{H}$ - $^{13}\text{C}$  coupling was used to assign quaternary carbons.  $^1\text{H}$  NMR,  $^{13}\text{C}$  NMR, IR and MS spectra for compounds *rac*-, and (*R*)-**7a** are given in Appendix Q to R.

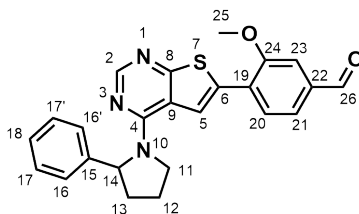


**Figure 3.16:** Numbering of positions in compound *rac*-**7a**



**Table 3.14:** Assigned  $^1\text{H}$  NMR (600 MHz) and  $^{13}\text{C}$  NMR (150 MHz) shifts for compound *rac*-**7a** in  $\text{DMSO-}d_6$ .

Position	$^{13}\text{C}$ [ppm]	$^1\text{H}$ [ppm] (mult., J [Hz], int.)	COSY	HMBC
2	153.9	8.31 (1H)		
4	155.7			
5	122.3	7.80-7.55 (m, 1H)		
6	131.1			
8	168.8			
9	116.0			
11	50.4	4.26 (br s, 1H) 4.0 (br s, 1H)		
12	27.8 <sup>a</sup>	1.95 (br s, 1H) 2.04 (br s, 1H)	13	
13	35.7 <sup>b</sup>	2.44 (br s, 1H) 1.95 (br s, 1H)	12	
14	62.7	5.72 (br s, 1H)		
15	143.8			
16/16'	126.0	7.33-7.29 (m, 2H)		
17/17'	129.0	7.33-7.29 (m, 2H)		
18	127.2	7.23-7.20 (m, 1H)		16/16'
19	127.9			
20	129.0	7.80-7.55 (m, 1H)		
21	123.3	7.80-7.55 (m, 1H)		
22	137.0			
23	112.3	7.80-7.55 (m, 1H)		
24	156.2			
25	56.6	4.0 (br s, 3H)		
26	192.7	10.0 (s, 1H)		21,22,23

<sup>a</sup> Poorly visible in  $^{13}\text{C}$  NMR. Shift confirmed by HSQC.

<sup>b</sup> Poorly visible in  $^{13}\text{C}$  NMR. Shift confirmed by HSQC.

### 3.11.6 Compound **7b**

The structure of **7b** with numbering positions is illustrated in Figure 3.17.

#### NMR

The results from  $^1\text{H}$  and  $^{13}\text{C}$  NMR are presented in Table 3.15. Long range  $^1\text{H}$ - $^{13}\text{C}$  coupling was used to assign quaternary carbons.  $^1\text{H}$  NMR,  $^{13}\text{C}$  NMR, IR and MS spectra for compound **7b** are given in Appendix S.

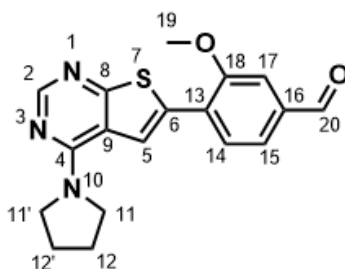


**Figure 3.17:** Numbering of positions in compound **7b**

**Table 3.15:** Assigned  $^1\text{H}$  NMR (600 MHz) and  $^{13}\text{C}$  NMR (150 MHz) shifts for compound **7b** in  $\text{DMSO-}d_6$ .

Position	$^{13}\text{C}$ [ppm]	$^1\text{H}$ [ppm] (mult., J [Hz], int.)	COSY	HMBC
2	154.0	8.33 (s, 1H)		4,8,9
4	155.6			
5	121.9	8.17 (s, 1H)		6,9,13
6	130.9			
8	168.6			
9	116.0			
11/11'	49.2	3.85 (br s, 4H)		
12/12'	25.5	2.01 (br s, 4H)		
13	128.1			
14	129.1	8.14-8.13 (m, 1H)	15	6,16,18
15	123.3	7.63-7.60 (m, 1H)	14	13,17,18,20
16	136.9			
17	112.2	7.63-7.60 (m, 1H)		13,15,18,20
18	156.1			
19	56.7	4.04 (s, 3H)		17,18
20	192.7	10.02 (s, 1H)		

### 3.11.7 Compound *rac*-**8a**

Compounds *rac*-, and (*R*)-**8a** have near identical  $^1\text{H}$  and  $^{13}\text{C}$  NMR shifts, and only the structure elucidation of *rac*-**8a** is therefore presented in this section. The structure of *rac*-**8a** with numbering positions is illustrated in Figure 3.18.

## NMR

The results from  $^1\text{H}$  and  $^{13}\text{C}$  NMR are presented in Table 3.18. Long range  $^1\text{H}$ - $^{13}\text{C}$  coupling was used to assign quaternary carbons.  $^1\text{H}$  NMR,  $^{13}\text{C}$  NMR, IR and MS spectra for compounds *rac*-, and (*R*)-**8a** are given in Appendix T to U.

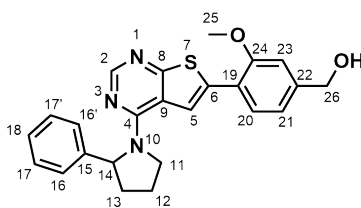


**Figure 3.18:** Numbering of positions in compound *rac-8a*

**Table 3.16:** Assigned  $^1\text{H}$  NMR (600 MHz) and  $^{13}\text{C}$  NMR (150 MHz) shifts for compound *rac-8a* in  $\text{DMSO-}d_6$ .

Position	$^{13}\text{C}$ [ppm]	$^1\text{H}$ [ppm] (mult., J [Hz], int.)	COSY	HMBC
2	153.3	8.28 (s, 1H)		
4	155.5			
5	120.4	7.86-7.53 (m, 1H)		
6	132.0			
8	167.9			
9	116.1			
11	50.3	4.22 (br s, 1H) 3.98 (br s, 1H)	12	
12	22.7 <sup>a</sup>	1.92 (br s, 1H) 2.01 (br s, 1H)	11	
13	35.5 <sup>b</sup>	2.42 (br s, 1H) 1.92 (br s, 1H)	14	
14	62.6	5.69 (s, 1H)	13	
15	144.0			
16/16'	126.0	7.32-7.31 (m, 2H)		14
17/17'	129.0	7.32-7.31 (m, 2H)		
18	127.1	7.22-7.20 (m, 1H)		
19	128.3			
20	129.0	7.86-7.53 (m, 1H)		
21	119.3	6.98-6.97 (m, 1H)		23,26
22	145.1			
23	110.5	7.10 (s, 1H)		21,26
24	155.9			
25	56.2	3.87 (s, 3H)		
26	63.0	4.53 (d, J = 5.0 Hz, 2H)	OH	21,22,23
OH		5.29 (t, J = 5.5 Hz, 1H)	26	22,26

<sup>a</sup> Poorly visible in  $^{13}\text{C}$  NMR. Shift confirmed by HSQC.

<sup>b</sup> Poorly visible in  $^{13}\text{C}$  NMR. Shift confirmed by HSQC.

### 3.11.8 Compound 8b

The structure of **8b** with numbering positions is illustrated in Figure 3.19.

#### NMR

The results from  $^1\text{H}$  and  $^{13}\text{C}$  NMR are presented in Table 3.17. Long range  $^1\text{H}$ - $^{13}\text{C}$  coupling was used to assign quaternary carbons.  $^1\text{H}$  NMR,  $^{13}\text{C}$  NMR, IR and MS spectra for compound **8b** are given in Appendix V.

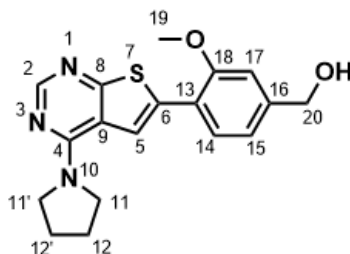


**Figure 3.19:** Numbering of positions in compound **8b**

**Table 3.17:** Assigned  $^1\text{H}$  NMR (600 MHz) and  $^{13}\text{C}$  NMR (150 MHz) shifts for compound **8b** in  $\text{DMSO-}d_6$ .

Position	$^{13}\text{C}$ [ppm]	$^1\text{H}$ [ppm] (mult., J [Hz], int.)	COSY	HMBC
2	153.4	8.29 (s, 1H)		4,8
4	155.9			
5	118.9	7.95 (s, 1H)		4,6,8,9,13
6	132.7			
8	167.7			
9	116.1			
11/11'	49.1	3.81 (br s, 4H)		
12/12'	25.5	2.0 (br s, 4H)		
13	120.6			
14	128.4	7.78 (s, 1H)	15	6,16,17,18
15	119.3	7.01 (s, 1H)	14	13,17,20
16	145.0			
17	110.5	7.13 (s, 1H)		13,16,18,20
18	155.9			
19	56.2	3.95 (s, 3H)		
20	63.1	4.55 (d, J = 5.7 Hz, 1H)	OH	15,16,17
OH		5.29 (t, J = 5.8 Hz, 1H)	20	16,20

## 4 | Concluding Remarks and Further Work

### 4.1 Summary

Investigation of several potential synthetic routes to (*R*)- and (*S*)-2-phenylpyrrolidine ((*R*)- and (*S*)-**4**) found palladium-catalyzed  $\alpha$ -arylation to be a viable and simple method for obtaining these compounds. The compounds were synthesized from pyrrolidine, starting with Boc protection to form compound **1** in 92-94 % yield. Palladium-catalyzed  $\alpha$ -Arylation of **1** gave the Boc-protected 2-phenylpyrrolidines (*R*)- and (*S*)-**3** in 62 % and 70 % yield, and with 81 % and 96 % ee, respectively. Differences in ee of (*R*)- and (*S*)-**3** is suspected due to divergences in the enantiopurity of (-)- and (+)-sparteine. Boc deprotection of compounds (*R*)- and (*S*)-**3** with TFA gave (*R*)- and (*S*)-**4** in 56 % and 49 % yield, respectively.

Racemic 2-phenylpyrrolidine (*rac*-**4**) was prepared from pyrrolidin-2-one in a two-step, one-pot procedure involving a silylation and Grignard reaction, followed by an imine reduction of the intermediary 2-phenylpyrroline (**2**). Achieving full conversion of starting material during the initial silylation proved challenging, and some erratic results were observed with the use of the Grignard reagent. Suspected causes for these issues are the attachment of Me<sub>3</sub>Si to both the nitrogen and the oxygen of pyrrolidin-2-one, and possible interactions between the Grignard reagent and the silyllactam at silicon. Attempted optimization of the one-pot reaction gave compound **2** in 12-36 % yield. Reduction of **2** with sodium borohydride gave *rac*-**4** in 72-89 % yield.

Nucleophilic aromatic substitution of 6-bromo-4-chlorothieno[2,3-*d*]pyrimidine with amines *rac*-, (*R*)-, and (*S*)-**4**, in addition to pyrrolidine, gave compounds **5a-b** in 50-91 % yield. Suboptimal conversion of the thieno[2,3-*d*]pyrimidine was observed in the synthesis of (*R*)- and (*S*)-**5a**, likely due to the presence of TFA salt in these amines. A surplus of Hünig's base was added in the reaction of (*R*)-**5a** to help deprotonate the salt, which gave considerably higher conversion and yield compared to the reaction of (*S*)-**5a**.

Suzuki cross-coupling of thieno[2,3-*d*]pyrimidines **5a-b** was done using catalyst

Pd(PPh<sub>3</sub>)<sub>4</sub>, and yielded compounds **6-7** in 60-99 % yield. Dimerization of the boronic acid was observed in the reactions of *rac*-**6a** and **-7a**, likely due to oxidation of the palladium catalyst because of insufficient degassing of the solvents. Proper degassing resulted in minute amounts of by-product and increased the yield of later reactions.

Reduction of thieno[2,3-*d*]pyrimidine aldehydes **7a-b** to primary alcohols **8a-b** was done using sodium borohydride, and gave full conversion and 48-99 % yields. Loss of yield from workup and purification was due to poor solubility of these compounds.

Target compounds (*R*)- and (*S*)-**6a**, and (*R*)-**8a** were analysed by CSP-HPLC to check the ee of the final products. The ee was found to be 65 % for compounds (*R*)- and (*S*)-**6a** and 84 % for (*R*)-**8a**, marking a significant decrease in enantiopurity from compounds (*R*)- and (*S*)-**3**. A suspected cause is racemization in the S<sub>N</sub>Ar reactions.

This masters's thesis has presented preliminary results in the structure-activity relationship study of thieno[2,3-*d*]pyrimidines with heterocyclic tertiary amines as a substituent on C-4. Of the 14 new thieno[2,3-*d*]pyrimidines, seven new thienopyrimidine-based inhibitor candidates were prepared. Single point analysis identified two of these compounds, *rac*- and (*R*)-**8a**, as potent EGFR-TK inhibitors with IC<sub>50</sub> values of 30.6 and 5.8 nM, respectively. This demonstrates that it is possible to obtain high EGFR-TK activity with tertiary amines at C-4. The single-point analyses further indicate that the 2-substituted phenyl moiety on the amines may contribute favourably to the EGFR-TK activity, depending on the stereochemistry. The (*R*)-enantiomers were found to exhibit better inhibition compared to the racemates, while the (*S*)-enantiomer exhibited poor activity. Removal of the phenyl group proved detrimental for the EGFR-TK activity, which supports the proposed theory that the EGFR-TK activity of thieno[2,3-*d*]pyrimidines is related to the conformation of the C-4 amino group, as opposed to hydrogen donor ability.

Single point analyses on CSF1R activity were also performed, and found compound (*R*)-**8a** to possess good activity with 86 % inhibition. Analyses found compounds without the 2-substituted phenyl group on the amine (compounds **6b** and **8b**) to possess activity on a par with, or higher than the racemates. This may suggest that the conformation of the pyrroline moiety is of importance to the CSF1R activity, and that the 2-substituted phenyl group interacts favourably or unfavourably, depending on the chirality. The activity of compounds (*S*)-**6a** (5 %) and (*R*)-**6a** (73 %), with opposite stereochemistry of the phenyl group, supports this statement.

## 4.2 Further work

The discovery of compounds *rac*- and (*R*)-**8a** with high EGFR-TK facilitates further investigation of thieno[2,3-*d*]-, pyrrolo-, and furopyrimidines with a tertiary amine as the substituent on C-4. These structures may open new areas of research with the preparation of different heterocyclic or non-heterocyclic tertiary amines as the

substituent. As an extension of this master's thesis, further analysis, modelling and X-ray co-crystal structure determination of the compounds *rac*- and (*R*)-**8a** should be performed for future SAR studies.

As the chirality of the 2-substituted phenyl moiety on the C-4 substituent has been found to influence the EGFR-TK activity, investigation of the possible racemization in the reactions from compounds (*R*)- and (*S*)-**3** to target compounds (*R*)- and (*S*)-**6a** and (*R*)-**8a** is imperative for future studies. A viable method for this study would be to perform chiral analyses after each reaction step, to check for any changes in ee. Methods for preparing the tertiary amines with higher ee could also be further investigated. Some alternate synthetic procedures with high enantioselectivity have been presented in this master's thesis, including asymmetric hydrogenation and chemoenzymatic routes. A method for improving upon the enantiopurity of the already synthesized compounds by recrystallization has also been suggested, which may present compounds with improved EGFR-TK activity.





# 5 | Experimental

## 5.1 General

6-bromo-4-chlorothieno[2,3-*d*]pyrimidine had been synthesized and purified as part of previous studies in our research group, and the available compound was used in the reactions mentioned below.<sup>[143]</sup> Unless otherwise stated, all other reagents in this project were of synthetic or analytical grade and were supplied by Sigma-Aldrich.

### 5.1.1 Separation techniques

Thin-layer chromatography (TLC) was used to follow the reaction progress, and to check for conversion of starting materials (Silica gel on aluminium sheets, F<sub>254</sub>). Silica gel column chromatography was performed using Silica gel 60A from EMD Millipore, pore size 40-63  $\mu\text{m}$ .

### 5.1.2 Spectroscopic analysis

NMR analyses were performed using Bruker 400 MHz Avance III HD equipped with a 5-mm SmartProbe z-gradient probe and SampleCase, and Bruker 600 MHz Avance III HD equipped with a 5-mm cryogenic CP-TCI z-gradient probe and SampleCase. DMSO-*d*<sub>6</sub> was used as solvent for the analyses, and the chemical shifts, reported in  $\delta$  (ppm), are relative to the solvent peak of DMSO-*d*<sub>6</sub> (2.50 ppm in <sup>1</sup>H NMR and 39.52 ppm in <sup>13</sup>C NMR<sup>[130]</sup>). Traces of water are usually present when using DMSO-*d*<sub>6</sub>, and can be detected at 3.33 ppm (s) in <sup>1</sup>H NMR.<sup>[130]</sup> Traces of solvents may also be present in the spectra: EtOAc (1.99 ppm (s), 4.03 ppm (q), 1.17 ppm (t)), n-pentane (0.86 ppm (t), 1.27 ppm (m)), dichloromethane (5.76 ppm (s)), 1,4-dioxane (3.57 ppm (s)).<sup>[130]</sup> Apiezon brand H grease (0.82-0.88 ppm (m), 1.24 ppm (br s)) may also be present in some of the spectra.<sup>[130]</sup> The coupling constants (J) are given in Hz, and the signals are defined according to their multiplicity: s (singlet), d (doublet), t (triplet), q (quartet). Multiplets (m) are defined as intervals.

HPLC was performed using an Agilent 1100 Series instrument with a 1260 infinity degasser, 1100 Series quaternary pump, 1100 Series autosampler, and a 1200 Series diode array detector. The software used was Agilent ChemStation. Spectra were recorded for wavelengths 230 nm, 254 nm, and 280 nm. The column was an Agilent Eclipse XDB-C18 (5  $\mu\text{m}$ , 4.6 x 150 mm) with a flow of 0.8 mL/min. The

method started with isocratic elution with water:CH<sub>3</sub>CN (90:10) for 5 min followed by a linear gradient ending at water:CH<sub>3</sub>CN (0:100) over 35 min. Chiral HPLC analyses were conducted through two methods. Method A: Chiralpak AD 0.46 x 25 cm chiral column (part no. 00CE-FE167), eluting with hexane:*i*-PrOH, 99:1, flow rate: 0.3 mL/min, detection at 254 nm. Method B: Lux 5u Cellulose-1 4.6 x 250 mm chiral column (part no. 00G-4459-E0), eluting with hexane (cont. 0.2% diethyl amine):*i*-PrOH, 85:15, flow rate: 1.5 mL/min, detection at 254 nm.

Accurate mass determination in positive and negative mode was performed on a "Synapt G2-S" Q-TOF instrument from Waters<sup>TM</sup>. Samples were ionized by the use of ASAP probe (APCI) or ESI probe. Calculated exact mass and spectra processing was done by Waters<sup>TM</sup> Software Masslynx V4.1 SCN871.

The IR analyses was performed using Bruker Alpha ECO-ATR FTIR-spectrometer, and processing software OPUS.

### 5.1.3 Melting point

The melting point analyses was performed using a Stuart automatic melting point SMP40 instrument (1 °C/min).

### 5.1.4 Optical rotation

Due to technical issues with the polarimeter, optical rotation measurements were not available for this master's thesis.

## 5.2 General procedure for $\alpha$ -arylations

*N*-Boc pyrrolidine (0.37 mL, 2.13 mmol) was dissolved in *tert*-butyl methyl ether (4.5 mL) and added (+)- or (-)-sparteine (500 mg, 2.1 mmol), depending on the desired enantiomer. The solution was cooled to -78 °C using dry ice, before adding *s*-BuLi (1.56 mL of a 1.4 M solution in cyclohexane, 2.18 mmol) dropwise slowly over 13 minutes. The solution was stirred at -78 °C for three hours. ZnCl<sub>2</sub> (1.3 mL of a 1 M solution in diethyl ether, 1.3 mmol) was added dropwise slowly over 11 minutes, and the solution was stirred at -78 °C for an 30 minutes. The mixture was allowed to warm to room temperature and stir for an additional 30 minutes. Bromobenzene (0.20 mL, 1.91 mmol) was added, followed by Pd(OAc)<sub>2</sub> (20.5 mg, 0.10 mmol) and *t*-Bu<sub>3</sub>P-HBF<sub>4</sub> (32.0 mg, 0.11 mmol), and the solution was stirred for 13 hours. Aqueous ammonia (2.0 mL) was added, and the solution was stired for one hour. The mixture was filtered through Celite and washed with *tert*-butyl methyl ether. The filtrate was washed with 1 N HCl and water, dried over MgSO<sub>4</sub>, filtered, and concentrated in vacuo. The crude product was purified by silica gel column chromatography.

### 5.3 General procedure for Boc-deprotection

Compound (*R*)- or (*S*)-**3** (227-293 mg, 0.92-1.19 mmol) was dissolved in CH<sub>2</sub>Cl<sub>2</sub> (10 mL), and cooled to 0 °C. TFA (19.6-24.8 mmol) was added, and the solution was stirred at room temperature for 4 hours. The solvent was removed in a rotary evaporator, before adding EtOAc (15 mL), 2M NaOH (10 mL), and NEt<sub>3</sub> (2.5 mL). The phases were separated, and the aquatic phase was extracted with more EtOAc.

### 5.4 General procedure for nucleophilic aromatic substitution

6-Bromo-4-chlorothieno[2,3-*d*]pyrimidine (0.3-2.5 g) was mixed with the selected amine (~1.5 eq.), Hünig's base (1.5-14 eq.), and *i*-PrOH (2-8 mL). The solution was stirred at 80 °C under a N<sub>2</sub> atmosphere until full conversion. The mixture was then cooled to room temperature and diluted with water (40 mL) and diethyl ether (40 mL). After phase separation, the water phase was extracted with more diethyl ether (2 x 40 mL). The combined organic phase was washed with saturated aq NaCl solution (15-20 mL), filtered and concentrated in vacuo. The crude product was purified by drying under reduced pressure to constant weight, and by silica gel column chromatography.

### 5.5 General procedure for Suzuki cross-coupling

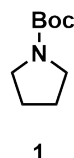
Compound **5a-b** (100-500 mg) was mixed with the selected arylboronic acid (1.2 eq.), fine powdered K<sub>2</sub>CO<sub>3</sub> (3 eq.), Pd(PPh<sub>3</sub>)<sub>4</sub> (0.01 eq.) and 1,4-dioxane:water (1:1 by vol.%, 2-12 mL). The 1,4-dioxane:water mixture was degassed using nitrogen. The reaction was stirred at 80 °C for 4.5-20 hours under a N<sub>2</sub> atmosphere. The solvent was removed and the product was diluted with water (50-100 mL), and diethyl ether or dichloromethane (50-100 mL). After phase separation the water phase was extracted with more diethyl ether or dichloromethane (2 x 25 mL). The combined organic phase was washed with saturated aq NaCl solution (25-50 mL), filtered and concentrated in vacuo. The crude product was purified by drying under reduced pressure to constant weight and by silica gel column chromatography.

### 5.6 General procedure for reduction using NaBH<sub>4</sub>

Compound **7a-b** was dissolved in THF:MeOH (3:1, 20 mL) and mixed with NaBH<sub>4</sub> (1 eq.). The reaction was stirred for 30 minutes at room temperature before additional NaBH<sub>4</sub> (1 eq.) was added. The mixture was stirred for another 30 minutes, and concentrated to about 5 mL. The residue was diluted with EtOAc (50 mL) and water (50 mL), and the water phase was extracted with more EtOAc (2 x 25 mL). The combined organic phase was washed with saturated aq NaCl solution (25 mL), filtered and concentrated in vacuo. The product was purified by drying under reduced pressure to constant weight.

### 5.6.1 *N*-Boc-pyrrolidine (**1**)<sup>[126]</sup>

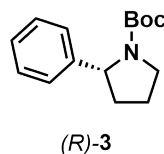
Pyrrolidine (1.0 mL, 12 mmol) was added to di-*tert*-butyl dicarbonate (2.62 g, 12.0 mmol), and the mixture was stirred at room temperature for 2 minutes. The solution was diluted with water, and extracted with EtOAc. The organic phase was washed with saturated aq. NaCl solution, filtered and concentrated in vacuo to yield 1.89 g (11.0 mmol, 92 %) of compound **1** as a yellow oil.



Spectroscopic data (Appendix A): <sup>1</sup>H NMR (400 MHz, DMSO-*d*<sub>6</sub>) δ: 3.19-3.18 (m, 4H), 1.77-1.76 (m, 4H), 1.39 (s, 9H). <sup>1</sup>H NMR data was in accordance with previously reported values.<sup>[126]</sup>

### 5.6.2 (*R*)-*N*-Boc-2-phenylpyrrolidine ((*R*)-**3**)<sup>[52][86]</sup>

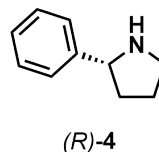
Compound (*R*)-**3** was prepared as described in section 5.2, using (-)-sparteine (500 mg, 2.13 mmol). The reaction was left for 13 hours, and purification by silica gel column chromatography (*n*-pentane:EtOAc, 6:1, *R<sub>f</sub>* = 0.48) yielded 329 mg (1.33 mmol, 62 %) of (*R*)-**3** as a white, crystalline solid; mp = 62.6-63.5 °C (lit.<sup>[86]</sup> 61.9-62.7 °C); Chiral HPLC (Method A): *t<sub>R</sub>* = 24.9 (major), *t<sub>R</sub>* = 26.7 (minor).



Spectroscopic data (Appendix C): <sup>1</sup>H NMR (400 MHz, DMSO-*d*<sub>6</sub>) (40:60 mixture of rotamers) δ: 7.33-7.29 (m, 2H), 7.23-7.15 (m, 3H), 4.82 (br s, 0.4H), 4.70 (br s, 0.6H), 3.56-3.46 (m, 2H), 2.30 (br s, 1H), 1.81-1.78 (m, 2H), 1.70 (br s, 1H), 1.40 (s, 4H), 1.09 (s, 5H). <sup>1</sup>H NMR data was in accordance with previously reported values.<sup>[86][52][89]</sup>

### 5.6.3 (*R*)-2-Phenylpyrrolidine ((*R*)-**4**)<sup>[52]</sup>

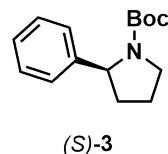
Compound (*R*)-**4** was prepared as described in Section 5.3, starting with (*R*)-**3** (293 mg, 1.19 mmol). The reaction time was 4 hours, and purification by silica gel column chromatography (*n*-pentane:EtOAc, 9:1, *R<sub>f</sub>* = 0.11) yielded 248 mg (0.66 mmol, 56 %) of (*R*)-**4**. The product was an orange oil.



Spectroscopic data (Appendix F): <sup>1</sup>H NMR (400 MHz, DMSO-*d*<sub>6</sub>) δ: 7.42-7.40 (m, 2H), 7.38-7.34 (m, 2H), 7.31-7.27 (m, 1H), 4.26 (t, *J* = 8.1, 1H), 3.20-3.14 (m, 1H), 3.13 (br s, 1H) (missing), 3.10-3.04 (m, 1H), 2.27-2.19 (m, 1H), 1.98-1.81 (m, 2H), 1.77-1.67 (m, 1H). <sup>1</sup>H NMR data was in accordance with previously reported values.<sup>[144]</sup>

### 5.6.4 (*S*)-*N*-Boc-2-phenylpyrrolidine ((*S*)-3)<sup>[52][86]</sup>

Compound (*S*)-3 was prepared as described in section 5.2, using (+)-sparteine (500 mg, 2.13 mmol). The reaction was for 17 hours, and purification by silica gel column chromatography (*n*-pentane:EtOAc, 6:1, *R<sub>f</sub>* = 0.67) yielded 374 mg (70 %, 1.51 mmol) of (*S*)-3 as a white, crystalline solid; mp = 62.6-63.5 °C (lit.<sup>[86]</sup> 61.9-62.7 °C); Chiral HPLC (Method A): *t<sub>R</sub>* = 24.9 (minor), *t<sub>R</sub>* = 26.7 (major).



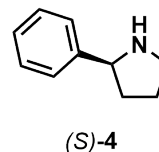
Spectroscopic data (Appendix D): <sup>1</sup>H NMR (400 MHz, DMSO-*d*<sub>6</sub>) (40:60 mixture of rotamers) δ 7.33-7.29 (m, 2H), 7.23-7.15 (m, 3H), 4.82 (br s, 0.4H), 4.70 (br s, 0.6H), 3.56-3.46 (m, 2H), 2.30 (br s, 1H), 1.80-1.78 (m, 2H), 1.70 (br s, 1H), 1.40 (s, 4H), 1.09 (s, 5H). <sup>1</sup>H NMR data was in accordance with previously reported values.<sup>[86][52][89]</sup>

### 5.6.5 (*S*)-2-Phenylpyrrolidine ((*S*)-4)

The synthesis of compound (*S*)-4 was carried out through two different synthetic routes:

#### Boc deprotection<sup>[52]</sup>

Compound (*S*)-4 was prepared as described in Section 5.3, starting with (*S*)-3 (227 mg, 0.92 mmol). The reaction time was 4 hours, and purification by silica gel column chromatography (*n*-pentane:EtOAc, 9:1, *R<sub>f</sub>* = 0.11) yielded 168 mg (0.45 mmol, 49 %) of (*S*)-4. The product was an orange oil.



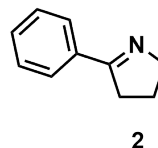
#### Chiral resolution<sup>[54]</sup>

Compounds(*rac*)-4 was dissolved in EtOH:EtOAc (35 %, 6 mL) and added Dibenzoyl-*D*-tartaric acid (1.24 g, 3.45 mmol). The solution was heated to reflux for 10 minutes, and then allowed to cool to room temperature for 24 hours. The solution was refrigerated for an additional 24 hours, and the crystals were then collected and rinsed with cold EtOAc. The crystals were dissolved in 2 M NaOH:CH<sub>2</sub>Cl<sub>2</sub> (50 mL) and stirred vigorously for 15 minutes. Phase separation and extraction with CH<sub>2</sub>Cl<sub>2</sub> (10 mL), followed by concentration in vacuo, yielded 500 mg (3.40 mmol, 49 %) of (*S*)-4 as an orange oil; Chiral HPLC (Method A): *t<sub>R</sub>* = 22.3 (minor), *t<sub>R</sub>* = 23.5 (major).

Spectroscopic data (Appendix G): <sup>1</sup>H NMR (400 MHz, DMSO-*d*<sub>6</sub>) δ: 7.43-7.42 (m, 2H), 7.39-7.36 (m, 2H), 7.32-7.29 (m, 1H), 4.33-4.28 (m, 1H), 3.23-3.17 (m, 1H), 3.14-3.07 (m, 1H), 3.13 (br s, 1H) (missing), 2.28-2.21 (m, 1H), 1.99-1.85 (m, 2H), 1.81-1.73 (m, 1H). <sup>1</sup>H NMR data was in accordance with previously reported values.<sup>[144]</sup>

### 5.6.6 2-Phenylpyrroline (2)<sup>[57]</sup>

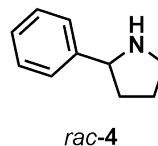
Pyrrolidin-2-one (524 mg, 6.16 mmol) was dissolved in dry ethyl ether (14 mL) and added NEt<sub>3</sub> (0.90 mL, 6.5 mmol). The solution was cooled to 0 °C in an ice bath. Me<sub>3</sub>SiCl (0.82 mL, 6.5 mmol) was added dropwise over 20 minutes using a syringe pump, and the reaction mixture was stirred vigorously using a mechanical stirrer. The reaction was heated to reflux, and stirred under reflux for 1 hour. After allowing to cool to room temperature, the reaction was filtered and washed with EtOAc. The filtrate was evaporated in vacuo, and dissolved in dry ethyl ether (10 mL). PhMgBr (4.20 mL of a 3M solution in diethyl ether, 12.6 mmol) was added to the solution under N<sub>2</sub> atmosphere. The solution was heated to reflux, and stirred at this temperature for 3 hours. The solution was allowed to cool to room temperature, before it was quenched with 1M HCl (6.3 mL). The layers were separated, and the aqueous phase was made basic with 2M NaOH (6.3 mL). The aqueous phase was extracted with EtOAc (3\*15 mL), and the combined organic phases were washed with brine (15 mL), filtered and concentrated in vacuo. The product was purified by silica-gel column chromatography (EtOAc:*n*-pentane, 2:1, *R<sub>f</sub>*= 0.43), yielding 322 mg (2.22 mmol, 36 %) of **2** as an orange oil.



Spectroscopic data (Appendix B): <sup>1</sup>H NMR (400 MHz, DMSO-*d*<sub>6</sub>) δ 7.85-7.83 (m, 2H), 7.46-7.45 (m, 3H), 3.97-3.93 (m, 2H), 2.94-2.90 (m, 2H), 1.99-1.91 (m, 2H). <sup>1</sup>H NMR data was in accordance with previously reported values.<sup>[57]</sup>

### 5.6.7 2-Phenylpyrrolidine (*rac*-4)

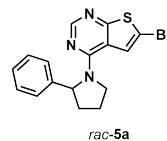
Compound **2** (1.36 g, 9.34 mmol) was dissolved in MeOH:H<sub>2</sub>O (4:1, 25 mL) and added NaBH<sub>4</sub> (405 mg, 10.7 mmol). The solution was stirred for 22 hours at room temperature. Then 2M HCl (15 mL) was added to bring the pH of the solution to 0-2, and the solution was stirred for an additional 30 minutes. 2M NaOH (15 mL) was added to bring the pH of the solution to 13-14, and the organic phase was extracted with dichloromethane (3 x 25 mL). The product was purified by column chromatography (EtOAc:*n*-pentane, 1:1, *R<sub>f</sub>*= 0.44), yielding 1.22 g (8.29 mmol, 89 %) of *rac*-**4** as a yellowish oil.



Spectroscopic data (Appendix E): (400 MHz, DMSO-*d*<sub>6</sub>) δ 7.37-7.35 (m, 2H), 7.30-7.26 (m, 2H), 7.20-7.17 (m, 1H), 4.01 (t, *J* = 7.62 Hz, 1H), 3.13 (br s, 1H), 3.05-3.00 (m, 1H), 2.91-2.85 (m, 1H), 2.14-2.06 (m, 1H), 1.83-1.67 (m, 2H), 1.51-1.42 (m, 1H). <sup>1</sup>H NMR data was in accordance with previously reported values.<sup>[53]</sup>

### 5.6.8 6-Bromo-4-(2-phenylpyrrolidin-1-yl)thieno[2,3-*d*]-pyrimidine (*rac*-5a)

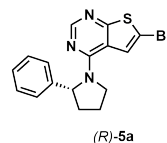
Compound *rac*-5a was prepared as described in Section 5.4, using 6-bromo-4-chlorothieno[2,3-*d*]pyrimidine (230 mg, 0.92 mmol), *rac*-4 (200 mg, 1.36 mmol) and Hünig's base (0.24 mL, 1.36 mmol). The reaction time was 1.25 hours, and purification by silica gel column chromatography (*n*-pentane:EtOAc, 6:1, *R<sub>f</sub>* = 0.24) yielded 265 mg (0.74 mmol, 80 %) of *rac*-5a as a white, crystalline solid; mp = 145.1-146.3 °C; HPLC purity: > 99%, *t<sub>R</sub>*=26.8 min.



Spectroscopic data (Appendix H): <sup>1</sup>H NMR (400 MHz, DMSO-*d*<sub>6</sub>) δ: 8.24 (s, 1H), 7.78 (br s, 1H), 7.31-7.30 (m, 2H), 7.23-7.21 (m, 3H), 5.60 (d, *J* = 7.8 Hz, 1H), 4.20 (br s, 1H), 3.92 (br s, 1H), 2.40 (br s, 1H), 2.01 (br s, 1H), 1.89 (br s, 2H); <sup>13</sup>C NMR (150 MHz, DMSO-*d*<sub>6</sub>) δ: 169.1, 154.7, 153.7, 143.6, 128.9 (2C), 127.1, 125.9 (2C), 125.4, 116.6, 108.7, 62.6, 50.4, 35.0, 23.8; IR (neat, *cm*<sup>-1</sup>): 2971, 2873, 1541, 1469, 1304, 1061, 840, 770, 698; HRMS(ESI/APCI, *m/z*): 360.0165 (calcd. C<sub>16</sub>H<sub>14</sub><sup>79</sup>BrN<sub>3</sub>S, 360.0170, [M+H]<sup>+</sup>).

### 5.6.9 (*R*)-6-Bromo-4-(2-phenylpyrrolidin-1-yl)thieno[2,3-*d*]-pyrimidine (*R*)-5a

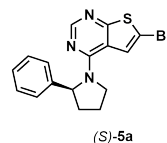
Compound (*R*)-5a was prepared as described in Section 5.4, using 6-bromo-4-chlorothieno[2,3-*d*]pyrimidine (302 mg, 1.21 mmol), (*R*)-4 (248 mg, 1.69 mmol), Hünig's base (3.0 mL, 17 mmol) and *i*-PrOH (8 mL). The reaction time was 24 hours, and purification by silica gel column chromatography (*n*-pentane:EtOAc, 6:1, *R<sub>f</sub>* = 0.38) yielded 320 mg (0.89 mmol, 74 %) of (*R*)-5a as a yellow oil.



Spectroscopic data (Appendix I): <sup>1</sup>H NMR (400 MHz, DMSO-*d*<sub>6</sub>) δ: 8.24 (br s, 1H), 7.78 (br s, 1H), 7.32-7.29 (m, 2H), 7.23-7.21 (m, 3H), 5.60 (d, *J* = 7.6 Hz, 1H), 4.19 (br s, 1H), 3.91 (br s, 1H), 2.38 (br s, 1H), 1.99 (br s, 1H), 1.90-1.88 (m, 2H); <sup>13</sup>C NMR (100 MHz, DMSO-*d*<sub>6</sub>) δ: 169.1, 154.6, 153.7, 143.6, 128.9 (2C), 127.1, 125.9 (2C), 125.4, 116.6, 108.7, 62.6, 50.4, 34.4, 23.6; IR (neat, *cm*<sup>-1</sup>): ; HRMS(ESI/APCI, *m/z*) 360.0169 (calcd. C<sub>16</sub>H<sub>14</sub><sup>79</sup>BrN<sub>3</sub>S, 360.0170, [M+H]<sup>+</sup>).

### 5.6.10 (*S*)-6-Bromo-4-(2-phenylpyrrolidin-1-yl)thieno[2,3-*d*]-pyrimidine (*S*)-5a

Compound (*S*)-5a was prepared as described in Section 5.4, using 6-bromo-4-chlorothieno[2,3-*d*]pyrimidine (203 mg, 0.81 mmol), (*S*)-4 (206 mg, 0.81 mmol), Hünig's base (0.19 mL, 1.1 mmol) and *i*-PrOH (8 mL). The reaction time was 24 hours, and purification by silica gel column chromatography (*n*-pentane:EtOAc, 6:1, *R<sub>f</sub>*

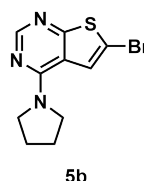


= 0.38) yielded 147 mg (0.41 mmol, 50 %) of (*S*)-**5a** as a yellow oil.

Spectroscopic data (Appendix J):  $^1\text{H}$  NMR (400 MHz,  $\text{DMSO-}d_6$ )  $\delta$ : 8.24 (s, 1H), 7.78 (br s, 1H), 7.32-7.29 (m, 2H), 7.23-7.21 (m, 3H), 5.60 (d,  $J = 7.7$  Hz, 1H), 4.19 (br s, 1H), 3.92 (m, 1H), 2.38 (br s, 1H), 2.0 (br s, 1H), 1.90-1.88 (m, 2H);  $^{13}\text{C}$  NMR (100 MHz,  $\text{DMSO-}d_6$ )  $\delta$ : 169.1, 154.6, 153.7, 143.6, 128.9 (2C), 127.1, 125.9 (2C), 125.4, 116.6, 108.7, 62.6, 50.4, 34.6, 24.7; IR (neat,  $\text{cm}^{-1}$ ); HRMS(ESI/APCI,  $m/z$ ) 360.0166 (calcd.  $\text{C}_{16}\text{H}_{14}^{79}\text{BrN}_3\text{S}$ , 360.0170,  $[\text{M}+\text{H}]^+$ )

### 5.6.11 6-Bromo-4-(pyrrolidin-1-yl)thieno[2,3-*d*]-pyrimidine (**5b**)

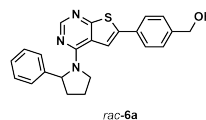
Compound **5b** was prepared as described in Section 5.4, using 6-bromo-4-chlorothieno[2,3-*d*]pyrimidine (416 mg, 1.67 mmol), pyrrolidine (0.21 mL, 2.56 mmol) and Hünig's base (0.42 mL, 2.41 mmol). The reaction time was 1.5 hours, and drying yielded 432 mg (1.52 mmol, 91 %) of **5b** as a brownish solid; mp = 131.2-132.2 °C.



Spectroscopic data (Appendix K):  $^1\text{H}$  NMR (600 MHz,  $\text{DMSO-}d_6$ )  $\delta$ : 8.28 (s, 1H), 7.74 (s, 1H), 3.71 (br s, 4H), 1.96 (br s, 4H);  $^{13}\text{C}$  NMR (150 MHz,  $\text{DMSO-}d_6$ )  $\delta$ : 168.8, 154.6, 153.8, 125.3, 116.6, 108.3, 49.1 (2C), 25.5 (2C); IR (neat,  $\text{cm}^{-1}$ ): 2971, 2871, 1534, 1495, 1341, 1218, 1026, 849, 770; HRMS (ESI/APCI,  $m/z$ ): 283.9861 (calcd.,  $\text{C}_{10}\text{H}_{11}\text{N}_3\text{S}^{79}\text{Br}$ , 283.9857,  $[\text{M}+\text{H}]^+$ ).

### 5.6.12 (4-(4-(2-Phenylpyrrolidin-1-yl)thieno[2,3-*d*]-pyrimidin-6-yl)phenyl)methanol (*rac*-**6a**)

Compound *rac*-**6a** was prepared as described in Section 5.5, starting with compound *rac*-**5a** (100 mg, 0.28 mmol) and 4-(hydroxymethyl)phenyl boronic acid (51.0 mg, 0.35 mmol). The reaction time was 55 minutes, and purification by silica gel column chromatography ( $\text{EtOAc:n-pentane}$ , 1:1,  $R_f = 0.12$ ) yielded 100 mg (0.26 mmol, 93 %) of *rac*-**6a** as a yellowish solid; mp = 171.8-173.0 °C; HPLC purity: 97%,  $t_R = 22.6$  min.

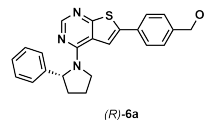


Spectroscopic data (Appendix L):  $^1\text{H}$  NMR (400 MHz,  $\text{DMSO-}d_6$ )  $\delta$ : 8.27 (br s, 1H), 7.64-7.61 (m, 2H), 7.56-7.53 (m, 1H), 7.39-7.38 (m, 2H), 7.31-7.30 (m, 2H), 7.28 (br s, 2H), 7.21-7.19 (m, 1H), 5.70 (s, 1H), 5.27 (t,  $J = 5.7$  Hz, 1H), 4.54 (d,  $J = 5.4$  Hz, 2H), 4.29 (br s, 1H), 4.00 (br s, 1H), 2.43 (br s, 1H), 2.04 (br s, 1H), 1.93 (m, 2H);  $^{13}\text{C}$  NMR (100 MHz,  $\text{DMSO-}d_6$ )  $\delta$ : 167.6, 155.6, 153.5, 144.0, 143.5, 136.7, 132.5, 132.0 (2C), 128.9 (3C), 127.6 (2C), 127.1, 126.0 (2C), 117.9, 62.9, 62.6, 50.5, 34.4, 24.0; IR (neat,  $\text{cm}^{-1}$ ): 3309, 2969, 1552, 1451, 1316, 1062, 1021, 773, 701; HRMS(ESI/APCI,  $m/z$ ): 388.1479 (calcd.  $\text{C}_{23}\text{H}_{23}\text{N}_3\text{O}_2\text{S}$ , 388.1484,  $[\text{M}+\text{H}]^+$ ).



### 5.6.13 (*R*)-(4-(4-(2-Phenylpyrrolidin-1-yl)thieno[2,3-*d*]-pyrimidin-6-yl)phenyl)methanol ((*R*)-**6a**)

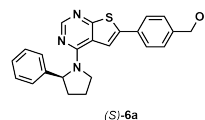
Compound (*R*)-**6a** was prepared as described in Section 5.5, starting with (*R*)-**5a** (146 mg, 0.405 mmol). The reaction time was 45 minutes, and purification by silica gel column chromatography (EtOAc:*n*-pentane, 1:1, *R<sub>f</sub>*= 0.25) yielded 145 mg (0.374 mmol, 92 %) of (*R*)-**6a** as a brown solid, mp = 200.1-202.4 °C; HPLC purity: 99%, *t<sub>R</sub>* = 22.6 min; Chiral HPLC (Method B): *t<sub>R</sub>* = 12.2 (minor), *t<sub>R</sub>* = 14.8 (major).



Spectroscopic data (Appendix N): <sup>1</sup>H NMR (600 MHz, DMSO-*d*<sub>6</sub>) δ: 8.26 (br s, 1H), 7.64-7.61 (m, 2H), 7.57-7.54 (m, 1H), 7.40-7.39 (m, 2H), 7.31-7.30 (m, 2H), 7.28 (br s, 2H), 7.22-7.20 (m, 1H), 5.71 (br s, 1H), 5.26 (t, J = 5.7 Hz, 1H), 4.54 (d, J = 5.5, 2H), 4.30 (br s, 1H), 4.0 (br s, 1H), 2.43 (br s, 1H), 2.04 (br s, 1H), 1.93 (br s, 2H); <sup>13</sup>C NMR (150 MHz, DMSO-*d*<sub>6</sub>) δ: 167.6, 155.6, 153.5, 144.0, 143.5, 136.7, 132.5, 131.5 (2C), 129.0 (3C), 127.6 (2C), 127.1, 126.0 (2C), 117.9, 62.9, 62.6, 50.5, 34.5, 24.3; IR (neat, *cm*<sup>-1</sup>): 3314, 3026, 2973, 2875, 1552, 1506, 1345, 1062, 773, 701; HRMS(ESI/APCI, *m/z*): 388.1487 (calcd. C<sub>23</sub>H<sub>21</sub>N<sub>3</sub>OS, 388.1484, [M+H]<sup>+</sup>).

### 5.6.14 (*S*)-(4-(4-(2-Phenylpyrrolidin-1-yl)thieno[2,3-*d*]-pyrimidin-6-yl)phenyl)methanol ((*S*)-**6a**)

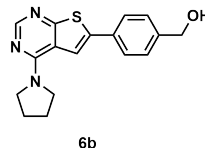
Compound (*S*)-**6a** was prepared as described in Section 5.5, starting with (*S*)-**5a** (131 mg, 0.362 mmol). The reaction time was 45 minutes, and purification by silica gel column chromatography (EtOAc:*n*-pentane, 1:1, *R<sub>f</sub>*= 0.25) yielded 129 mg (0.33 mmol, 92 %) of (*S*)-**6a** as a brown solid; mp = 200.1-202.4 °C; HPLC purity: 98%, *t<sub>R</sub>* = 22.6 min; Chiral HPLC (Method B): *t<sub>R</sub>* = 12.3 (major), *t<sub>R</sub>* = 14.8 (minor).



Spectroscopic data (Appendix O): <sup>1</sup>H NMR (600 MHz, DMSO-*d*<sub>6</sub>) δ: 8.27 (br s, 1H), 7.64-7.61 (m, 2H), 7.57-7.54 (m, 1H), 7.40-7.39 (m, 2H), 7.32-7.31 (m, 2H), 7.28 (br s, 2H), 7.22-7.20 (m, 1H), 5.71 (br s, 1H), 5.26 (t, J = 5.7 Hz, 1H), 4.54 (d, J = 5.5, 2H), 4.30 (br s, 1H), 4.04-3.98 (m, 1H), 2.43 (br s, 1H), 2.04 (br s, 1H), 1.93 (br s, 2H); <sup>13</sup>C NMR (150 MHz, DMSO-*d*<sub>6</sub>) δ: 167.6, 155.6, 153.5, 144.0, 143.5, 136.7, 132.5, 132.0 (2C), 129.0 (3C), 127.6 (2C), 127.1, 126.0 (2C), 117.9, 62.9, 62.6, 50.5, 34.5, 24.4; IR (neat, *cm*<sup>-1</sup>): 3311, 3026, 2973, 2873, 1552, 1495, 1345, 1180, 1021, 772, 701; HRMS (ESI/APCI, *m/z*): 388.1482 (calcd., C<sub>23</sub>H<sub>22</sub>N<sub>3</sub>OS, 388.1484, [M+H]<sup>+</sup>).

### 5.6.15 (4-(4-(Pyrrolidin-1-yl)thieno[2,3-*d*]pyrimidin-6-yl)-phenyl)methanol (**6b**)

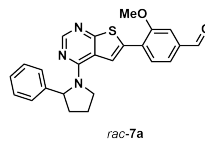
Compound **6b** was prepared as described in Section 5.5, starting with **5b** (103 mg, 0.36 mmol). The reaction time was 55 minutes, and purification by silica gel column chromatography (EtOAc:*n*-pentane, 9:1,  $R_f$ = 0.20) yielded 64.0 mg (0.21 mmol, 58 %) of **6b** as a white solid; mp = 216.5-221.3 °C; HPLC purity: 99%,  $t_R$  = 18.1 min.



Spectroscopic data (Appendix P):  $^1\text{H}$  NMR (600 MHz, DMSO- $d_6$ )  $\delta$ : 8.29 (s, 1H), 7.90 (s, 1H), 7.75-7.33 (m, 2H), 7.40-7.39 (m, 2H), 5.26 (t,  $J$  = 5.7 Hz, 1H), 4.54 (d,  $J$  = 5.7 Hz, 2H), 3.82 (br s, 4H), 1.99 (br s, 4H);  $^{13}\text{C}$  NMR (150 MHz, DMSO- $d_6$ )  $\delta$ : 167.3, 155.5, 153.6, 143.4, 136.6, 132.1, 127.5 (2C), 126.1 (2C), 117.5, 117.4, 63.0, 49.2 (2C), 25.5 (2C); IR (neat,  $\text{cm}^{-1}$ ): 3274, 2971, 2870, 1558, 1500, 1331, 1178, 811, 723, 696; HRMS (ESI/APCI,  $m/z$ ): 312.1175 (calcd.,  $\text{C}_{17}\text{H}_{18}\text{N}_3\text{OS}$ , 312.1171,  $[\text{M}+\text{H}]^+$ ).

### 5.6.16 3-Methoxy-4-(4-(2-phenylpyrrolidin-1-yl)-thieno[2,3-*d*]pyrimidin-6-yl)benzaldehyde (*rac*-**7a**)

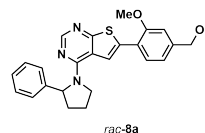
Compound *rac*-**7a** was prepared as described in Section 5.5, starting with *rac*-**5a** (372 mg, 1.03 mmol). The reaction time was 1.5 hours, and purification by silica gel column chromatography (EtOAc:*n*-pentane, 1:1,  $R_f$ = 0.16) yielded 422 mg (1.02 mmol, 99 %) of *rac*-**7a** as a yellow solid; mp = 205.5-207.0 °C.



Spectroscopic data (Appendix Q):  $^1\text{H}$  NMR (400 MHz, DMSO- $d_6$ )  $\delta$ : 10.0 (s, 1H), 8.31 (m, 2H), 7.80-7.55 (m, 4H), 7.33-7.29 (m, 4H), 7.23-7.20 (m, 1H), 5.72 (br s, 1H), 4.26 (br s, 1H), 4.0 (br s, 3H), 2.44 (br s, 1H), 2.04 (br s, 1H), 1.95 (br s, 2H);  $^{13}\text{C}$  NMR (100 MHz, DMSO- $d_6$ )  $\delta$ : 192.7, 168.8, 156.2, 155.7, 153.9, 143.8, 137.0, 131.1, 129.0 (3C), 127.9, 127.2, 126.0 (2C), 123.3, 122.3, 116.0, 112.3, 62.7, 56.6, 50.4, 35.7, 27.8; IR (neat,  $\text{cm}^{-1}$ ): 2971, 2876, 2731, 1690, 1546, 1474, 1302, 1121, 1030, 777, 702; HRMS (ESI/APCI,  $m/z$ ): 416.1427 (calcd.,  $\text{C}_{24}\text{H}_{22}\text{N}_3\text{O}_2\text{S}$ , 416.1433,  $[\text{M}+\text{H}]^+$ ).

### 5.6.17 (3-Methoxy-4-(4-(2-phenylpyrrolidin-1-yl)-thieno[2,3-*d*]pyrimidin-6-yl)phenyl)methanol (*rac*-**8a**)

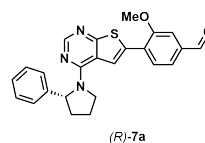
Compound *rac*-**8a** was synthesized as described in Section 5.6, starting with *rac*-**7a** (350 mg, 0.84 mmol). The reaction time was 1 hours, and purification by silica gel column chromatography (EtOAc:*n*-pentane, 1:1,  $R_f = 0.28$ ) yielded 167 mg (0.40 mmol, 48 %) of *rac*-**8a** as a yellowish solid; mp = 177-179.2 °C; HPLC purity: 96%,  $t_R = 22.5$  min.



Spectroscopic data (Appendix R): <sup>1</sup>H NMR (600 MHz, DMSO-*d*<sub>6</sub>) δ: 8.28 (s, 1H), 7.86-7.53 (m, 2H), 7.32-7.31 (m, 4H), 7.22-7.20 (m, 1H), 7.1 (s, 1H), 6.98-6.97 (m, 1H), 5.69 (s, 1H), 5.29 (t, J = 5.5 Hz, 1H), 4.53 (d, J = 5.0 Hz, 2H), 4.22 (br s, 1H), 3.98 (br s, 1H), 3.87 (s, 3H), 2.42 (br s, 1H), 2.01 (br s, 1H), 1.92 (br s, 2H), <sup>13</sup>C NMR (150 MHz, DMSO-*d*<sub>6</sub>) δ: 167.9, 155.9, 155.5, 153.3, 145.1, 144.0, 132.0, 129.0 (3C), 128.3, 127.1, 126.0 (2C), 120.4, 119.3, 116.1, 110.5, 63.0, 62.6, 56.2, 50.3, 35.5, 22.7; IR (neat,  $cm^{-1}$ ): 3297, 3206, 2938, 2873, 1550, 1451, 1388, 1215, 1160, 1063, 775, 701; HRMS (ESI/APCI,  $m/z$ ): 418.1586 (calcd., C<sub>24</sub>H<sub>24</sub>N<sub>3</sub>O<sub>2</sub>S, 418.1589, [M+H]<sup>+</sup>).

### 5.6.18 (*R*)-3-Methoxy-4-(4-(2-phenylpyrrolidin-1-yl)-thieno[2,3-*d*]pyrimidin-6-yl)benzaldehyde (*R*)-**7a**)

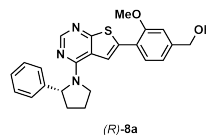
Compound (*R*)-**7a** was prepared as described in Section 5.5, starting with (*R*)-**5a** (172 mg, 0.48 mmol). The reaction time was 45 minutes, and purification by silica gel column chromatography (EtOAc:*n*-pentane, 1:1,  $R_f = 0.19$ ) yielded 183 mg (0.44 mmol, 92 %) of (*R*)-**7a** as a yellowish solid; mp = 156.6-158.2 °C (decomp.).



Spectroscopic data (Appendix S): <sup>1</sup>H NMR (600 MHz, DMSO-*d*<sub>6</sub>) δ: 10.0 (s, 1H), 8.30 (s, 1H), 7.88-7.61 (m, 4H), 7.33-7.29 (m, 4H), 7.22-7.21 (m, 1H), 5.71 (br s, 1H), 4.30 (br s, 1H), 4.0 (br s, 4H), 2.44 (br s, 1H), 2.04 (br s, 1H), 1.94 (br s, 2H); <sup>13</sup>C NMR (150 MHz, DMSO-*d*<sub>6</sub>) δ: 192.7, 168.8, 156.2, 155.7, 153.9, 143.8, 137.0, 131.1, 129.0 (3C), 127.9, 172.2, 126.0 (2C), 123.3, 122.3, 116.0, 112.3, 62.7, 56.6, 50.4, 35.7, 27.3; IR (neat,  $cm^{-1}$ ) 2969, 2877, 1690, 1570, 1474, 1345, 1214, 1122, 1030, 816, 702; HRMS (ESI/APCI,  $m/z$ ): 416.1439 (calcd., C<sub>24</sub>H<sub>22</sub>N<sub>3</sub>O<sub>2</sub>S, 416.1433, [M+H]<sup>+</sup>).

### 5.6.19 (R)-(3-Methoxy-4-(4-(2-phenylpyrrolidin-1-yl)-thieno[2,3-d]pyrimidin-6-yl)phenyl)methanol ((R)-8a)

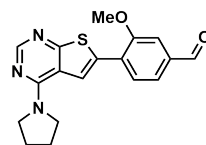
Compound (R)-8a was prepared as described in Section 5.6, starting with (R)-7a (145 mg, 0.35 mmol). The reaction time was 50 minutes, and purification by silica gel column chromatography (EtOAc:*n*-pentane, 1:1,  $R_f = 0.12$ ) yielded 146 mg (0.35 mmol, > 99%) of (R)-8a as a white solid; mp = 162.0-163.5 °C; HPLC purity >99%,  $t_R = 22.5$  min; Chiral HPLC (Method B):  $t_R = 14.6$  (minor),  $t_R = 17.7$  (major).



Spectroscopic data (Appendix T):  $^1\text{H}$  NMR (600 MHz, DMSO- $d_6$ )  $\delta$ : 8.27 (br s, 1H), 7.59 (m, 2H), 7.34-7.27 (m, 4H), 7.23-7.19 (m, 1H), 7.10 (s, 1H), 6.98-6.97 (m, 1H), 5.69 (br s, 1H), 5.28 (t,  $J = 5.7$  Hz, 1H), 4.54 (d,  $J = 5.7$  Hz, 2H), 4.24 (br s, 1H), 4.0 (br s, 1H), 3.87 (s, 3H), 2.43 (br s, 1H), 2.02 (br s, 1H), 1.92 (br s, 2H);  $^{13}\text{C}$  NMR (150 MHz, DMSO- $d_6$ )  $\delta$ : 167.9, 155.9, 155.5, 153.1, 145.1, 144.0, 132.8, 129.0 (3C), 128.3, 127.1, 126.0 (2C), 120.4, 119.3, 116.1, 110.5, 63.0, 62.6, 56.2, 50.3, 35.8, 22.7; IR (neat,  $\text{cm}^{-1}$ ): 3301, 3027, 2972, 2876, 1551, 1474, 1389, 1216, 1063, 849, 701; HRMS (ESI/APCI,  $m/z$ ): 418.1591 (calcd.,  $\text{C}_{24}\text{H}_{24}\text{N}_3\text{O}_2\text{S}$ , 418.1589,  $[\text{M}+\text{H}]^+$ ).

### 5.6.20 3-Methoxy-4-(4-(pyrrolidin-1-yl)thieno[2,3-d]-pyrimidin-6-yl)benzaldehyde (7b)

Compound 7b was synthesized as described in Section 3.5, starting with 5b (418 mg, 1.47 mmol). The reaction time was 45 minutes, and purification by silica gel column chromatography (EtOAc:*n*-pentane, 9:1,  $R_f = 0.32$ ) yielded 468 mg (1.38 mmol, 94 %) of 7b as a yellow solid; mp = 185.6-186.5 °C.

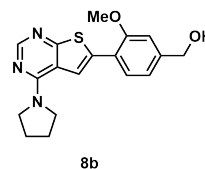


7b

Spectroscopic data (Appendix U):  $^1\text{H}$  NMR (600 MHz, DMSO- $d_6$ )  $\delta$ : 10.02 (s, 1H), 8.33 (s, 1H), 8.17 (s, 1H), 8.14-8.13 (m, 1H), 7.63-7.61 (m, 2H), 4.04 (s, 3H), 3.85 (br s, 4H), 2.01 (br s, 4H);  $^{13}\text{C}$  NMR (150 MHz, DMSO- $d_6$ )  $\delta$ : 192.7, 168.6, 156.1, 155.6, 154.0, 136.9, 130.9, 129.1, 128.1, 123.3, 121.9, 116.0, 112.2, 56.7, 49.2 (2C), 25.5 (2C); IR (neat,  $\text{cm}^{-1}$ ): 2971, 2872, 2729, 1688, 1552, 1483, 1386, 1122, 1028, 815, 775, 736; HRMS (ESI/APCI,  $m/z$ ): 340.1124 (calcd.,  $\text{C}_{18}\text{H}_{18}\text{N}_3\text{O}_2\text{S}$ , 340.1120,  $[\text{M}+\text{H}]^+$ ).

### 5.6.21 (3-Methoxy-4-(4-(pyrrolidin-1-yl)thieno[2,3-*d*]-pyrimidin-6-yl)phenyl)methanol (**8b**)

Compound **8b** was synthesized as described in Section 5.6, starting with **7b** (199 mg, 0.59 mmol). The reaction time was 1.5 hours, and purification by silica gel column chromatography (EtOAc:*n*-pentane, 9:1, *R<sub>f</sub>* = 0.11) yielded 134 mg (0.39 mmol, 67 %) of **8b** as a yellowish solid; mp = 199.0-201.1 °C (decomp.); HPLC purity: 98%, *t<sub>R</sub>* = 18.5 min.



Spectroscopic data (Appendix V): <sup>1</sup>H NMR (600 MHz, DMSO-*d*<sub>6</sub>) δ: 8.29 (s, 1H), 7.94 (s, 1H), 7.79-7.78 (m, 1H), 7.12 (s, 1H), 7.01-7.0 (m, 1H), 5.29 (t, 5.8 Hz, 1H), 4.55 (d, *J* = 5.7 Hz, 2H), 3.92 (s, 3H), 3.81 (br s, 4H), 2.0 (br s, 4H); <sup>13</sup>C NMR (150 MHz, DMSO-*d*<sub>6</sub>) δ: 167.7, 155.9, 155.4, 153.4, 145.0, 132.7, 128.4, 120.6, 119.3, 118.9, 116.1, 110.5, 63.1, 56.2, 49.1 (2C), 25.5 (2C); IR (neat, *cm*<sup>-1</sup>): 3256, 2969, 2871, 1578, 1500, 1330, 1125, 1028, 773; HRMS (ESI/APCI, *m/z*): 342.1282 (calcd., C<sub>18</sub>H<sub>20</sub>N<sub>3</sub>O<sub>2</sub>S, 342.1276, [M+H]<sup>+</sup>).

# Bibliography

- [1] Ferlay, J., Soerjomataram, I., Dikshit, R., Eser, S., Mathers, C., Rebelo, M., Parkin, D. M., Forman, D., Bray, F., *Int. J. Cancer* **2014**, *136*, E359–E386.
- [2] *NCI Dictionary of Cancer Terms*.
- [3] Huang, M., Shen, A., Ding, J., Geng, M., *Trends Pharmacol. Sci.* **2014**, *35*, 41–50.
- [4] Sun, C., Bernards, R., *Trends Biochem. Sci.* **2014**, *39*, 465–474.
- [5] Hanahan, D., Weinberg, R., *Cell* **2011**, *144*, 646–674.
- [6] Gutschner, T., Diederichs, S., *RNA Biology* **2012**, *9*, 703–719.
- [7] Sgambato, A., Casaluce, F., Maione, P., Rossi, A., Rossi, E., Napolitano, A., Palazzolo, G., Bareschino, M. A., Schettino, C., Sacco, P. C., Ciadiello, F., Gridelli, C., *Curr. Med. Chem.* **2012**, *19*, 3337–3352.
- [8] Köhler, J., Schuler, M., *Onkologie* **2013**, *36*, 5–5.
- [9] Bugge, S., Buene, A. F., Jurisch-Yaksi, N., Moen, I. U., Skjønsvjell, E. M., Sundby, E., Hoff, B. H., *Eur. J. Med. Chem.* **2016**, *107*, 255–274.
- [10] Bugge, S., Moen, I. U., Sylte, K.-O. K., Sundby, E., Hoff, B. H., *Eur. J. Med. Chem.* **2015**, *94*, 175–194.
- [11] Bugge, S., Kaspersen, S. J., Larsen, S., Nonstad, U., Bjørkøy, G., Sundby, E., Hoff, B. H., *Eur. J. Med. Chem.* **2014**, *75*, 354–374.
- [12] Normanno, N., Luca, A. D., Bianco, C., Strizzi, L., Mancino, M., Maiello, M. R., Carotenuto, A., Feo, G. D., Caponigro, F., Salomon, D. S., *Gene* **2006**, *366*, 2–16.
- [13] Ono, M., Kuwano, M., *Clin. Cancer Res.* **2006**, *12*, 7242–7251.
- [14] Hubbard, S. R., Miller, W. T., *Curr. Opin. Cell Biol.* **2007**, *19*, 117–123.
- [15] Zhang, H., Berezov, A., Wang, Q., Zhang, G., Drebin, J., Murali, R., Greene, M. I., *J. Clin. Invest.* **2007**, *117*, 2051–2058.
- [16] Guren, T. K., Christoffersen, T., Thoresen, G. H., Wisløff, F., Dajani, O., Tveit, K. M., *Tidsskrift for den Norske lægeforening : tidsskrift for praktisk medicin ny raekke* **2005**, *125*, 3115–3119.
- [17] Grandis, J. R., Sok, J. C., *Pharmacol. Ther.* **2004**, *102*, 37–46.

- [18] Seshacharyulu, P., Ponnusamy, M. P., Haridas, D., Jain, M., Ganti, A. K., Batra, S. K., *Expert Opin. Ther. Targets* **2012**, *16*, 15–31.
- [19] Sullivan, I., Planchard, D., *Front. Med.* **2017**, *3*.
- [20] Nan, X., Xie, C., Yu, X., Liu, J., *Oncotarget* **2017**, *8*.
- [21] Morgillo, F., Corte, C. M. D., Fasano, M., Ciardiello, F., *ESMO Open* **2016**, *1*, e000060.
- [22] Barnes, T. A., O’Kane, G. M., Vincent, M. D., Leighl, N. B., *Front. Oncol.* **2017**, *7*.
- [23] Wang, S., Song, Y., Liu, D., *Cancer Lett.* **2017**, *385*, 51–54.
- [24] Patel, H., Pawara, R., Ansari, A., Surana, S., *Eur. J. Med. Chem.* **2017**, *142*, 32–47.
- [25] Kerru, N., *Med. Chem.* **2014**, *4*.
- [26] Li, S.-G., Vilchèze, C., Chakraborty, S., Wang, X., Kim, H., Anisetti, M., Ekins, S., Rhee, K. Y., Jacobs, W. R., Freundlich, J. S., *Tetrahedron Lett.* **2015**, *56*, 3246–3250.
- [27] Rashad, A. E., Ali, M. A., *Nucleosides Nucleotides Nucleic Acids* **2006**, *25*, 17–28.
- [28] El-Gazzar, A.-R., Hussein, H., Hafez, H., *Acta Pharm* **2007**, *57*.
- [29] Dai, Y., Guo, Y., Frey, R. R., Ji, Z., Curtin, M. L., Ahmed, A. A., Albert, D. H., Arnold, L., Arries, S. S., Barlozzari, T., Bauch, J. L., Bouska, J. J., Bousquet, P. F., Cunha, G. A., Glaser, K. B., Guo, J., Li, J., Marcotte, P. A., Marsh, K. C., Moskey, M. D., Pease, L. J., Stewart, K. D., Stoll, V. S., Tapang, P., Wishart, N., Davidsen, S. K., Michaelides, M. R., *J. Med. Chem.* **2005**, *48*, 6066–6083.
- [30] Bridges, A., *Curr. Med. Chem.* **1999**, *6*, 825–844.
- [31] Bridges, A. J., Zhou, H., Cody, D. R., Rewcastle, G. W., McMichael, A., Showalter, H. D. H., Fry, D. W., Kraker, A. J., Denny, W. A., *J. Med. Chem.* **1996**, *39*, 267–276.
- [32] Beckers, T., Sellmer, A., Eichhorn, E., Pongratz, H., Schächtele, C., Totzke, F., Kelter, G., Krumbach, R., Fiebig, H.-H., Böhmer, F.-D., Mahboobi, S., *Bioorg. Med. Chem.* **2012**, *20*, 125–136.
- [33] Bysting, F., Bugge, S., Sundby, E., Hoff, B. H., *RSC Advances* **2017**, *7*, 18569–18577.
- [34] Kim, E. S., *Drugs* **2016**, *76*, 1153–1157.
- [35] Liao, B.-C., Lin, C.-C., Lee, J.-H., Yang, J. C.-H., *J. Biomed. Sci.* **2016**, *23*.
- [36] Ji, X., Peng, T., Zhang, X., Li, J., Yang, W., Tong, L., Qu, R., Jiang, H., Ding, J., Xie, H., Liu, H., *Bioorg. Med. Chem.* **2014**, *22*, 2366–2378.
- [37] Lee, K.-O., Cha, M. Y., Kim, M., Song, J. Y., Lee, J.-H., Kim, Y. H., Lee, Y.-M., Suh, K. H., Son, J., *Cancer Res.* **2014**, *74*, LB–100–LB–100.
- [38] Borah, M., Saikia, A. K., *ChemistrySelect* **2018**, *3*, 2162–2166.

- [39] Siegmund, B., Leitner, E., Pfannhauser, W., *J. Agric. Food Chem.* **1999**, *47*, 3113–3120.
- [40] Hammond, C. in *Cellular and Molecular Neurophysiology*, Elsevier, **2015**, pp. 221–244.
- [41] Mathieu, C., Degrande, E., *Vasc Health Risk Manag.* **2008**, *4*, 1349.
- [42] Grollman, A. P. et al., *J. Biol. Chem.* **1967**, *242*, 3226–3233.
- [43] Watanabe, H., Okue, M., Kobayashi, H., Kitahara, T., *Tetrahedron Lett.* **2002**, *43*, 861–864.
- [44] Held, P., **2015**.
- [45] Bajar, B., Wang, E., Zhang, S., Lin, M., Chu, J., *Sensors* **2016**, *16*, 1488.
- [46] Moss, G. P., *Pure Appl. Chem.* **1996**, *68*, 2193–2222.
- [47] Belyk, K. M., Beguin, C. D., Palucki, M., Grinberg, N., DaSilva, J., Askin, D., Yasuda, N., *Tetrahedron Lett.* **2004**, *45*, 3265–3268.
- [48] Denmark, S. E., Marcin, L. R., *J. Org. Chem.* **1995**, *60*, 3221–3235.
- [49] Katritzky, A. R., Cui, X.-L., Yang, B., Steel, P. J., *J. Org. Chem.* **1999**, *64*, 1979–1985.
- [50] Duncan, D., Livinghouse, T., *J. Org. Chem.* **2001**, *66*, 5237–5240.
- [51] Matteson, D. S., Kim, G. Y., *Org. Lett.* **2002**, *4*, 2153–2155.
- [52] Trost, B. M., Silverman, S. M., Stambuli, J. P., *Journal of the American Chemical Society* **2011**, *133*, 19483–19497.
- [53] Dunsmore, C. J., Carr, R., Fleming, T., Turner, N. J., *J. Am. Chem. Soc.* **2006**, *128*, 2224–2225.
- [54] Blum, A. P., Lester, H. A., Dougherty, D. A., *Proc. Natl. Acad. Sci.* **2010**, *107*, 13206–13211.
- [55] Chen, F., Ding, Z., Qin, J., Wang, T., He, Y., Fan, Q.-H., *Org. Lett.* **2011**, *13*, 4348–4351.
- [56] Willoughby, C. A., Buchwald, S. L., *J. Am. Chem. Soc.* **1994**, *116*, 8952–8965.
- [57] Coindet, C., Comel, A., Kirsch, G., *Tetrahedron Lett.* **2001**, *42*, 6101–6104.
- [58] Tang, W., Zhang, X., *Chem. Rev.* **2003**, *103*, 3029–3070.
- [59] Nugent, T., El-Shazly, M., *Adv. Synth. Catal.* **2010**, *352*, 753–819.
- [60] Knowles, W. S., Sabacky, M. J., *Chem. Commun.* **1968**, 1445–1446.
- [61] Horner, L., Siegel, H., Büthe, H., *Angew Chem Int Ed Engl* **1968**, *7*, 942–942.
- [62] Vineyard, B. D., Knowles, W. S., Sabacky, M. J., Bachman, G. L., Weinkauff, D. J., *J. Am. Chem. Soc.* **1977**, *99*, 5946–5952.
- [63] Mashima, K., Kusano, K.-h., Sato, N., Matsumura, Y.-i., Nozaki, K., Kumabayashi, H., Sayo, N., Hori, Y., Ishizaki, T., *J. Org. Chem.* **1994**, *59*, 3064–3076.



- [64] Verdaguer, X., Lange, U. E. W., Reding, M. T., Buchwald, S. L., *J. Am. Chem. Soc.* **1996**, *118*, 6784–6785.
- [65] Willoughby, C. A., Buchwald, S. L., *J. Am. Chem. Soc.* **1992**, *114*, 7562–7564.
- [66] Chin, B., Buchwald, S. L., *J. Org. Chem.* **1996**, *61*, 5650–5651.
- [67] Nishibayashi, Y., Takei, I., Uemura, S., Hidai, M., *Organometallics* **1998**, *17*, 3420–3422.
- [68] Zhang, Y., Kong, D., Wang, R., Hou, G., *Org. Biomol. Chem.* **2017**, *15*, 3006–3012.
- [69] Yamagata, T., Tadaoka, H., Nagata, M., Hirao, T., Kataoka, Y., Ratovelomanana-Vidal, V., Genet, J. P., Mashima, K., *Organometallics* **2006**, *25*, 2505–2513.
- [70] Nishimura, S. et al., *Handbook of heterogeneous catalytic hydrogenation for organic synthesis*, Wiley New York etc, **2001**, Chapter 2.2.1.
- [71] Marcazzan, P., Patrick, B. O., James, B. R., *Organometallics* **2003**, *22*, 1177–1179.
- [72] Hansen, K. B., Rosner, T., Kubryk, M., Dormer, P. G., Armstrong, J. D., *Org. Lett.* **2005**, *7*, 4935–4938.
- [73] Chen, F., Wang, T., He, Y., Ding, Z., Li, Z., Xu, L., Fan, Q.-H., *Chemistry - A European Journal* **2011**, *17*, 1109–1113.
- [74] Fabrello, A., Bachelier, A., Urrutigoity, M., Kalck, P., *Coord. Chem. Rev.* **2010**, *254*, 273–287.
- [75] Wild, F. R., Zsolnai, L., Huttner, G., Brintzinger, H. H., *J. Organomet. Chem.* **1982**, *232*, 233–247.
- [76] Claver, C., Fernandez, E. in *Modern Reduction Methods*, Wiley-VCH Verlag GmbH & Co. KGaA, **2008**, pp. 235–269.
- [77] Guo, C., Sun, D.-W., Yang, S., Mao, S.-J., Xu, X.-H., Zhu, S.-F., Zhou, Q.-L., *J. Am. Chem. Soc.* **2015**, *137*, 90–93.
- [78] Fan, Q., Zhang, J., Chen, F., He, Y., CN104610256A, **2015**.
- [79] Porter, W. H., *Pure Appl. Chem.* **1991**, *63*, 1119–1122.
- [80] Springuel, G., Leyssens, T., *Cryst. Growth Des.* **2012**, *12*, 3374–3378.
- [81] Binanzer, M., Hsieh, S.-Y., Bode, J. W., *J. Am. Chem. Soc.* **2011**, *133*, 19698–19701.
- [82] Pellissier, H., *Adv. Synth. Catal.* **2011**, *353*, 1613–1666.
- [83] Ilisz, I., Berkecz, R., Péter, A., *J. Sep. Sci.* **2006**, *29*, 1305–1321.
- [84] Machida, Y., Nishi, H., Nakamura, K., Nakai, H., Sato, T., *J. Chromatogr. A* **1998**, *805*, 85–92.
- [85] Okamoto, Y., Ikai, T., *Chem. Soc. Rev.* **2008**, *37*, 2593.
- [86] Campos, K. R., Klapars, A., Waldman, J. H., Dormer, P. G., Chen, C.-y., *J. Am. Chem. Soc.* **2006**, *128*, 3538–3539.

- [87] Brinner, K. M., Ellman, J. A., *Org. Biomol. Chem.* **2005**, *3*, 2109.
- [88] Beak, P., Basu, A., Gallagher, D. J., Park, Y. S., Thayumanavan, S., *Acc. Chem. Res.* **1996**, *29*, 552–560.
- [89] Barker, G., McGrath, J. L., Klapars, A., Stead, D., Zhou, G., Campos, K. R., O'Brien, P., *J. Org. Chem.* **2011**, *76*, 5936–5953.
- [90] Gallagher, D. J., Kerrick, S. T., Beak, P., *J. Am. Chem. Soc.* **1992**, *114*, 5872–5873.
- [91] Gallagher, D. J., Beak, P., *J. Org. Chem.* **1995**, *60*, 7092–7093.
- [92] Negishi, E., Takahashi, T., Baba, S., Horn, D. E. V., Okukado, N., *J. Am. Chem. Soc.* **1987**, *109*, 2393–2401.
- [93] Yuryev, R., Strompen, S., Liese, A., *Beilstein J. Org. Chem.* **2011**, *7*, 1449–1467.
- [94] Pàmies, O., Bäckvall, J.-E., *Chem. Rev.* **2003**, *103*, 3247–3262.
- [95] Muthana, S., Cao, H., Chen, X., *Curr. Opin. Chem. Biol.* **2009**, *13*, 573–581.
- [96] Mathew, S., Yun, H., *ACS Catalysis* **2012**, *2*, 993–1001.
- [97] Ghislieri, D., Green, A. P., Pontini, M., Willies, S. C., Rowles, I., Frank, A., Grogan, G., Turner, N. J., *J. Am. Chem. Soc.* **2013**, *135*, 10863–10869.
- [98] Turner, N. J., Truppo, M. D. in *Chiral Amine Synthesis*, Wiley-VCH Verlag GmbH & Co. KGaA, **2010**, pp. 431–459.
- [99] Mitsukura, K., Suzuki, M., Tada, K., Yoshida, T., Nagasawa, T., *Org. Biomol. Chem.* **2010**, *8*, 4533.
- [100] Aleku, G. A., Man, H., France, S. P., Leipold, F., Hussain, S., Toca-Gonzalez, L., Marchington, R., Hart, S., Turkenburg, J. P., Grogan, G., Turner, N. J., *ACS Catalysis* **2016**, *6*, 3880–3889.
- [101] Bugge, S., PhD thesis, NTNU, **2015**.
- [102] Hozien, Z., Atta, F., Hassan, K., Abdel-Wahab, A., Ahmed, S., *Synth. Commun.* **1996**, *26*, 3733–3755.
- [103] Peng, J., Lin, W., Jiang, D., Yuan, S., Chen, Y., *J. Comb. Chem.* **2007**, *9*, 431–436.
- [104] Bunnett, J. F., Zahler, R. E., *Chem. Rev.* **1951**, *49*, 273–412.
- [105] Acevedo, O., Jorgensen, W. L., *Org. Lett.* **2004**, *6*, 2881–2884.
- [106] Um, I.-H., Min, S.-W., Dust, J. M., *J. Org. Chem.* **2007**, *72*, 8797–8803.
- [107] Banjoko, O., Babatunde, I. A., *Tetrahedron* **2005**, *61*, 8035–8040.
- [108] Miyaura, N., Yanagi, T., Suzuki, A., *Synth. Commun.* **1981**, *11*, 513–519.
- [109] Lennox, A. J. J., Lloyd-Jones, G. C., *Chem. Soc. Rev.* **2014**, *43*, 412–443.
- [110] Miyaura, N., Suzuki, A., *Chem. Rev.* **1995**, *95*, 2457–2483.
- [111] Matos, K., Soderquist, J. A., *J. Org. Chem.* **1998**, *63*, 461–470.
- [112] Carrow, B. P., Hartwig, J. F., *J. Am. Chem. Soc.* **2011**, *133*, 2116–2119.

- [113] Thomas, A. A., Denmark, S. E., *Science* **2016**, *352*, 329–332.
- [114] Amatore, C., Jutand, A., Le Duc, G., *Chem. Eur. J.* **2011**, *17*, 2492–2503.
- [115] Amatore, C., Jutand, A., Le Duc, G., *Chem. Eur. J.* **2012**, *18*, 6616–6625.
- [116] Amatore, C., Le Duc, G., Jutand, A., *Chem. Eur. J.* **2013**, *19*, 10082–10093.
- [117] Suzuki, A., *J. Organomet. Chem.* **1999**, *576*, 147–168.
- [118] Chaikin, S. W., Brown, W. G., *J. Am. Chem. Soc.* **1949**, *71*, 122–125.
- [119] Bayer, A., *Pure Appl. Chem.* **1977**, *49*, 733–743.
- [120] Rickborn, B., Wuesthoff, M. T., *J. Am. Chem. Soc.* **1970**, *92*, 6894–6904.
- [121] O'Brien, K., *Aust. J. Chem.* **1957**, *10*, 91.
- [122] Wigfield, D. C., *Tetrahedron* **1979**, *35*, 449–462.
- [123] Davis, R. E., Gottbrath, J. A., *J. Am. Chem. Soc.* **1962**, *84*, 895–898.
- [124] Shechter, H., Ley, D. E., Roberson, E. B., *J. Am. Chem. Soc.* **1956**, *78*, 4984–4991.
- [125] Kadin, S. B., *J. Org. Chem.* **1966**, *31*, 620–622.
- [126] Mojtahedi, M. M., Niknejad, N., Veisi, H., *Lett. Org. Chem.* **2013**, *10*, 121–125.
- [127] Hua, D. H., Miao, S. W., Bharathi, S. N., Katsuhira, T., Bravo, A. A., *J. Org. Chem.* **1990**, *55*, 3682–3684.
- [128] Abraham, R., Mobli, M. in *Modelling<sup>1</sup>H NMR Spectra of Organic Compounds: Theory, Applications and NMR Prediction Software*, John Wiley & Sons, Ltd, Chichester, **2008**, pp. 1–21.
- [129] Coleman, G. H., Hauser, C. R., *J. Am. Chem. Soc.* **1928**, *50*, 1193–1196.
- [130] Fulmer, G. R., Miller, A. J. M., Sherden, N. H., Gottlieb, H. E., Nudelman, A., Stoltz, B. M., Bercaw, J. E., Goldberg, K. I., *Organometallics* **2010**, *29*, 2176–2179.
- [131] Castillo, A. M., Patiny, L., Wist, J., *J. Magn. Reson.* **2011**, *209*, 123–130.
- [132] Aires-de-Sousa, J., Hemmer, M. C., Gasteiger, J., *Anal. Chem.* **2002**, *74*, 80–90.
- [133] Banfi, D., Patiny, L., *CHIMIA International Journal for Chemistry* **2008**, *62*, 280–281.
- [134] Malz, F., Jancke, H., *J. Pharm. Biomed. Anal.* **2005**, *38*, 813–823.
- [135] Benito, J., Meldal, M., *QSAR & Combinatorial Science* **2004**, *23*, 117–129.
- [136] Moreno-Mañas, M., Pérez, M., Pleixats, R., *J. Org. Chem.* **1996**, *61*, 2346–2351.
- [137] Miller, W. D., Fray, A. H., Quatroche, J. T., Sturgill, C. D., *Org. Process Res. Dev.* **2007**, *11*, 359–364.
- [138] Wagaw, S., Rennels, R. A., Buchwald, S. L., *J. Am. Chem. Soc.* **1997**, *119*, 8451–8458.

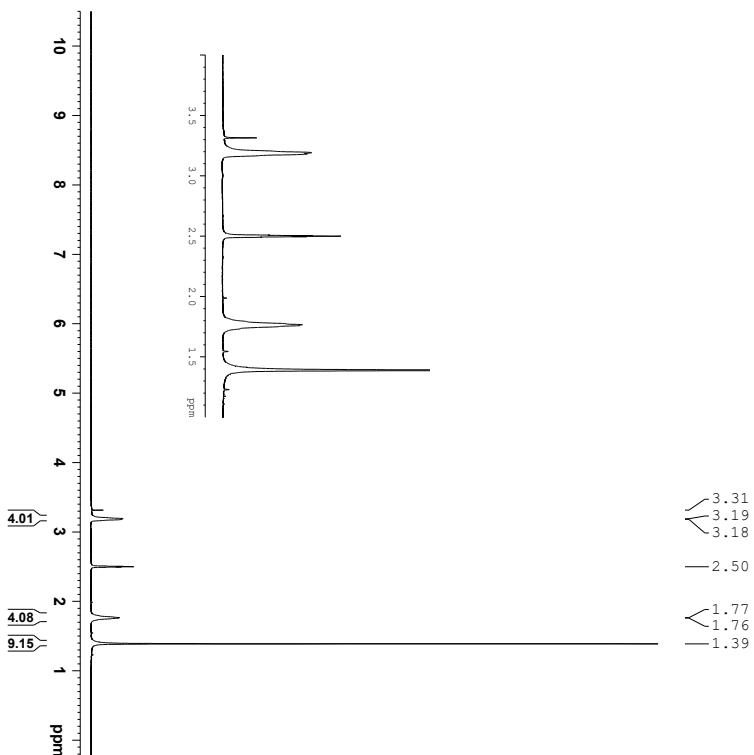
- [139] Shieh, W. C., Carlson, J. A., *J. Org. Chem.* **1992**, *57*, 379–381.
- [140] Ramsnes, A., *Synthesis of thienopyrimidine-based EGFR inhibitors.* **2017**.
- [141] Rewcastle, G. W., Denny, W. A., Bridges, A. J., Zhou, H., Cody, D. R., McMichael, A., Fry, D. W., *J. Med. Chem.* **1995**, *38*, 3482–3487.
- [142] Silverstein, R., Webster, F., Kiemle, D., Bryce, D., *Spectrometric Identification of Organic Compounds*, 8th Edition, John Wiley & Sons, Singapore, **2015**.
- [143] Bugge, S., Kaspersen, S. J., Sundby, E., Hoff, B. H., *Tetrahedron* **2012**, *68*, 9226–9233.
- [144] Reddy, L. R., Prashad, M., *Chem. Commun.* **2010**, *46*, 222–224.



# Appendix



# A | Spectroscopic Data - Compound I



```

Current Data Parameters
=====
EXNO          2
PROCNO        1
F2 - Acquisition Parameters
=====
Date_         20180205
Time          11.30
INSTRUM       spect
PROBHD        5 mm BBO5
PULPROG       zg30
TD            65536
SOLVENT       DMSO
DS            2
SWH           8012.820 Hz
AQ           0.168446 sec
RG           128.06
DM           62.400 usec
DE           298.0 K
TE           1.00000000 sec
D1           1
D0           1
===== CHANNEL f1 =====
SFO1          400.1324710 MHz
NUC1          1H
P1           9.00 usec
PL1          0.00000000 W
F2 - Processing parameters
=====
SI           32768
SF           400.1300033 MHz
WDW          EM
SSB          0
GB           0
PC           1.00
  
```

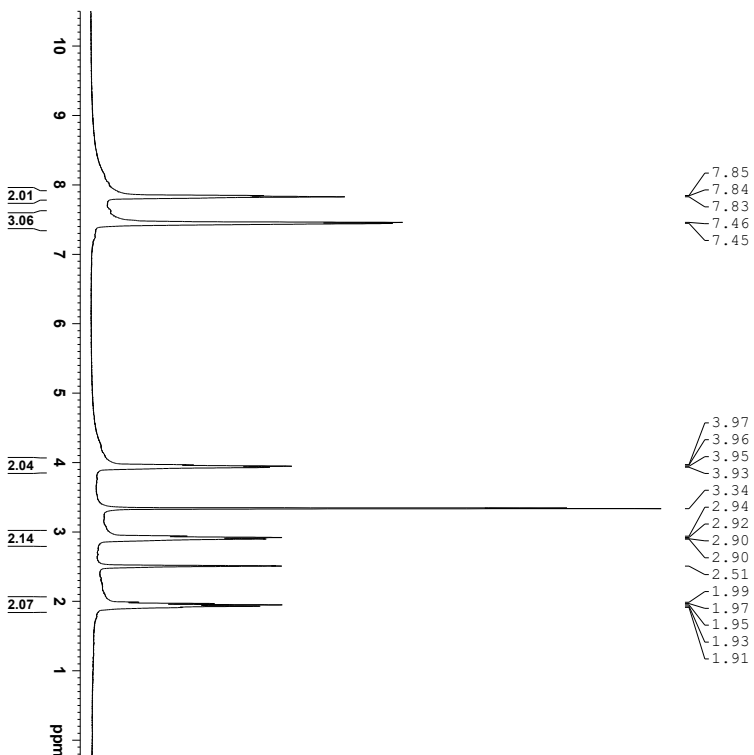


<sup>1</sup>H NMR (400 MHz, DMSO-*d*<sub>6</sub>) spectrum of compound 1.





# B | Spectroscopic Data - Compound 2



```

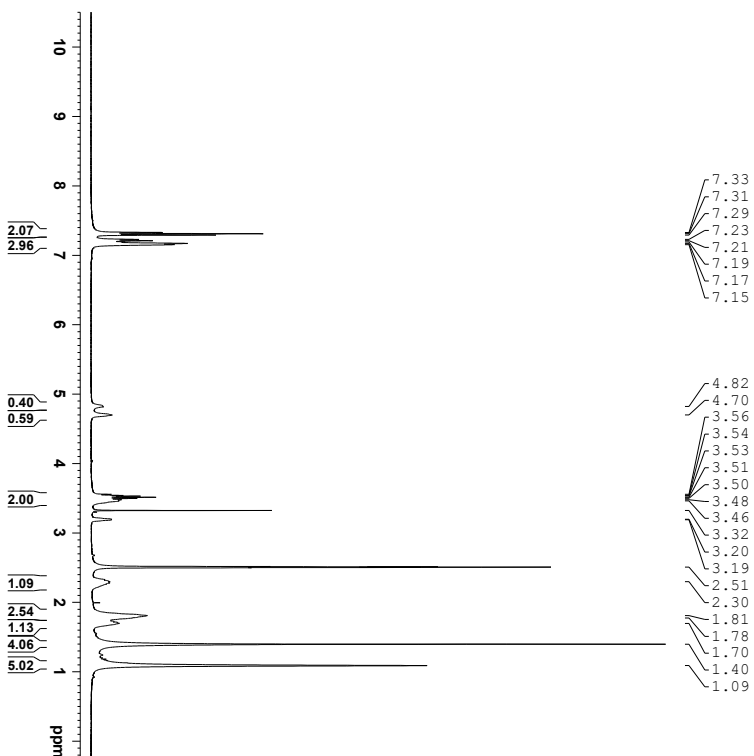
Current Data Parameters
=====
EXNO          1
PROCNO       1
F2 - Acquisition Parameters
=====
Date_         20180309
Time_        11.10
INSTRUM      spect
PROBHD       5 mm PABBO
PULPROG      zg30
TD            65536
SOLVENT      DMSO
DS            2
AQ            8012.820 Hz
RG            0.08446 Hz
RG            4.08446 Hz
RG            82.93 Hz
DM            62.400 usec
TE            297.9 K
D1            1.00000000 sec
TD0           1
===== CHANNEL f1 =====
SFO1          400.1324710 MHz
NUC1           1H
P1            9.00 usec
PL1           17.00000000 W
F2 - Processing parameters
=====
SI            32768
SF            400.1300000 MHz
WDW           EM
SSB           0
GB            0.30 Hz
PC            1.00
  
```



<sup>1</sup>H NMR (400 MHz, DMSO-*d*<sub>6</sub>) spectrum of compound 2.



# C | Spectroscopic Data - Compound (R)-3



```

Current Data Parameters
=====
EXNO          1
PROCNO        1
F2 - Acquisition Parameters
=====
Date_         20180219
Time          6.33
INSTRUM      spect
PROBHD       5 mm BBO-2
PULPROG      zg30
TD            65536
SOLVENT      DMSO
DS            2
SWH           8012.820 Hz
AQ           4.084465 sec
RG            143.52
DM            62.400 usec
TE            298.3 K
D1            1.00000000 sec
TD0           1
===== CHANNEL f1 =====
SFO1          400.1324710 MHz
NUC1          1H
P1            9.14 usec
PL1           0.00000000 W
F2 - Processing parameters
=====
SI            32768
SF            400.1300000 MHz
WDW           EM
SSB           0
GB            0
PC            1.00
  
```

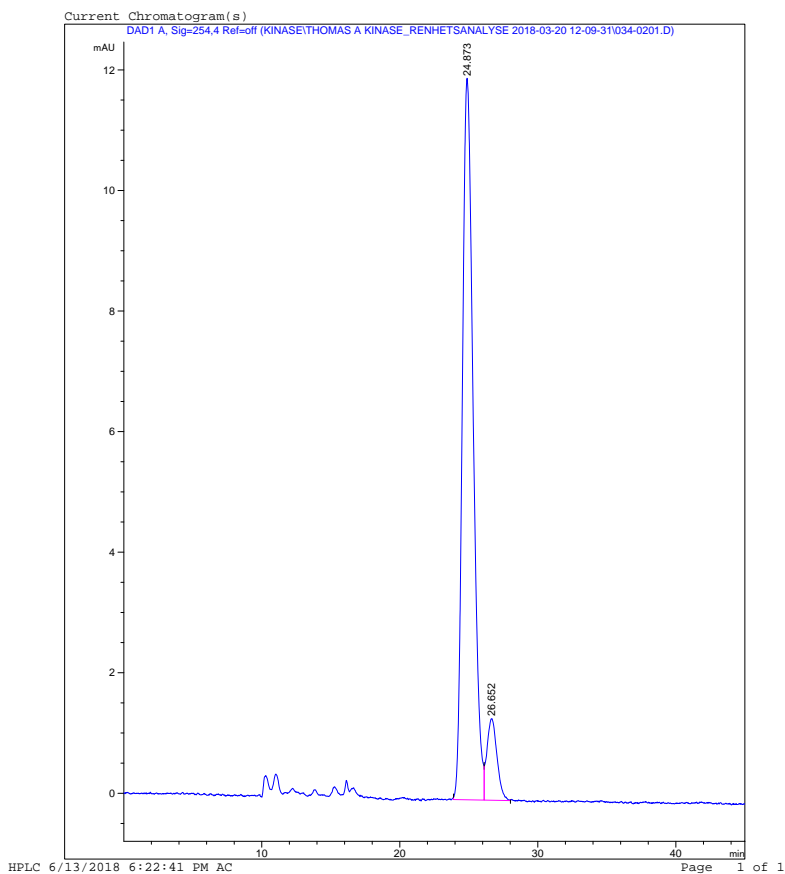


<sup>1</sup>H NMR (400 MHz, DMSO-*d*<sub>6</sub>) spectrum of compound (R)-3.

Print of window 38: Current Chromatogram(s)  
Data File : C:\CHEM32\...INASE\THOMAS A KINASE\_RENHETSANALYSE 2018-03-20 12-09-31\034-0201.D  
Sample Name : ABR1-03-Rflow0.3  
=====

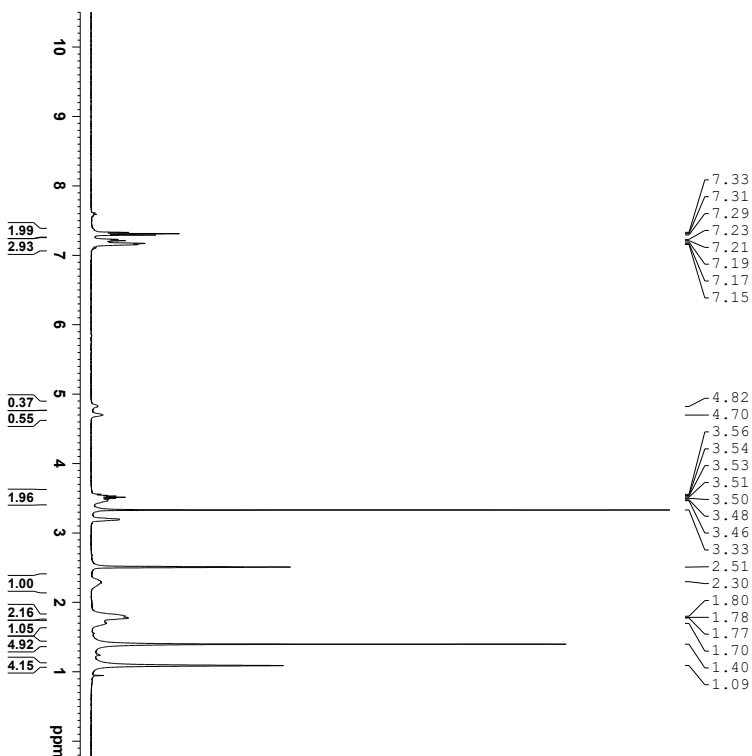
Acq. Operator	: Thomas A	Seq. Line	: 2
Acq. Instrument	: HPLC	Location	: Vial 34
Injection Date	: 3/20/2018 1:06:48 PM	Inj	: 1
		Inj Volume	: 10.000 µl

Acq. Method : C:\CHEM32\1\DATA\KINASE\THOMAS A KINASE\_RENHETSANALYSE 2018-03-20 12-09-31\RENHETSANALYSE FELLES\_NEUTRAL.M  
Last changed : 3/20/2018 12:09:31 PM by Thomas A  
Analysis Method : C:\CHEM32\1\METHODS\FELLES\RENHETSANALYSE FELLES\_NEUTRAL.M  
Last changed : 6/13/2018 6:16:27 PM by AC  
(modified after loading)



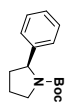
CSP-HPLC (Chiralpak AD 0.46 x 25 cm, hexane:*i*-PrOH, 99:1, flow 0.3 mL/min, detection at 254 nm) of compound (R)-3

# D | Spectroscopic Data - Compound (S)-3



```

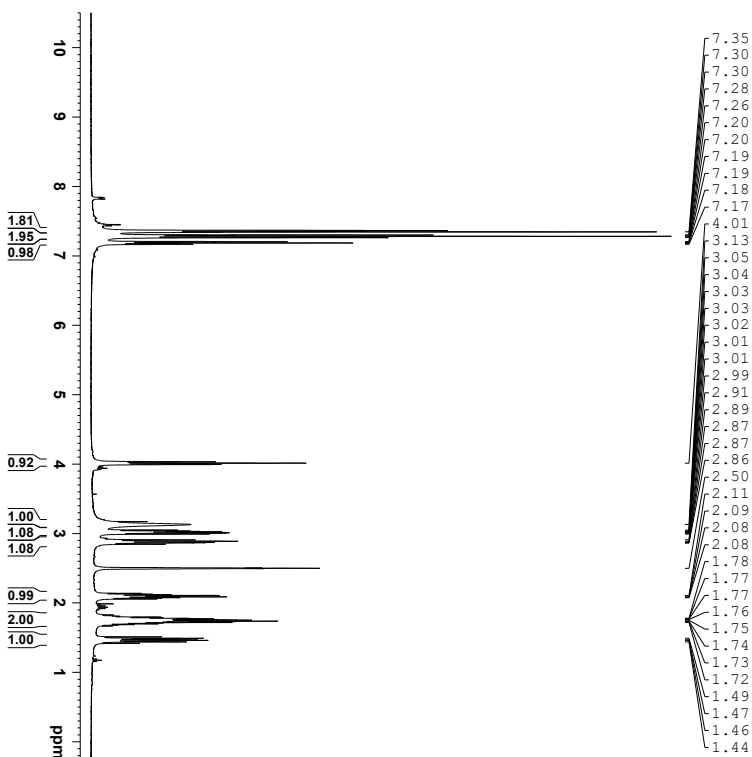
Current Data Parameters
=====
EXNO          5
PROCNO       1
F2 - Acquisition Parameters
=====
Date_         20180227
Time_         13:19
INSTRUM      spect
PROBHD       5 mm BBBO
PULPROG      zg30
TD            65536
SOLVENT      DMSO
DS            2
SWH           8012.820 Hz
AQ            0.168445 sec
RG            128.06
DM            62.400 usec
TE            298.0 K
D1            1.00000000 sec
TD0           1
===== CHANNEL f1 =====
SFO1          400.1324710 MHz
NUC1          1H
P1            9.00 usec
PL1           0.00 dB
PL11          17.00000000 W
F2 - Processing parameters
=====
SI            32768
SF            400.1300000 MHz
WDW           EM
SSB           0
GB            0
PC            1.00
  
```



<sup>1</sup>H NMR (400 MHz, DMSO-d<sub>6</sub>) spectrum of compound (S)-3.



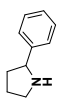
# E | Spectroscopic Data - *rac*-4



```

Current Data Parameters
NAME          RHM137-1
EXPNO        1
PROCNO       1
F2 - Acquisition Parameters
Date_         20180315
Time         21.40
INSTRUM      spect
PROBHD       5 mm BBO-zg30
PULPROG      zg30
TD           65536
SOLVENT      DMSO
NS           2
DS           2
SWH          8012.820 Hz
FIDRES      4.084465 Hz
AQ          49.07 sec
RG          62.400 usec
DM          289.0 usec
DE          289.0 usec
TE          300.2 K
D1          1.00000000 sec
TD0         1

===== CHANNEL f1 =====
SFO1         400.1324710 MHz
NUC1         1H
P1          9.48 usec
PL1         17.00000000 W
F2 - Processing parameters
SI          32768
SF          400.1300033 MHz
WDW         EM
SSB         0
GB          0
PC          1.00
  
```

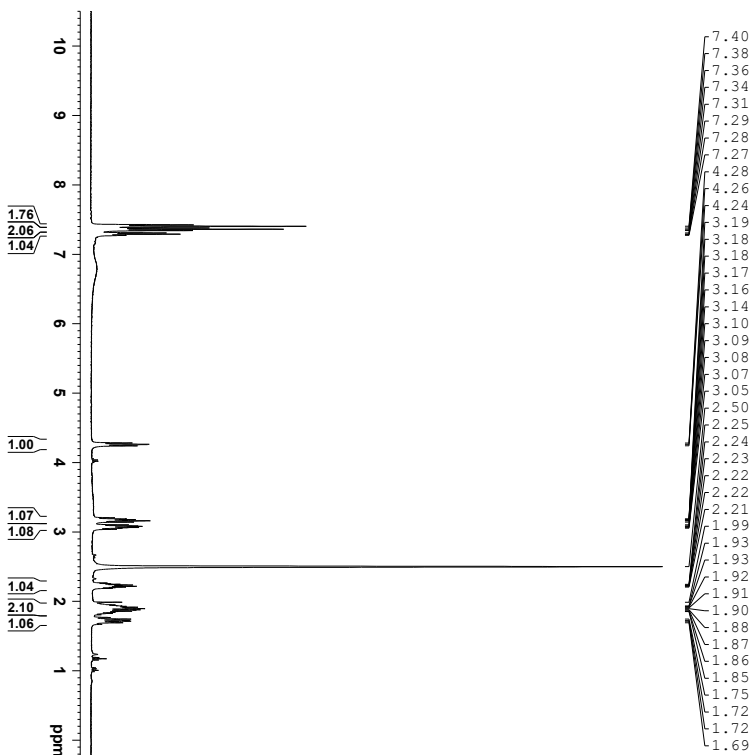


<sup>1</sup>H NMR (400 MHz, DMSO-*d*<sub>6</sub>) spectrum of compound (*rac*)-4.





# F | Spectroscopic Data - Compound (R)-4



```

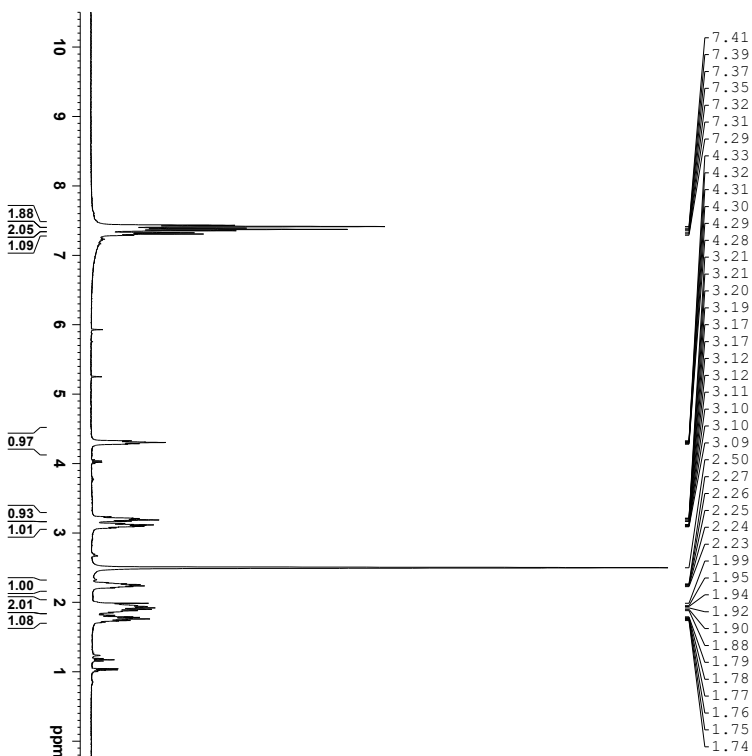
Current Data Parameters
=====
EXNO          1
PROCNO       1
F2 - Acquisition Parameters
=====
Date_         20180406
Time_        1.54
INSTRUM      spect
PROBHD       5 mm PABBO
PULPROG      zg30
TD           65536
SOLVENT      DMSO
DS           2
SWH          8012.820 Hz
AQ           4.064465 sec
RG           112.06
DM           62.400 usec
TE           298.0 K
D1           1.00000000 sec
TD0          1
===== CHANNEL f1 =====
SFO1         400.1324710 MHz
NUC1         1H
P1           9.00 usec
PL1         17.00000000 W
F2 - Processing parameters
=====
SI           32768
SF           400.1300031 MHz
WDW          EM
SSB          0
GB           0
PC           1.00
  
```



<sup>1</sup>H NMR (400 MHz, DMSO-*d*<sub>6</sub>) spectrum of compound (R)-4.

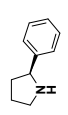


# G | Spectroscopic Data - Compound (S)-4



```

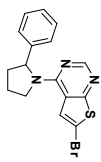
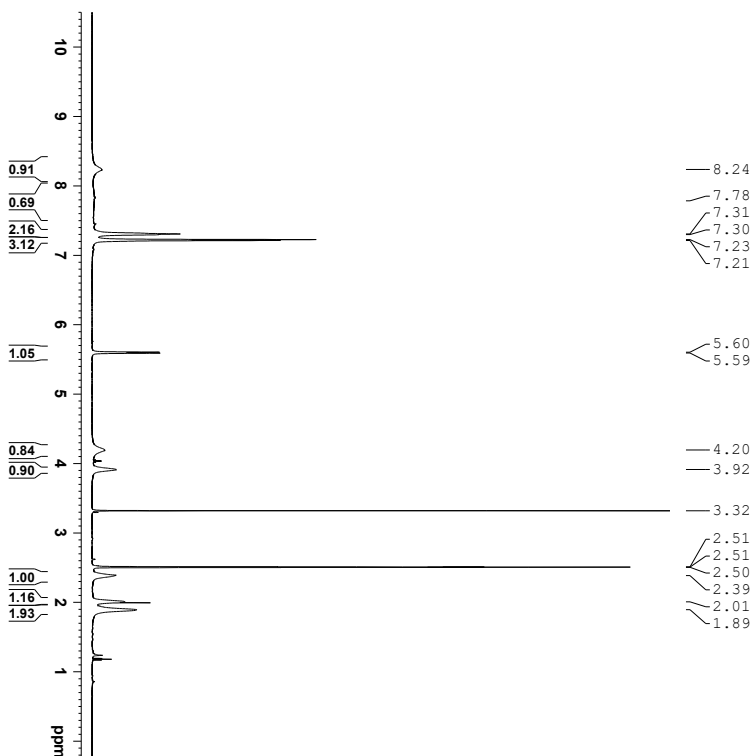
Current Data Parameters
=====
EXNO      MARI-34-Group
PROBHD    1
F2 - Acquisition Parameters
=====
Date_     20180406
Time      1.48
INSTRUM   spect
PROBHD    5 mm BBO5
PULPROG   zg30
TD         65536
SOLVENT   DMSO
DS         2
SWH        8012.820 Hz
AQ         4.064465 sec
RG         112.06
DM         62.400 usec
TE         298.0 K
D1         1.00000000 sec
TD0        1
=====
CHANNEL F1
SFO1      400.1324710 MHz
NUC1      1H
P1         9.00 usec
PL1       0.00 dB
PL12      17.00000000 W
F2 - Processing parameters
=====
SI         32768
SF         400.130032 MHz
WDW        EM
SSB        0
GB         0
PC         1.00
  
```



<sup>1</sup>H NMR (400 MHz, DMSO-*d*<sub>6</sub>) spectrum of compound (S)-4.



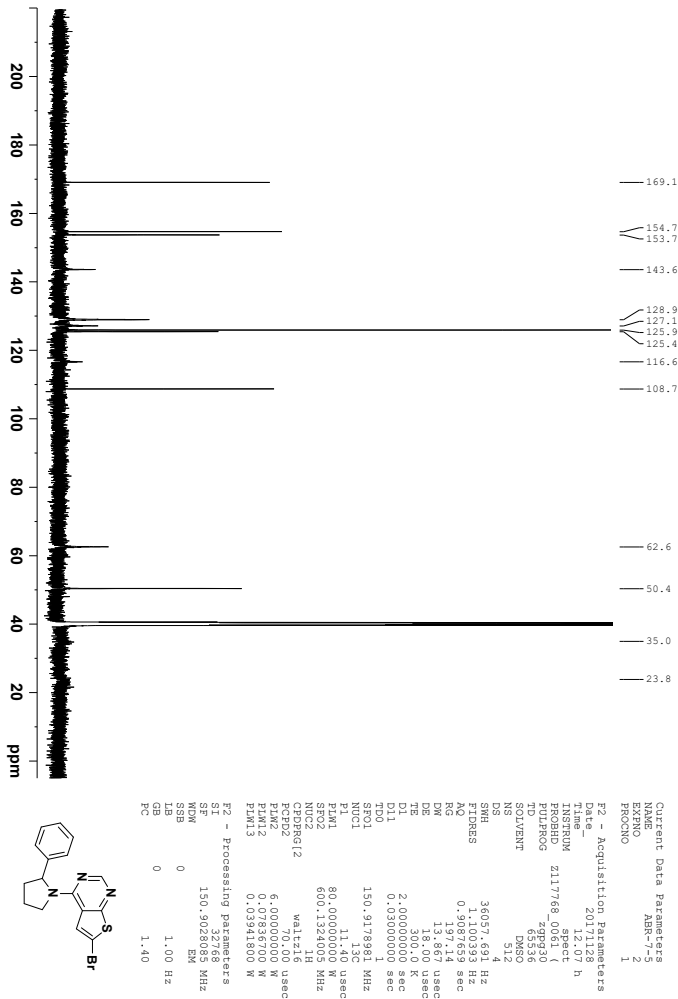
# H | Spectroscopic Data - Compound *rac-5a*



```

Current Data Parameters
NAME      AMN-7
EXPNO     1
PROCNO    1
F2 - Acquisition Parameters
Date_     20171128
Time      11.41 h
INSTRUM   spect
PROBHD    zgpg30
PULPROG   zg30
TD         65536
SOLVENT   DMSO
DS         2
SWH        12019.230 Hz
AQ         0.782976 sec
RG         16.28
DM         41.600 usec
DE         300.0 K
TE         1.00000000 sec
D1         600.1337043 MHz
TDO1      0.01
NUC1       1H
P1         8.00 usec
PL1        6.00000000 W
F2 - Processing parameters
SI         65536
SF         600.1300000 MHz
SFO1      600.1300000 MHz
SSB        0
LB         0.30 Hz
GB         0
PC         1.00
    
```

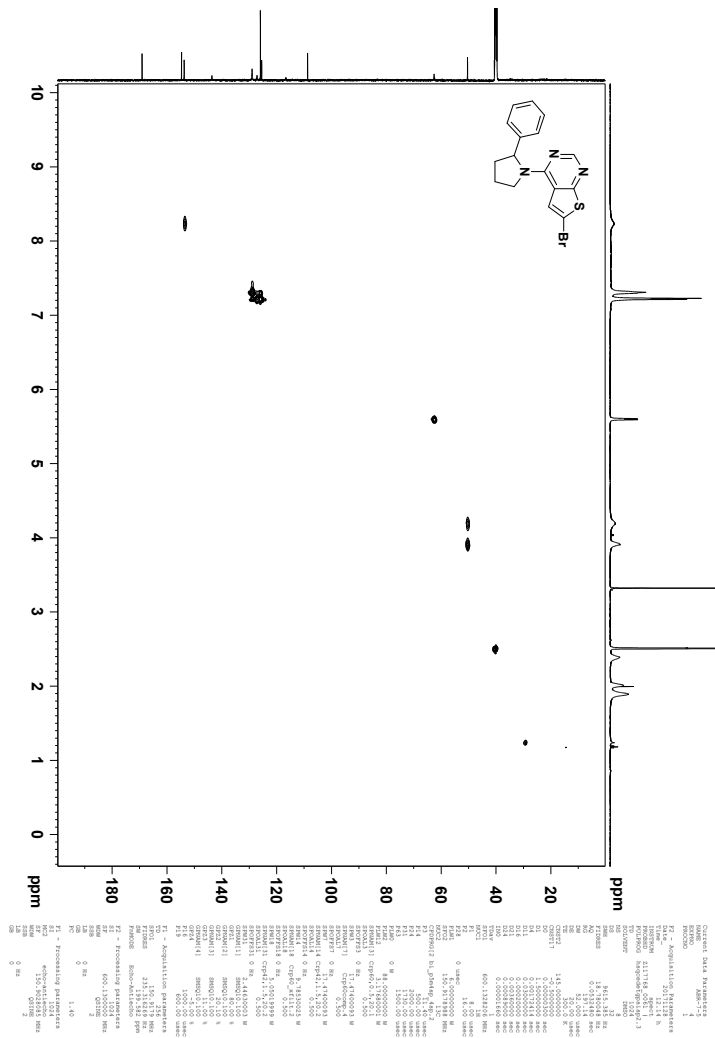
<sup>1</sup>H NMR (600 MHz, DMSO-*d*<sub>6</sub>) spectrum of compound (*rac*)-**5a**.

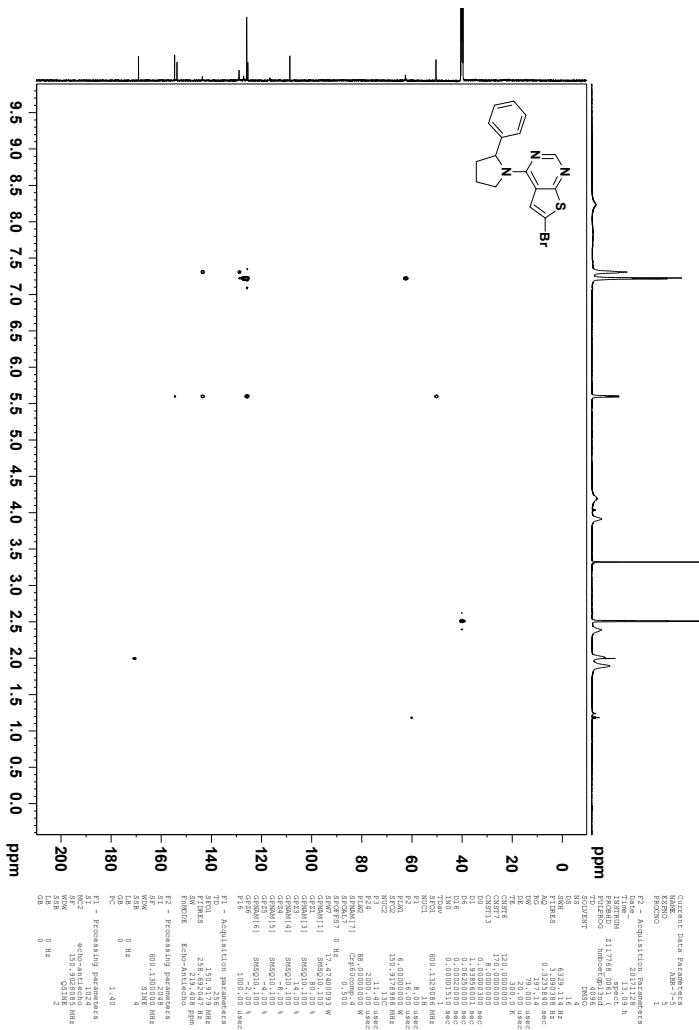


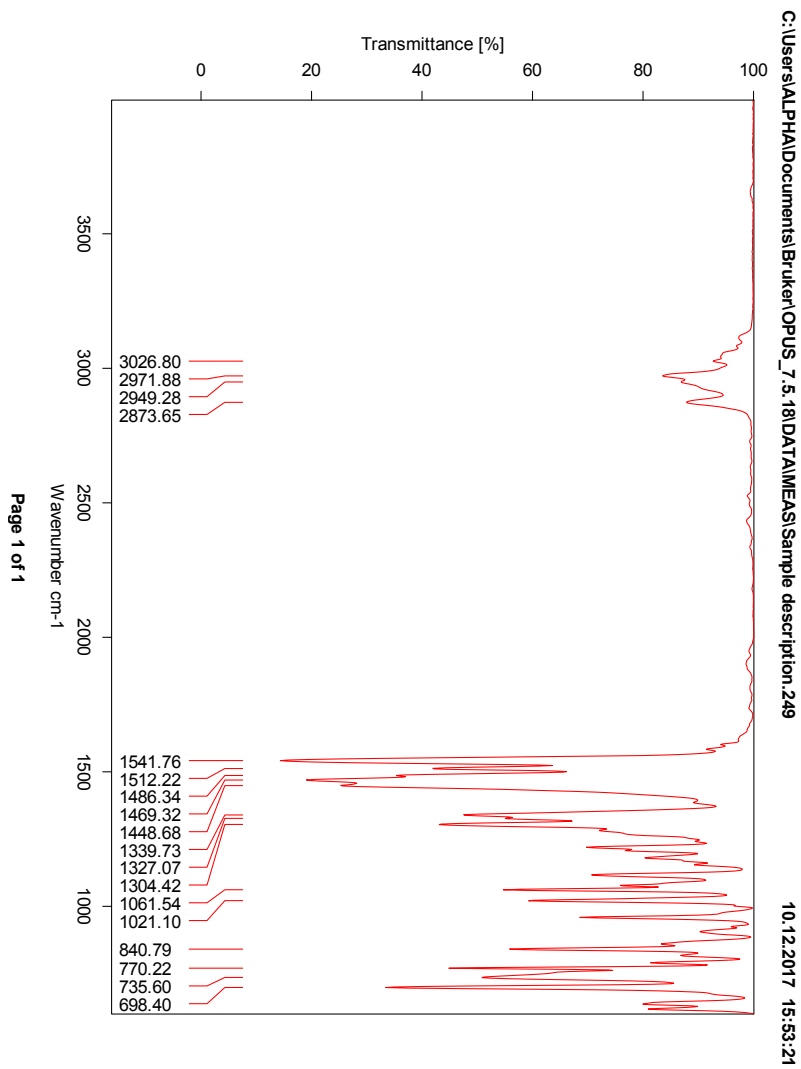
$^{13}\text{C}$  NMR (150 MHz, DMSO- $d_6$ ) spectrum of compound (*rac*)-5a.





HSQC spectrum of compound *rac-5a*.

HMBC spectrum of compound *rac*-5a.

IR spectrum of compound *rac-5a*.

## Elemental Composition Report

Page 1

## Single Mass Analysis

Tolerance = 2.0 PPM / DBE: min = -1.5, max = 50.0

Element prediction: Off

Number of isotope peaks used for i-FIT = 3

Monoisotopic Mass, Even Electron Ions

2848 formula(e) evaluated with 4 results within limits (up to 50 closest results for each mass)

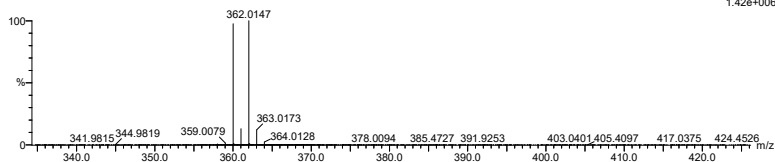
Elements Used:

C: 1-500 H: 0-1000 N: 0-20 O: 0-100 S: 0-1 Br: 0-3

2017-439 43 (0.863) AM2 (Ar,35000.0,0.00,0.00); Cm (41:45)

1: TOF MS ASAP+

1.42e+006



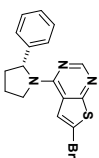
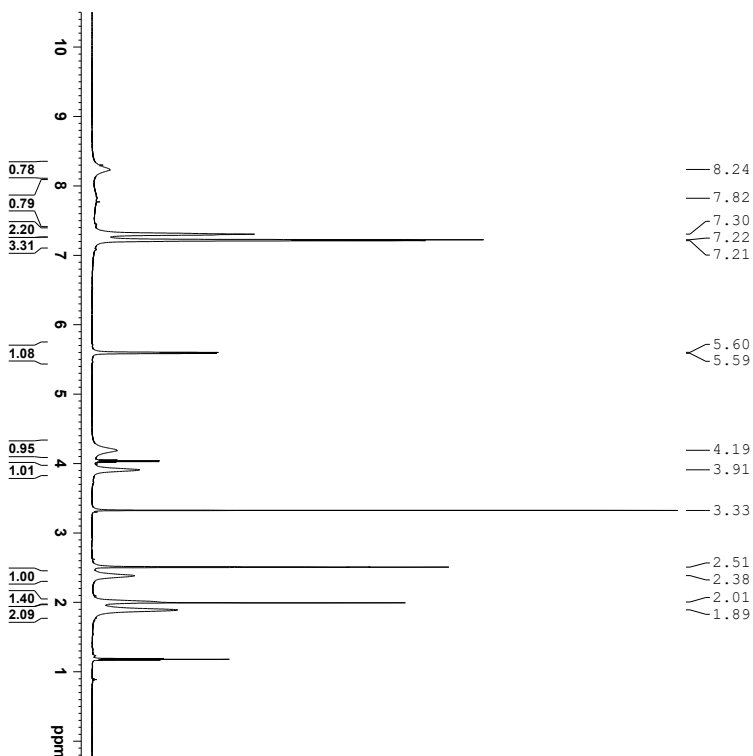
Minimum: -1.5  
Maximum: 50.0

Mass	Calc. Mass	mDa	PPM	DBE	i-FIT	Norm	Conf(%)	Formula
360.0165	360.0170	-0.5	-1.4	10.5	1220.7	9.472	0.01	C16 H15 N3 S Br
	360.0164	0.1	0.3	18.5	1224.5	13.291	0.00	C13 H2 N11 O S
	360.0168	-0.3	-0.8	7.5	1211.2	0.000	99.99	C8 H11 N9 O3 Br
	360.0163	0.2	0.6	4.5	1234.7	23.528	0.00	C7 H10 N3 O14

Mass spectrum of compound *rac*-5a.



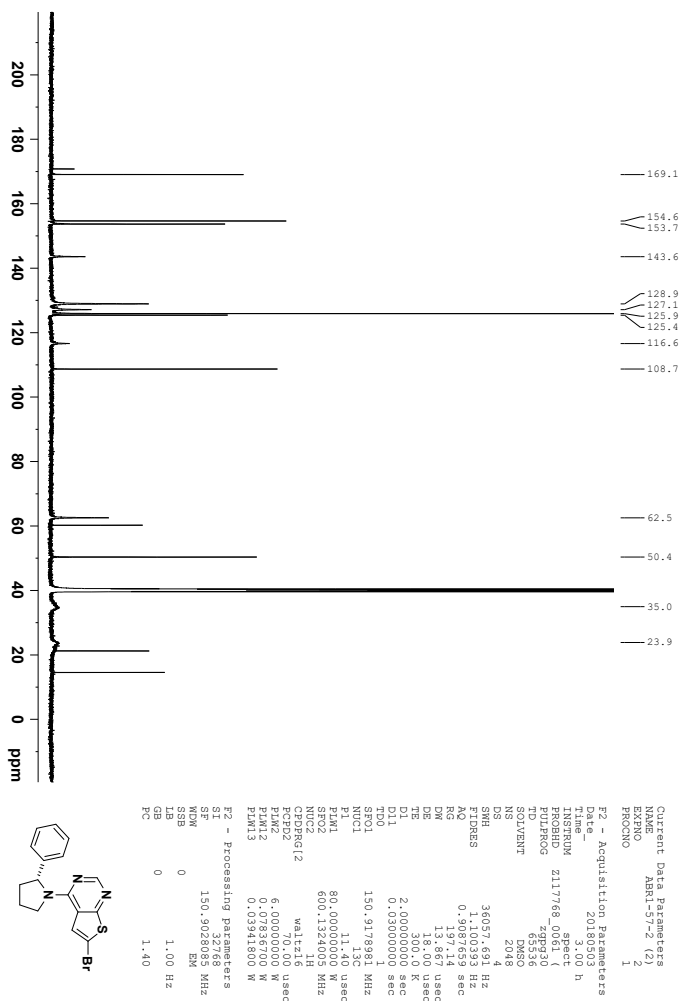
# I | Spectroscopic Data - Compound (R)-5a



```

Current Data Parameters
EXNO          1
PROCNO       1
F2 - Acquisition Parameters
Date_         20180503
Time         1.18 h
INSTRUM      spect
PROBHD       5mm
PULPROG      zg30
TD           65536
SOLVENT      DMSO
DS           2
SWH          12019.230 Hz
AQ           0.742276 sec
RG           10.05
DM           41.600 usec
DE           300.0 K
TE           300.0 K
D1           1.00000000 sec
TDO1        600.1337043 MHz
NUC1         1H
P1           8.00 usec
PL1         6.00000000 W
F2 - Processing parameters
SI           65536
SF           600.1300000 MHz
SFO          600.1300000 MHz
SSB          0
LB           0.30 Hz
GB           0
PC           1.00
  
```

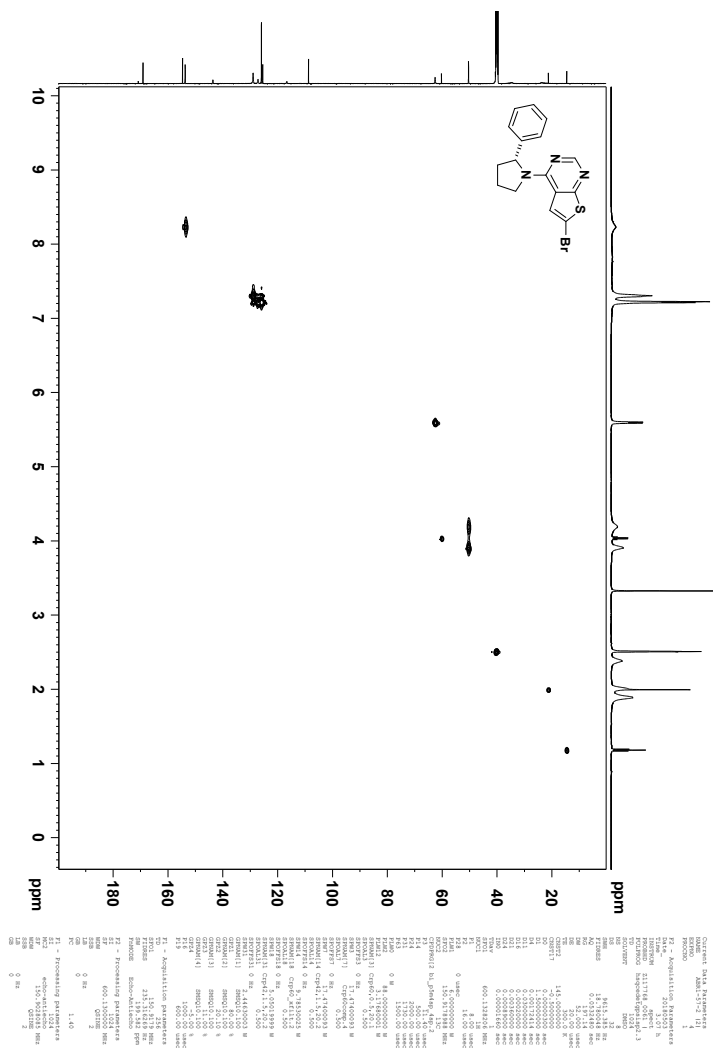
<sup>1</sup>H NMR (600 MHz, DMSO-*d*<sub>6</sub>) spectrum of compound (R)-5a.

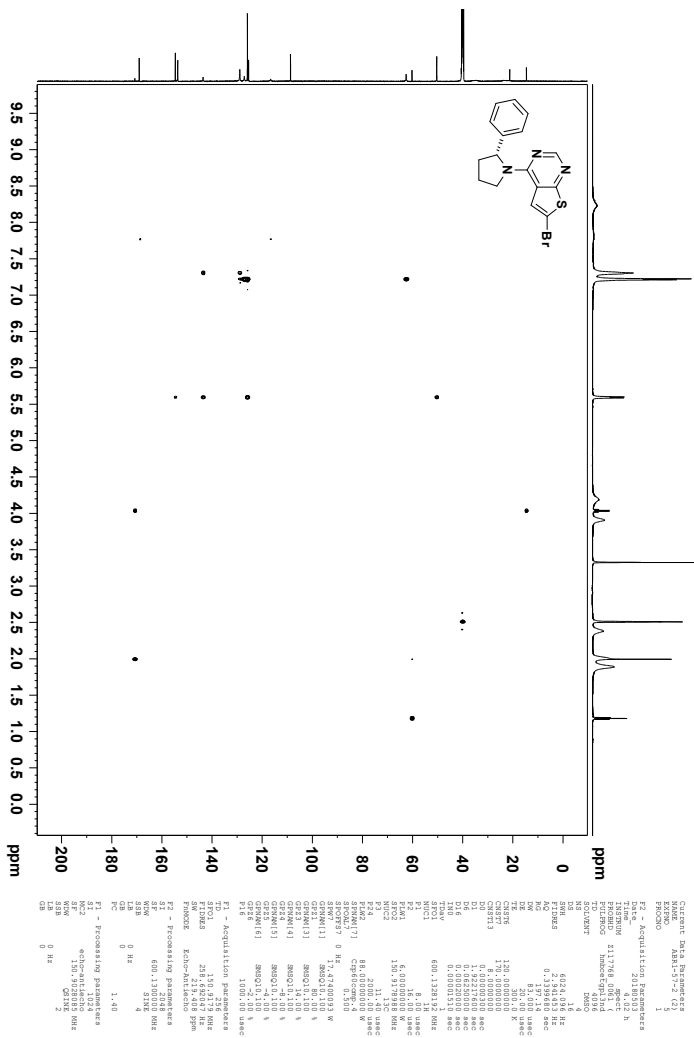


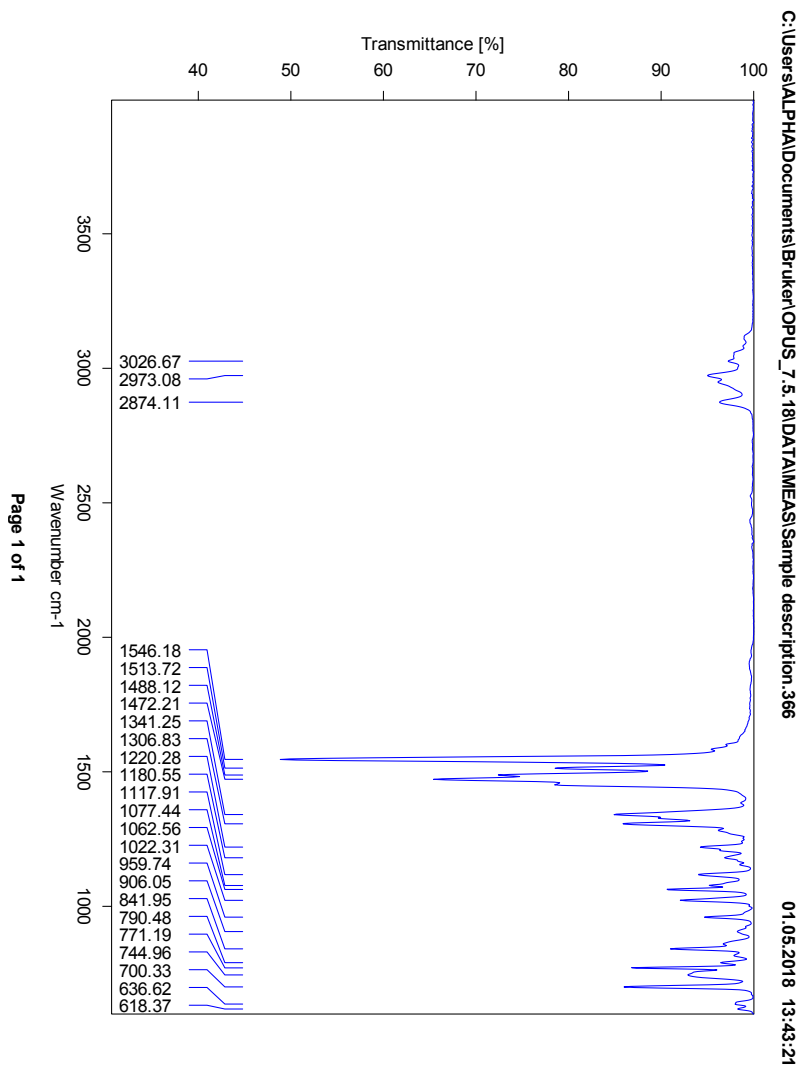
$^{13}\text{C}$  NMR (150 MHz,  $\text{DMSO-}d_6$ ) spectrum of compound (*R*)-5a.





HSQC spectrum of compound (*R*)-5a.

HMBC spectrum of compound (*R*)-5a.

IR spectrum of compound (*R*)-5a.

## Elemental Composition Report

Page 1

## Single Mass Analysis

Tolerance = 2.0 PPM / DBE: min = -1.5, max = 50.0

Element prediction: Off

Number of isotope peaks used for i-FIT = 3

Monoisotopic Mass, Even Electron Ions

4829 formula(e) evaluated with 7 results within limits (all results (up to 1000) for each mass)

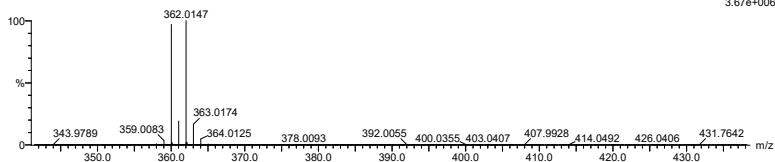
Elements Used:

C: 0-500 H: 0-1000 N: 0-10 O: 0-10 Na: 0-1 S: 0-2 Br: 0-4

2018-174 21 (0.431) AM2 (Ar,35000.0,0.00,0.00); Cm (19:22)

1: TOF MS ASAP+

3.67e+006



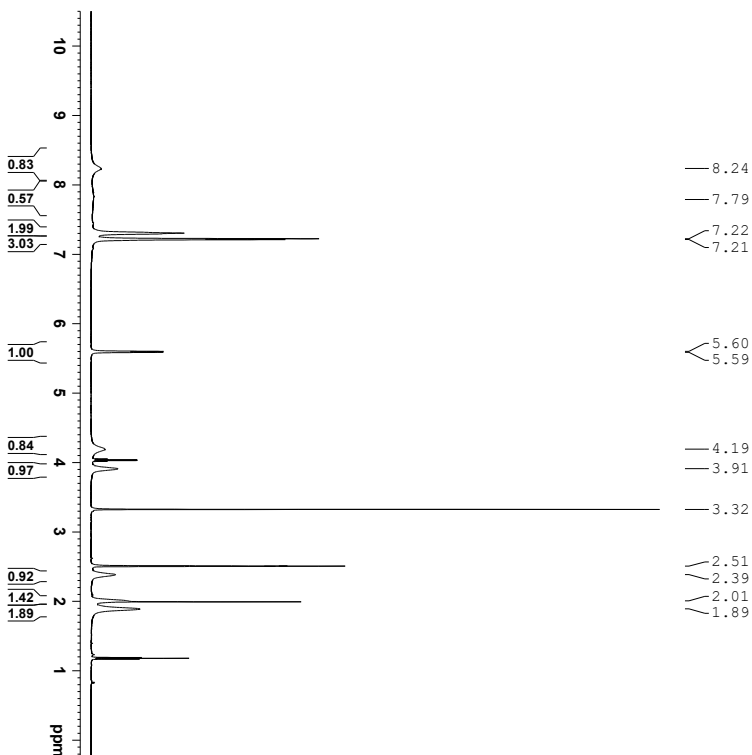
Minimum: -1.5  
Maximum: 50.0

Mass	Calc. Mass	mDa	PPM	DBE	i-FIT	Norm	Conf(%)	Formula
360.0166	360.0170	-0.4	-1.1	10.5	1462.3	0.001	99.95	C16 H15 N3 S Br
	360.0168	-0.2	-0.6	7.5	1470.2	7.823	0.04	C8 H11 N9 O3 Br
	360.0164	0.2	0.6	1.5	1471.4	9.041	0.01	C8 H19 N5 O2 S2 Br
	360.0171	-0.5	-1.4	3.5	1474.6	12.261	0.00	C10 H16 N3 O5 Na Br
	360.0171	-0.5	-1.4	3.5	1480.7	18.358	0.00	C8 H14 N3 O9 S2
	360.0167	-0.1	-0.3	14.5	1480.8	18.472	0.00	C15 H7 N5 O3 Na S
	360.0161	0.5	1.4	5.5	1481.0	18.646	0.00	C7 H11 N7 O5 Na S2

Mass spectrum of compound (R)-5a.

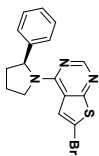


# J | Spectroscopic Data - Compound (S)-5a

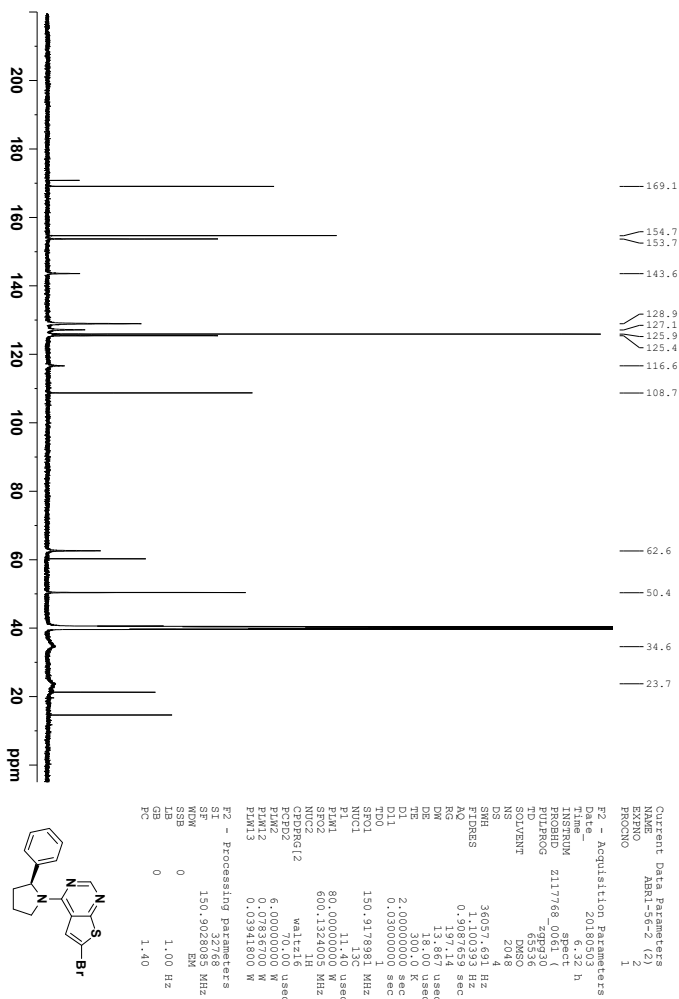


```

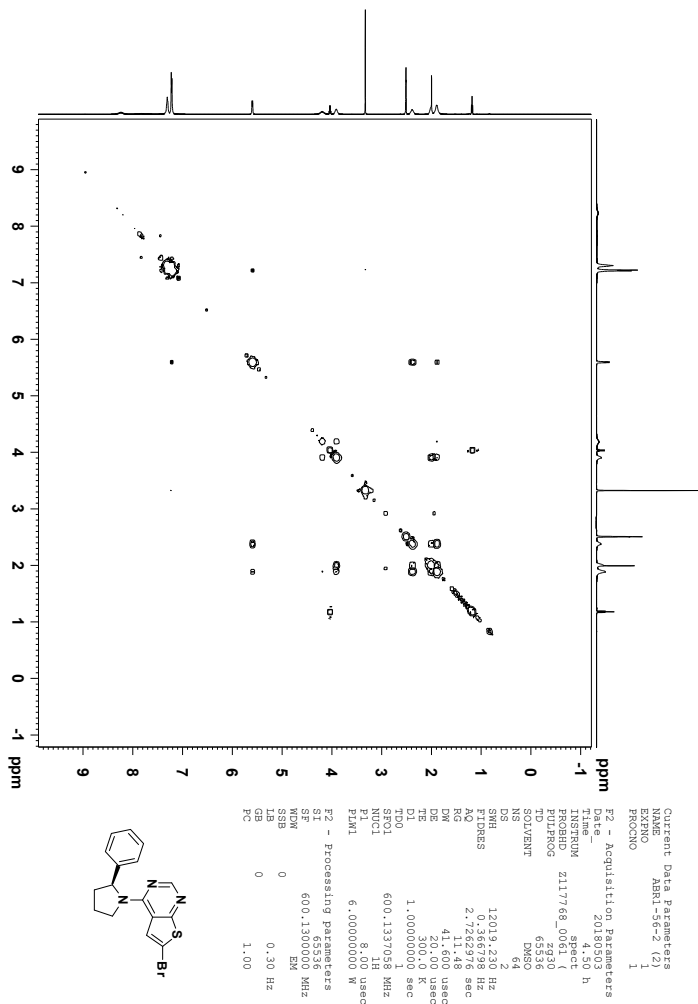
Current Data Parameters
=====
EXNO          1
PROCNO        1
F2 - Acquisition Parameters
=====
Date_         20180503
Time          4.50 h
INSTRUM       spect
PROBHD        5mm QNP 1H/1
PULPROG       zgpg30
TD            65536
AQ            0.987
RG            2
DS            2
SOLVENT       DMSO
NS            12019.230 Hz
SMH           12019.230 Hz
AQURESZ       0.782978 Hz
RG            11.48 sec
DM            41.600 usec
DE            300.0 K
TE            300.0 K
D1            1.00000000 sec
TDO1         600.1337043 MHz
NUC1          1H
P1            8.00 usec
PL1           6.00000000 W
F2 - Processing parameters
=====
SI            65536
SF            600.1300000 MHz
SFO           600.1300000 MHz
SSB           0
LB            0.30 Hz
GB            0
PC            1.00
  
```



<sup>1</sup>H NMR (600 MHz, DMSO-*d*<sub>6</sub>) spectrum of compound (S)-5a.



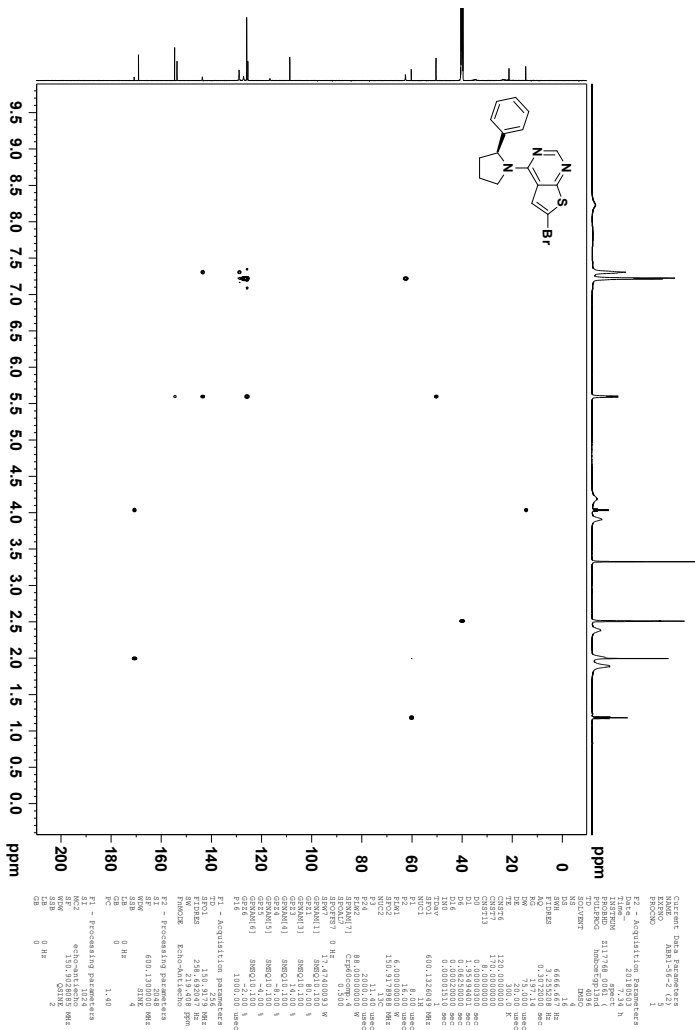
$^{13}\text{C}$  NMR (150 MHz,  $\text{DMSO-}d_6$ ) spectrum of compound (*S*)-**5a**.

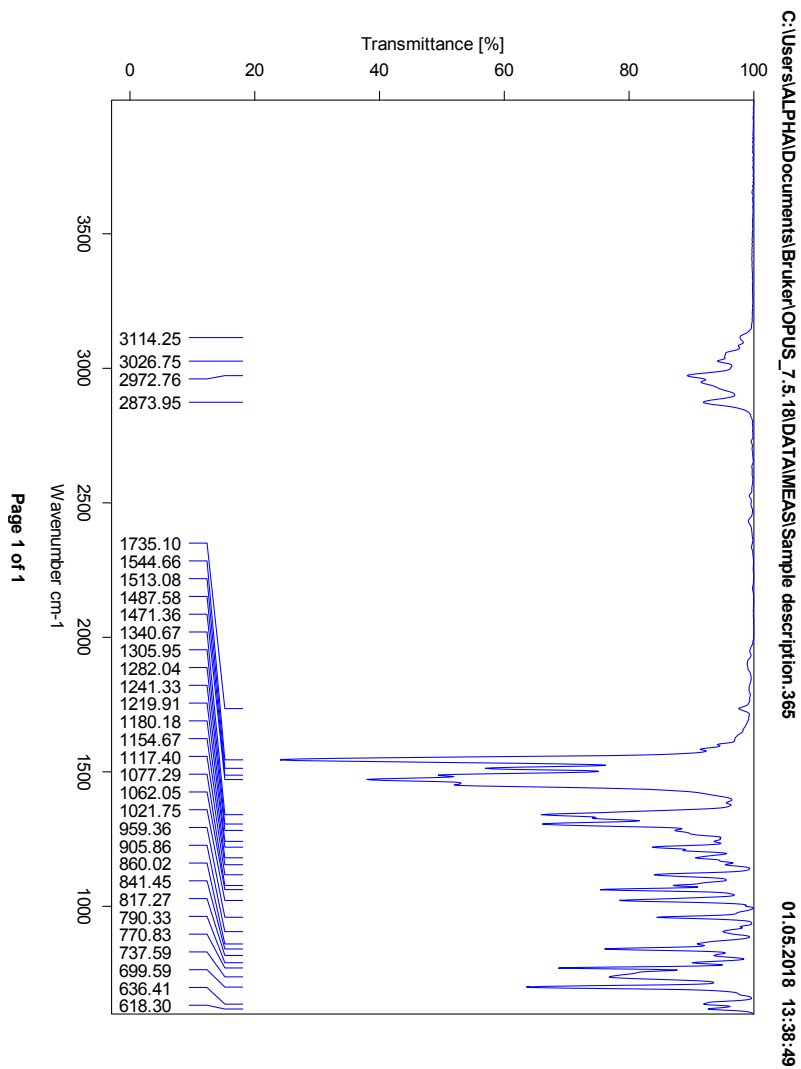


COSY spectrum of compound (S)-5a.





HMBC spectrum of compound (*S*)-5a.

IR spectrum of compound (*S*)-5a.

## Elemental Composition Report

Page 1

## Single Mass Analysis

Tolerance = 2.0 PPM / DBE: min = -1.5, max = 50.0

Element prediction: Off

Number of isotope peaks used for i-FIT = 3

Monoisotopic Mass, Even Electron Ions

4829 formula(e) evaluated with 9 results within limits (all results (up to 1000) for each mass)

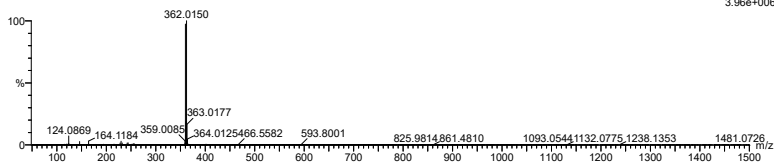
Elements Used:

C: 0-500 H: 0-1000 N: 0-10 O: 0-10 Na: 0-1 S: 0-2 Br: 0-4

2018-175 21 (0.431) AM2 (Ar,35000.0,0.00,0.00); Cm (17.21)

1: TOF MS ASAP+

3.96e+006



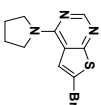
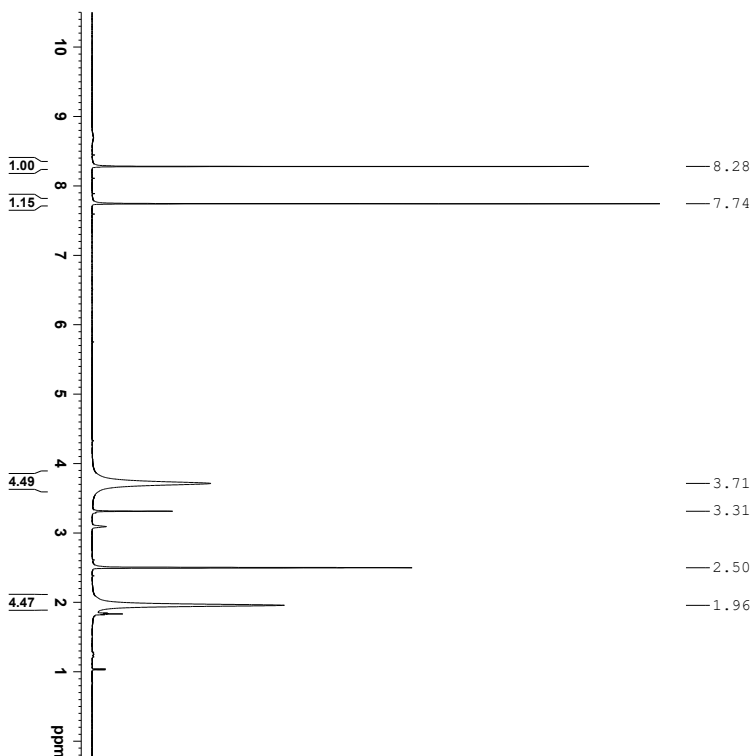
Minimum: -1.5  
Maximum: 50.0

Mass	Calc. Mass	mDa	PPM	DBE	i-FIT	Norm	Conf(%)	Formula
360.0169	360.0170	-0.1	-0.3	10.5	1423.9	0.000	99.99	C16 H15 N3 S Br
	360.0168	0.1	0.3	7.5	1433.4	9.516	0.01	C8 H11 N9 O3 Br
	360.0164	0.5	1.4	1.5	1435.5	11.682	0.00	C8 H19 N5 O2 S2 Br
	360.0171	-0.2	-0.6	3.5	1437.7	13.838	0.00	C10 H16 N3 O5 Na Br
	360.0174	-0.5	-1.4	-0.5	1443.7	19.816	0.00	C11 H24 N O2 Br2
	360.0167	0.2	0.6	14.5	1443.9	20.028	0.00	C15 H7 N5 O3 Na S
	360.0171	-0.2	-0.6	3.5	1443.9	20.031	0.00	C8 H14 N3 O9 S2
	360.0176	-0.7	-1.9	9.5	1451.3	27.434	0.00	C8 H6 N7 O10
	360.0174	-0.5	-1.4	23.5	1452.1	28.282	0.00	C23 H3 N3 O Na

Mass spectrum of compound (S)-5a.



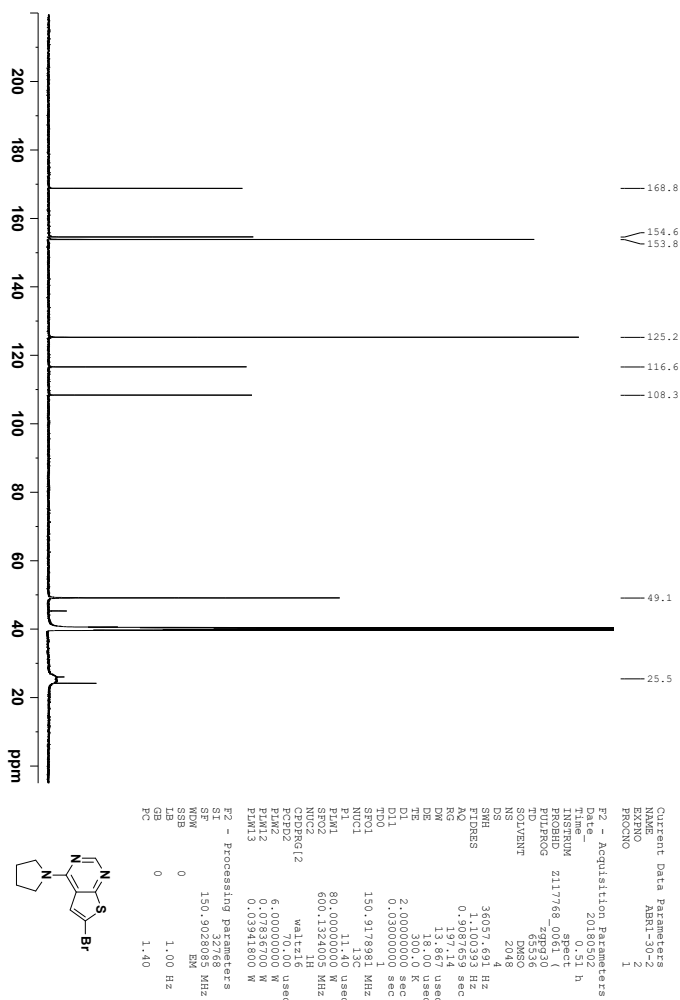
# K | Spectroscopic Data - Compound 5b



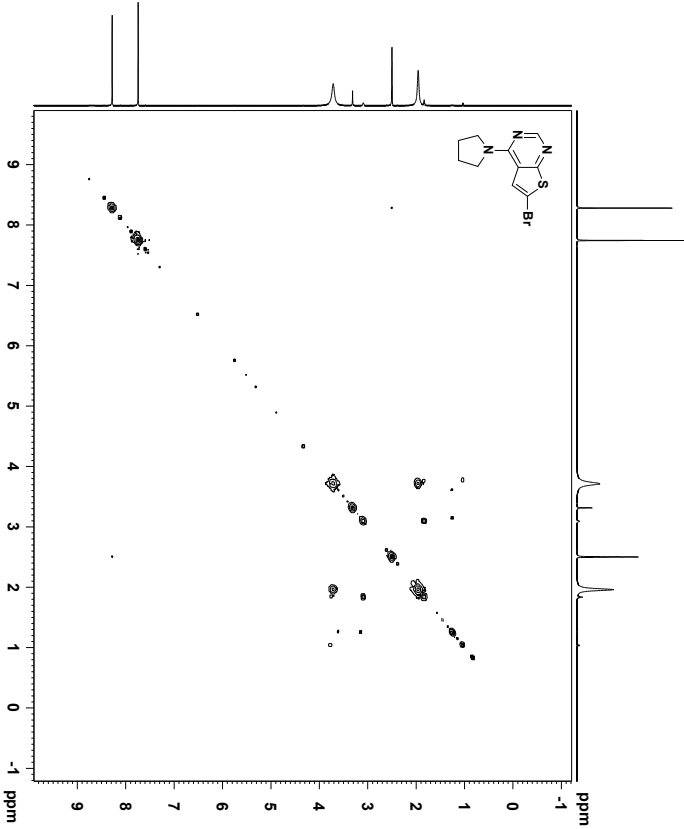
```

Current Data Parameters
=====
EXNO          1
PROCNO       1
F2 - Acquisition Parameters
=====
Date_         20180501
Time_        23:09 h
INSTRUM      spect
PROBHD       5mm
PULPROG      zg30
TD           65536
AQ           1.2
RG           128
DS           2
SOLVENT      DMSO
NS           128
SMH          12019.230 Hz
AQPERS       0.782978 sec
RG           11.48 sec
DM           41.600 usec
TE           300.0 K
D1           1.00000000 sec
TDO1         600.1337043 MHz
NUC1         1H
P1           8.00 usec
PL1          6.000000000 W
F2 - Processing Parameters
=====
SI           65536
SF           600.1300448 MHz
SFO          600.1300448 MHz
SSB          0
LB           0.30 Hz
GB           0
PC           1.00
  
```

<sup>1</sup>H NMR (600 MHz, DMSO-*d*<sub>6</sub>) spectrum of compound **5b**.



<sup>13</sup>C NMR (150 MHz, DMSO-*d*<sub>6</sub>) spectrum of compound **5b**.

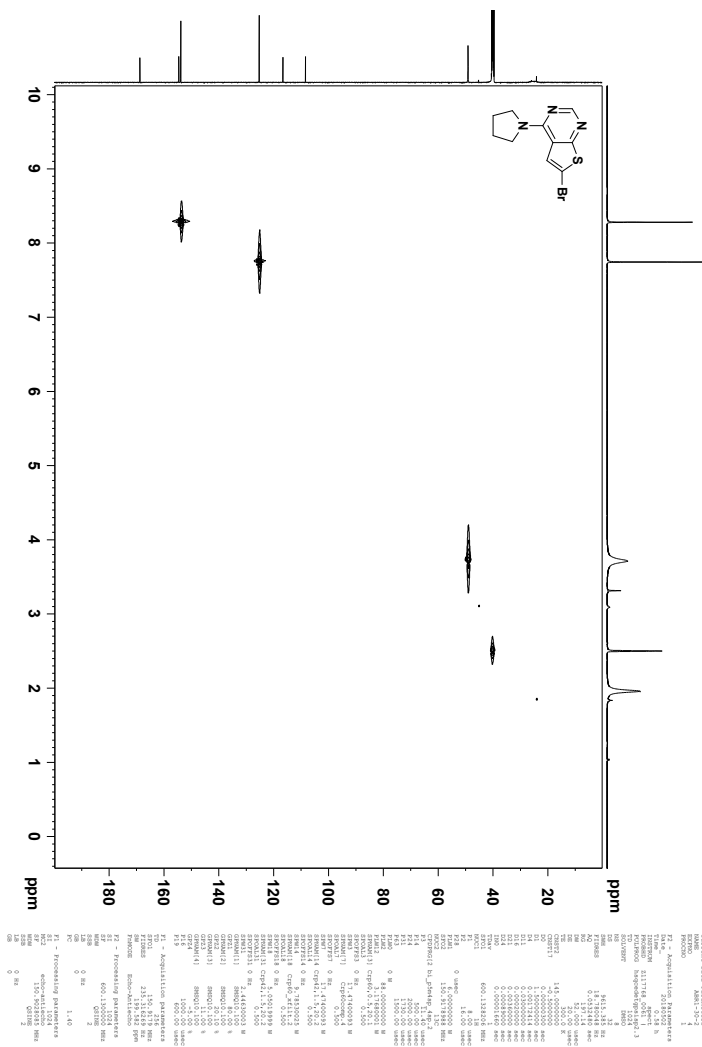


```

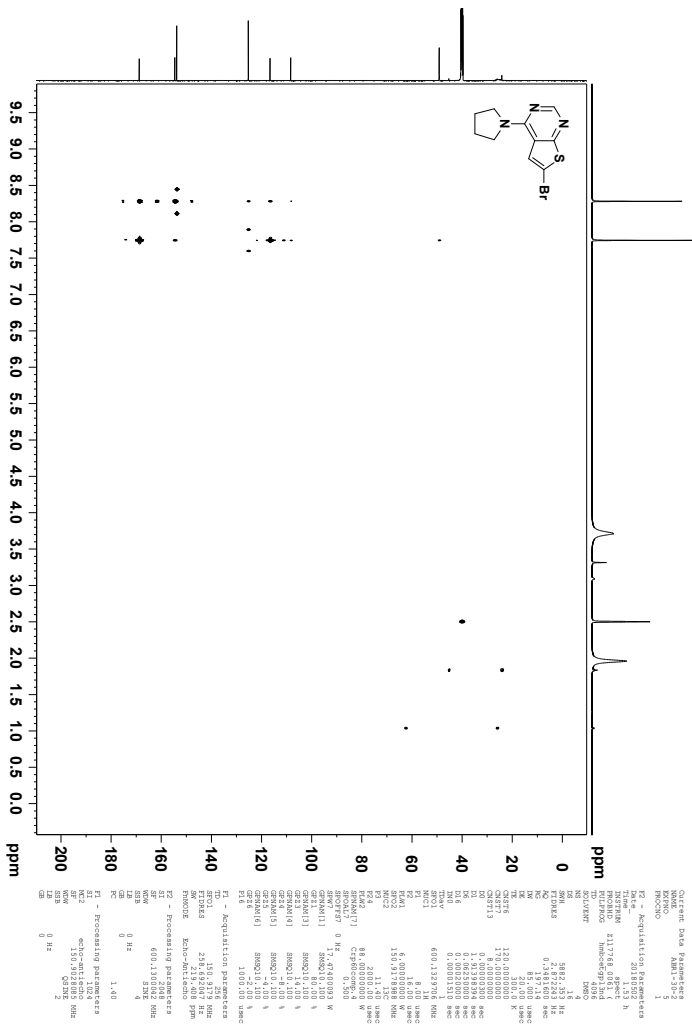
Current Data Parameters
EXPNO 3
PROCNO 1
F2 - Acquisition Parameters
Date_ 20130306
Time 13:55:43
Pulseprog zgpg30
AcqDate 20130306
AcqTime 13:55:43
SOLVENT DMF-DMSO
DS 16
SH 2822.4453 Hz
SHF 500.132809 MHz
AQC 0.1446607 sec
AQ 85.7400 usec
DE 20.00 usec
TE 300.2 K
D0 0.10000000 sec
D1 0.40000000 sec
D11 0.40000000 sec
D12 0.00000000 sec
D13 0.00000000 sec
D16 0.00000000 sec
F2 - Processing parameters
SI 600.13024 MHz
SF 600.13024 MHz
WDW 0 Hertz
SSB 0 Hertz
LB 0 Hertz
GB 1.40 Hertz
FI - Acquisition parameters
SFO 500.132809 MHz
WDW EM
SSB 0
SF 600.13024 MHz
AQ 0.1446607 sec
DE 20.00 usec
TE 300.2 K
F1 - Processing parameters
SI 600.13024 MHz
SF 600.13024 MHz
WDW 0 Hertz
SSB 0 Hertz
LB 0 Hertz
GB 1.40 Hertz
  
```

COSY spectrum of compound **5b**.

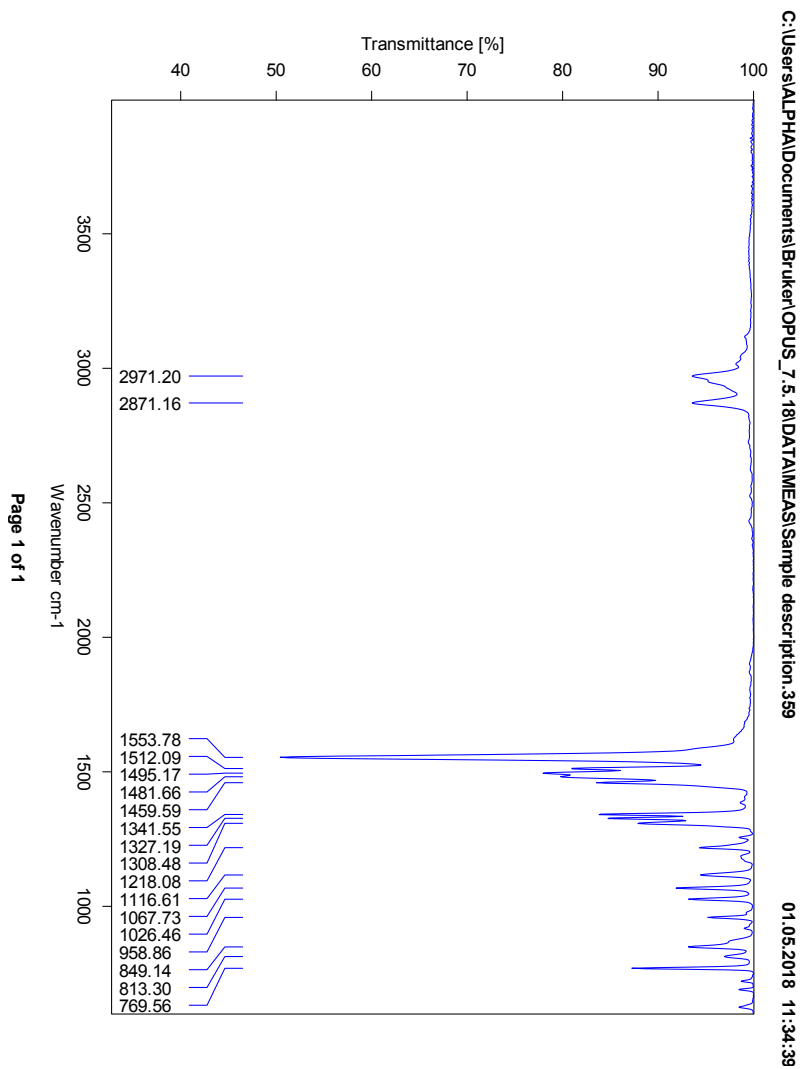




HSQC spectrum of compound **5b**.



HMBC spectrum of compound 5b.

IR spectrum of compound **5b**.

Elemental Composition Report

Single Mass Analysis

Tolerance = 2.0 PPM / DBE: min = -1.5, max = 50.0

Element prediction: Off

Number of isotope peaks used for i-FIT = 3

Monoisotopic Mass, Even Electron Ions

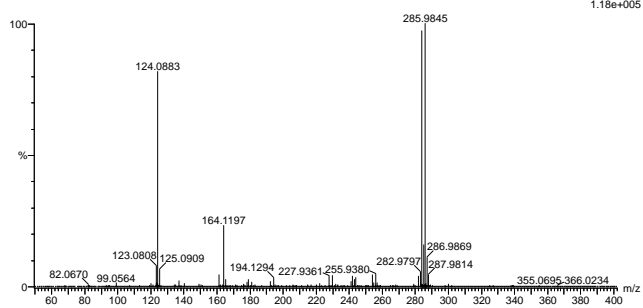
1804 formula(e) evaluated with 4 results within limits (all results (up to 1000) for each mass)

Elements Used:

C: 0-500 H: 0-1000 N: 0-10 O: 0-20 S: 0-3 Br: 0-2

2018-248B 91 (1.793) AM2 (Ar,35000.0,0.00,0.00); Cm (91.92)

1: TOF MS ASAP+



Minimum: 5.0 2.0 -1.5

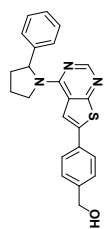
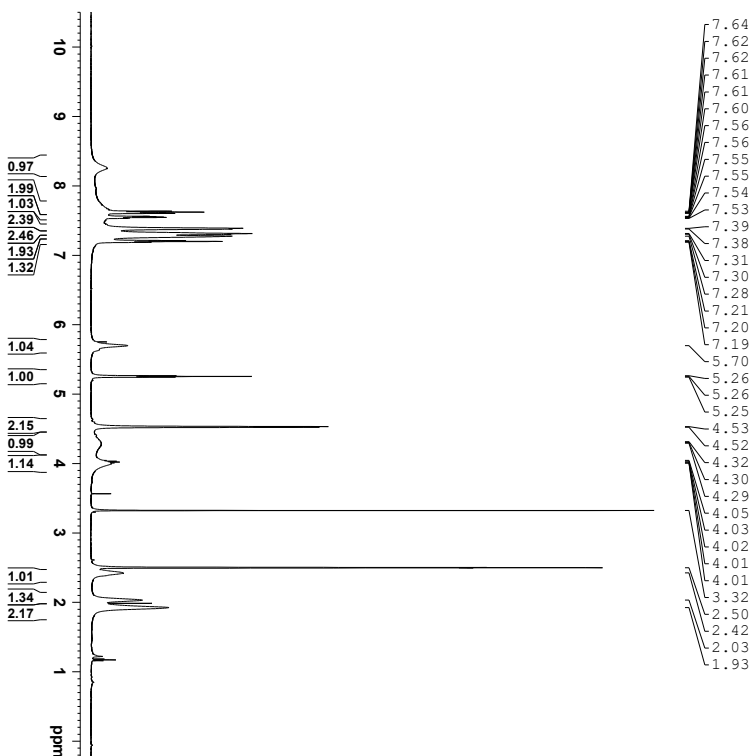
Maximum: 50.0

Mass	Calc. Mass	mDa	PPM	DBE	i-FIT	Norm	Conf (%)	Formula
283.9861	283.9863	-0.2	-0.7	5.5	1022.0	12.438	0.00	C2 H2 N7 O10
	283.9858	0.3	1.1	-0.5	1018.1	8.476	0.02	C2 H10 N3 O9 S2
	283.9865	-0.4	-1.4	8.5	1020.1	10.477	0.00	C10 H6 N O7 S
	283.9857	0.4	1.4	6.5	1009.6	0.000	99.98	C10 H11 N3 S Br

Mass spectrum of compound 5b.



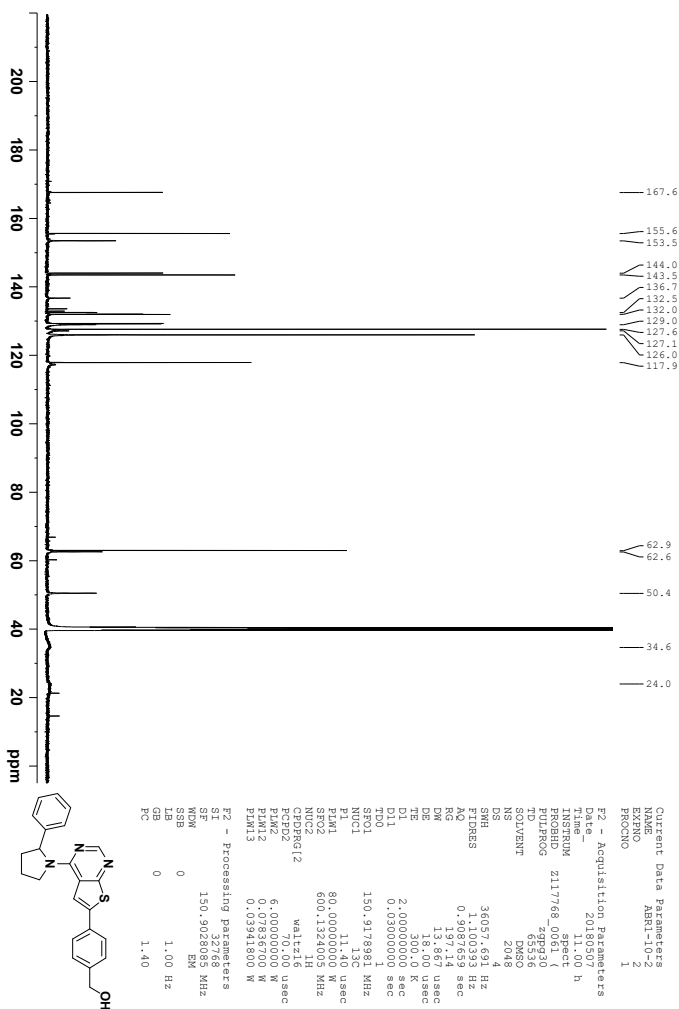
# L | Spectroscopic Data - Compound *rac-6a*



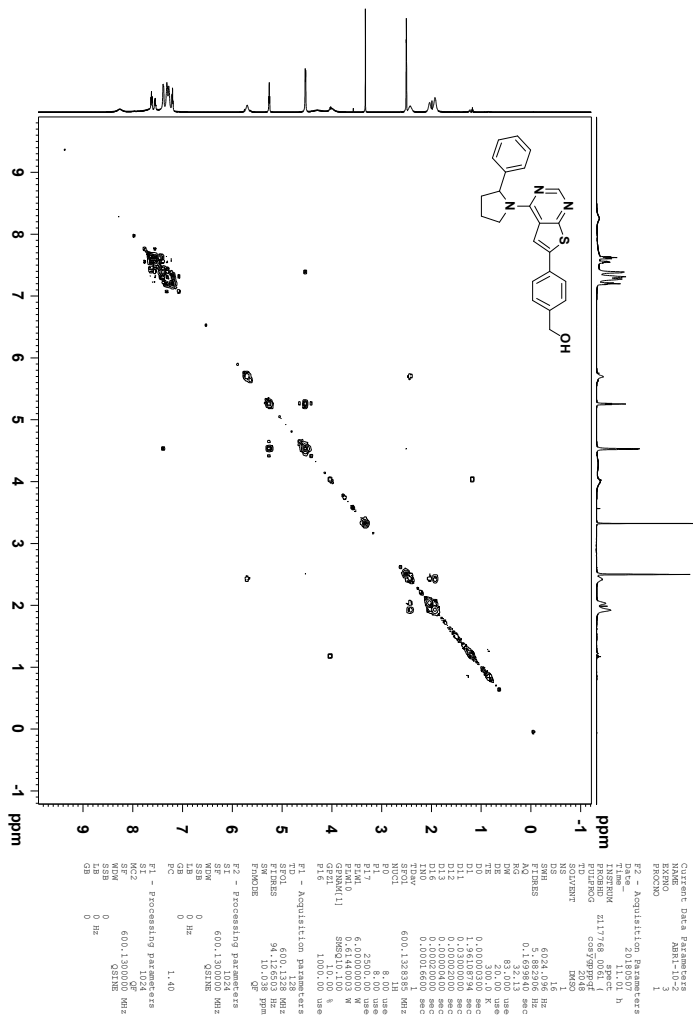
```

Current Data Parameters
NAME      AMN1-10
EXPNO     1
PROCNO    1
F2 - Acquisition Parameters
Date_     20180507
Time      9.18 h
INSTRUM   spect
PROBHD    5mm QNP 1H/1
PULPROG   zgpg30
TD         65536
SOLVENT   DMSO
DS         2
SWH        12019.230 Hz
AQ         0.782976 sec
RG          10.05
DM          41.600 usec
TE          300.0 K
TD1         1.00000000 sec
FID01      600.1337043 MHz
NUC1       1H
P1          8.00 usec
PL1        6.00000000 W
F2 - Processing parameters
SI         65536
SF         600.130048 MHz
SFO        600.130048 MHz
SSB        0
LB         0.30 Hz
GB         0
PC         1.00
  
```

<sup>1</sup>H NMR (600 MHz, DMSO-*d*<sub>6</sub>) spectrum of compound *rac-6a*.

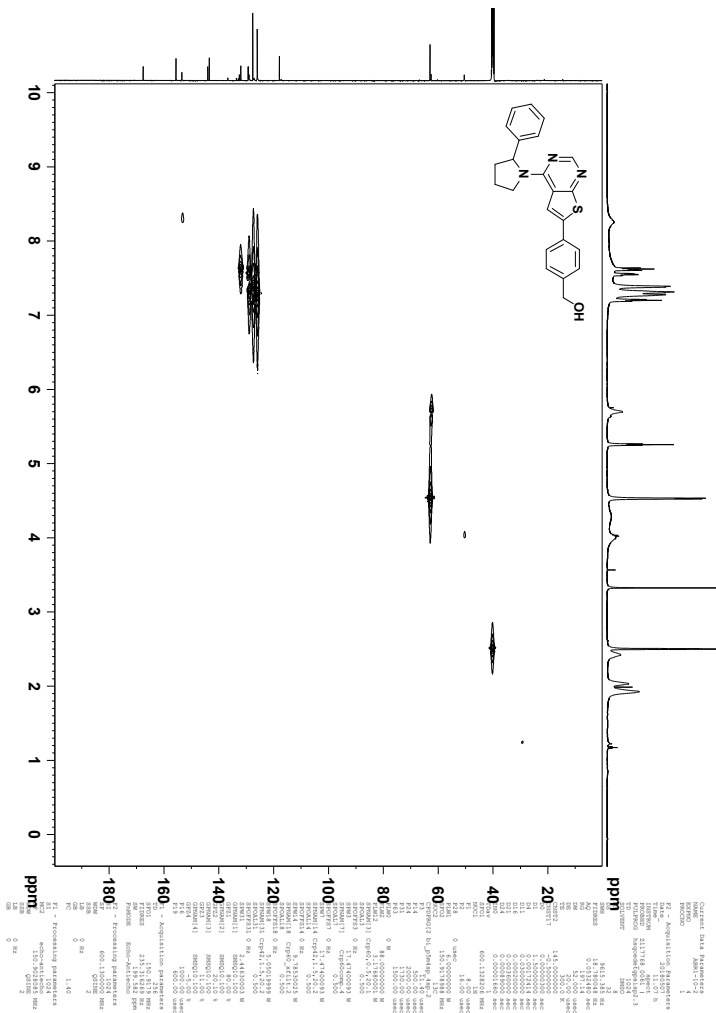


$^{13}\text{C}$  NMR (150 MHz,  $\text{DMSO-}d_6$ ) spectrum of compound *rac-6a*.

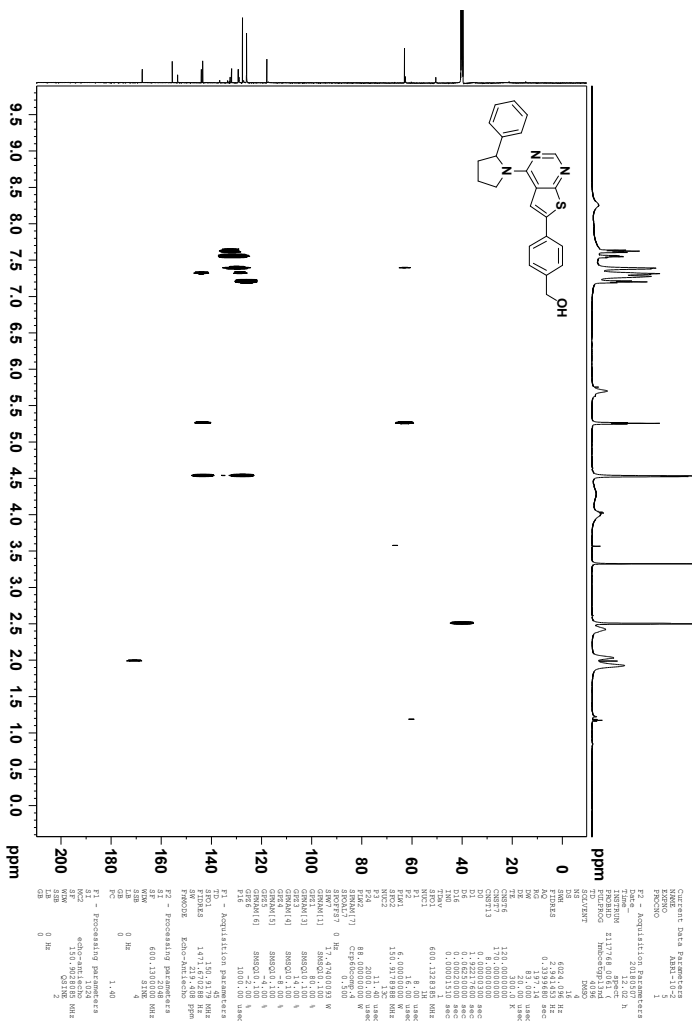


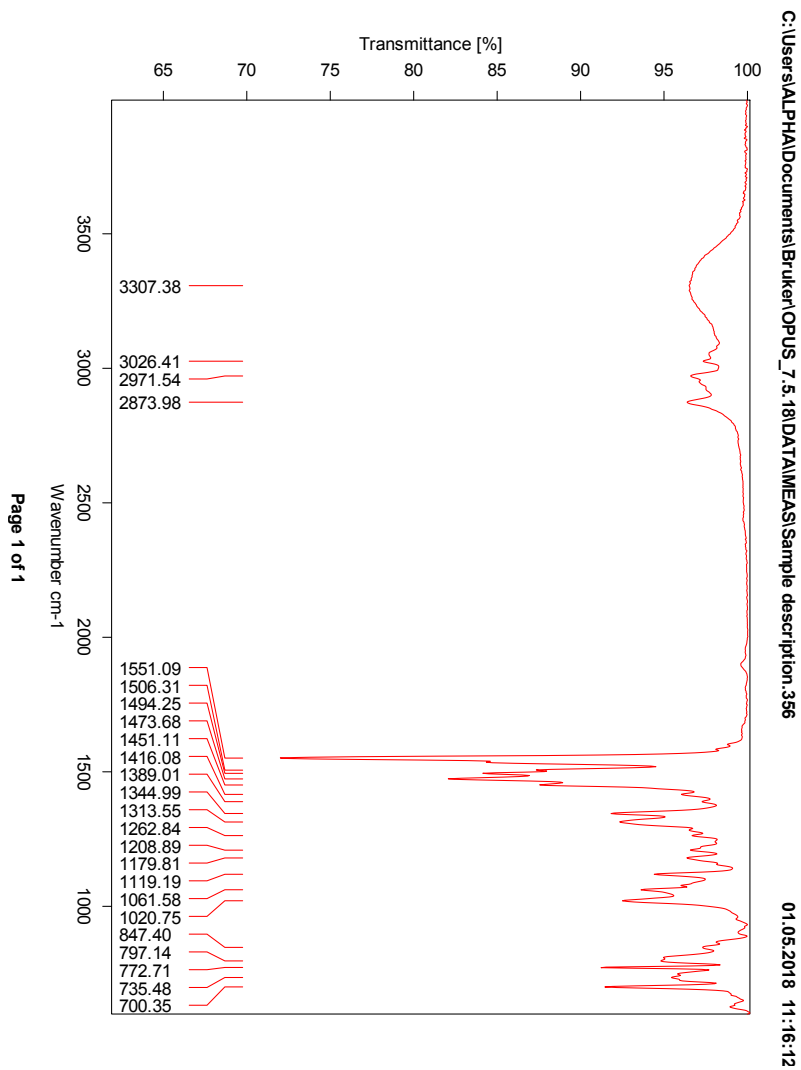
COSY spectrum of compound *rac*-6a.





HSQC spectrum of compound *rac-6a*.

HMBC spectrum of compound *rac*-6a.

IR spectrum of compound *rac-6a*.

## Elemental Composition Report

Page 1

## Single Mass Analysis

Tolerance = 2.0 PPM / DBE: min = -1.5, max = 50.0

Element prediction: Off

Number of isotope peaks used for i-FIT = 3

Monoisotopic Mass, Even Electron Ions

4739 formula(e) evaluated with 4 results within limits (up to 50 closest results for each mass)

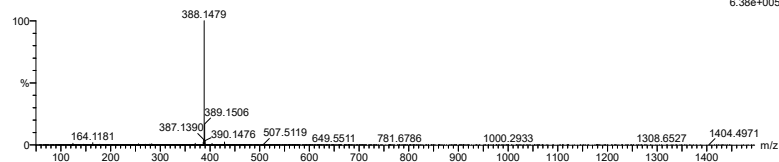
Elements Used:

C: 1-500 H: 0-1000 N: 0-20 O: 0-100 S: 0-2 Br: 0-3

2017-440 118 (2.309)AM2 (Ar.35000.0,0.00,0.00), Cm (113:118)

1: TOF MS ASAP+

6.38e+005



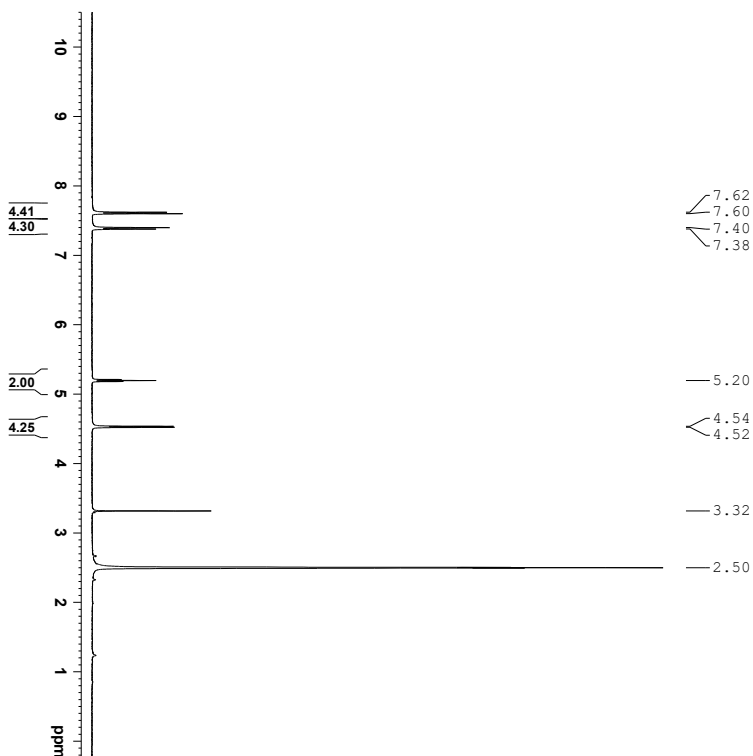
Minimum: -1.5  
Maximum: 50.0

Mass	Calc. Mass	mDa	PPM	DBE	i-FIT	Norm	Conf(%)	Formula
388.1479	388.1484	-0.5	-1.3	14.5	921.1	0.451	63.69	C23 H22 N3 O S
	388.1482	-0.3	-0.8	11.5	922.4	1.728	17.77	C15 H18 N9 O4
	388.1475	0.4	1.0	2.5	922.5	1.756	17.28	C7 H22 N11 O6 S
	388.1477	0.2	0.5	5.5	925.1	4.371	1.26	C15 H26 N5 O3 S2

Mass spectrum of compound *rac-6a*.



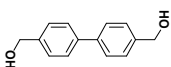
# M | Spectroscopic Data - Dimer by-product



```

Current Data Parameters
=====
EXPNO      1
PROCNO     1
Date_      20180201
Time       12.03
INSTRUM    spect
PROBHD     5 mm BBO5B
PULPROG    zg30
TD          65536
SOLVENT    DMSO
DS          2
SWH         8012.820 Hz
AQ          4.06445 sec
RG          2091.8
DM          62.400 usec
TE          298.0 K
D1          1.00000000 sec
TD0         1

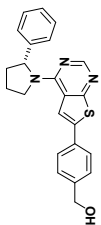
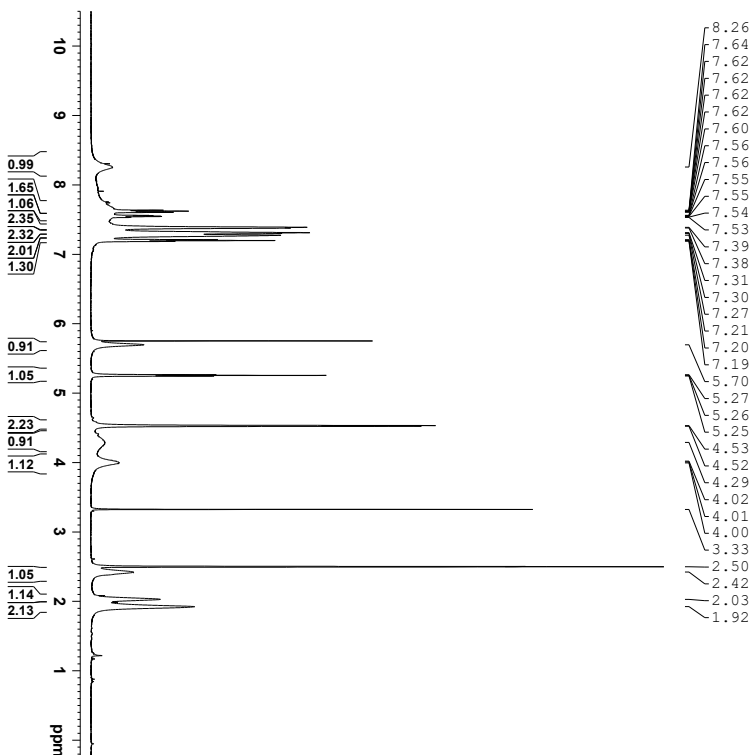
===== CHANNEL f1 =====
SFO1       400.1324710 MHz
NUC1       1H
P1         9.00 usec
PL1        0.00 dB
=====
F2 - Processing parameters
SF         400.1300034 MHz
WDW        EM
SSB        0
GB         0
PC         1.00
  
```



<sup>1</sup>H NMR (400 MHz, DMSO-*d*<sub>6</sub>) spectrum of [1,1'-biphenyl]-4,4'-diyl dimethanol, as a byproduct in the synthesis of *rac*-**6a**.



# N | Spectroscopic Data - Compound (R)-6a



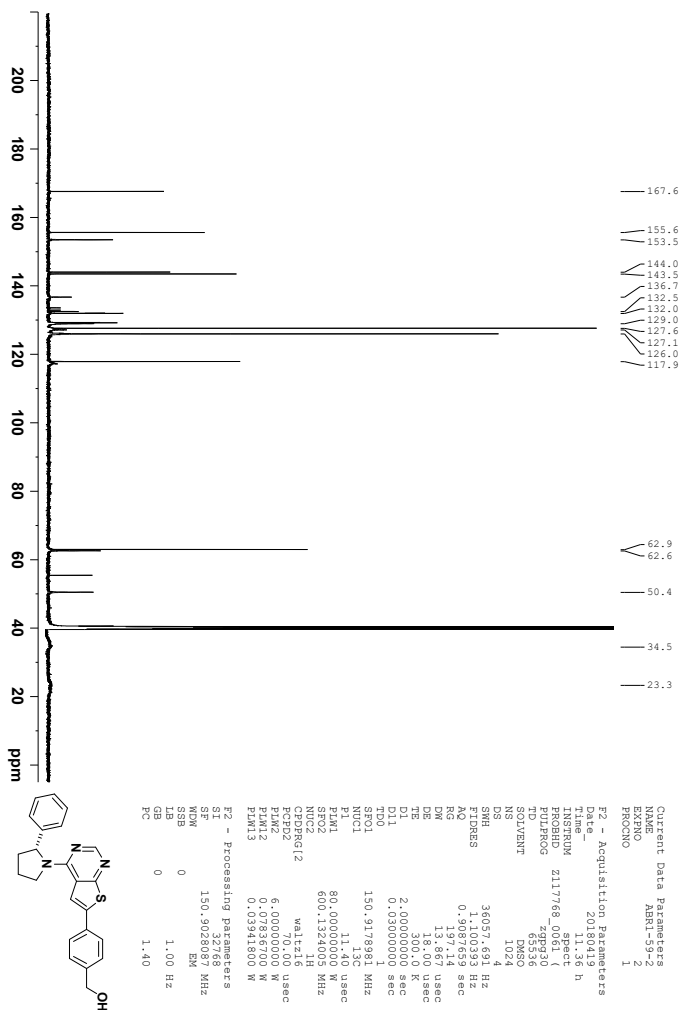
```

Current Data Parameters
=====
EXNO          1
PROCNO       1
F2 - Acquisition Parameters
=====
Date_         20180419
Time_        10.45 h
INSTRUM      spect
PROBHD       5mm QNP 1H/1
PULPROG      zgpg30
TD           65536
AQ           1.00000000 sec
RG           300.0 K
WDW           EM
SSB           0
GB           0
PC           1.00
SOLVENT      DMSO
DS           2
SWH          12019.230 Hz
AQUREFS     2.7282978 sec
RG           10.05
DM           41.600 usec
DE           300.0 K
TE           300.0 K
D1           1.00000000 sec
TDO1        600.1337043 MHz
NUC1         1H
P1           8.00 usec
PLM1        6.00000000 W
F2 - Processing Parameters
=====
SI           65536
SF           600.130050 MHz
SFO          600.130050 MHz
AQ           1.00000000 sec
RG           300.0 K
WDW           EM
SSB           0
GB           0
PC           1.00

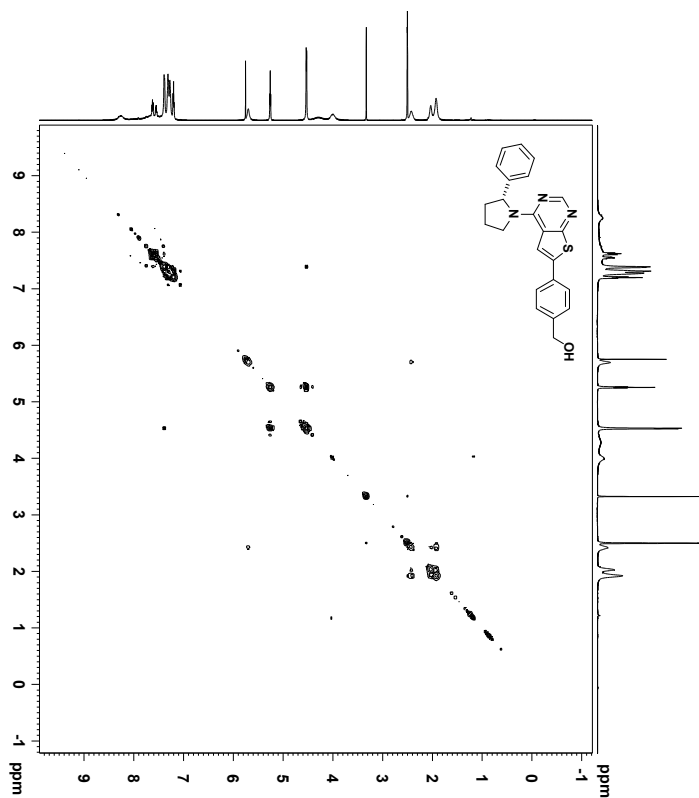
```

<sup>1</sup>H NMR (600 MHz, DMSO-*d*<sub>6</sub>) spectrum of compound (R)-6a.





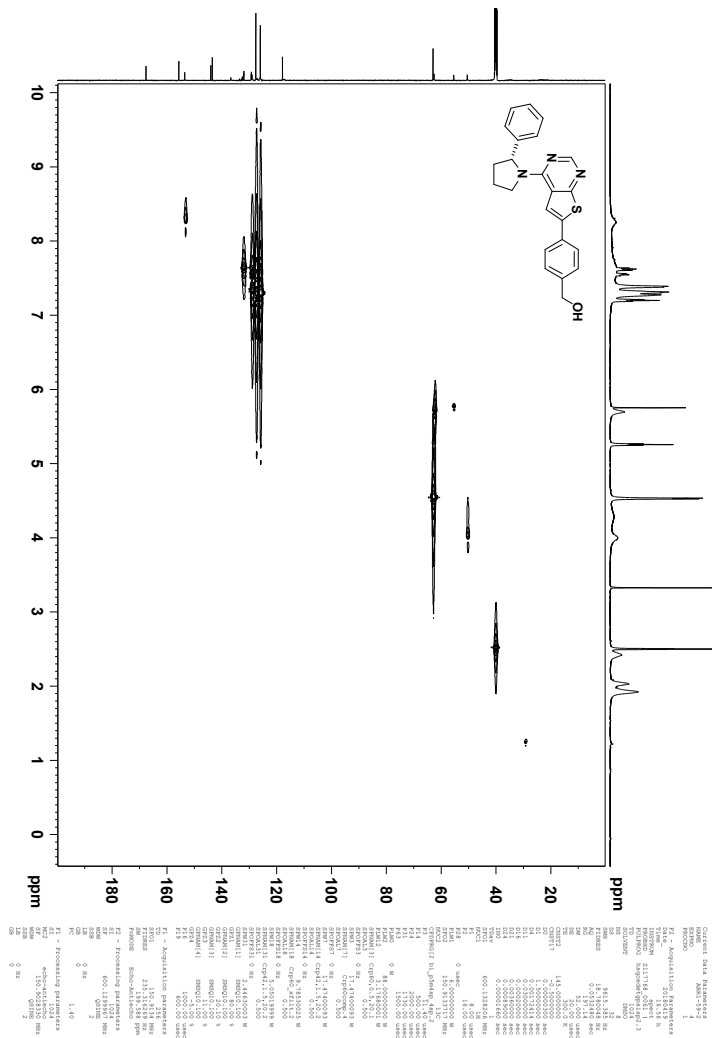
<sup>13</sup>C NMR (150 MHz, DMSO-*d*<sub>6</sub>) spectrum of compound (*R*)-6a.



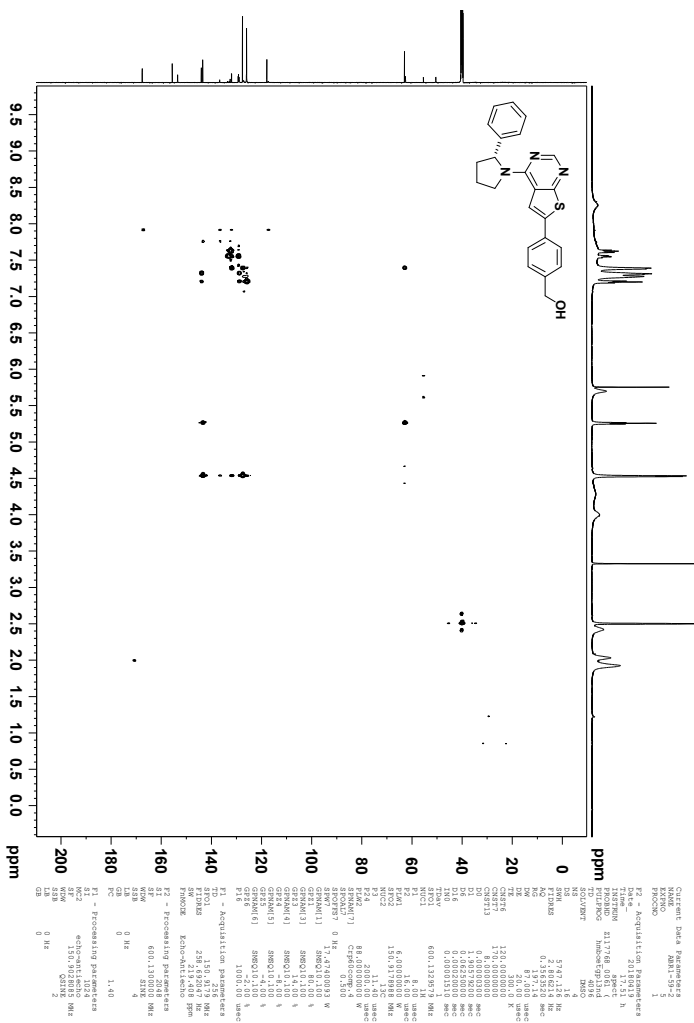
```

Current Data Parameters
EXPNO          3
PROCNO         1
F2 - Acquisition Parameters
Time          16:50 h
Date_         21/11/08 06:01
PULPROG       zgpg30
PRGNAME       cosy2d
SOLVENT       DMSO
DS            16
SI            512
SF            500.136060 MHz
AQ            0.1781760 sec
RG            67.000
DM            87.000
TE            300.0 K
TD            320.0
DE            0.00000000 sec
D0            0.00000000 sec
D1            0.02000000 sec
D11           0.02000000 sec
D12           0.02000000 sec
D13           0.00000000 sec
D16           0.00000000 sec
TEMB         0.00000000 sec
TD0          600.1329714 MHz
NUC1          13C
NUC2          1H
P0            8.00 usec
PC            1.00 usec
PL1           200.00 usec
PL2           200.00 usec
PL3           6.41440093 N
PL4           6.41440093 N
PL5           6.41440093 N
PL6           6.41440093 N
PL7           6.41440093 N
PL8           6.41440093 N
PL9           6.41440093 N
PL10          6.41440093 N
PL11          6.41440093 N
PL12          6.41440093 N
PL13          6.41440093 N
PL14          6.41440093 N
PL15          6.41440093 N
PL16          6.41440093 N
PL17          6.41440093 N
PL18          6.41440093 N
PL19          6.41440093 N
PL20          6.41440093 N
PL21          6.41440093 N
PL22          6.41440093 N
PL23          6.41440093 N
PL24          6.41440093 N
PL25          6.41440093 N
PL26          6.41440093 N
PL27          6.41440093 N
PL28          6.41440093 N
PL29          6.41440093 N
PL30          6.41440093 N
PL31          6.41440093 N
PL32          6.41440093 N
PL33          6.41440093 N
PL34          6.41440093 N
PL35          6.41440093 N
PL36          6.41440093 N
PL37          6.41440093 N
PL38          6.41440093 N
PL39          6.41440093 N
PL40          6.41440093 N
PL41          6.41440093 N
PL42          6.41440093 N
PL43          6.41440093 N
PL44          6.41440093 N
PL45          6.41440093 N
PL46          6.41440093 N
PL47          6.41440093 N
PL48          6.41440093 N
PL49          6.41440093 N
PL50          6.41440093 N
PL51          6.41440093 N
PL52          6.41440093 N
PL53          6.41440093 N
PL54          6.41440093 N
PL55          6.41440093 N
PL56          6.41440093 N
PL57          6.41440093 N
PL58          6.41440093 N
PL59          6.41440093 N
PL60          6.41440093 N
PL61          6.41440093 N
PL62          6.41440093 N
PL63          6.41440093 N
PL64          6.41440093 N
PL65          6.41440093 N
PL66          6.41440093 N
PL67          6.41440093 N
PL68          6.41440093 N
PL69          6.41440093 N
PL70          6.41440093 N
PL71          6.41440093 N
PL72          6.41440093 N
PL73          6.41440093 N
PL74          6.41440093 N
PL75          6.41440093 N
PL76          6.41440093 N
PL77          6.41440093 N
PL78          6.41440093 N
PL79          6.41440093 N
PL80          6.41440093 N
PL81          6.41440093 N
PL82          6.41440093 N
PL83          6.41440093 N
PL84          6.41440093 N
PL85          6.41440093 N
PL86          6.41440093 N
PL87          6.41440093 N
PL88          6.41440093 N
PL89          6.41440093 N
PL90          6.41440093 N
PL91          6.41440093 N
PL92          6.41440093 N
PL93          6.41440093 N
PL94          6.41440093 N
PL95          6.41440093 N
PL96          6.41440093 N
PL97          6.41440093 N
PL98          6.41440093 N
PL99          6.41440093 N
PL100         6.41440093 N
F1 - Acquisition parameters
SFO1          500.136060 MHz
SFO2          500.136060 MHz
SFO3          500.136060 MHz
SFO4          500.136060 MHz
SFO5          500.136060 MHz
SFO6          500.136060 MHz
SFO7          500.136060 MHz
SFO8          500.136060 MHz
SFO9          500.136060 MHz
SFO10         500.136060 MHz
SFO11         500.136060 MHz
SFO12         500.136060 MHz
SFO13         500.136060 MHz
SFO14         500.136060 MHz
SFO15         500.136060 MHz
SFO16         500.136060 MHz
SFO17         500.136060 MHz
SFO18         500.136060 MHz
SFO19         500.136060 MHz
SFO20         500.136060 MHz
SFO21         500.136060 MHz
SFO22         500.136060 MHz
SFO23         500.136060 MHz
SFO24         500.136060 MHz
SFO25         500.136060 MHz
SFO26         500.136060 MHz
SFO27         500.136060 MHz
SFO28         500.136060 MHz
SFO29         500.136060 MHz
SFO30         500.136060 MHz
SFO31         500.136060 MHz
SFO32         500.136060 MHz
SFO33         500.136060 MHz
SFO34         500.136060 MHz
SFO35         500.136060 MHz
SFO36         500.136060 MHz
SFO37         500.136060 MHz
SFO38         500.136060 MHz
SFO39         500.136060 MHz
SFO40         500.136060 MHz
SFO41         500.136060 MHz
SFO42         500.136060 MHz
SFO43         500.136060 MHz
SFO44         500.136060 MHz
SFO45         500.136060 MHz
SFO46         500.136060 MHz
SFO47         500.136060 MHz
SFO48         500.136060 MHz
SFO49         500.136060 MHz
SFO50         500.136060 MHz
SFO51         500.136060 MHz
SFO52         500.136060 MHz
SFO53         500.136060 MHz
SFO54         500.136060 MHz
SFO55         500.136060 MHz
SFO56         500.136060 MHz
SFO57         500.136060 MHz
SFO58         500.136060 MHz
SFO59         500.136060 MHz
SFO60         500.136060 MHz
SFO61         500.136060 MHz
SFO62         500.136060 MHz
SFO63         500.136060 MHz
SFO64         500.136060 MHz
SFO65         500.136060 MHz
SFO66         500.136060 MHz
SFO67         500.136060 MHz
SFO68         500.136060 MHz
SFO69         500.136060 MHz
SFO70         500.136060 MHz
SFO71         500.136060 MHz
SFO72         500.136060 MHz
SFO73         500.136060 MHz
SFO74         500.136060 MHz
SFO75         500.136060 MHz
SFO76         500.136060 MHz
SFO77         500.136060 MHz
SFO78         500.136060 MHz
SFO79         500.136060 MHz
SFO80         500.136060 MHz
SFO81         500.136060 MHz
SFO82         500.136060 MHz
SFO83         500.136060 MHz
SFO84         500.136060 MHz
SFO85         500.136060 MHz
SFO86         500.136060 MHz
SFO87         500.136060 MHz
SFO88         500.136060 MHz
SFO89         500.136060 MHz
SFO90         500.136060 MHz
SFO91         500.136060 MHz
SFO92         500.136060 MHz
SFO93         500.136060 MHz
SFO94         500.136060 MHz
SFO95         500.136060 MHz
SFO96         500.136060 MHz
SFO97         500.136060 MHz
SFO98         500.136060 MHz
SFO99         500.136060 MHz
SFO100        500.136060 MHz
F2 - Processing parameters
SI            512
SF            500.136060 MHz
SFO           500.136060 MHz
WDW           EM
SSB           0
GB            0
PC            1.40
  
```

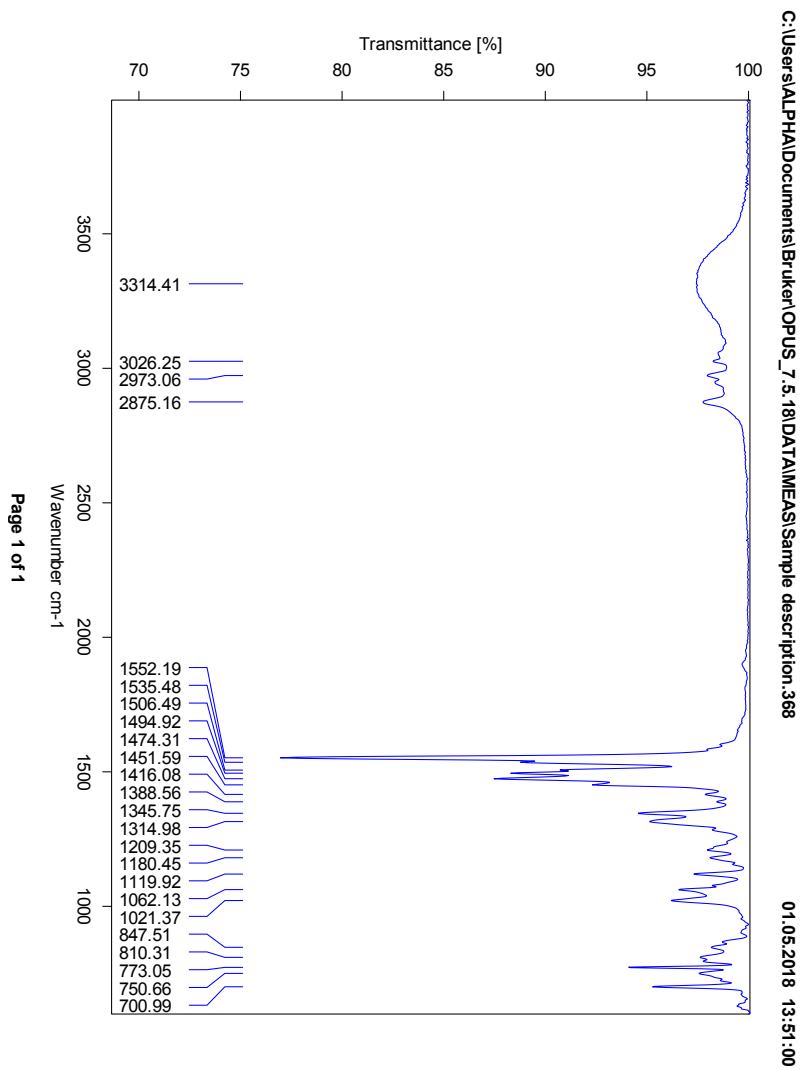
COSY spectrum of compound (*R*)-6a.



HSQC spectrum of compound (R)-6a.



HMBC spectrum of compound (R)-6a.

IR spectrum of compound (*R*)-6a.

## Elemental Composition Report

Page 1

## Single Mass Analysis

Tolerance = 2.0 PPM / DBE: min = -100.0, max = 100.0

Element prediction: Off

Number of isotope peaks used for i-FIT = 3

Monoisotopic Mass, Even Electron Ions

7239 formula(e) evaluated with 8 results within limits (all results (up to 1000) for each mass)

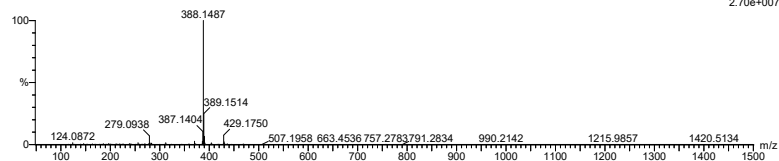
Elements Used:

C: 0-500 H: 0-1000 N: 0-10 O: 0-20 S: 0-2

2018-211 133 (2.602) AM2 (Ar.35000.0.0.00.0.00); Cm (128:133)

1: TOF MS ASAP+

2.70e+007



Minimum: -100.0  
Maximum: 100.0

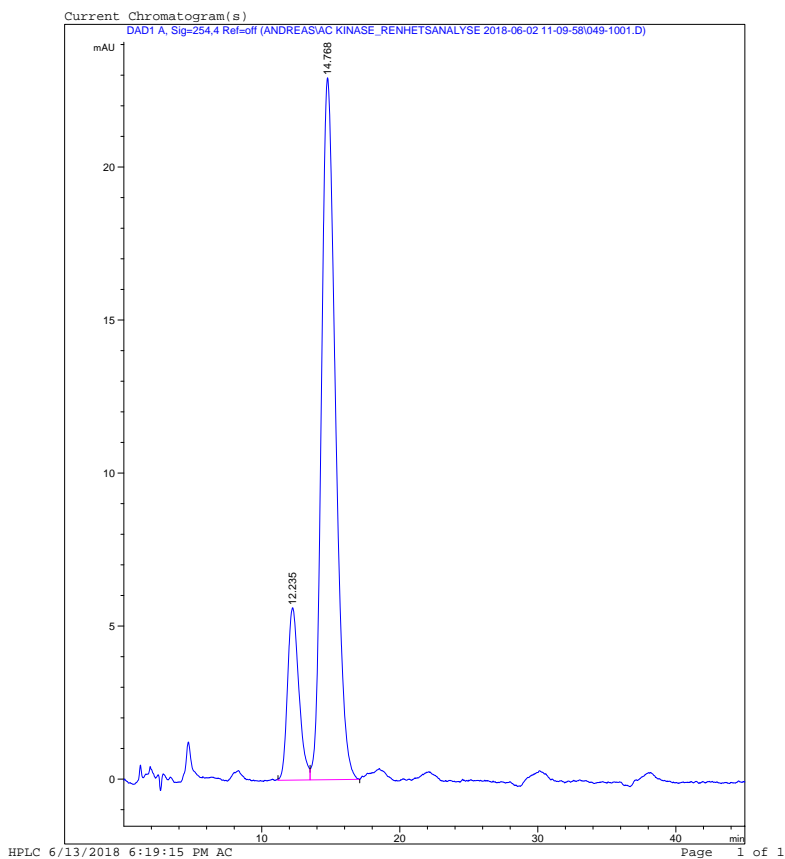
Mass	Calc. Mass	mDa	PPM	DBE	i-FIT	Norm	Conf(%)	Formula
388.1487	388.1484	0.3	0.8	14.5	1614.0	0.008	99.19	C23 H22 N3 O S
	388.1489	-0.2	-0.5	-3.5	1618.8	4.819	0.81	C10 H30 N O12 S
	388.1482	0.5	1.3	11.5	1625.6	11.654	0.00	C15 H18 N9 O4
	388.1490	-0.3	-0.8	-70.5	1626.0	12.049	0.00	C4 H155 N4 O4 S2
	388.1482	0.5	1.3	-12.5	1626.2	12.220	0.00	C2 H34 N3 O14 S2
	388.1481	0.6	1.5	-69.5	1628.8	14.772	0.00	C3 H151 N4 O9
	388.1494	-0.7	-1.8	-64.5	1628.8	14.857	0.00	C4 H147 N8 O5
	388.1487	0.0	0.0	-6.5	1629.6	15.573	0.00	C2 H26 N7 O15

Mass spectrum of compound (R)-6a.

Print of window 38: Current Chromatogram(s)  
Data File : C:\CHEM32\1\DATA\ANDREAS\AC KINASE\_RENHETSANALYSE 2018-06-02 11-09-58\049-1001.D  
Sample Name : ABR1-59-2 85/15,DEA, FLOW 1.5  
=====

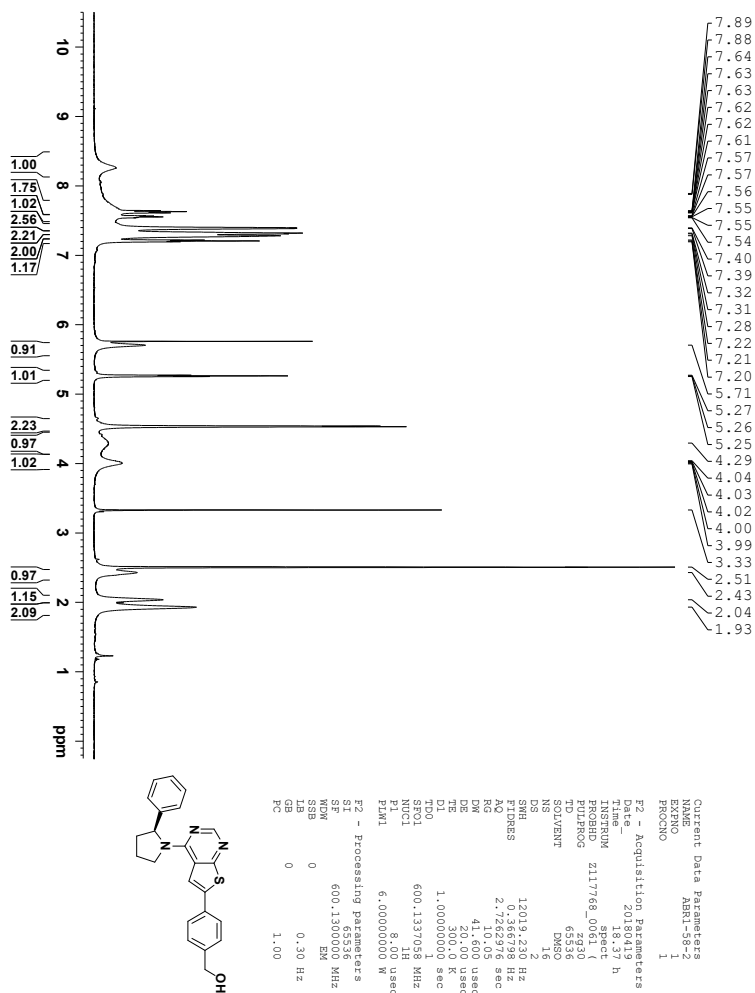
Acq. Operator	: AC	Seq. Line	: 10
Acq. Instrument	: HPLC	Location	: Vial 49
Injection Date	: 6/2/2018 7:35:19 PM	Inj	: 1
		Inj Volume	: 5.000 µl

Acq. Method : C:\CHEM32\1\DATA\ANDREAS\AC KINASE\_RENHETSANALYSE 2018-06-02 11-09-58\  
ANDREAS CHIRAL 85 FLOW 1.5.M  
Last changed : 5/31/2018 10:18:31 AM by AC  
Analysis Method : C:\CHEM32\1\METHODS\FELLES\RENHETSANALYSE FELLES\_NEUTRAL.M  
Last changed : 6/13/2018 6:16:27 PM by AC  
(modified after loading)  
Additional Info : Peak(s) manually integrated



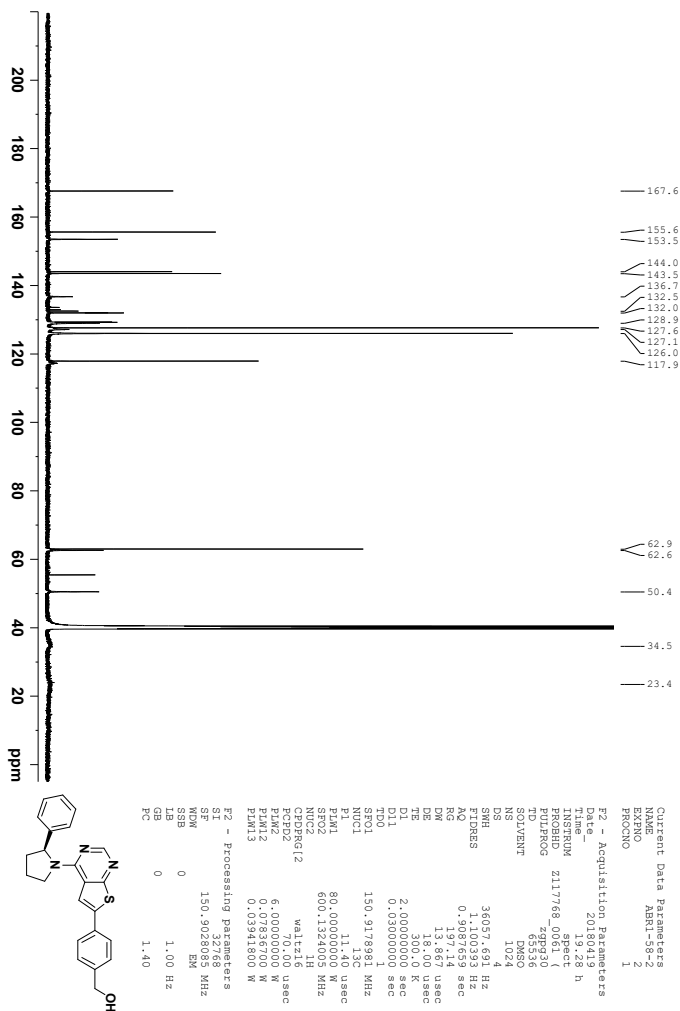
CSP-HPLC (Lux 5u Cellulose-1 4.6 x 250 mm, hexane(cont. 0.2% diethyl amine):*i*-PrOH, flow 1.5 mL/min, detection at 254 nm) of compound (*R*)-6a

# O | Spectroscopic Data - Compound (S)-6a

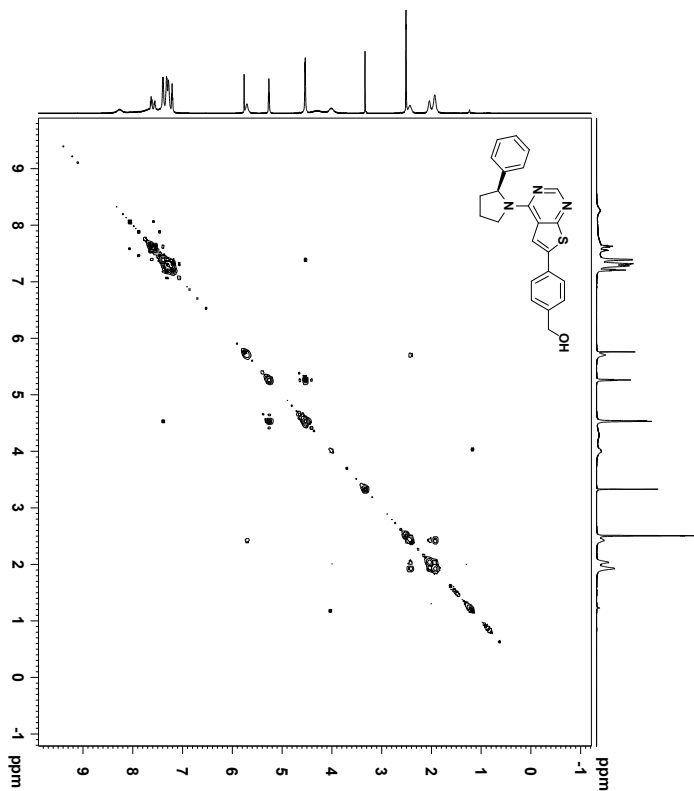


<sup>1</sup>H NMR (600 MHz, DMSO-*d*<sub>6</sub>) spectrum of compound (S)-6a.





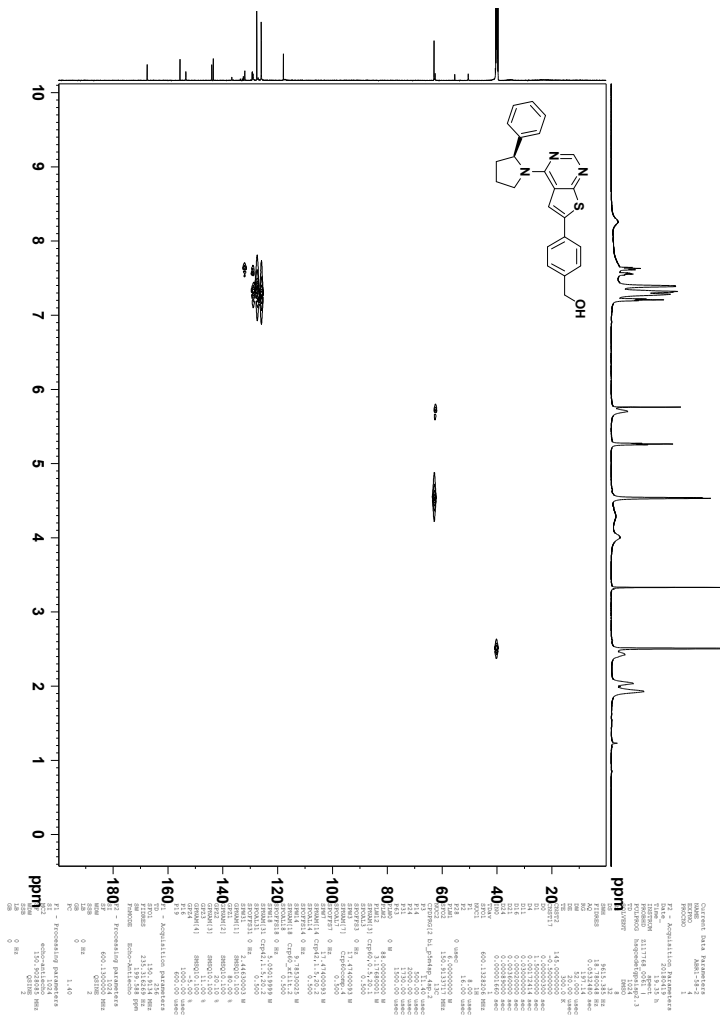
$^{13}\text{C}$  NMR (150 MHz,  $\text{DMSO-}d_6$ ) spectrum of compound (S)-6a.



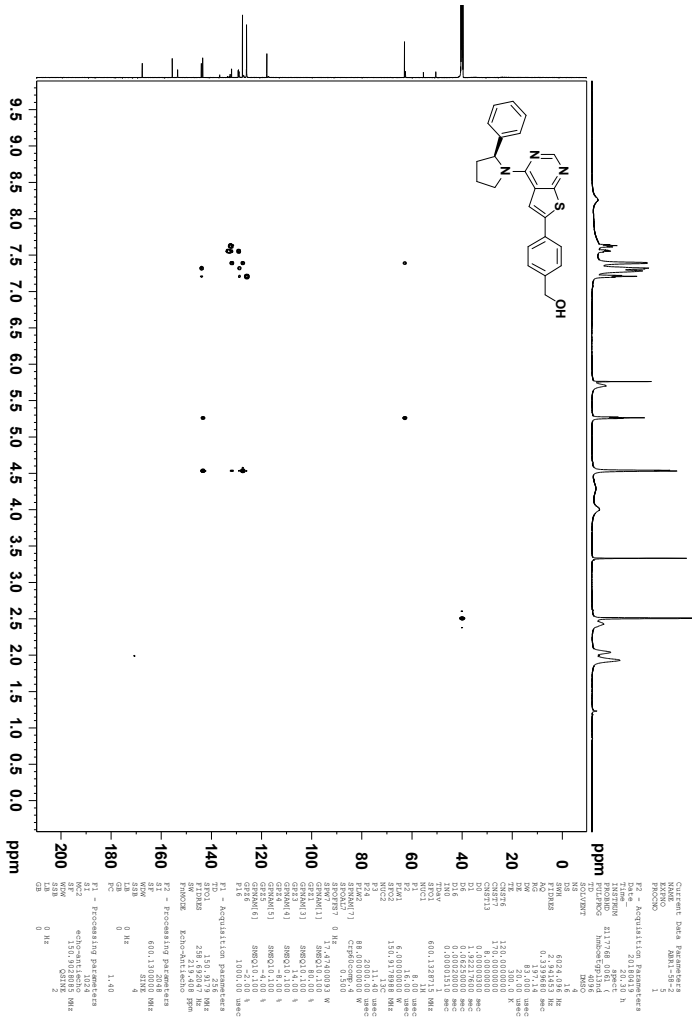
```

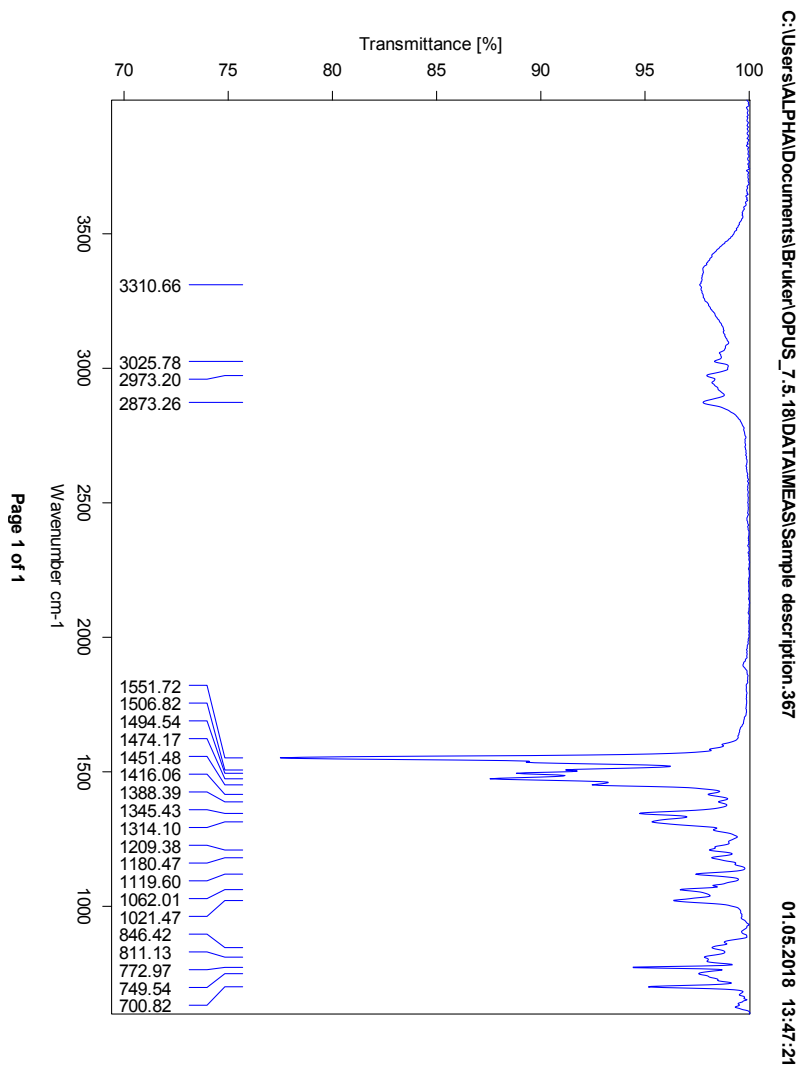
Current Data Parameters
EXPNO          3
PROCNO         1
F2 - Acquisition Parameters
Time          19.29 h
PROBHD1       211768_0061_1
PULPROG       zgpg30
TD             65536
SOLVENT       DMSO
NS             624
DS             16
FIDRES        0.582906 Hz
AQ             0.1699840 sec
EM          83.1000 usec
TE             300.0 K
DE             0.001000000 sec
DQ             380.0 K
E2             0.001000000 sec
D11            0.030000000 sec
D12            0.000000000 sec
D13            0.000000000 sec
D10            0.001000000 sec
TH0V          600.1329711 MHz
NUC1           1H
NUC2           1H
PC             8.00 usec
RG             6.2500000 usec
SI             32768
SF             600.1329 MHz
WDW            EM
SSB            0
GB             0
PCMODE        GP
F2 - Processing parameters
SI             1024
SF             600.1300000 MHz
WDW            GEM
SSB            0
PC             0 Hz
RG             1.40
PC             0 Hz
  
```

COSY spectrum of compound (*S*)-6a.



HSQC spectrum of compound (S)-6a.

HMBC spectrum of compound (*S*)-6a.

IR spectrum of compound (*S*)-6a.

## Elemental Composition Report

Page 1

## Single Mass Analysis

Tolerance = 5.0 PPM / DBE: min = -1.5, max = 100.0

Element prediction: Off

Number of isotope peaks used for i-FIT = 3

Monoisotopic Mass, Even Electron Ions

3485 formula(e) evaluated with 10 results within limits (all results (up to 1000) for each mass)

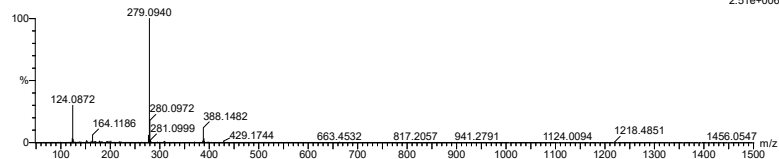
Elements Used:

C: 0-500 H: 0-1000 N: 0-10 O: 0-20 Na: 0-1 S: 0-2

2018-214 68 (1.345) AM2 (Ar,35000.0,0.00,0.00); Cm (68:73)

1: TOF MS ASAP+

2.51e+006



Minimum: -1.5  
Maximum: 5000.0 5.0 100.0

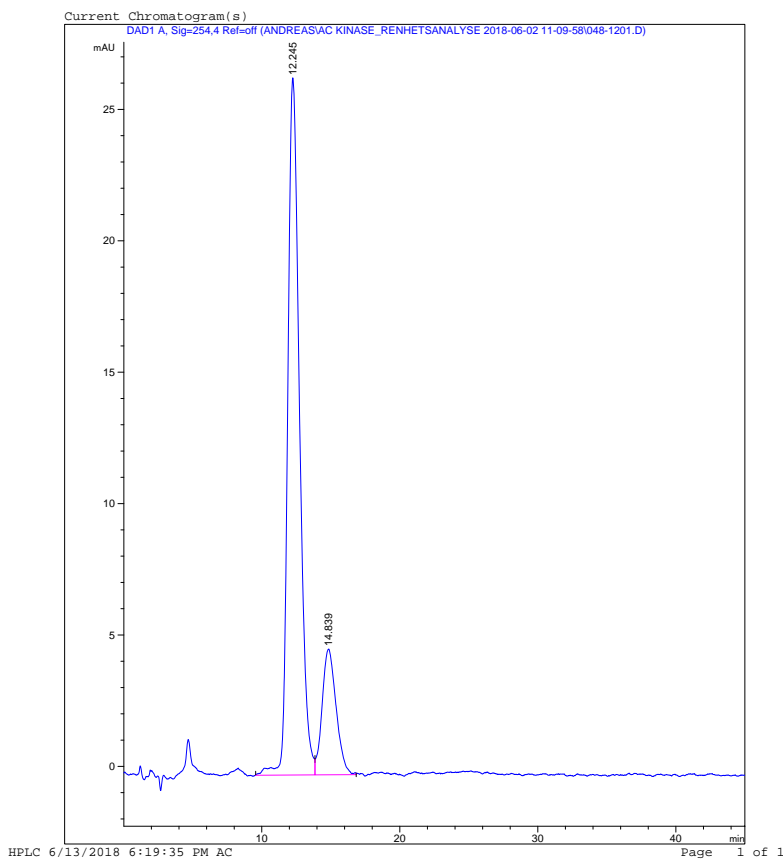
Mass	Calc. Mass	mDa	PPM	DBE	i-FIT	Norm	Conf(%)	Formula
388.1482	388.1484	-0.2	-0.5	14.5	868.2	0.000	100.00	C23 H22 N3 O S
	388.1493	-1.1	-2.8	6.5	881.4	13.241	0.00	C18 H27 N3 O Na S2
	388.1491	-0.9	-2.3	3.5	881.5	13.298	0.00	C10 H23 N9 O4 Na S
	388.1478	0.4	1.0	-1.5	881.6	13.391	0.00	C9 H27 N5 O8 Na S
	388.1477	0.5	1.3	5.5	882.4	14.164	0.00	C15 H26 N5 O3 S2
	388.1464	1.8	4.6	0.5	883.5	15.291	0.00	C14 H30 N O7 S2
	388.1482	0.0	0.0	11.5	884.6	16.419	0.00	C15 H18 N9 O4
	388.1498	-1.6	-4.1	12.5	884.8	16.596	0.00	C18 H19 N7 O2 Na
	388.1485	-0.3	-0.8	7.5	884.8	16.607	0.00	C17 H23 N3 O6 Na
	388.1468	1.4	3.6	6.5	884.9	16.727	0.00	C14 H22 N5 O8

Mass spectrum of compound (S)-6a.

Print of window 38: Current Chromatogram(s)  
Data File : C:\CHEM32\1\DATA\ANDREAS\AC KINASE\_RENHETSANALYSE 2018-06-02 11-09-58\048-1201.D  
Sample Name : ABR1-58-52 85/15,DEA, FLOW 1.5  
=====

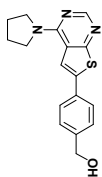
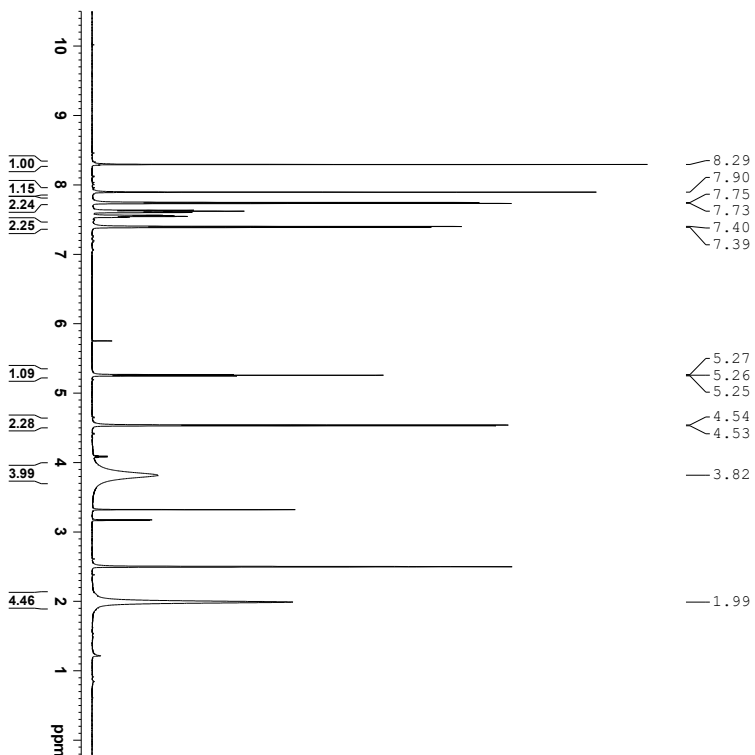
Acq. Operator : AC	Seq. Line : 12
Acq. Instrument : HPLC	Location : Vial 48
Injection Date : 6/2/2018 9:27:24 PM	Inj : 1
	Inj Volume : 5.000 µl

Acq. Method : C:\CHEM32\1\DATA\ANDREAS\AC KINASE\_RENHETSANALYSE 2018-06-02 11-09-58\  
ANDREAS CHIRAL 85 FLOW 1.5.M  
Last changed : 5/31/2018 10:18:31 AM by AC  
Analysis Method : C:\CHEM32\1\METHODS\FELLES\RENHETSANALYSE FELLES\_NEUTRAL.M  
Last changed : 6/13/2018 6:16:27 PM by AC  
(modified after loading)  
Additional Info : Peak(s) manually integrated



CSP-HPLC (Lux 5u Cellulose-1 4.6 x 250 mm, hexane(cont. 0.2% diethyl amine):*i*-PrOH, flow 1.5 mL/min, detection at 254 nm) of compound (*S*)-**6a**

# P | Spectroscopic Data - Compound 6b

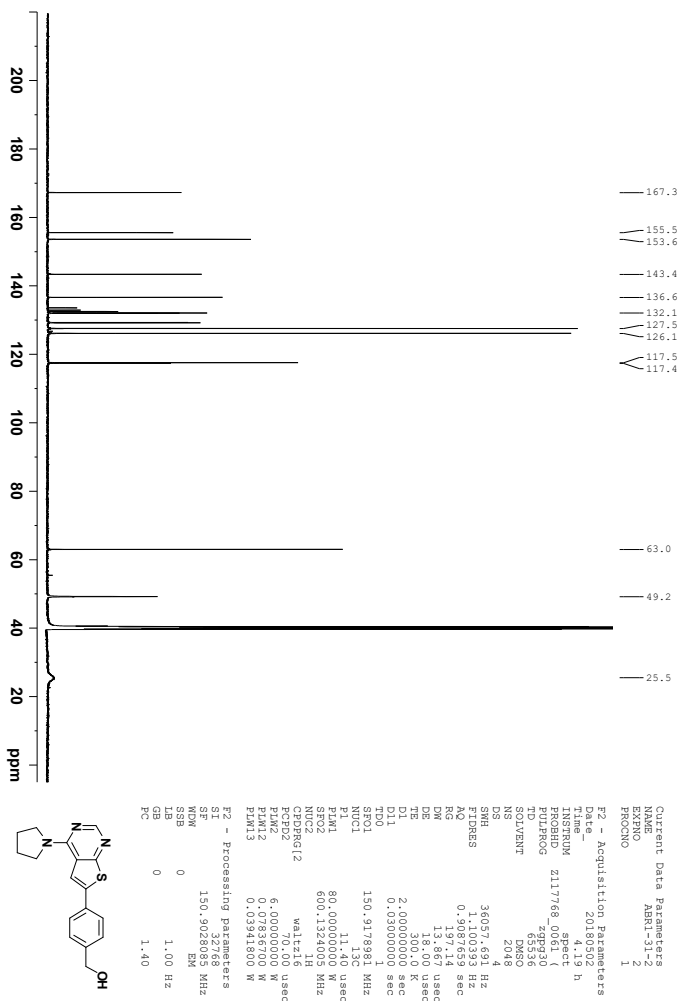


```

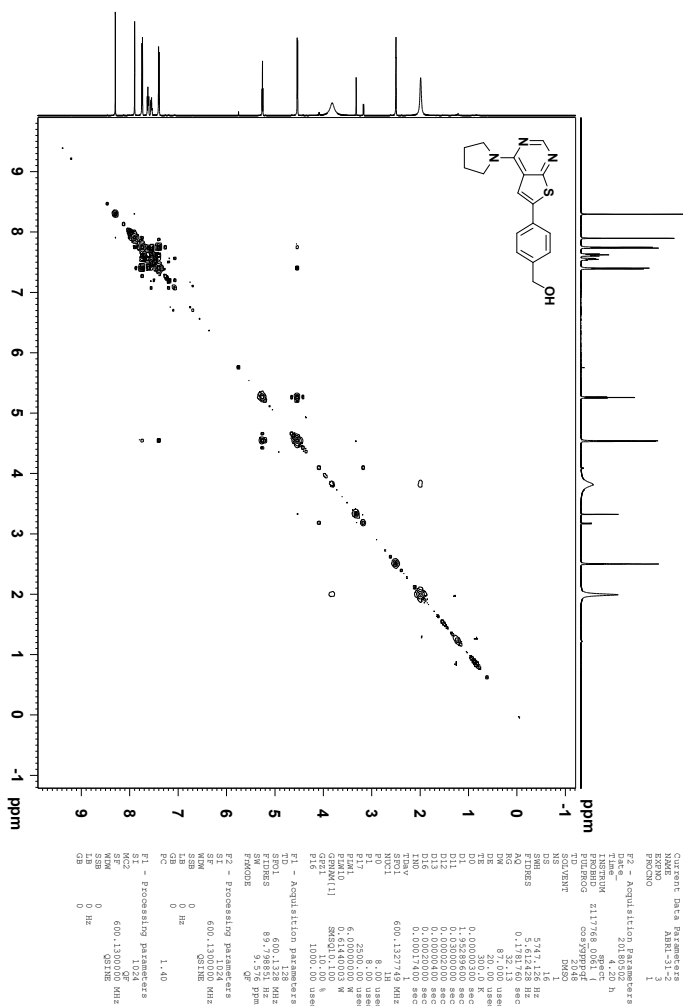
Current Data Parameters
=====
EXNO          1
PROCNO       1
F2 - Acquisition Parameters
=====
Date_         20180902
Time         2:37 h
INSTRUM      spect
PROBHD       5mm
PULPROG      zg30
TD           65536
SOLVENT      DMSO
DS           2
SWH          12019.230 Hz
AQ           0.782976 sec
RG           11.48
DM           41.600 usec
DE           300.0 K
TE           300.0 K
D1           1.00000000 sec
TDO1        600.1337045 MHz
NUC1         1H
P1           8.00 usec
PL1         6.000000000 W
F2 - Processing parameters
=====
SI           65536
SF           600.130052 MHz
SFO          600.130052 MHz
SSB          0
LB           0.30 Hz
GB           0
PC           1.00
  
```

<sup>1</sup>H NMR (600 MHz, DMSO-*d*<sub>6</sub>) spectrum of compound **6b**.

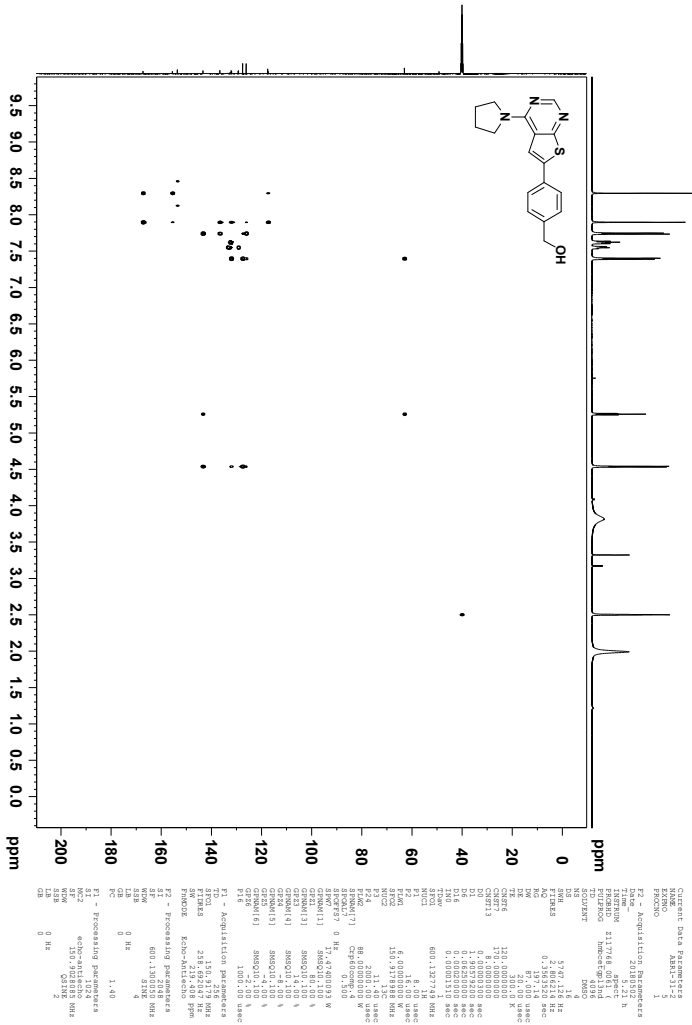




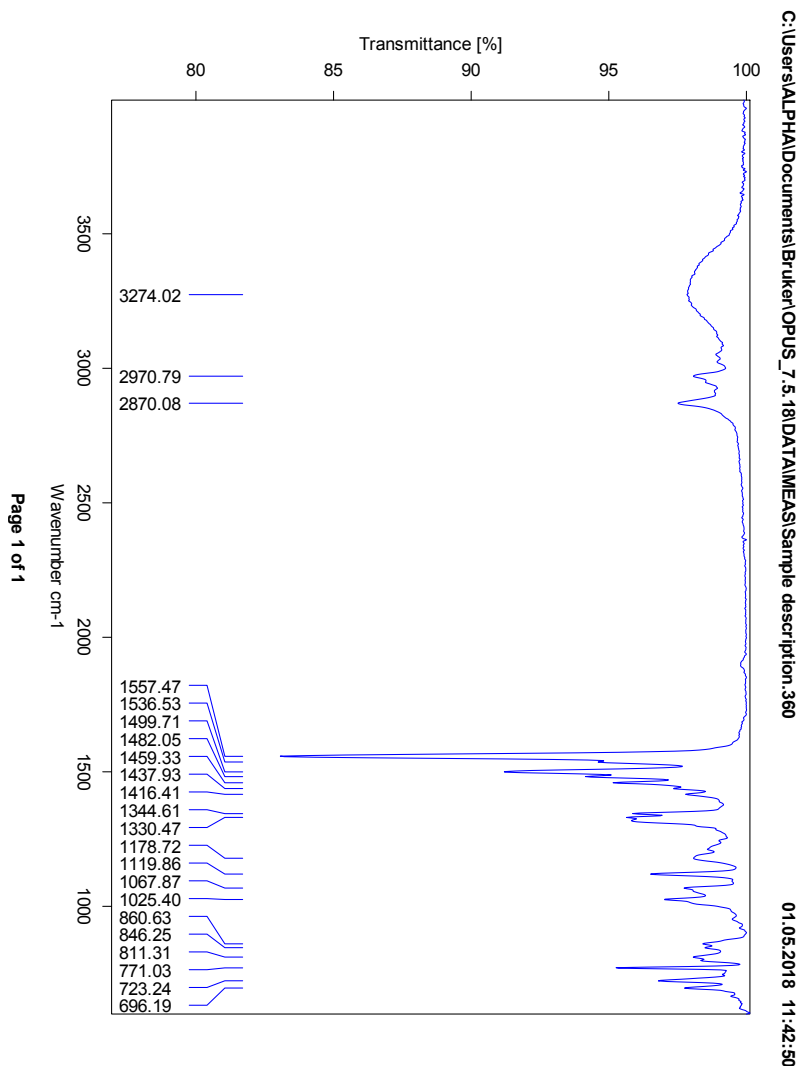
<sup>13</sup>C NMR (150 MHz, DMSO-*d*<sub>6</sub>) spectrum of compound **6b**.

COSY spectrum of compound **6b**.





HMBC spectrum of compound 6b.

IR spectrum of compound **6b**.

## Elemental Composition Report

Page 1

## Single Mass Analysis

Tolerance = 2.0 PPM / DBE: min = -1.5, max = 50.0

Element prediction: Off

Number of isotope peaks used for i-FIT = 3

Monoisotopic Mass, Even Electron Ions

1411 formula(e) evaluated with 1 results within limits (all results (up to 1000) for each mass)

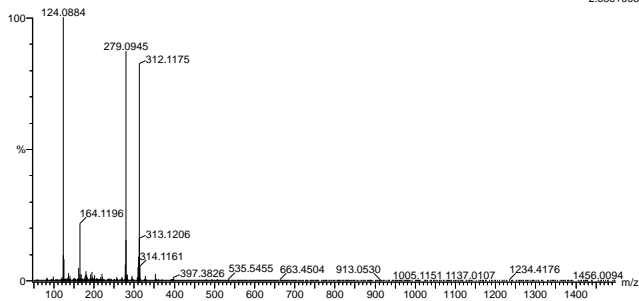
Elements Used:

C: 0-500 H: 0-1000 N: 0-10 O: 0-20 S: 0-3

2018-247.91 (1.793) AM2 (Ar:35000.0,0.00,0.00); Cm (89.91)

1: TOF MS ASAP+

2.63e+005



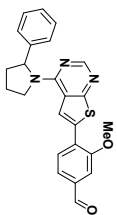
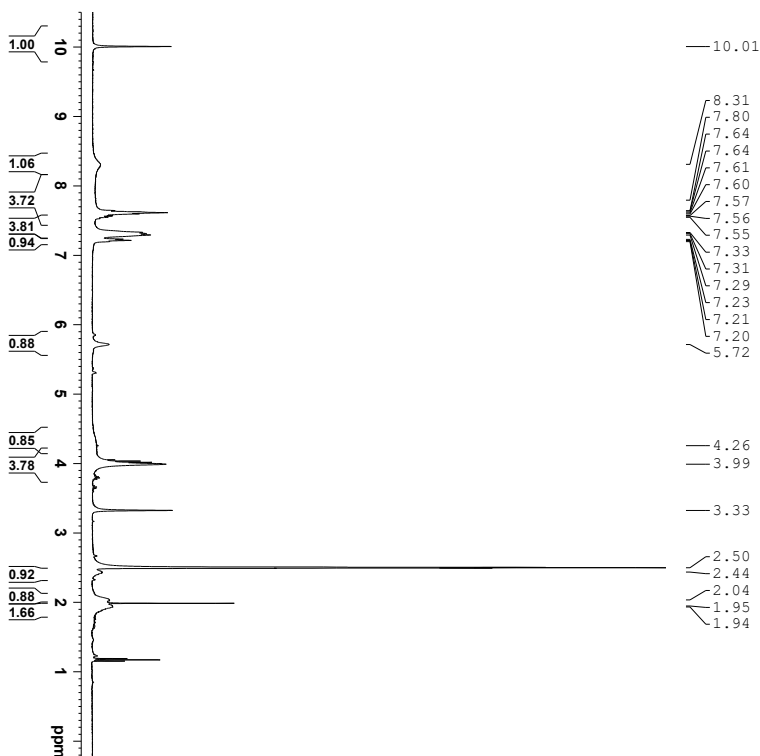
Minimum: -1.5  
Maximum: 5.0 2.0 50.0

Mass	Calc. Mass	mDa	PPM	DBE	i-FIT	Norm	Conf (%)	Formula
312.1175	312.1171	0.4	1.3	10.5	913.7	n/a	n/a	C17 H18 N3 O S

Mass spectrum of compound **6b**.



# Q | Spectroscopic Data - Compound *rac-7a*

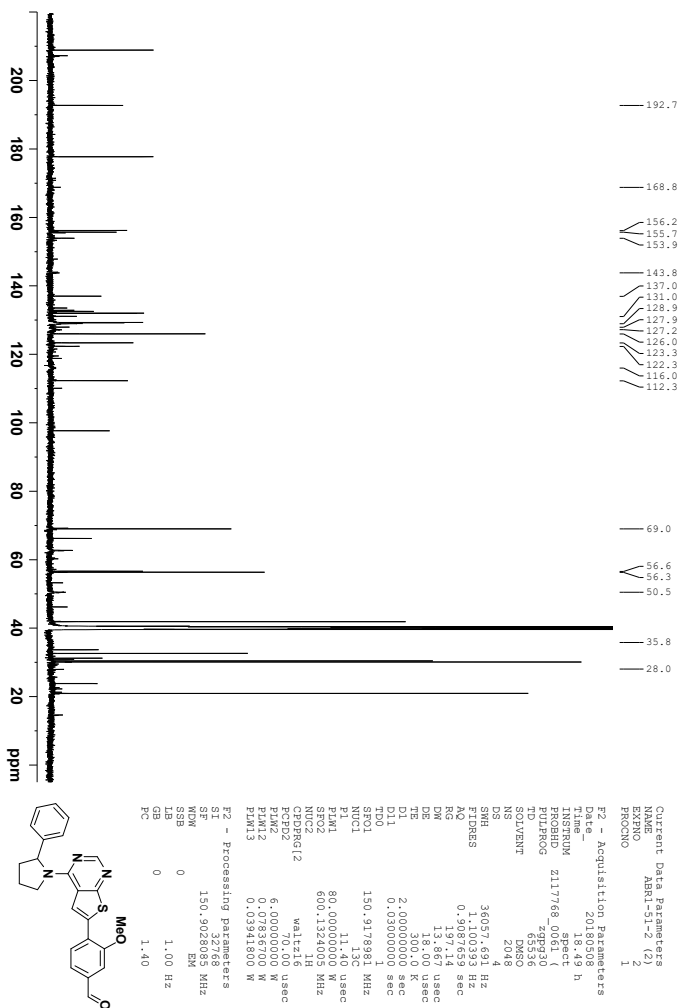


```

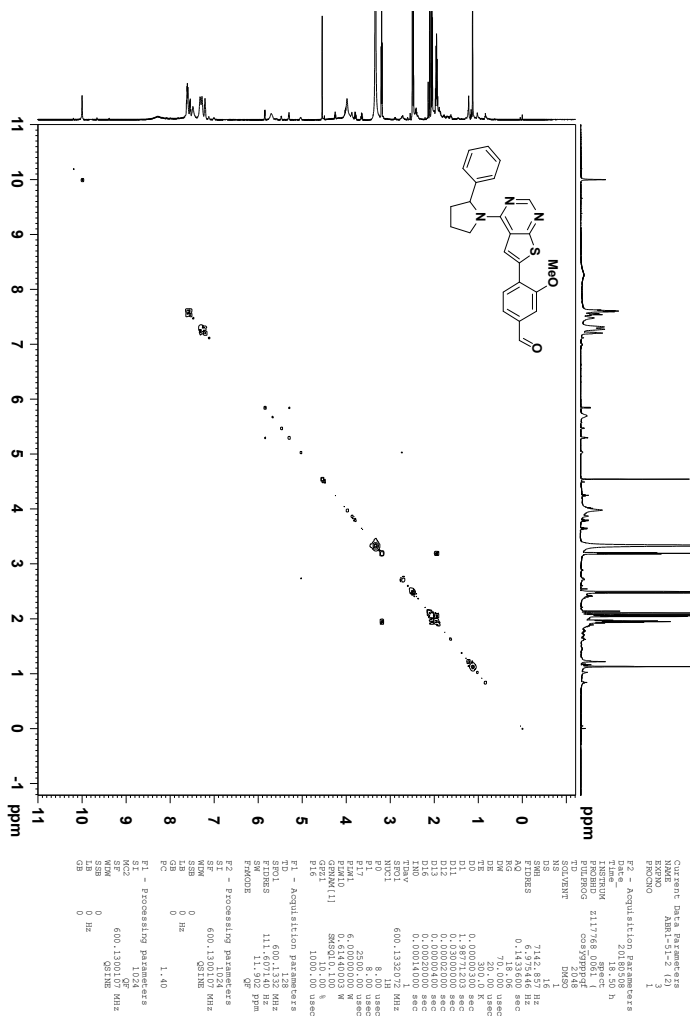
Current Data Parameters
=====
EXNO          1
PROCNO       1
Date_         20180406
Time_         0
INSTRUM      spect
PROBHD       5 mm PABBO
PULPROG      zg30
TD           65536
SOLVENT      DMSO
DS           2
SWH          8012.820 Hz
AQ           4.084465 sec
RG           112.06
DM           62.400 usec
TE           298.0 K
D1           1.00000000 sec
TD0          1
=====
CHANNEL F1 =====
SFO1         400.1324710 MHz
NUC1         1H
P1           9.00 usec
PL1         17.00000000 W
F2 - Processing parameters
SF           400.1300033 MHz
WDW          EM
SSB          0
GB           0
PC           1.00
  
```

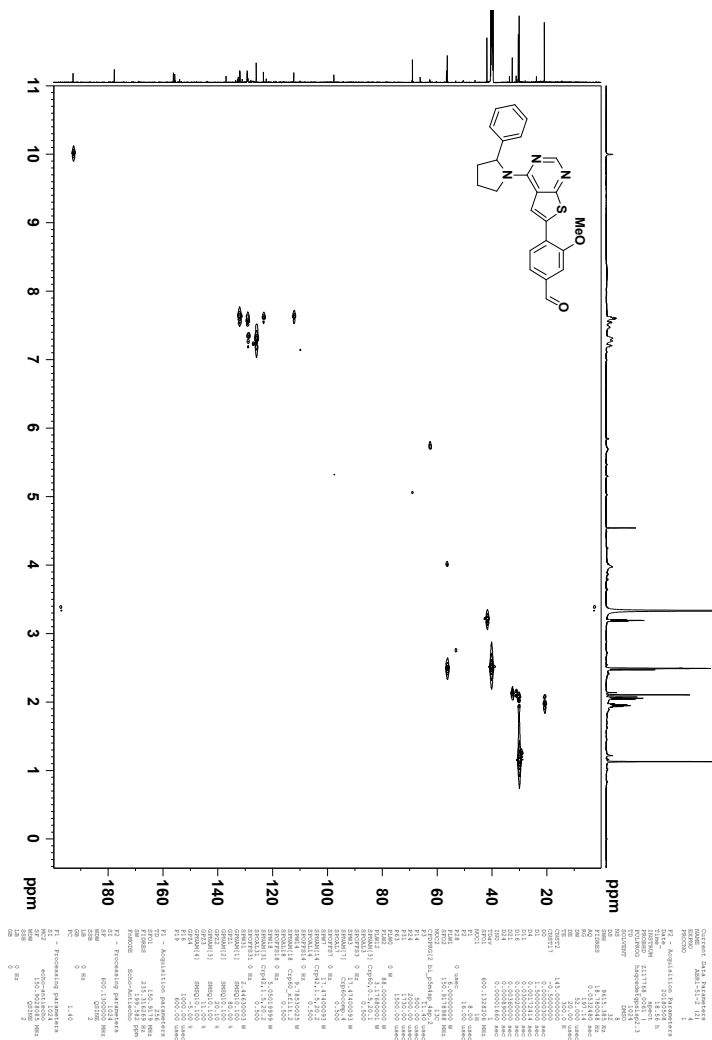
<sup>1</sup>H NMR (600 MHz, DMSO-*d*<sub>6</sub>) spectrum of compound *rac-7a*.



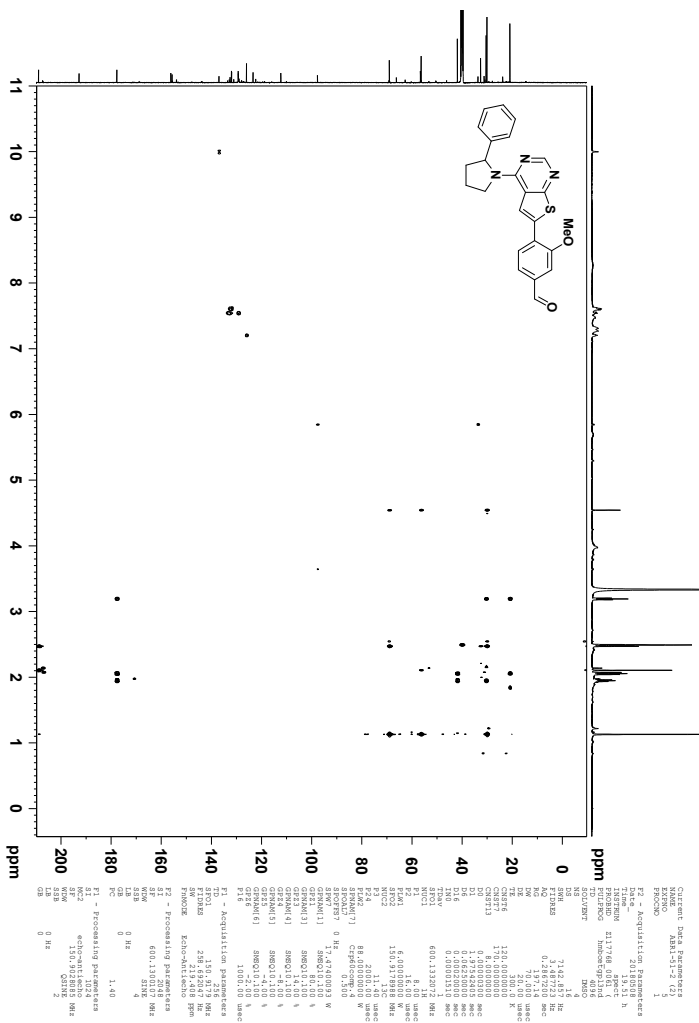


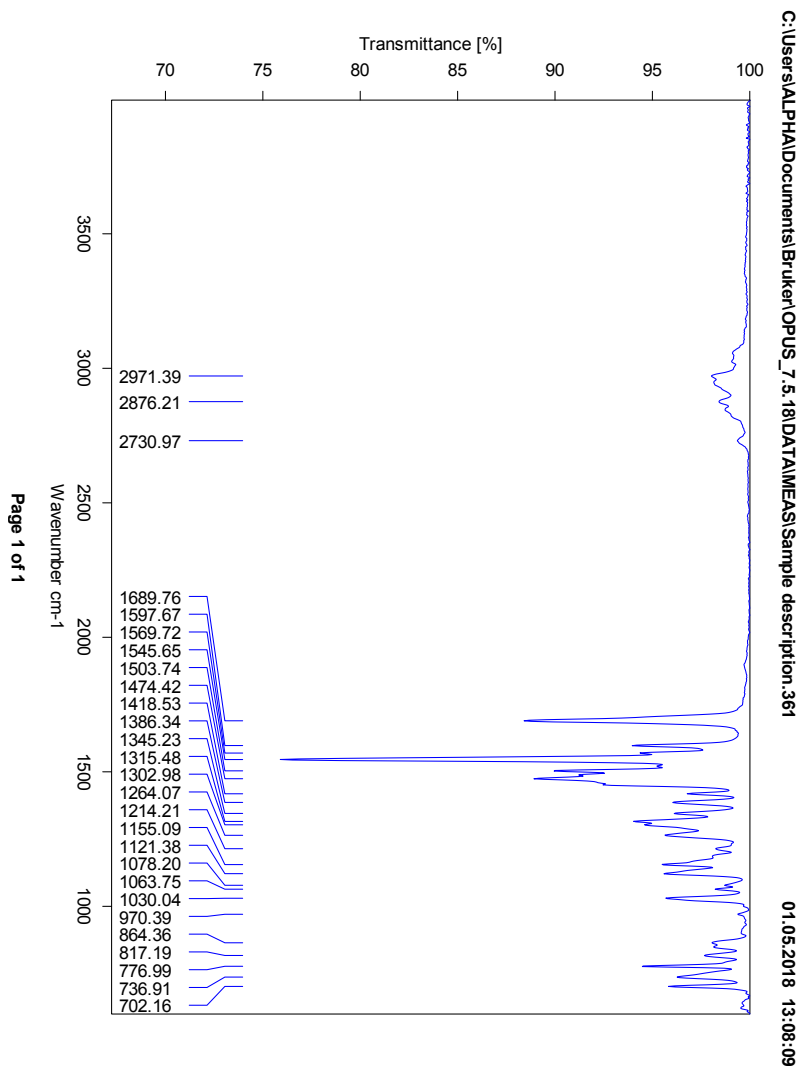
<sup>13</sup>C NMR (150 MHz, DMSO-*d*<sub>6</sub>) spectrum of compound *rac-7a*.

COSY spectrum of compound *rac*-7a.



HSQC spectrum of compound *rac-7a*.

HMBC spectrum of compound *rac-7a*.

IR spectrum of compound *rac-7a*.

## Elemental Composition Report

Page 1

## Single Mass Analysis

Tolerance = 2.0 PPM / DBE: min = -1.5, max = 50.0

Element prediction: Off

Number of isotope peaks used for i-FIT = 3

Monoisotopic Mass, Even Electron Ions

6815 formula(e) evaluated with 6 results within limits (all results (up to 1000) for each mass)

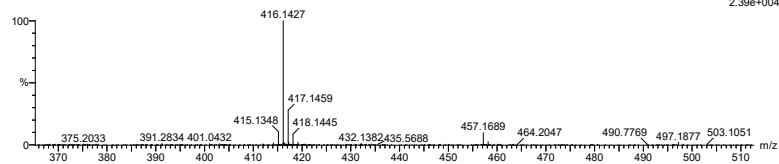
Elements Used:

C: 0-500 H: 0-1000 N: 0-10 O: 0-10 Na: 0-1 S: 0-2 Br: 0-4

2018-176 62 (1.224) AM2 (Ar,35000.0,0.00,0.00); Cm (61:62)

1: TOF MS ASAP+

2.39e+004



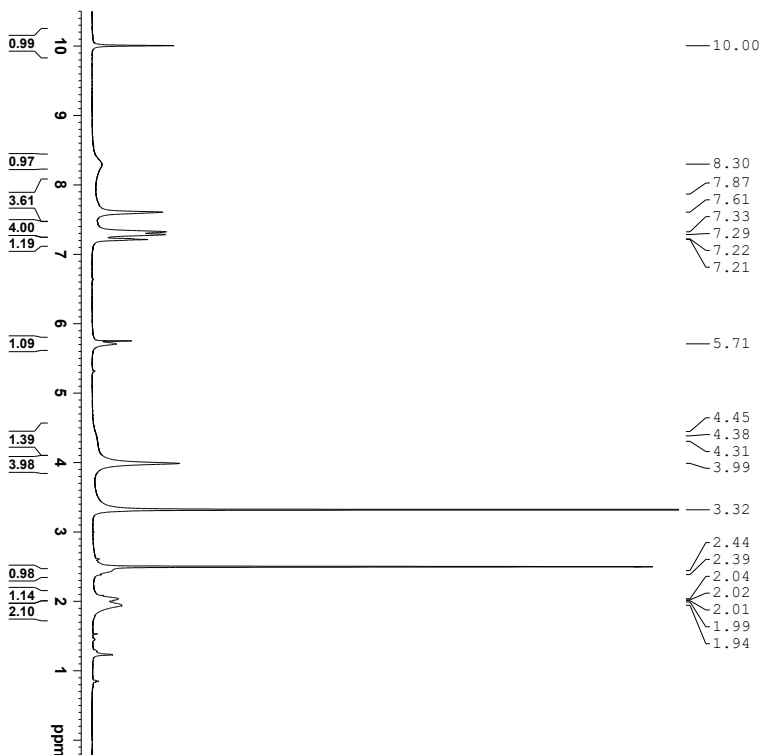
Minimum: -1.5  
Maximum: 50.0

Mass	Calc. Mass	mDa	PPM	DBE	i-FIT	Norm	Conf(%)	Formula
416.1427	416.1433	-0.6	-1.4	15.5	431.2	0.000	100.00	C24 H22 N3 O2 S
	416.1426	0.1	0.2	6.5	446.1	14.847	0.00	C16 H26 N5 O4 S2
	416.1427	0.0	0.0	-0.5	446.1	14.881	0.00	C10 H27 N5 O9 Na S
	416.1431	-0.4	-1.0	12.5	446.4	15.128	0.00	C16 H18 N9 O5
	416.1434	-0.7	-1.7	8.5	446.8	15.565	0.00	C18 H23 N3 O7 Na
	416.1426	0.1	0.2	6.5	453.6	22.369	0.00	C18 H28 N5 Na Br

Mass spectrum of compound *rac*-7a.

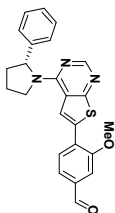


# R | Spectroscopic Data - Compound (R)-7a



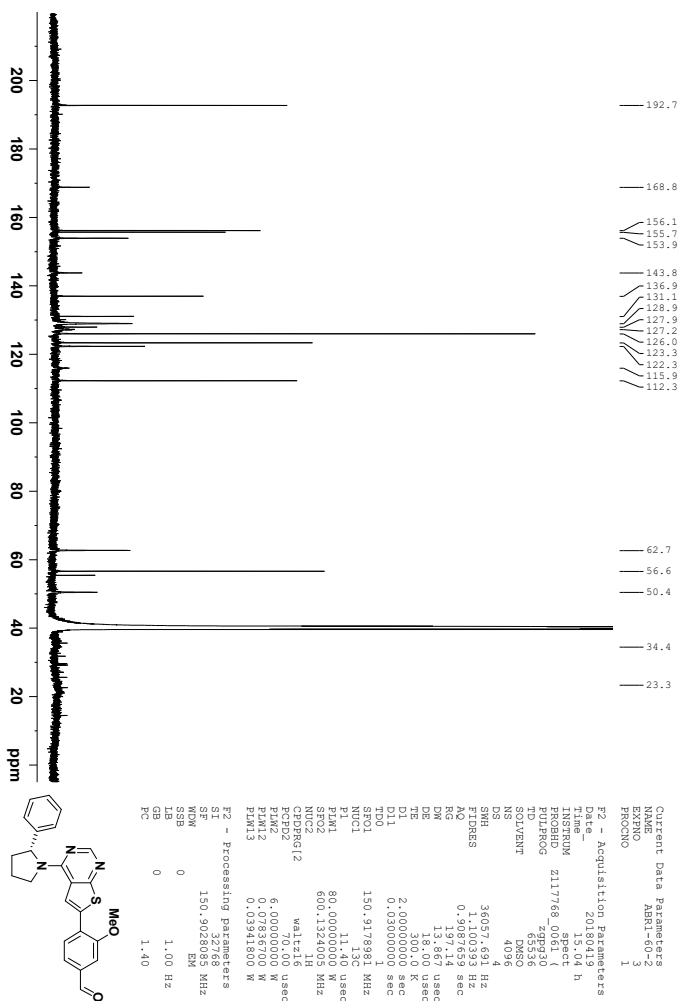
```

Current Data Parameters
NAME          AMN1-60-1
EXPNO         1
PROCNO        1
F2 - Acquisition Parameters
Date_         20180419
Time          10.24 h
INSTRUM      spect
PROBHD       5mm QNP 1H/1
PULPROG      zgpg30
TD            65536
SOLVENT      DMSO
DS            2
SWH           12019.230 Hz
AQ           0.782976 sec
RG            10.05
DM            41.600 usec
DE            300.0 K
TE            1.00000000 sec
D1            1.00000000 sec
TDO1         600.1337043 MHz
NUC1          1H
P1            8.00 usec
PL1           6.00000000 W
F2 - Processing parameters
SI            65536
SF            600.130048 MHz
SFO           600.130048 MHz
SSB           0
LB            0.30 Hz
GB            0
PC            1.00
  
```

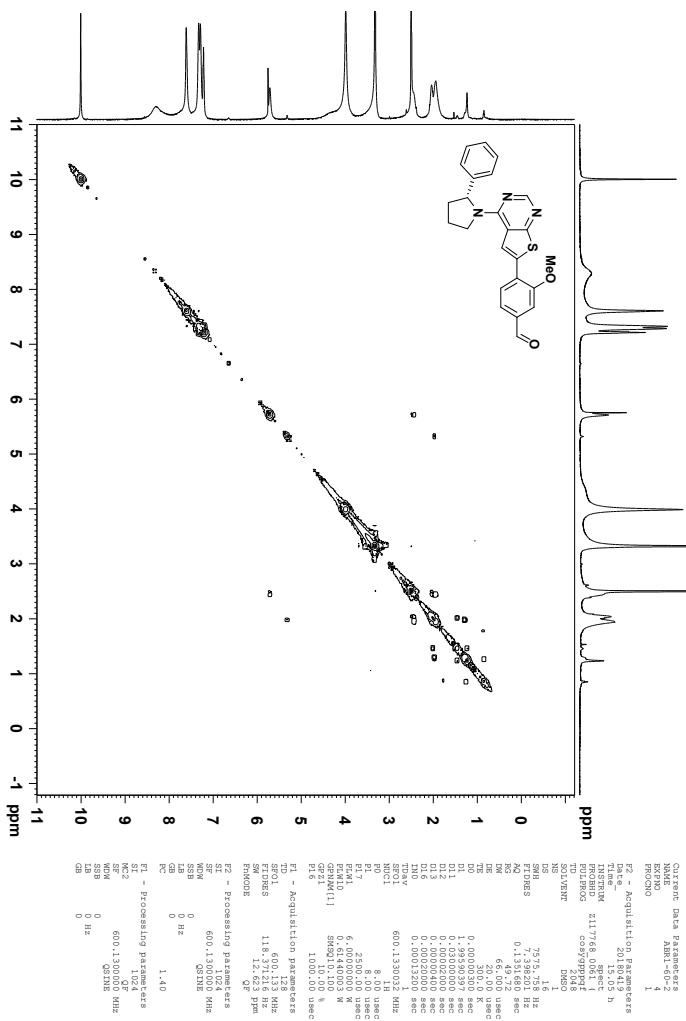


<sup>1</sup>H NMR (600 MHz, DMSO-*d*<sub>6</sub>) spectrum of compound (R)-7a.

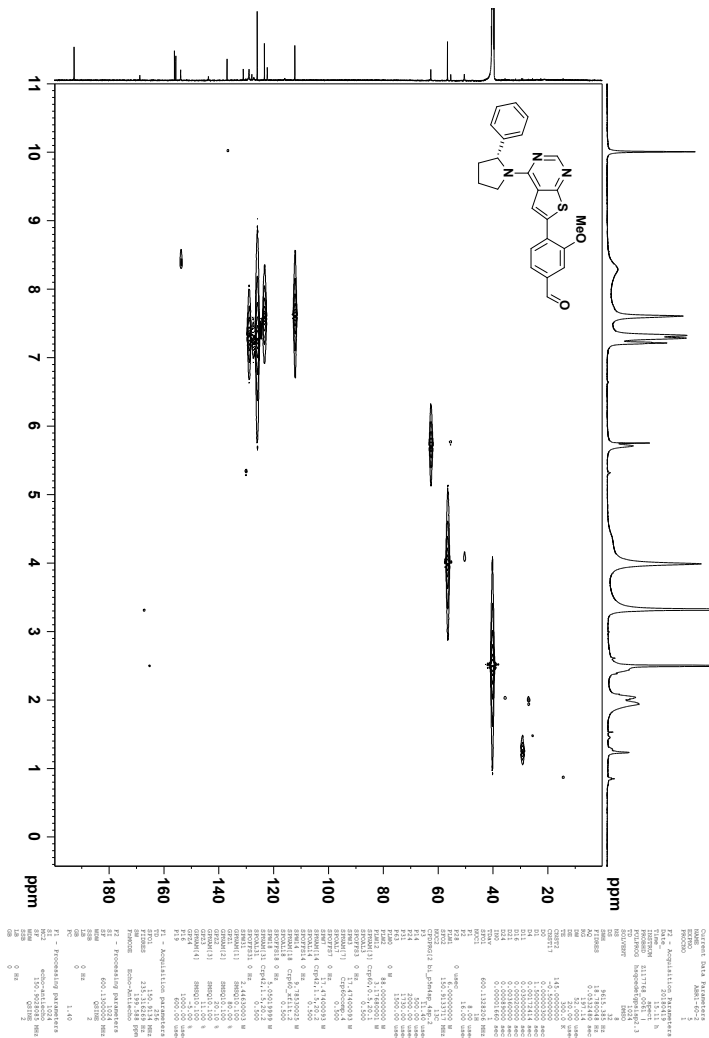




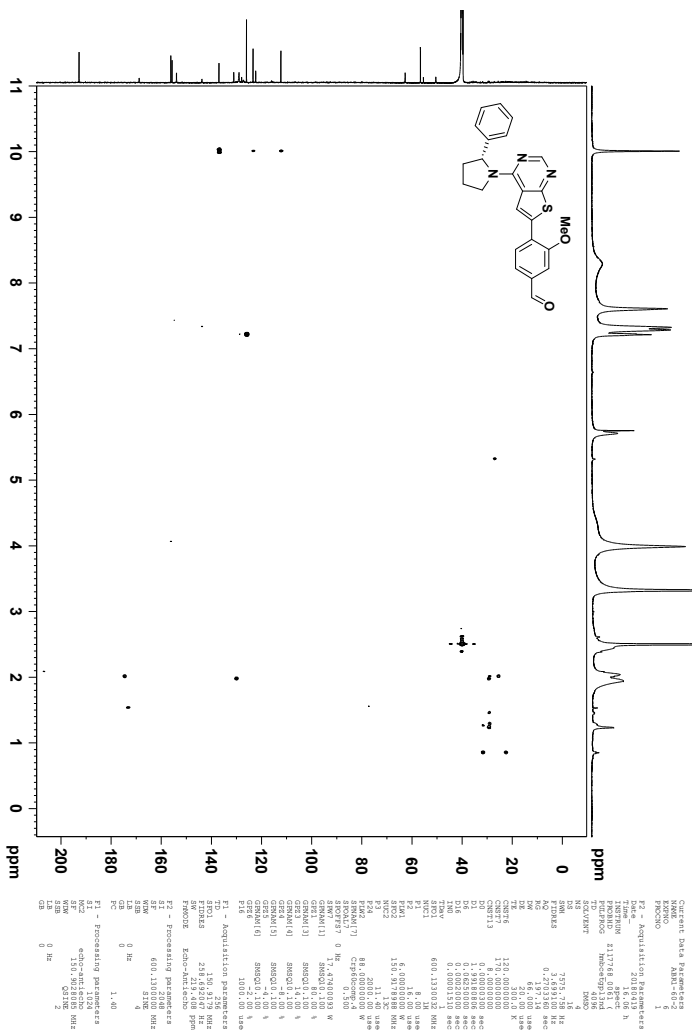
$^{13}\text{C}$  NMR (150 MHz,  $\text{DMSO-}d_6$ ) spectrum of compound (*R*)-7a.



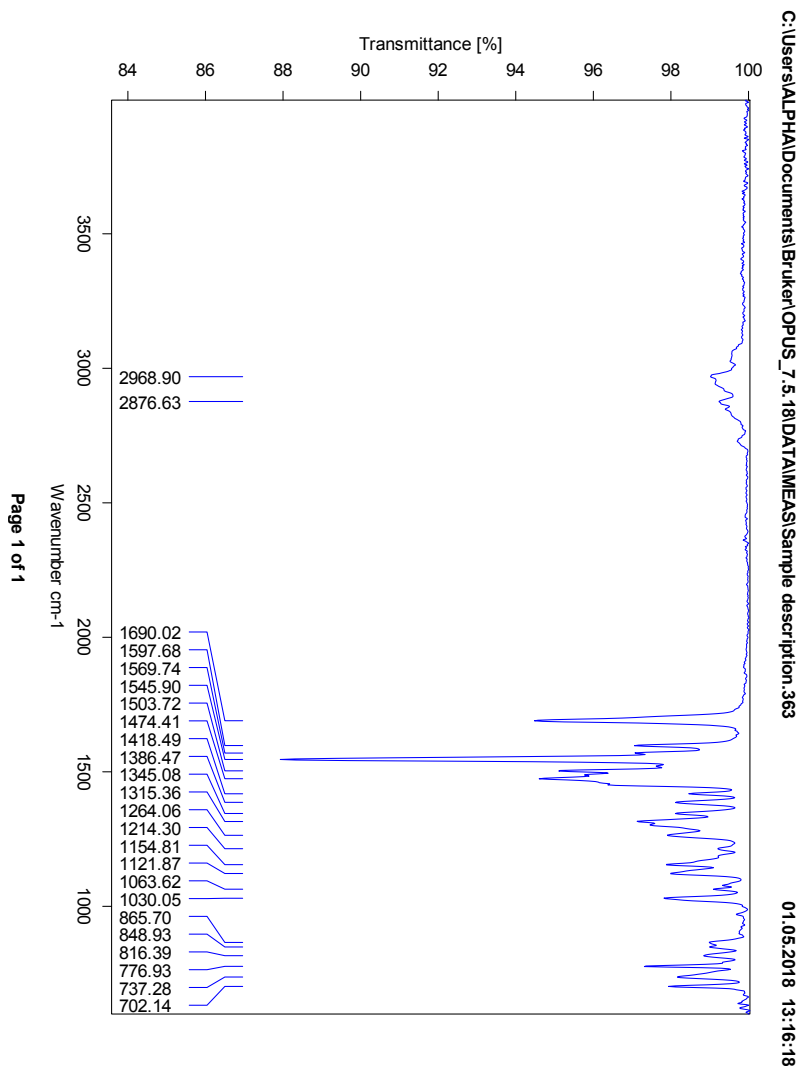
COSY spectrum of compound (R)-7a.



HSQC spectrum of compound (R)-7a.



HMBC spectrum of compound (R)-7a.

IR spectrum of compound (*R*)-7a.

## Elemental Composition Report

Page 1

## Single Mass Analysis

Tolerance = 2.0 PPM / DBE: min = -1.5, max = 50.0

Element prediction: Off

Number of isotope peaks used for i-FIT = 3

Monoisotopic Mass, Even Electron Ions

2625 formula(e) evaluated with 4 results within limits (all results (up to 1000) for each mass)

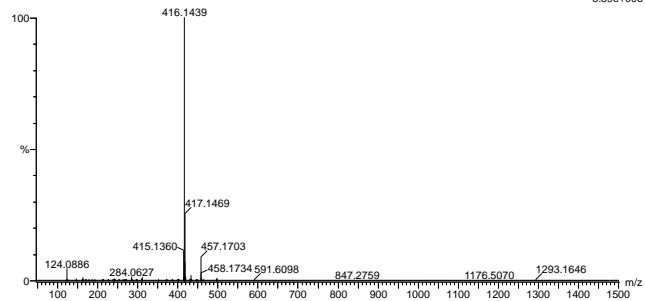
Elements Used:

C: 0-500 H: 0-1000 N: 0-10 O: 0-20 S: 0-3

2018-246 135 (2.638) AM2 (Ar:35000.0,0.00,0.00); Cm (131:136)

1: TOF MS ASAP+

8.59e+006



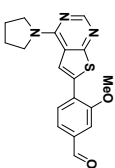
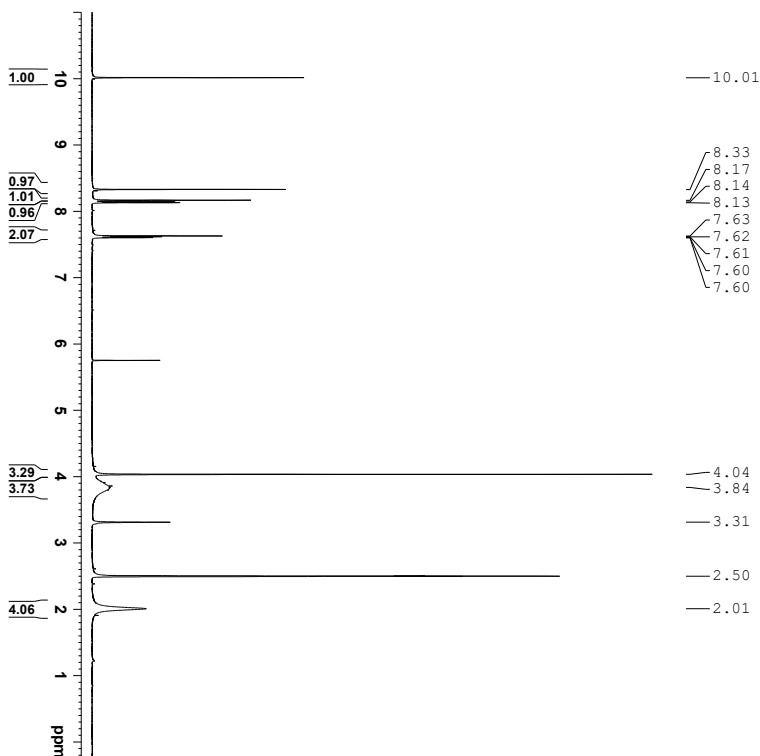
Minimum: -1.5  
Maximum: 5.0 2.0 50.0

Mass	Calc. Mass	mDa	PPM	DBE	i-FIT	Norm	Conf (%)	Formula
416.1439	416.1439	0.0	0.0	24.5	1251.9	11.790	0.00	C32 H18 N
	416.1440	-0.1	-0.2	11.5	1248.4	8.252	0.03	C17 H22 N9 S2
	416.1433	0.6	1.4	15.5	1240.1	0.000	99.97	C24 H22 N3 O2 S
	416.1431	0.8	1.9	12.5	1250.1	10.008	0.00	C16 H18 N9 O5

Mass spectrum of compound (R)-7a.



# S | Spectroscopic Data - Compound 7b



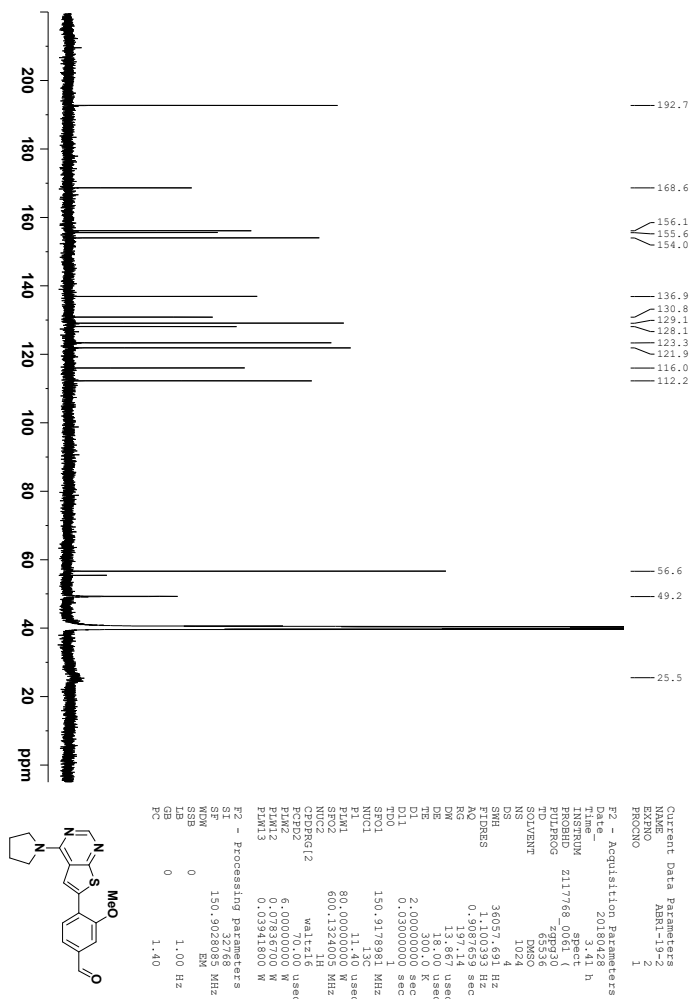
```

Current Data Parameters
NAME      AMR1-19
EXPNO     1
PROCNO    1
F2 - Acquisition Parameters
Date_     20180428
Time      2.50 h
INSTRUM   spect
PROBHD    zgpg30
PULPROG   zgpg30
TD         65536
SOLVENT   DMSO
DS         2
SWH        12019.230 Hz
AQ         0.782976 sec
RG         11.48 sec
DM         41.600 usec
TE         300.0 K
D1         1.00000000 sec
TDO1      600.1337043 MHz
NUC1       1H
P1         8.00 usec
PL1        6.00000000 W
F2 - Processing parameters
SI         65536
SF         600.130047 MHz
SFO        60
SSB        0
LB         0.30 Hz
GB         0
PC         1.00
    
```

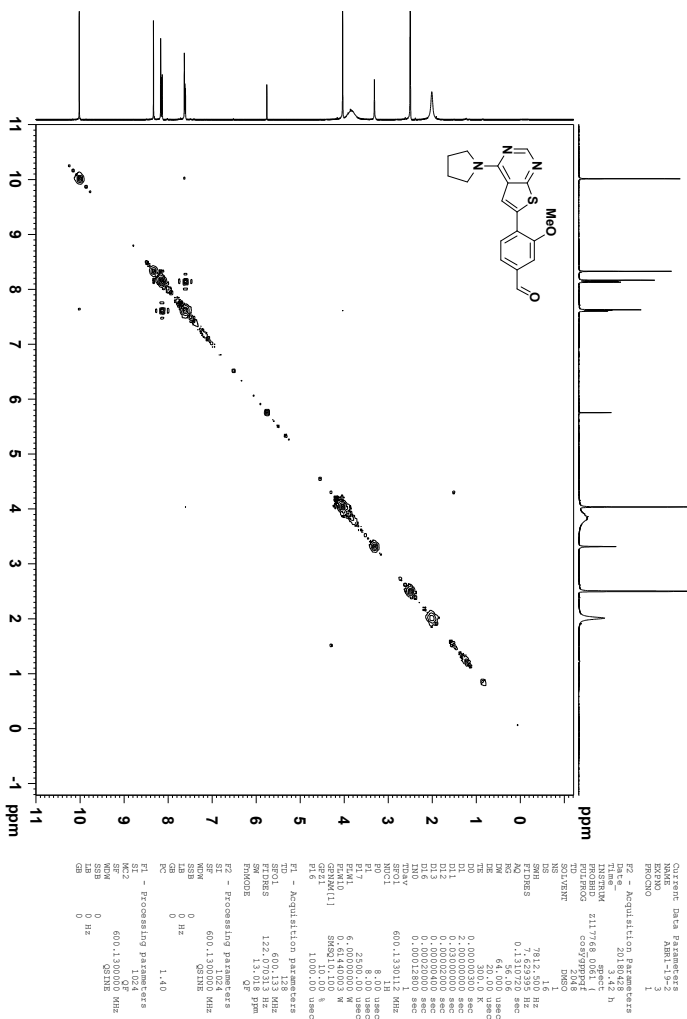
<sup>1</sup>H NMR (600 MHz, DMSO-*d*<sub>6</sub>) spectrum of compound **7b**.

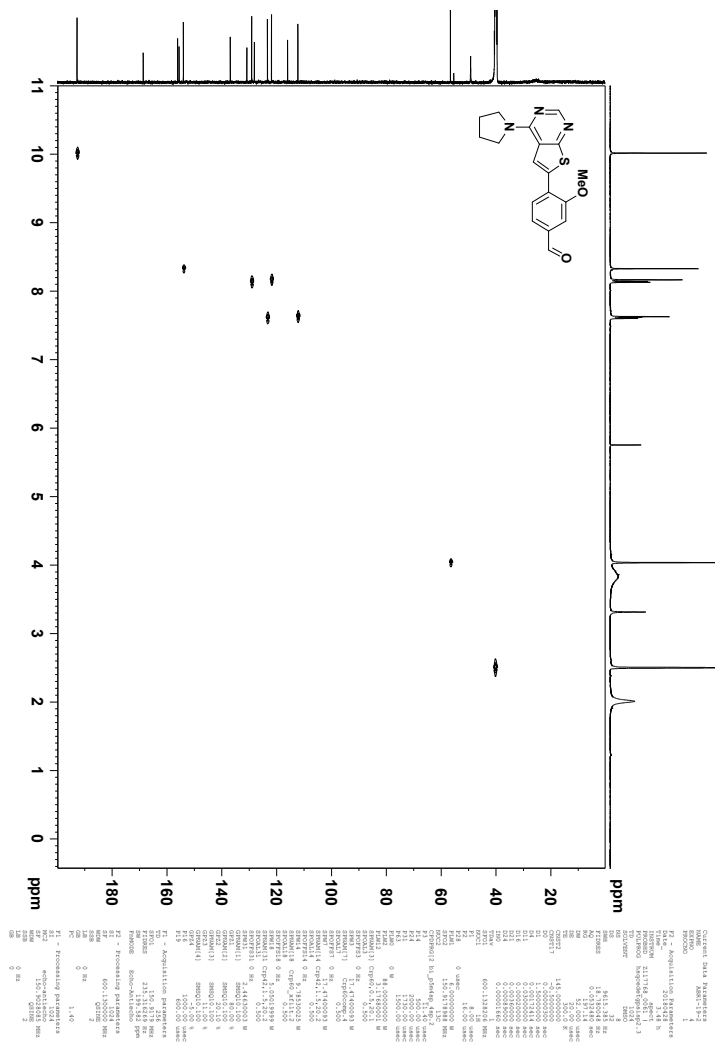


c



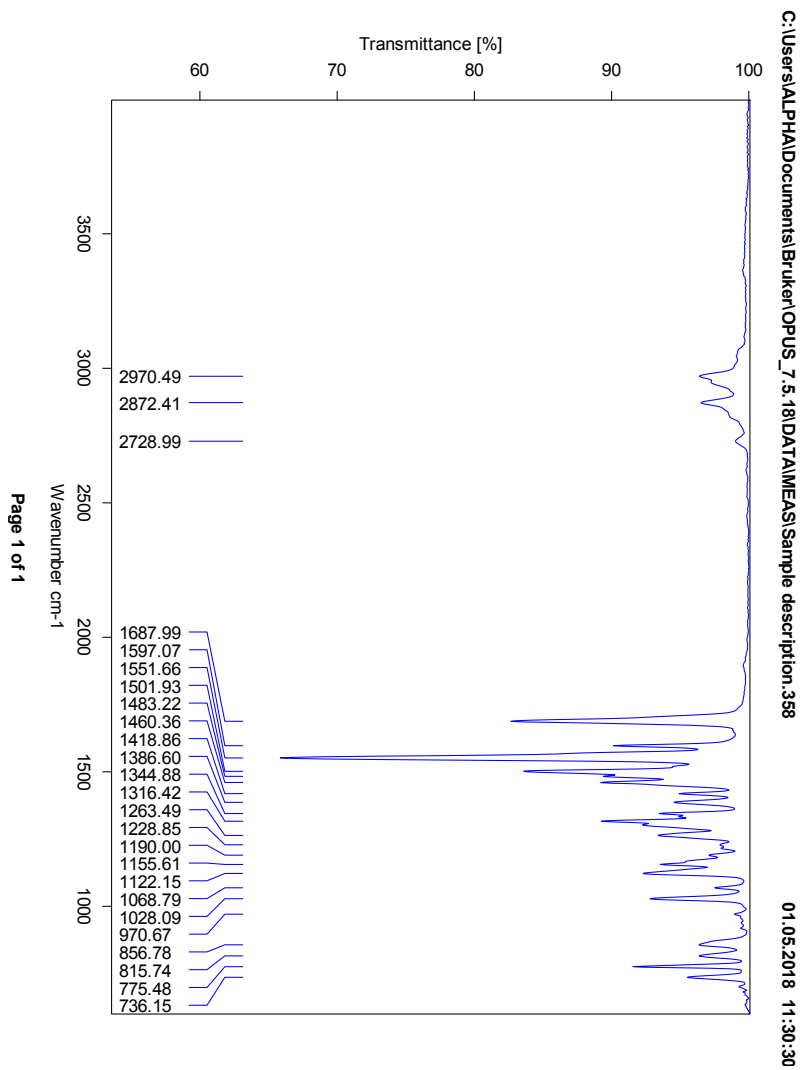
<sup>13</sup>C NMR (150 MHz, DMSO-*d*<sub>6</sub>) spectrum of compound 7b.

COSY spectrum of compound **7b**.



HSQC spectrum of compound 7b.



IR spectrum of compound **7b**.

## Elemental Composition Report

Page 1

## Single Mass Analysis

Tolerance = 2.0 PPM / DBE: min = -1.5, max = 50.0

Element prediction: Off

Number of isotope peaks used for i-FIT = 3

Monoisotopic Mass, Even Electron Ions

3752 formula(e) evaluated with 9 results within limits (all results (up to 1000) for each mass)

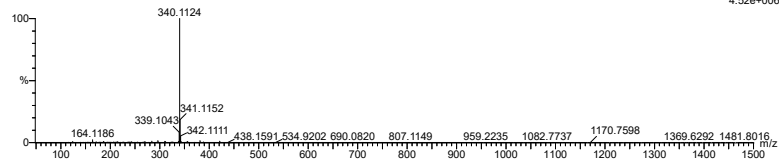
Elements Used:

C: 0-500 H: 0-1000 B: 0-1 N: 0-50 O: 0-50 S: 0-2

2018-84 140 (2.740) AM2 (Ar,35000.0,0.00,0.00); Cm (138:142)

1: TOF MS ASAP+

4.52e+006

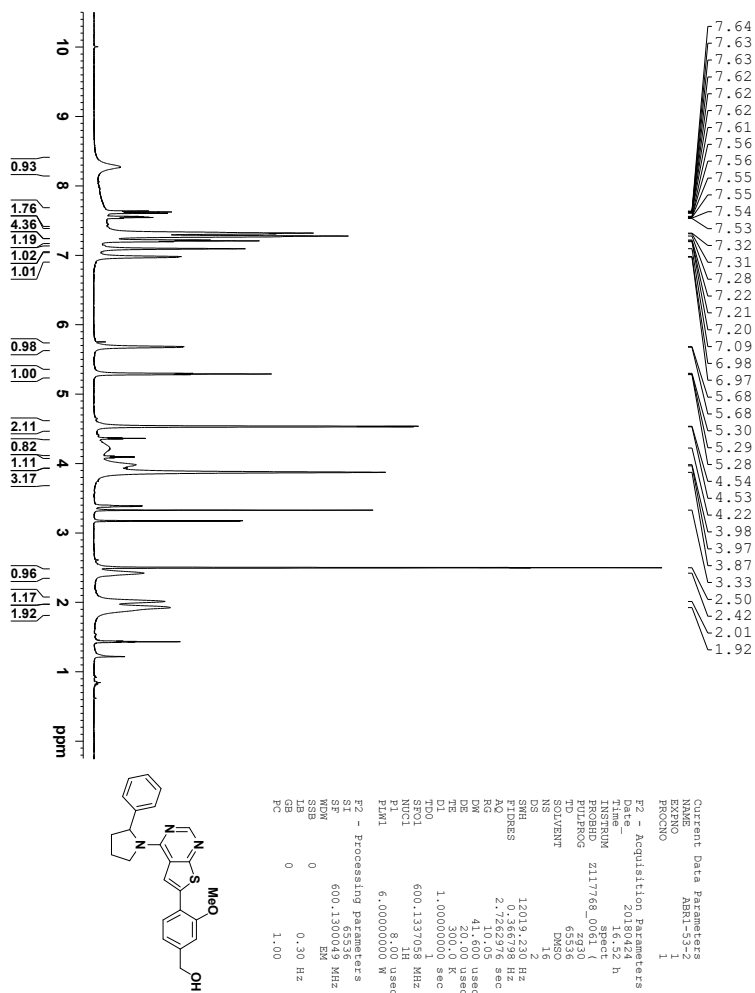
Minimum: -1.5  
Maximum: 50.0

Mass	Calc. Mass	mDa	PPM	DBE	i-FIT	Norm	Conf(%)	Formula
340.1124	340.1120	0.4	1.2	11.5	1547.5	0.001	99.88	C18 H18 N3 O2 S
	340.1127	-0.3	-0.9	7.5	1554.4	6.866	0.10	C11 H18 N9 S2
	340.1125	-0.1	-0.3	4.5	1556.3	8.841	0.01	C3 H14 N15 O3 S
	340.1118	0.6	1.8	8.5	1557.8	10.331	0.00	C10 H14 N9 O5
	340.1126	-0.2	-0.6	20.5	1560.3	12.831	0.00	C26 H14 N
	340.1118	0.6	1.8	16.5	1564.1	16.639	0.00	C17 H11 B N7 O
	340.1123	0.1	0.3	-1.5	1569.2	21.669	0.00	C4 H19 B N5 O12
	340.1118	0.6	1.8	3.5	1573.3	25.825	0.00	C2 H15 B N15 O S2
	340.1123	0.1	0.3	9.5	1574.4	26.867	0.00	C2 H7 B N19 O2

Mass spectrum of compound 7b.

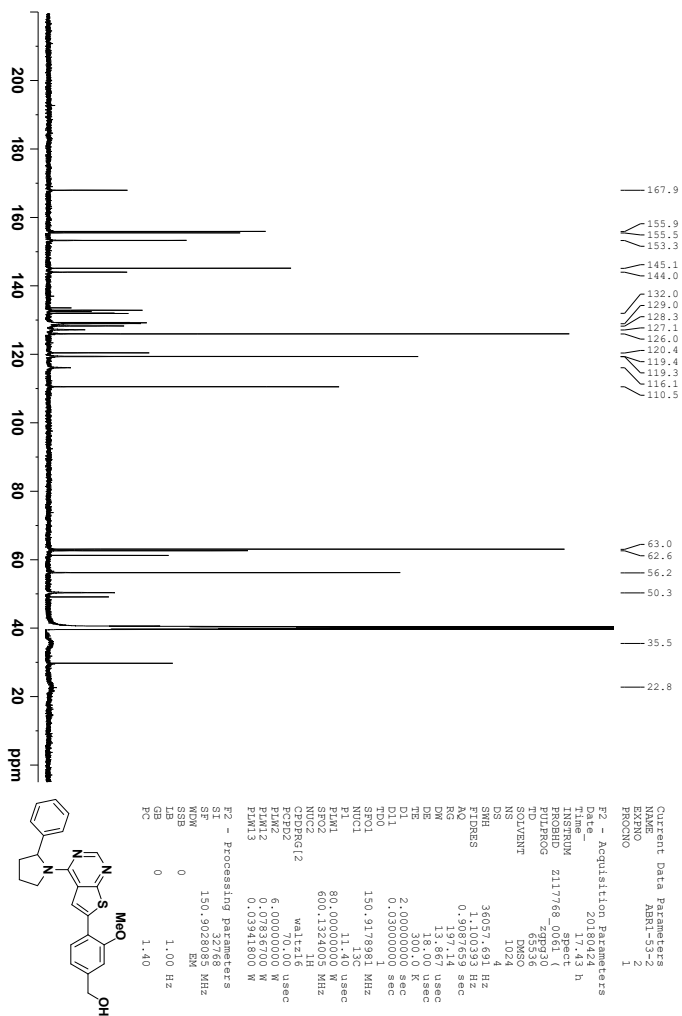


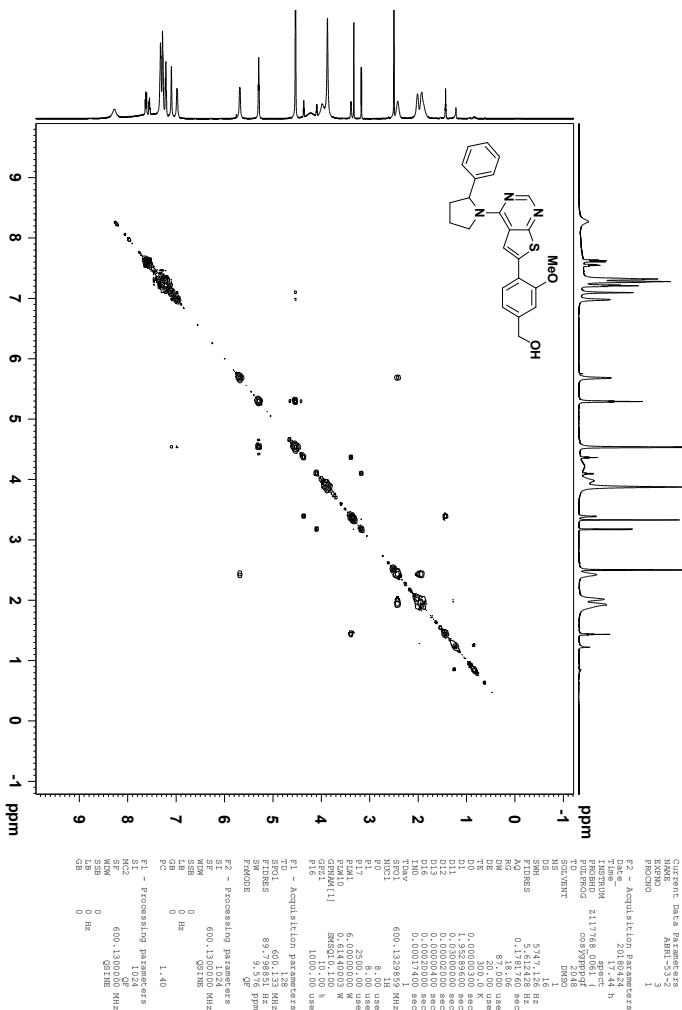
# T | Spectroscopic Data - Compound *rac-8a*



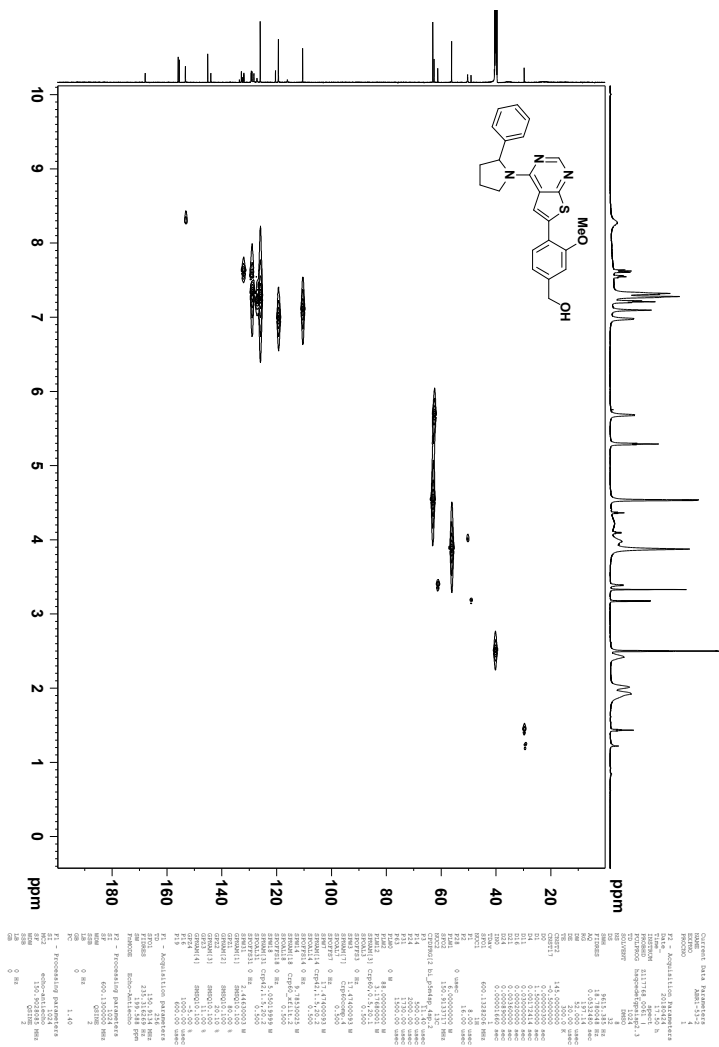
<sup>1</sup>H NMR (600 MHz, DMSO-*d*<sub>6</sub>) spectrum of compound *rac-8a*.



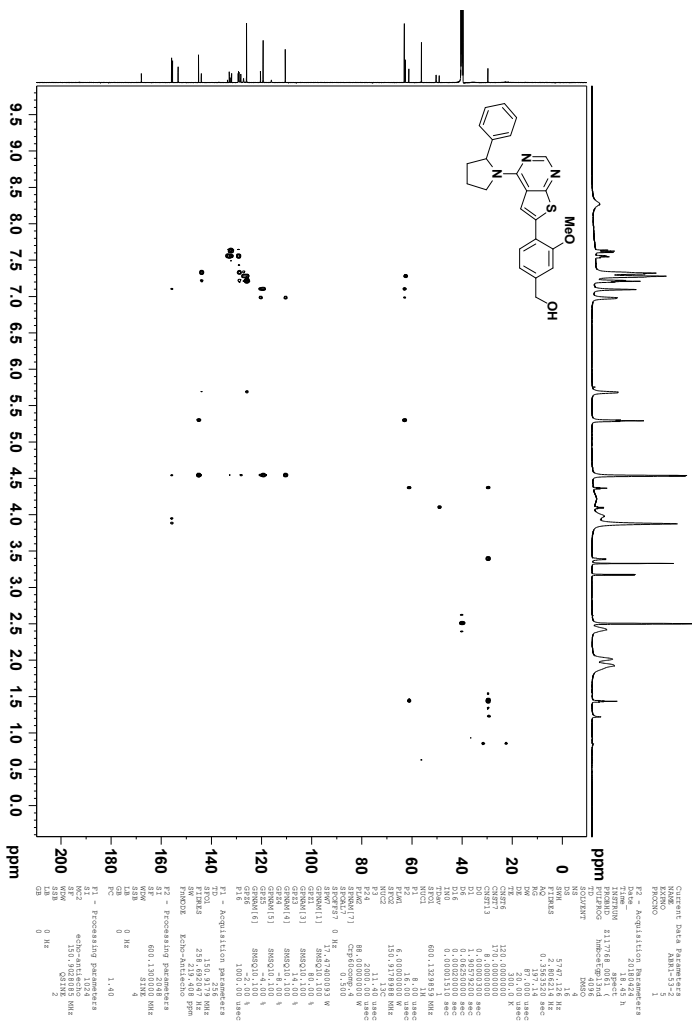
 $^{13}\text{C}$  NMR (150 MHz,  $\text{DMSO-}d_6$ ) spectrum of compound *rac-8a*.

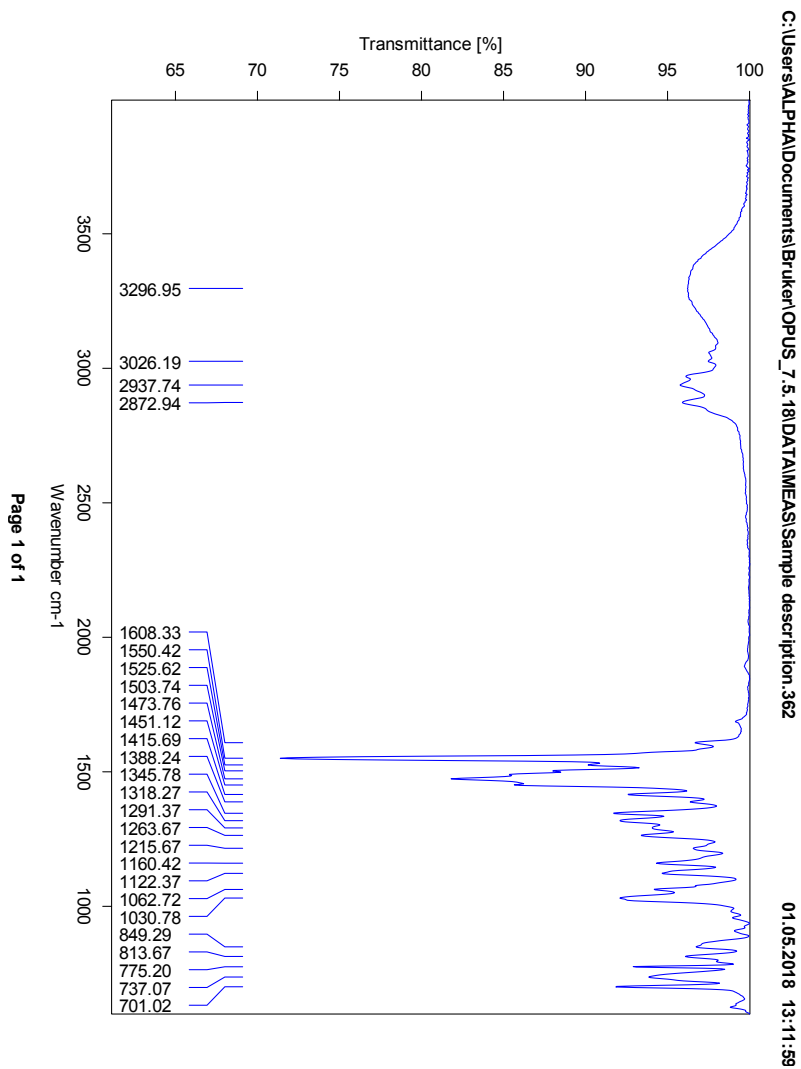


COSY spectrum of compound *rac*-8a.



HSQC spectrum of compound *rac-8a*.

HMBC spectrum of compound *rac*-8a.

IR spectrum of compound *rac-8a*.

## Elemental Composition Report

Page 1

## Single Mass Analysis

Tolerance = 2.0 PPM / DBE: min = -1.5, max = 50.0

Element prediction: Off

Number of isotope peaks used for i-FIT = 3

Monoisotopic Mass, Even Electron Ions

6889 formula(e) evaluated with 7 results within limits (all results (up to 1000) for each mass)

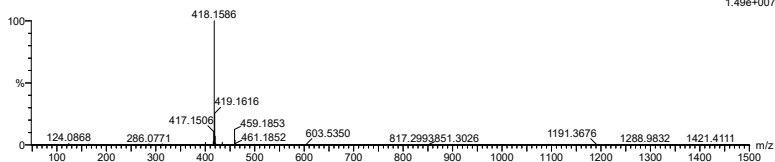
Elements Used:

C: 0-500 H: 0-1000 N: 0-10 O: 0-10 Na: 0-1 S: 0-2 Br: 0-4

2018-177 149 (2.912) AM2 (Ar:35000.0,0.00,0.00); Cm (144:149)

1: TOF MS ASAP+

1.49e+007



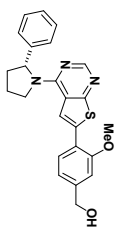
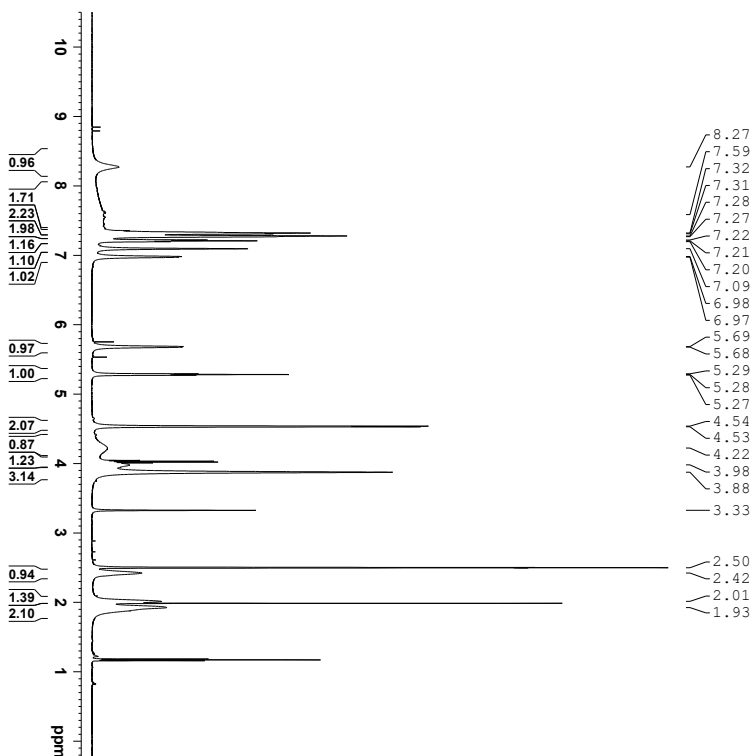
Minimum: -1.5  
Maximum: 5000.0 2.0 50.0

Mass	Calc. Mass	mDa	PPM	DBE	i-FIT	Norm	Conf(%)	Formula
418.1586	418.1589	-0.3	-0.7	14.5	1400.4	0.001	99.90	C24 H24 N3 O2 S
	418.1584	0.2	0.5	-1.5	1407.5	7.057	0.09	C10 H29 N5 O9 Na S
	418.1583	0.3	0.7	5.5	1409.6	9.111	0.01	C16 H28 N5 O4 S2
	418.1587	-0.1	-0.2	11.5	1411.0	10.555	0.00	C16 H20 N9 O5
	418.1590	-0.4	-1.0	7.5	1411.1	10.681	0.00	C18 H25 N3 O7 Na
	418.1593	-0.7	-1.7	3.5	1416.3	15.887	0.00	C19 H33 N O4 Br
	418.1582	0.4	1.0	5.5	1416.6	16.174	0.00	C18 H30 N5 Na Br

Mass spectrum of compound *rac*-8a.



# U | Spectroscopic Data - Compound (R)-8a

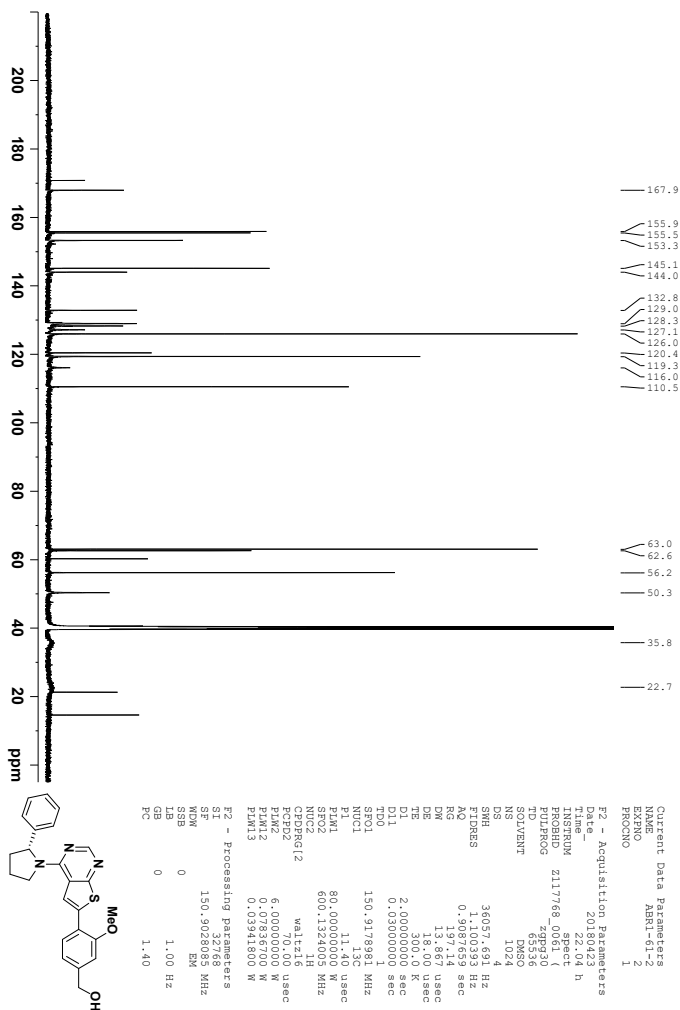


```

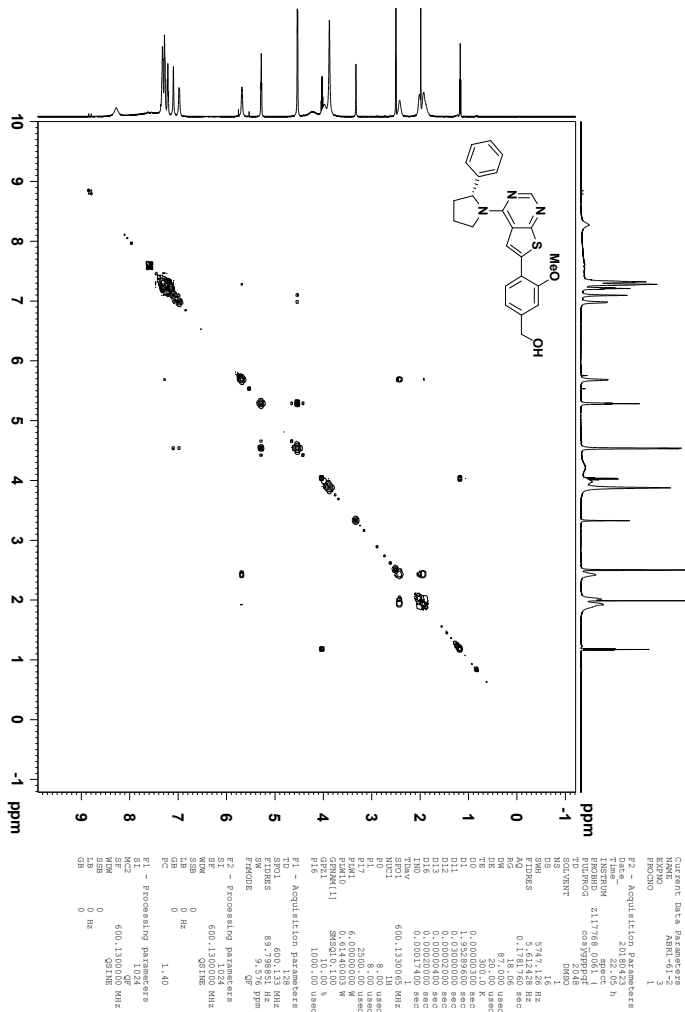
Current Data Parameters
NAME: F2-1
EXPNO: 1
PROCNO: 1
F2 - Acquisition Parameters
Date_ 20180423
Time 21.13 h
INSTRUM spect
PROBHD 5mm QNP 1H/13
PULPROG zgpg30
TD 65536
SOLVENT DMSO
DS 2
SWH 12019.230 Hz
AQ 0.728276 sec
RG 10.05
DM 41.600 usec
DE 300.0 K
TE 300.0 K
D1 1.00000000 sec
TD01 600.1337043 MHz
NUC1 1H
P1 8.00 usec
PL1 6.00000000 W
F2 - Processing parameters
SI 65536
SF 600.130048 MHz
SFO 600.130048 MHz
SSB 0
LB 0.30 Hz
GB 0
PC 1.00
  
```

<sup>1</sup>H NMR (600 MHz, DMSO-*d*<sub>6</sub>) spectrum of compound (R)-8a.

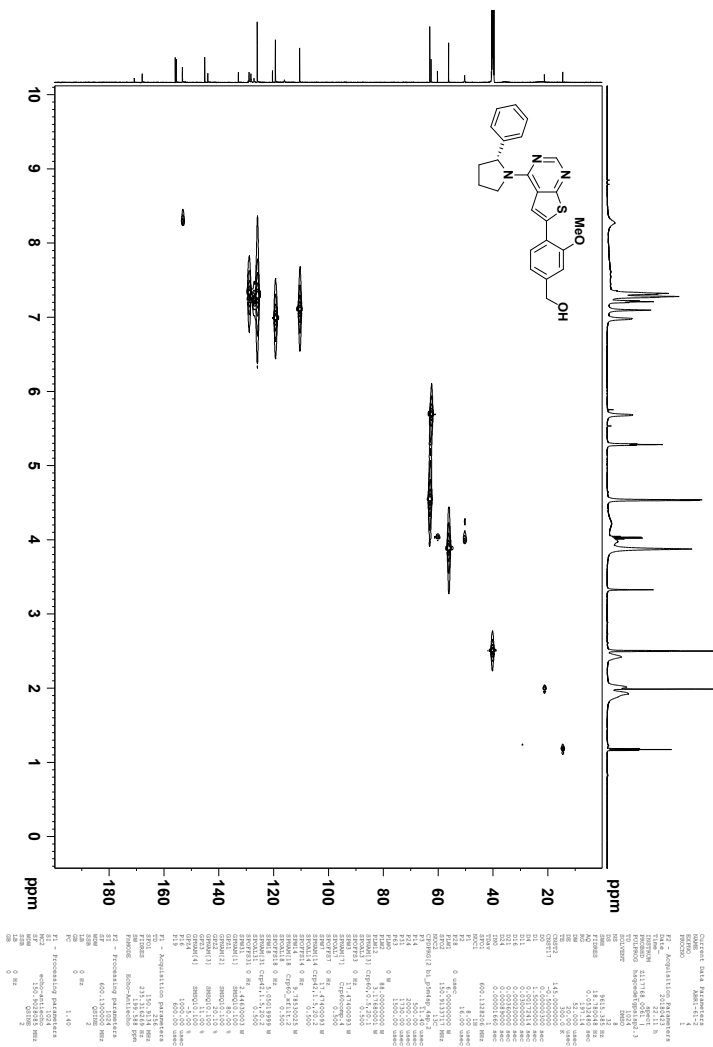




<sup>13</sup>C NMR (150 MHz, DMSO-*d*<sub>6</sub>) spectrum of compound (*R*)-8a.

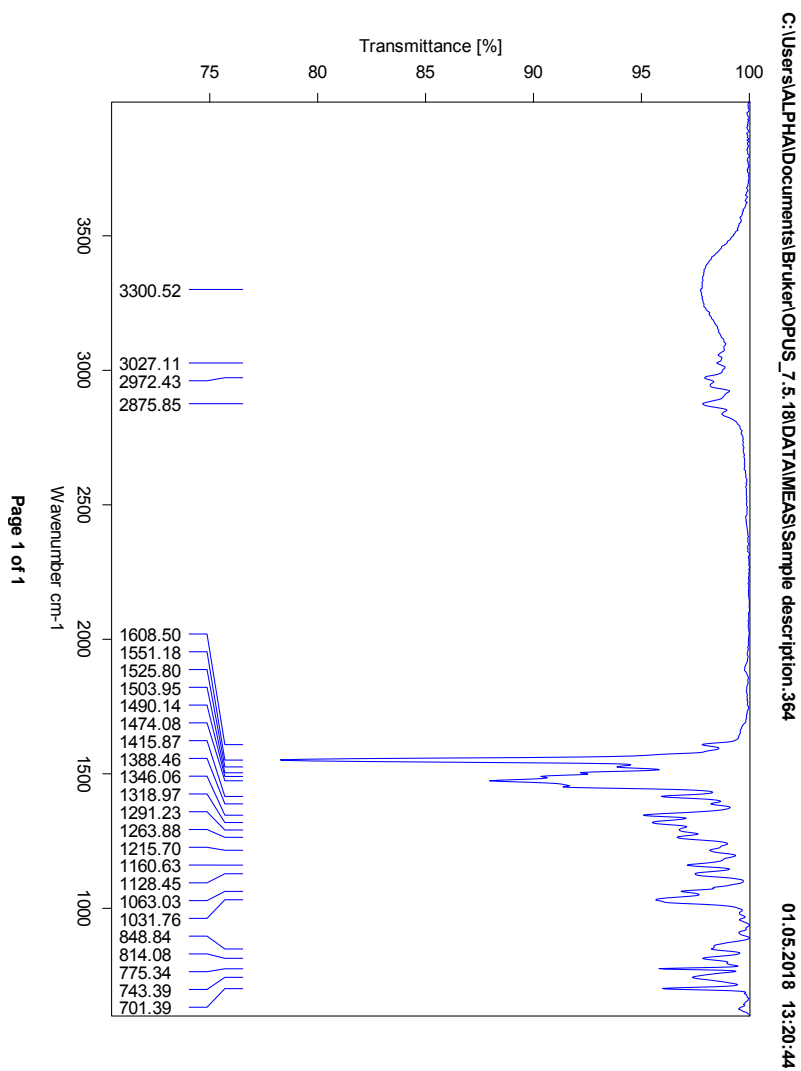


COSY spectrum of compound (R)-8a.



HSQC spectrum of compound (*R*)-**8a**.



IR spectrum of compound (*R*)-8a.

## Elemental Composition Report

Page 1

## Single Mass Analysis

Tolerance = 2.0 PPM / DBE: min = -1.5, max = 100.0

Element prediction: Off

Number of isotope peaks used for i-FIT = 3

Monoisotopic Mass, Even Electron Ions

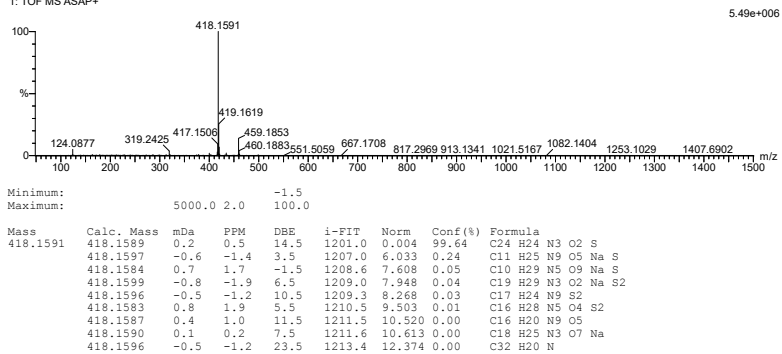
4042 formula(e) evaluated with 9 results within limits (all results (up to 1000) for each mass)

Elements Used:

C: 0-500 H: 0-1000 N: 0-10 O: 0-20 Na: 0-1 S: 0-2

2018-225 144 (2.808) AM2 (Ar:35000.0,0.00,0.00); Cm (137:144)

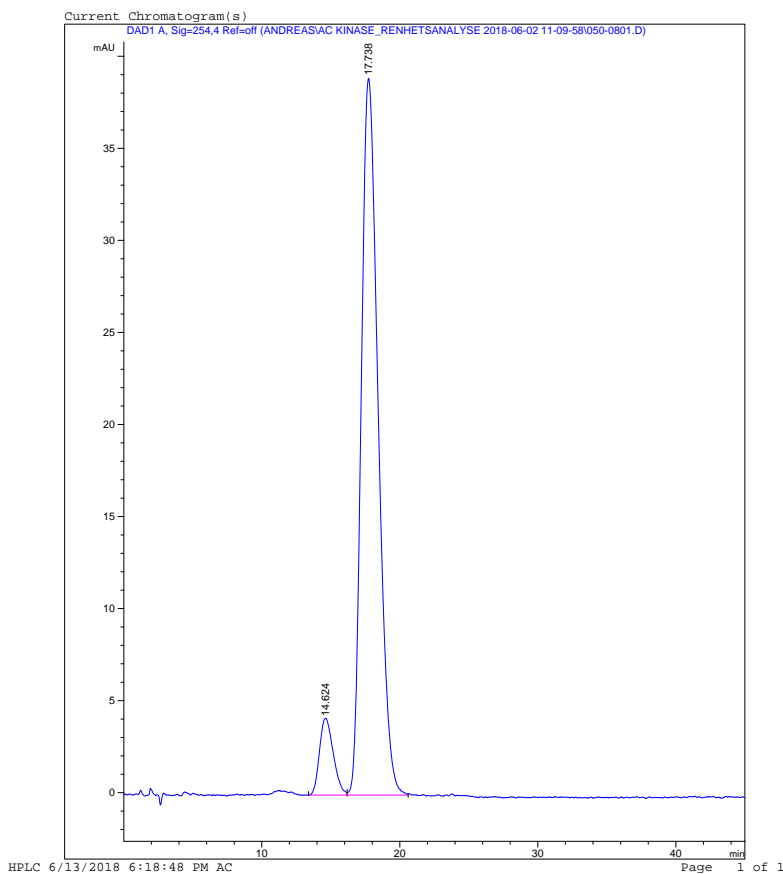
1: TOF MS ASAP+

Mass spectrum of compound (*R*)-8a.

Print of window 38: Current Chromatogram(s)  
Data File : C:\CHEM32\1\DATA\ANDREAS\AC KINASE\_RENHETSANALYSE 2018-06-02 11-09-58\050-0801.D  
Sample Name : ABR1-61-2 85/15,DEA, FLOW 1.5  
=====

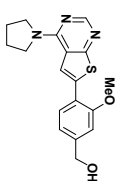
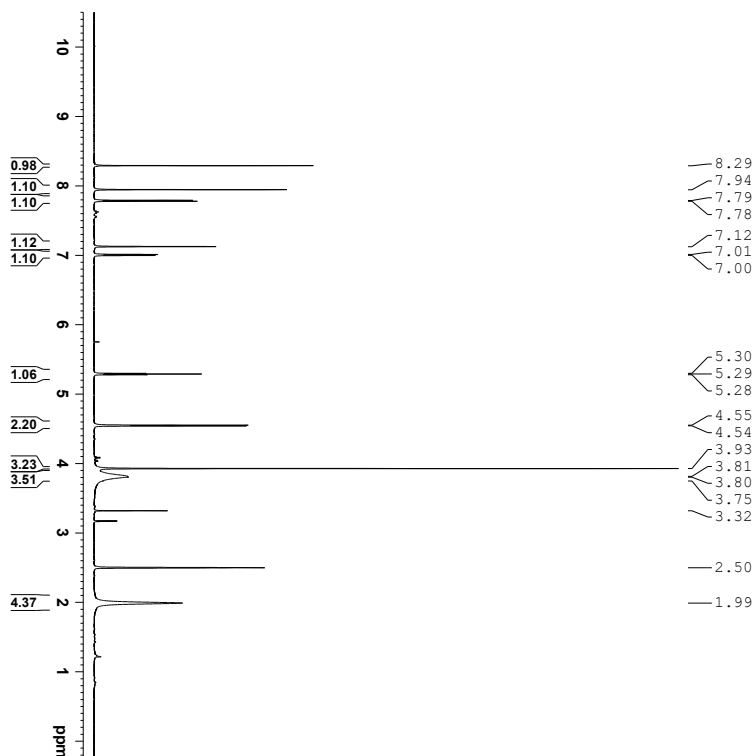
Acq. Operator	: AC	Seq. Line	: 8
Acq. Instrument	: HPLC	Location	: Vial 50
Injection Date	: 6/2/2018 5:43:15 PM	Inj	: 1
		Inj Volume	: 5.000 µl

Acq. Method : C:\CHEM32\1\DATA\ANDREAS\AC KINASE\_RENHETSANALYSE 2018-06-02 11-09-58\  
ANDREAS CHIRAL 85 FLOW 1.5.M  
Last changed : 5/31/2018 10:18:31 AM by AC  
Analysis Method : C:\CHEM32\1\METHODS\FELLES\RENHETSANALYSE FELLES\_NEUTRAL.M  
Last changed : 6/13/2018 6:16:27 PM by AC  
(modified after loading)



CSP-HPLC (Lux 5u Cellulose-1 4.6 x 250 mm, hexane(cont. 0.2% diethyl amine):*i*-PrOH, flow 1.5 mL/min, detection at 254 nm) of compound (*R*)-**8a**

# V | Spectroscopic Data - Compound 8b

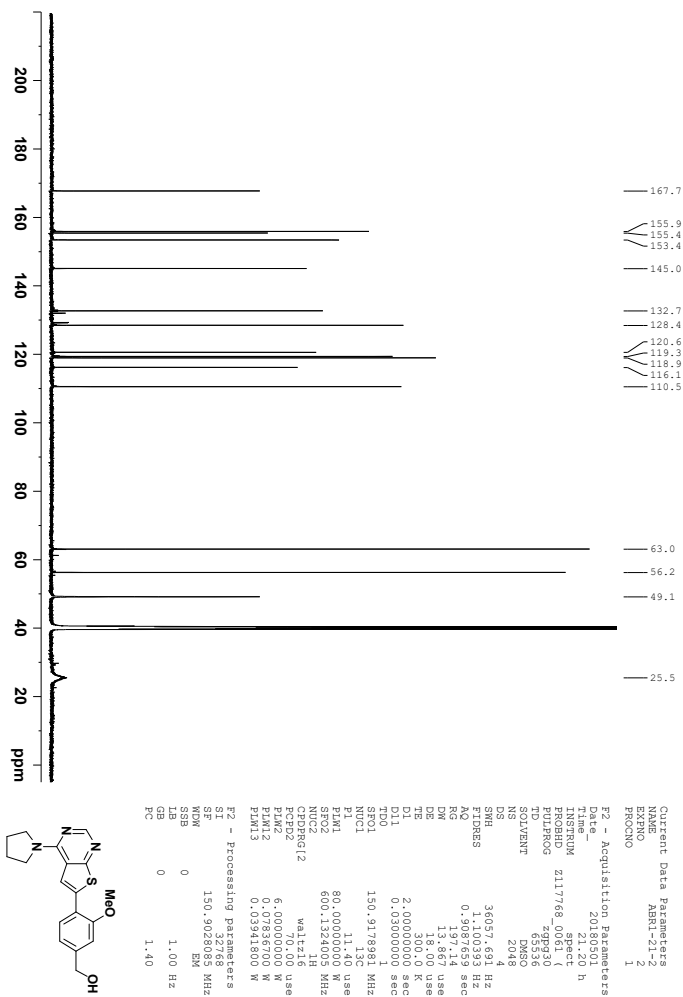


```

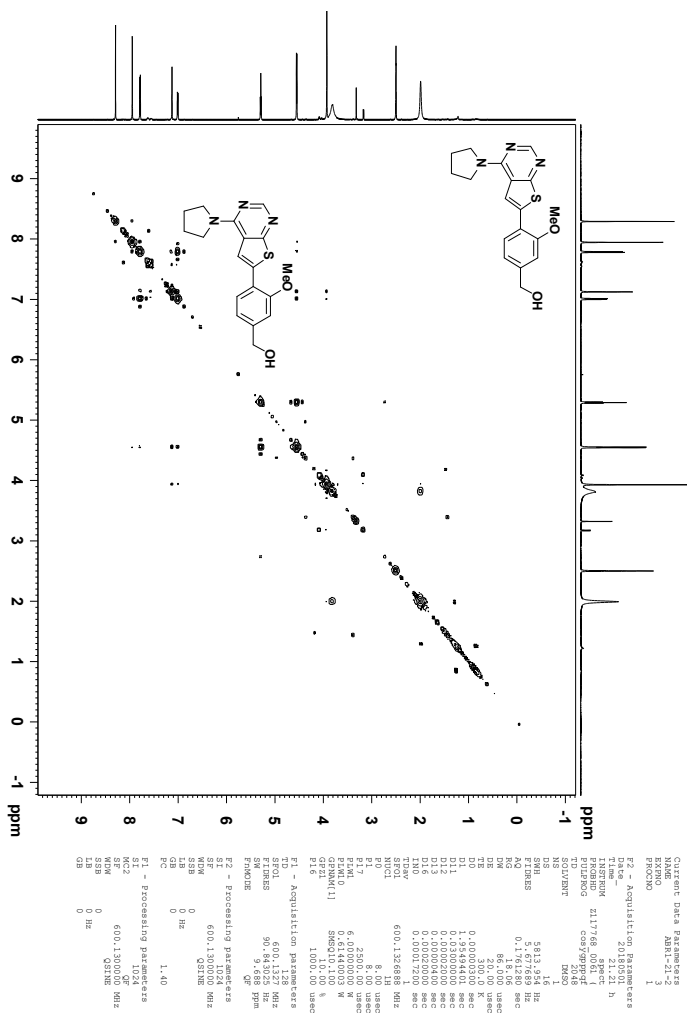
Current Data Parameters
=====
EXNO          1
PROCNO       1
F2 - Acquisition Parameters
=====
Date_         20180501
Time_        19.38 h
INSTRUM      spect
PROBHD       5mm QNP1H
PULPROG      zgpg30
TD           65536
AQ           1.00000000 sec
RG           10.05
SOLVENT      DMSO
DS           2
SWH          12019.230 Hz
AQPRES      0.782976 atm
RG           10.05
DM           41.600 usec
TE           300.0 K
TU           500.0 K
D1           1.00000000 sec
TDO1        600.1337043 MHz
NUC1         1H
P1           8.00 usec
PL1         6.000000000 W
F2 - Processing Parameters
=====
SI           65536
SF           600.130051 MHz
SFO          600.130051 MHz
SSB          0
LB           0.30 Hz
GB           0
PC           1.00
  
```

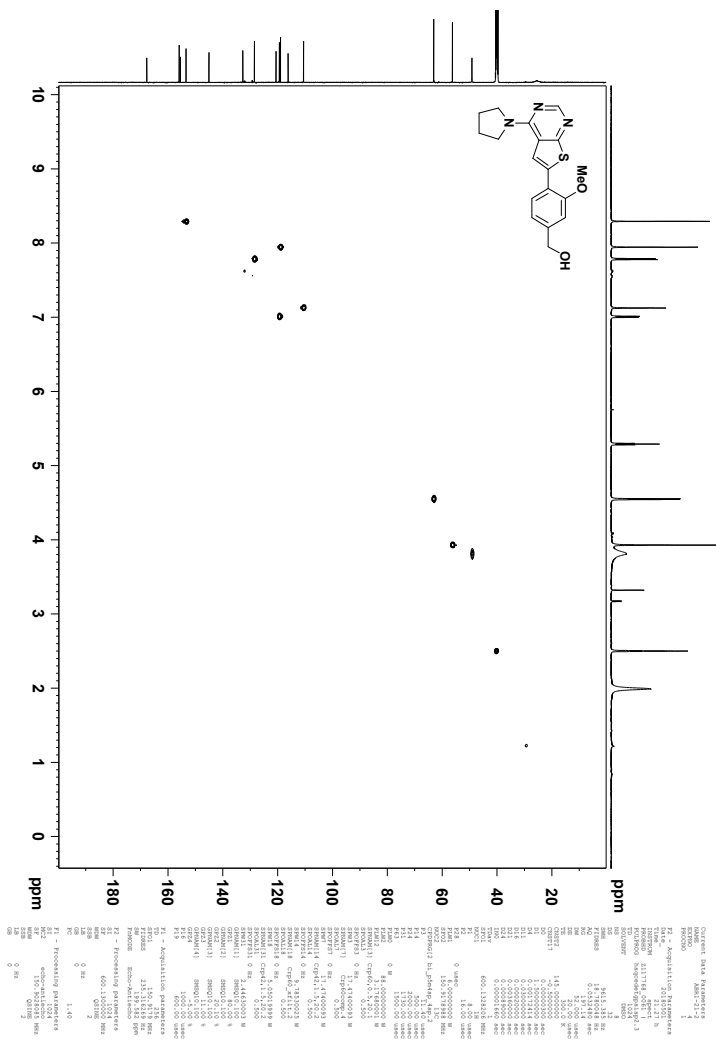
<sup>1</sup>H NMR (600 MHz, DMSO-*d*<sub>6</sub>) spectrum of compound **8b**.

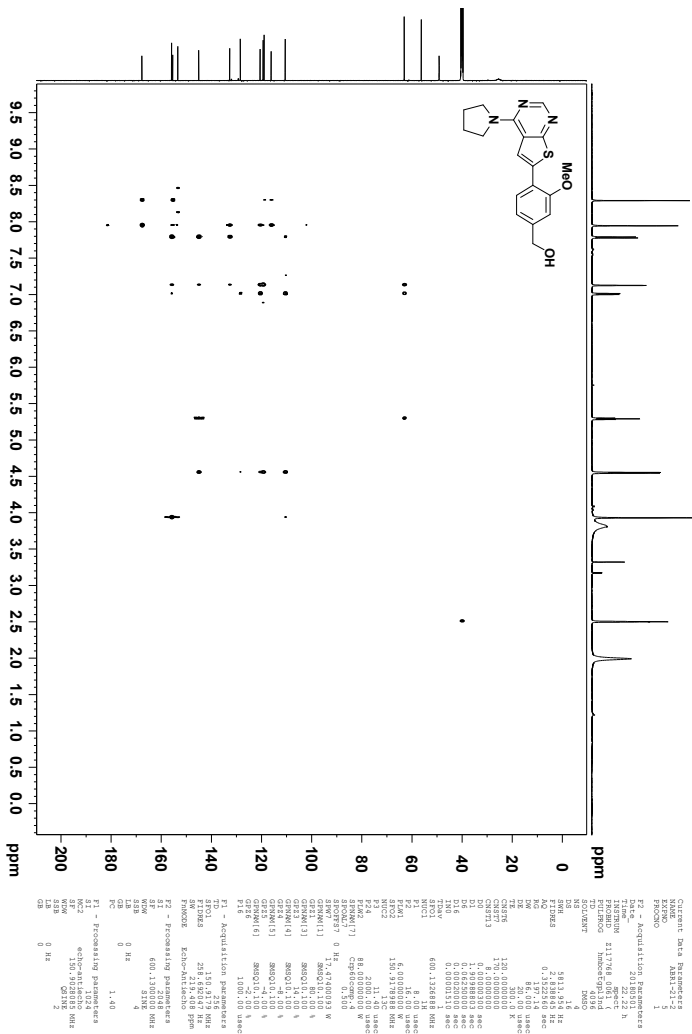


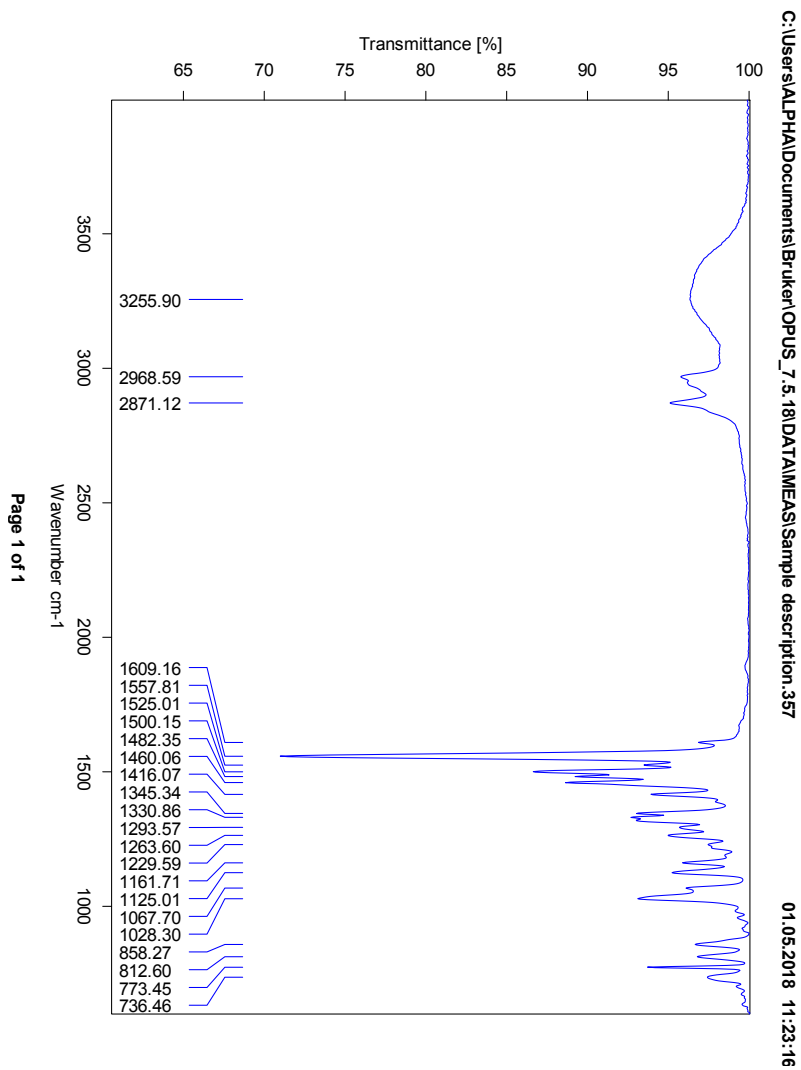


<sup>13</sup>C NMR (150 MHz, DMSO-*d*<sub>6</sub>) spectrum of compound **8b**.

COSY spectrum of compound **8b**.

HSQC spectrum of compound **8b**.

HMBC spectrum of compound **8b**.

IR spectrum of compound **8b**.

## Elemental Composition Report

Page 1

## Single Mass Analysis

Tolerance = 2.0 PPM / DBE: min = -1.5, max = 50.0

Element prediction: Off

Number of isotope peaks used for i-FIT = 3

Monoisotopic Mass, Even Electron Ions

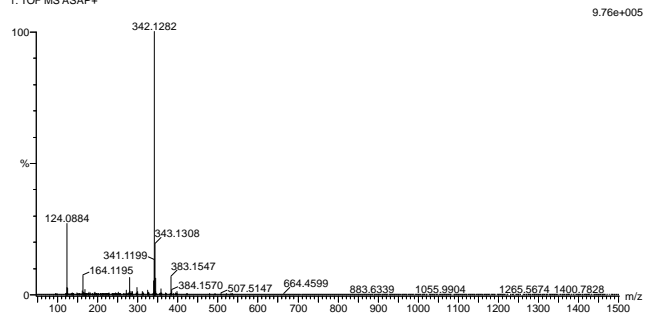
3002 formula(e) evaluated with 4 results within limits (all results (up to 1000) for each mass)

Elements Used:

C: 0-500 H: 0-1000 N: 0-10 O: 0-20 S: 0-3 Br: 0-2

2018-249 94 (1.843) AM2 (Ar:35000.0,0.00,0.00); Cm (91:94)

1: TOF MS ASAP+



Minimum: -1.5  
Maximum: 50.0

Mass	Calc. Mass	mDa	PPM	DBE	i-FIT	Norm	Conf (%)	Formula
342.1282	342.1276	0.6	1.8	10.5	1229.2	0.000	99.99	C18 H20 N3 O2 S
	342.1283	-0.1	-0.3	6.5	1238.1	8.924	0.01	C11 H20 N9 S2
	342.1283	-0.1	-0.3	19.5	1244.1	14.883	0.00	C26 H16 N
	342.1280	0.2	0.6	-0.5	1244.1	14.929	0.00	C13 H29 N O4 Br

Mass spectrum of compound **8b**.